DEPARTMENT OF THEORY OF STRUCTURE OF MATTER
DIVISION OF THEORETICAL PHYSICS
THE HENRYK NIEWODNICZAŃSKI INSTITUTE OF NUCLEAR PHYSICS
POLISH ACADEMY OF SCIENCES
KRAKÓW, POLAND

Collective dynamics of polarized spin-half fermions in relativistic heavy-ion collisions

Rajeev Singh

Presented in Partial Fulfillment of the Requirements for the Degree of Doctor of Philosophy in Physics.

Supervisor   **Coordinator**
dr. hab. prof. IFJ PAN Radoslaw Ryblewski

Co-Supervisor
dr. Arpan Das   ...

2018 − 2022

To my parents

ABSTRACT

Standard relativistic hydrodynamics, through the years, has been extremely successful in describing the properties of the strongly-interacting matter produced in the heavy-ion collision experiments. Recently, there has been a significant theoretical advancement in this field to explain a new phenomenon of spin polarization of hadrons emitted in these processes. Although current models have successfully explained some of the experimental data based on the coupling between spin polarization and vorticity of the medium, they still lack a clear understanding of the differential measurements. This is commonly interpreted as an indication that the spin needs to be treated as an independent degree of freedom whose dynamics is not entirely bound to flow circulation. In particular, if the spin is a macroscopic property of the system, in equilibrium its dynamics should follow hydrodynamic laws.

In this thesis, we develop a framework of relativistic perfect-fluid hydrodynamics which includes spin degrees of freedom from the quantum kinetic theory for Dirac fermions and use it for modeling the dynamics of matter produced in relativistic heavy-ion collisions. Following experimental observations, we assume that the polarization effects are small and derive conservation laws for the net-baryon current, the energy-momentum tensor, and the spin tensor based on the so-called de Groot–van Leeuwen–van Weert definitions of these currents.

Subsequently, we present various properties of the spin polarization tensor and its components, analyze the propagation properties of the spin polarization components, and derive the spin-wave velocity for arbitrary statistics. We find that only the transverse spin components propagate, analogously to the electromagnetic waves.

Finally, using our hydrodynamic framework, we study the spacetime evolution of the spin polarization for the systems respecting certain spacetime symmetries and calculate the mean spin polarization per particle, which can be compared to the experimental data. We find that, for some observables, our spin polarization results agree qualitatively with the experimental findings and other model calculations. Considering the importance of electromagnetic fields in the heavy-ion collisions, we also analyze the effect of external electric fields on the dynamics of spin polarization in the Bjorken-expanding background.

Streszczenie

Standardowa hydrodynamika relatywistyczna przez lata była niezwykle skuteczna w opisywaniu właściwości silnie oddziałującej materii produkowanej w eksperymentach zderzeń ciężkich jonów. W ostatnim czasie nastąpił znaczny postęp teoretyczny w tej dziedzinie, mający na celu wyjaśnienie nowego zjawiska jakim jest polaryzacja spinowa hadronów emitowanych w tych procesach. Chociaż obecne modele z powodzeniem wyjaśniają niektóre dane eksperymentalne tłumacząc je sprzężeniem między polaryzacją spinu a wirowością ośrodka, nadal brakuje jasnego zrozumienia danych różniczkowych. Jest to powszechnie interpretowane jako wskazówka, że spin należy traktować jako niezależny stopień swobody, którego dynamika nie jest sztywno związana z cyrkulacją przepływu materii. W szczególności, jeśli spin jest makroskopową właściwością układu, w równowadze jego dynamika powinna być zgodna z prawami hydrodynamicznymi.

W tej pracy przedstawiamy formalizm relatywistycznej hydrodynamiki płynu doskonałego obejmującej spinowe stopnie swobody otrzymanej w oparciu z kwantową teorię kinetyczną dla fermionów o spinie $1/2$ i wykorzystujemy ją do modelowania dynamiki materii wytwarzanej w relatywistycznych zderzeniach ciężkich jonów. W oparciu o obserwacje eksperymentalne przyjmujemy, że efekty polaryzacji są małe i wyprowadzamy prawa zachowania dla prądu barionowego, tensora energii-pędu i tensora spinu w używając definicji tych prądów zaproponowane przez de Groota, van Leeuwena i van Weerta .

W dalszej części przeprowadzamy analizę właściwości tensora polaryzacji i jego składowych, badamy właściwości propagacyjne składowych polaryzacji i wyprowadzamy prędkość fali spinowej dla dowolnych statystyk kwantowych. Pokazujemy, że poprzeczne składowe polaryzacji podlegają propagacji, analogicznie do fal elektromagnetycznych.

Wreszcie, korzystając z naszego formalizmu hydrodynamicznego, badamy czasoprzestrzenną ewolucję polaryzacji dla systemów respektujących pewne symetrie czasoprzestrzenne oraz wyznaczamy średnią polaryzację spinu cząstek na hiperpowierzchni wymrożenia, którą możemy porównać z danymi eksperymentalnymi. Stwierdzamy, że w przypadku niektórych obserwabli, nasze wyniki są jakościowo zgodne z wynikami eksperymentów i innymi obliczeniami modelowymi. Biorąc pod uwagę znaczenie pól elektromagnetycznych w zderzeniach ciężkich jonów, analizujemy również wpływ zewnętrznych pól elektrycznych na dynamikę polaryzacji spinu przy założeniu ekspansji Bjorkena.

Acknowledgements

"Adapt yourself to the life you have been given;
and truly love the people with whom
destiny has surrounded you"
– Marcus Aurelius

Before going to the main part of this Thesis, here I would like to acknowledge all the living and non-living with whom I have interacted directly or indirectly and they somehow motivated me to embark on the journey of my Ph.D.

First and most important of all, I would like to thank my parents, and my supportive brother and sister. They are the reason I am here. I am grateful to them for believing in me, and constantly supporting me in all aspects of my life. Teachers play an important role in shaping the lives of students. They inspire me to take up challenges, I am thankful to all my teachers who taught me and inspired me throughout my life.

Now I would like to take the opportunity to sincerely thank my Ph.D. supervisor Prof. Radoslaw Ryblewski. Without his guidance, support, and help, I could never be able to start this journey in the first place. His passion for excellence and perfection inspired me to think and imagine beyond limits. I would like to mention that my supervisor was always there for me, pushing me to reach my true potential. Thank you very much for listening every time I knocked on your door.

I am grateful to Prof. Wojciech Florkowski who, in a sense, mentored me to learn and go deep into the field and also inspired me to take up challenges in other fields and be curious. His support was always with me. Then I would like to thank my co-supervisor Dr. Arpan Das without whom I would never have realized many important aspects of academics and ethics. I am glad to be grateful to all my friends (especially Karishma Dhanmeher, Himanshu Sharma and Tomoki Goda), collaborators, and colleagues who encouraged, sustained, inspired, and tolerated me during this journey.

Contents

EM	Electromagnetic
QCD	Quantum Chromodynamics
QGP	Quark-Gluon Plasma
CERN	Conseil Européen pour la Recherche Nucléaire
BNL	Brookhaven National Laboratory
SPS	Super Proton Synchrotron
LHC	Large Hadron Collider
AGS	Alternating Gradient Synchrotron
RHIC	Relativistic Heavy-Ion Collider
LTE	Local Thermodynamic Equilibrium
QFT	Quantum Field Theory
EoS	Equation of State
NS	Navier-Stokes
LRF	Local Rest Frame
Can	Canonical
BR	Belinfante-Rosenfeld
GR	General Relativity
HW	Hilgevoord-Wouthuysen
GLW	de Groot, van Leeuwen, van Weert
MJ	Maxwell-Jüttner
FD	Fermi-Dirac
PL	Pauli-Lubański
PRF	Particle-Rest Frame
BV	Boltzmann–Vlasov
MHD	Magnetohydrodynamics
JH	Joule Heating

Table 1: List of acronyms in order of appearance in the Thesis.

NOTATION

In this Thesis the following notations/conventions have been adopted:

- "Mostly minus" signature for the spacetime metric, unless specified otherwise

$$
g_{\alpha\beta} = \begin{pmatrix} 1 & 0 & 0 & 0 \\ 0 & -1 & 0 & 0 \\ 0 & 0 & -1 & 0 \\ 0 & 0 & 0 & -1 \end{pmatrix},
\tag{1}
$$

  where $g^{\mu\nu} g_{\mu\nu} = 4$ and $x^\mu = (t, \, x, \, y, \, z)$ in the Cartesian coordinate.

- For the scalar (dot) product of four-vectors: $a \cdot b = a^\alpha b_\alpha = g_{\alpha\beta} a^\alpha b^\beta = a^0 b^0 - \boldsymbol{a} \cdot \boldsymbol{b}$, where bold font denotes three-vectors.

- For Levi-Civita symbol $\epsilon^{\alpha\beta\gamma\delta}$: $\epsilon^{0123} = 1 = -\epsilon_{0123}$.

- We denote symmetrization by $A_{(\mu\nu)} = \frac{1}{2} \left(A_{\mu\nu} + A_{\nu\mu} \right)$.

- To represent anti-symmetrization we use $A_{[\mu\nu]} = \frac{1}{2} \left(A_{\mu\nu} - A_{\nu\mu} \right)$.

- We represent commutator and anti-commutator between A and B as $[A, B] = AB - BA$ and $\{A, B\} = AB + BA$, respectively.

- Dual of any tensor is denoted by a star and obtained by contracting it with the Levi-Civita symbol as

$$
\overset{\star}{A}{}^{\alpha\beta} = \frac{1}{2} \epsilon^{\alpha\beta\gamma\delta} A_{\gamma\delta} .
\tag{2}
$$

- $\slashed{A} = \gamma^\mu A_\mu$ represents Feynman slashed notation.

- $\langle : A : \rangle$ denotes ensemble (statistical) average of the normal ordered quantity A.

- Directional derivatives along basis vectors are denoted as $U^\alpha \partial_\alpha \equiv (\overset{\bullet}{})$, $X^\alpha \partial_\alpha \equiv (\overset{\blacksquare}{})$, $Y^\alpha \partial_\alpha \equiv (\overset{\square}{})$, $Z^\alpha \partial_\alpha \equiv (\overset{\circ}{})$.

- Divergence of a four-vector A is written as $\partial_\alpha A^\alpha \equiv \theta_A$.

- Einstein summation convention is assumed unless mentioned otherwise.

Throughout the work we assume natural units *i.e.* $c = \hbar = k_B = 1$, unless mentioned otherwise. Here c, $\hbar$, and k_B is speed of light, reduced Planck constant and Boltzmann constant, respectively.

1

INTRODUCTION

"What is not started
will never get finished."
– JOHANN WOLFGANG VON GOETHE

Understanding the origin of our universe, its physical properties, its composition, etc. are among the primary goals of modern science. According to the standard model of cosmology, the theory of the Big Bang proposed by G. Lemaître [1] in the year 1927 [1], has been considered the most reliable framework to date to study the evolution of the universe. Extrapolated back in time the Big Bang model gives us crucial information about its origin. According to this model, our universe is expanding and it was much hotter and much smaller in the beginning. The experimental validation of its expansion came after galaxy red-shift measurements by E. Hubble in 1929 [10]. His observational evidence along with the cosmic microwave background [11] and Big Bang nucleosynthesis [12,13] became the key milestones of modern cosmology. To explore the physical properties and the matter content of our universe, physicists have considered different approaches. One of the approaches is the direct astrophysical and astronomical observation, meaning observation at large length scales using telescopes probing different electromagnetic (EM) wavelengths. The other approach is to reproduce the conditions which existed during the very early stages of the universe in terrestrial laboratories producing hot and dense medium in relativistic heavy-ion collisions [14,15].

According to the thermal history of our universe, its temperature and its age, at the very beginning, during the Planck era, were of the order of 10^{19} GeV and 10^{-43} s, respectively [16]. The universe, being in a very hot and dense early stage, then cooled and diluted due to its expansion. It has been speculated that due to the cooling, our universe also went through several phase transitions, for instance, grand unification [2], electroweak and QCD (quantum chromodynamics) phase transitions, etc. at different time scales [17,18]. Among

---

[1]Historically speaking, A. Friedmann was the first who came up with the idea that the Universe can be dynamic [3] after finding the solutions of A. Einstein's field equations. However, he did not link his findings to any astronomical observations. There were many attempts to obtain the dynamic universe solution from Einstein's equations but none of them suggested that the universe is expanding [4]. It was K. Lundmark in 1924, who estimated extra-galactic distances and suggested that galaxies are red-shifted [5]. Then in 1927, G. Lemaître discovered new dynamical solutions to Einstein's equations and obtained the relationship between linear velocity and distance, which he then linked to astronomical observations. This solution was also independently discovered later by H. P. Robertson [6] and A. G. Walker [9].

[2]This is a phase transition where the strong force got disentangled from the weak and electromagnetic forces.

these phase transitions, the dynamics of the QCD one is the most important for our current discussion. QCD transition which can also be understood as the transition from the deconfined quark-gluon matter, more commonly known as the quark-gluon plasma (QGP), to confined hadronic matter occurred when the temperature was of the order of $T \sim \Lambda_{\mathrm{QCD}} \approx 200$ MeV and the age of the universe was a few microseconds ($\sim 10^{-6}$ s) after the Big Bang [18]. It turns out that the QCD transition is the only phase transition of the early Universe history that can be studied in the relativistic heavy-ion collision experiments. Due to the direct experimental access, we can explore various aspects of the dynamics of QCD phase transition, which is otherwise not possible. We should emphasize that the study of the QCD phase transition dynamics is also crucial for the existence of nuclear matter in the universe. As the universe cooled across the QCD transition scale, bound states of elementary particles such as baryons were formed out of quark-gluon matter. Subsequent evolution of the universe and due to the big bang nucleosynthesis, protons and neutrons combined to form certain species of atomic nuclei. Today most of the observed matter in our universe is in the form of atomic nuclei. Therefore, understanding the QCD dynamics in the early universe is of paramount importance. Moreover, large compact objects, such as neutron stars may also help us to understand the properties of matter under extreme conditions. These compact objects can also contain various phases of QCD matter *e.g.* QGP, hadronic matter, etc. Since we cannot access the QCD plasma of the early universe or the interior of astrophysical objects directly, relativistic heavy-ion collision experiments across a wide range of collision energies provide us a unique opportunity to explore the QCD dynamics [19–22].

1.1 Quark-gluon plasma

The dynamics of strongly-interacting matter namely quark-gluon matter and the hadronic matter is governed by the fundamental theory of QCD. Two key aspects of the QCD are *asymptotic freedom* and *color confinement*. The QCD coupling constant becomes very small at the high energy scale or a large momentum transfer scale in microscopic collisions. This phenomenon is known as the asymptotic freedom [23, 24] which can be shown analytically using the methods of perturbative QCD and has been well tested in deep inelastic scattering experiments. Interestingly, the momentum dependence of the QCD coupling also indicates that in the low energy scale of Λ_{QCD}, this coupling is rather large leading to the breakdown of the perturbative QCD techniques. Such non-perturbative nature at the low energy scale is very interesting and it can be argued to be associated with the non-abelian nature of the QCD gauge fields. Due to this non-abelian nature, gluons can self-interact leading to the phenomenon of color confinement which prevents us to observe directly the 'colored' partons, *i.e.* quarks, antiquarks, and gluons. These colored partons are confined within color singlet (color neutral) hadrons [3] which can be observed in the experiments.

Fundamental properties of QCD are also manifested in its phase transition dynamics. In the QCD medium, at a very high temperature ($T \gg \Lambda_{\mathrm{QCD}}$) or high baryon number density ($\mathcal{N} \gg \Lambda_{\mathrm{QCD}}^3$) [4], partons are expected to be liberated from individual hadrons and form

---

[3]Hadrons can be considered as the low-energy states of QCD, although a framework describing color confinement from a microscopic point of view is still lacking. Nevertheless, various lattice QCD numerical calculations unambiguously predict the existence of various hadronic states starting from the fundamental QCD Lagrangian.

[4]Understanding the extreme properties has always been important in paving the way to discover new states of matter [25]. The first exploration of the properties of matter at high densities was performed by

a deconfined phase of quarks and gluons. In this deconfined medium, partons can move across length scales that are larger than the confinement length scale *i.e.*, the mean size of hadrons. The transition from the confined hadronic phase to the deconfined QGP phase is known as the confinement-deconfinement phase transition. We should note that, although the confinement-deconfinement transition was predicted as a true phase transition, lattice QCD calculations (with physical quark masses) showed that this is not a phase transition but rather a crossover. Such conclusions can be drawn by considering the variation of the thermal expectation value of the Polyakov loop with various physical scales. The thermal expectation value of the Polyakov loop can be considered as an order parameter of the confinement-deconfinement transition [29–31]. At vanishing baryon chemical potential with physical quark masses, the thermal expectation value of the Polyakov loop changes continuously from the confined phase to the deconfined phase with temperature. On the other hand in the pure gauge sector, QCD phase transition is of first order [32].

Apart from the $SU(3)_c$ gauge symmetry, QCD Lagrangian can also have other global symmetries. One such symmetry of the massless QCD Lagrangian is the chiral symmetry, denoted as $SU(3)_V \otimes SU(3)_A$ with V and A representing the vector and axial-vector transformation in the fermionic sector of the QCD Lagrangian. In the high energy scale ($\gg \Lambda_{QCD}$), one can safely neglect masses of light quarks (including strange quark). The chiral symmetry of QCD is exact only in the vanishing quark mass limit, however, in reality, chiral symmetry is only an approximate symmetry. Note that, if we only consider u and d quarks, the physical masses of these quarks can be neglected in comparison to Λ_{QCD} scale. Thus, in the non-strange light quark sector, chiral symmetry is physically motivated. If chiral symmetry is a symmetry of nature then one would expect parity doublets of observed hadrons, which are not observed [5]. This implies that, although the chiral symmetry is the symmetry of the QCD Lagrangian, in the QCD vacuum this symmetry is not manifested. Hence, the chiral symmetry is 'spontaneously' broken, $SU(3)_V \otimes SU(3)_A \to SU(3)_V$. For two light-flavor quarks (u and d) case, pions are the Goldstone bosons of the spontaneous chiral symmetry breaking [33, 34]. Spontaneous breaking of chiral symmetry can be argued in various QCD-inspired effective models due to the presence of non-vanishing quark-antiquark scalar condensate (chiral condensate) which is an order parameter of the chiral phase transition [35, 36]. Various QCD effective model calculations indicate that in the high temperature and/or high chemical potential limit the chiral condensate has a vanishing value. This phase is called the chirally symmetric, or chirally restored, phase. On the other hand, in the low-temperature limit, chiral condensate can have a non-vanishing value. This phase is known as the chiral symmetry broken phase. The quark matter phase is expected to be a chiral symmetry restored phase and in the hadronic phase, the chiral symmetry is spontaneously broken. Spontaneous breaking of chiral symmetry also gives rise to non-perturbative corrections to the masses of quarks and hadrons [33]. One should emphasize that the chiral symmetry group is only defined in the fermionic sector of the QCD Lagrangian. On the other hand, the local $SU(3)_c$ symmetry deals with color gauge fields. Hence, it is not expected that the chiral phase transition and the confinement-deconfinement transitions are connected. However, lattice QCD calculations suggest that the chiral transition temperature and confinement-deconfinement transition temperature coincide indicating that these two transitions can be connected [37].

J. R. Oppenheimer and G. M. Volkoff [26] in the context of star formation, followed by the investigations in other areas of physics [27, 28].

[5]Pions have specific parity, and pions with opposite parity have not been observed in low energy experiments.

Based on the concept of asymptotic freedom, J. C. Collins and M. J. Perry in 1975 [38] proposed the idea of superdense matter in the interiors of neutron star and noted that there is a qualitative difference between QCD at high temperature (and/or density) and QCD at low temperature (and/or density). In the same year, N. Cabibo and G. Parisi gave a schematic phase diagram of baryonic matter and suggested that Hagedorn temperature [39] might be the temperature of phase transition between the quark matter and hadronic matter [40]. They also noted that hadronic matter, at high temperature and/or density, should have a phase transition into a new state where quarks are deconfined. E. V. Shuryak called this new phase of deconfined matter *quark-gluon plasma* [41, 42].

The idea of investigating the characteristics of highly dense and hot matter in laboratory conditions came in 1970's [43–45] after the study of supernovae and neutron stars. This led to the idea that the collisions of heavy-ions at very high energy may be able to produce dense matter like the QGP giving birth to a new field of physics, namely relativistic heavy-ion collisions [46–55]. To mimic the conditions existing in the very early universe, the experimental study of the QGP properties was initiated using ultra-relativistic collisions of heavy-ions [14, 15, 56] in facilities like Conseil Européen pour la Recherche Nucléaire (CERN), founded in 1952, and Brookhaven National Laboratory (BNL), founded in 1947.

1.1.1 Search for QGP and its possible signatures

Significant efforts have been put forward through the years to understand the phase transition dynamics of QCD in heavy-ion collision experiments *e.g.* at CERN (SPS, LHC) and BNL (AGS, RHIC). Fixed target experiments at AGS and SPS where one collides Au + Au at up to 11 GeV per nucleon beam energy (AGS) and Pb + Pb at up to 160 AGeV (SPS) indicated the possible existence of a new form of hot and dense state of QCD matter. In these low-energy heavy-ion collision experiments the target and the projectile nuclei cannot pass through each other due to the nuclear stopping and strong QCD coupling. Such low-energy collisions provide an opportunity to systematically study the baryon-rich matter or the QGP at high baryon density which is expected to exist in the interior of neutron stars. On the other hand, with the help of the heavy-ion collision program at RHIC (BNL) with the collision energy up to $\sqrt{s_{NN}} = 200$ GeV and at LHC (CERN) with the center of mass collision energy per nucleon $\sqrt{s_{NN}} = 2.76$ TeV and higher, we can explore the QCD dynamics at temperature and baryon chemical potential relevant for understanding the QCD phase transition dynamics in the early universe.

Figure 1.1 shows the possible evolution stages of the matter created in the ultra-relativistic collisions. Contrary to a fixed target experiment, in collider experiments heavy-ion beams collide at a very high energy scale where QCD coupling is relatively small and, due to the nuclear transparency, the target and projectile nuclei almost pass through each other [58]. Therefore, in the high-energy collider experiments, the interaction region remains almost baryon free. Despite the nuclear transparency at ultra-relativistic energies, when the highly Lorentz contacted nuclei pass through each other, a large amount of energy density can be deposited in the reaction zone forming secondary partons. Due to a large number of rescatterings, these secondary partons redistribute energy among themselves to produce a (locally) thermally equilibrated plasma which is expected to be the QGP phase, which then expands due to high internal pressure. Because of the expansion, after some time, the fireball cools down and it undergoes the quark-hadron transition to form a hadronic medium at freeze-out [6]. These intermediate stages are not observed in

---

[6]Freeze-out is the stage where the interaction between particles stops and final hadrons are freely
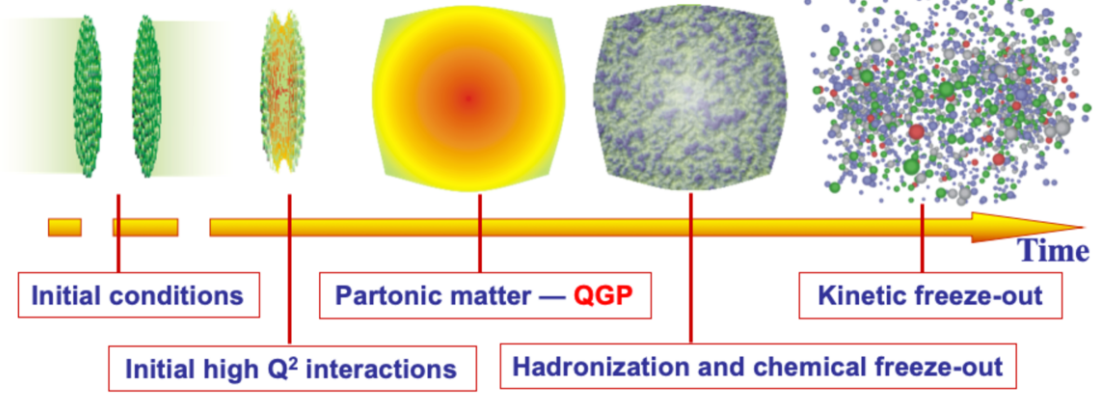
Figure 1.1: Schematic picture of the evolution stages of ultra-relativistic heavy-ion collision. Time in the horizontal axis has the unit of fm/c and Q^2 denotes four-momentum transfer squared [57].

the experiments. Moreover, in detectors, we observe quantities such as momentum spectra and multiplicities of hadrons, but not their actual positions [60–62].

Since QGP is a color-charged medium with a very short lifetime (of the order of femtometers), it can not be detected in the experiments directly. Thus, one needs to propose physical observables which can provide information about the QGP indirectly. Some signatures of the QGP formation which are commonly studied are:

- **Hard thermal dilepton and photon radiation** [63, 64] Direct photon radiation and dileptons such as e^+, e^- and μ^+, μ^- contain the thermodynamic information of the QGP fireball. Even though they are difficult to interpret, they are probably the best observables to study the relativistic collisions of heavy-ions as they penetrate the matter easily and are not affected by the process of hadronization. They are also helpful in providing the initial stage information as their momentum distributions depend on the partons temperature. Since the temperature of the QGP phase is supposed to be higher than the hadronic phase, there should be an increase in higher transverse momenta due to the momentum of direct photons.

- **Quarkonia suppression** [65–67] As heavy quarks are produced in the initial hard scattering processes, these quarks witness the entire evolution of the strongly-interacting matter produced in the heavy-ion collisions. Heavy quarks and antiquarks interact to produce bound states which are known as quarkonia, for instance, the bound states of charm and anti-charm (charmonia) and bottom and anti-bottom (bottomonia) quarks [7]. It was proposed in 1986 that suppression of J/ψ (bound state of c and $\bar{c}$) can be used as a probe for QGP. The key concept can be understood as follows: c and $\bar{c}$ are produced at a very early stage of QGP formation. The high gluon density in the deconfined matter, due to the color deconfinement, causes Debye screening of c and $\bar{c}$ effective interaction. This Debye screening can be characterized by the Debye mass or Debye screening length scale which depends on the temperature of

---

streaming to the detector. There are two types of freeze-outs: *thermal* and *chemical*. *Thermal* or *kinetic* freeze-out is the stage where final hadrons stop interacting completely, whereas, *chemical* freeze-out is the stage where there are no inelastic collisions between the particles [54]. Some experimental data can be explained with the so-called single-freeze-out model where these two types of freeze-outs coincide [59].

[7]Top quarks form bound state but they have a very short lifetime and thus decay quickly.

21

the medium. Whenever the Debye screening length becomes smaller than the radius of charmonium, the charm quarks and antiquarks cease to interact with each other giving rise to the decay and hence suppression of charmonium states. Moreover, such Debye screened c and $\bar{c}$ particles may form hadrons, like D and $\bar{D}$ mesons, with their light quark partners. Since the Debye screening length is sensitive to the temperature of the medium, different quarkonia states having different binding energies will dissociate in the medium at different temperatures. Hence, quarkonia suppression can also be considered a 'thermometer' for the QGP.

- **Strangeness enhancement** [68,69] Enhancement in the strange quark production relative to the up and down quarks in the heavy-ion collisions has been proposed in the year 1982 as a probe to study QGP properties as more pairs of $s\bar{s}$ are supposed to be produced in the QGP because of high energy density and fusion of gluons contributing almost of 80% to the production of strange quarks. Note that colliding nuclei do not contain strange quarks, therefore all strangeness must be created during the collisions. We should emphasize that the strangeness production mechanism in a hadronic medium can be significantly different from the one in the QGP. Since strangeness is conserved in QCD, strange particles and antiparticles must be produced in a pairs. Therefore, the threshold for strange hadron production in a hadronic medium is rather high compared to others, *e.g.*, the threshold energy of strangeness production in a pion nucleon scattering $\pi + N \rightarrow \Lambda + K$ is ~ 540 MeV. On the other hand, in the QGP medium, due to the chiral symmetry restoration [70], the *constituent* quark masses can be replaced by the *current* mass. Therefore, above the chiral symmetry restoration threshold, strange–anti-strange quark pair production gets reduced, enhancing the strangeness production in the deconfined partonic medium. Assuming that the produced strange particles and antiparticles take part in the hadronization, the strangeness abundance in the partonic phase should be imprinted in the relative yield of the strange and non-strange hadrons. As compared to the $e^+ - e^-$ collision or proton-proton collision, in the heavy-ion collisions strangeness enhancement has been, indeed, observed [71].

- **Jet quenching** [72,73] Jets originating from the initial hard scattering of partons can be considered as an important probe for the hot and dense QGP matter created in heavy-ion collisions. Jets are composed of highly collimated and correlated partons having large transverse momentum (p_T) (transverse to the beam direction) and are mostly produced back to back due to the conservation of energy and momentum (although three and four jet events can also take place). These high p_T particles lose their energy through collinear radiation. Jets produced at the initial stage traverse through the thermalized medium before escaping the QGP. While passing through the medium, they lose their energy much more significantly than the ones traversing hadronic matter, as jet energy loss or parton energy loss can be significantly different in the medium from energy loss in the vacuum. As a result, jets that are produced at the edge of the QGP fireball can escape easily, while jets emitted in the opposite direction traverse a longer length through the thermalized medium and undergo significant medium modification. Such phenomenon is known as 'jet quenching' in a medium. Medium effects on jets can also be quantified by the jet nuclear modification factor (jet-R_{AA}). Quantitatively, values of jet-R_{AA} less than one imply medium modification. The experimentally observed 'jet-quenching' indicates the formation of a partonic medium [74,75].

Evidences provided by CERN [76], in 2000, and by RHIC at BNL [77,78], in 2005, confirmed the production of a new state of hot and dense matter. This was possible due to both high-quality experimental data, coming from the experiments, and theoretical models, which gave a precise quantitative description. Opposite to theoretical expectations, it was shown that this new state of matter behaves as a strongly-coupled system whose evolution follows the dynamics of a perfect fluid [79, 80] [8]. This is due to the very small kinematic shear viscosity (η/s) obtained from the transverse momentum spectra of the charged particles; here η is the dynamic shear viscosity coefficient and s is the entropy density. In fact, η/s of the QGP, which, by the way, is the smallest value observed in nature, is also very close to the so-called Kovtun-Son-Starinet bound, $\eta/s = 1/(4\pi)$ [84, 85], derived using gauge-gravity correspondence [86].

1.2   Spin polarization of $\Lambda(\bar{\Lambda})$ hyperons

Recently, new directions in heavy-ion collision physics have opened up after the speculation that the non-central relativistic collisions can be the source of a large magnetic field and angular momentum. The presence of a large magnetic field (of the order of Λ_{QCD}^2) can give rise to charge-parity violating effects, *e.g.*, chiral magnetic effect [87,88], etc. which are not yet confirmed by the experiments. Moreover, non-central nuclear collisions at high energies can induce, in quark-gluon matter, a large angular momentum ($\sim 10^5\hbar$) [89] which leads to measurable spin polarization of the emitted hadrons [90].
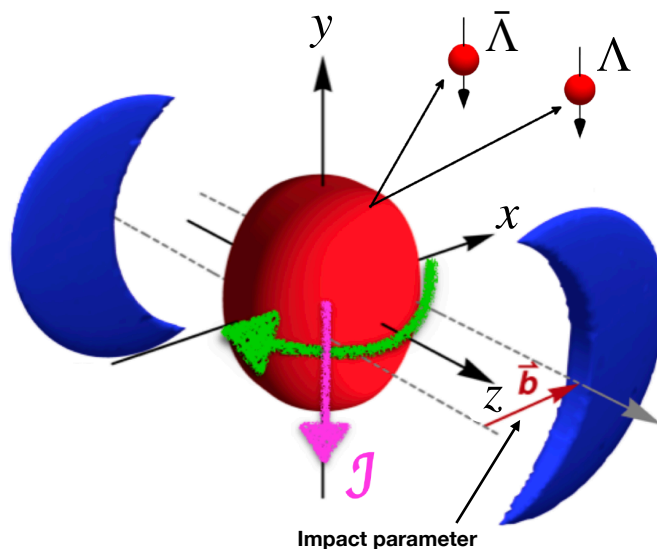
Figure 1.2: (Color online) Schematic diagram of the initial angular momentum orientation in non-central heavy-ion collision [91].

In 2005, it was proposed [92] that the spatial inhomogeneity of the colliding system in non-central heavy-ion collisions leads to the deposition of large initial orbital angular momentum in the produced matter along the direction orthogonal to the reaction plane (y-axis), whose significant fraction may be transferred in partonic collision processes to the

---

[8]See Refs. [81–83] for the studies related to the strongly-interacting systems in the area of condensed matter physics.

spin of the QGP constituents, see Fig. 1.2. As a result, due to angular momentum conservation, it may lead to polarization of quarks and antiquarks, which can be subsequently transferred to the hadrons resulting in their global spin polarization along y direction.

A macroscopic interpretation of this phenomenon was provided in 2008 using the hydrodynamic considerations [89]. According to it, the spatial inhomogeneities, arising from the initial orbital angular momentum, lead to the generation of fluid vorticity. The particles emerging from such a vortical system, through the so-called spin-vorticity coupling, should exhibit a global polarization along the same direction [9].
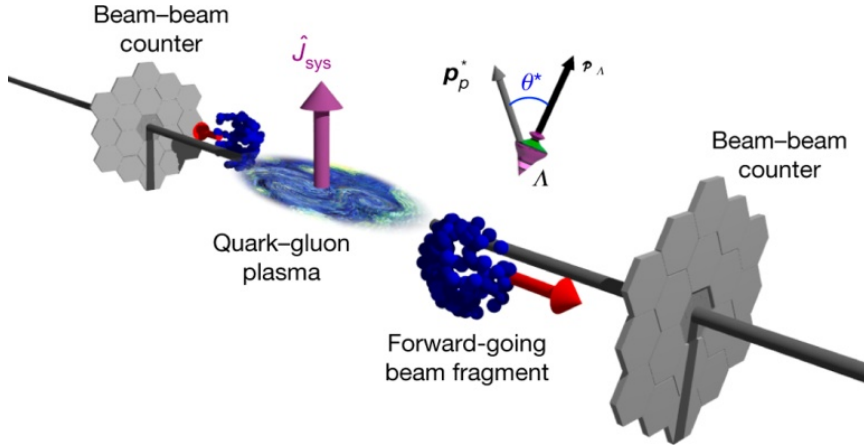
Figure 1.3: (Color online) Schematic diagram of a Au + Au collision (not to scale) where $\hat{J}_{\mathrm{sys}}$ is the direction of the angular momentum of the collision, see Ref. [90].

Among various spin-polarizable hadrons, weakly decaying $\Lambda(\bar{\Lambda})$ hyperons are of special interest for quantitative estimation of the vorticity-driven polarization. In the parity-violating decay of the Λ particle the outgoing proton is preferentially emitted along the spin direction of its parent particle, see Fig. 1.3. Hence, measuring the direction of the proton's momentum in the hyperon's rest frame can provide information about the spin polarization of the hyperon. Such 'self-analyzing' weak-decay channel of $\Lambda(\bar{\Lambda})$ hyperons makes them excellent probes for the polarization measurements.

The first positive experimental observation of *global spin polarization* [10] of $\Lambda(\bar{\Lambda})$ hyperons [11] published by STAR Collaboration [90,96] provided experimental evidence of vortical structure of the QGP. Using the spin-vorticity coupling, which holds for spin-polarized systems in thermal equilibrium [97], the experimentally observed value of polarization, see Fig. 1.4, leads to prediction of the value of vorticity of the order of 10^{21} s^{-1} which is much larger than the vorticity of any other physical system. From the Fig. 1.4 one may notice that the magnitude of the average global spin polarization of both Λ and $\bar{\Lambda}$ increases with

---

[9]Interestingly, a non-relativistic analog of such a mechanism has been observed in experiments by A. Einstein and W. de Haas [93], and S. J. Barnett [94].

[10]Here 'global' means the average polarization in the event with respect to the direction of the global orbital angular momentum of the colliding system, see Fig. 1.2.

[11]The discovery of Ξ and Ω hyperon global polarization was also reported recently [95].
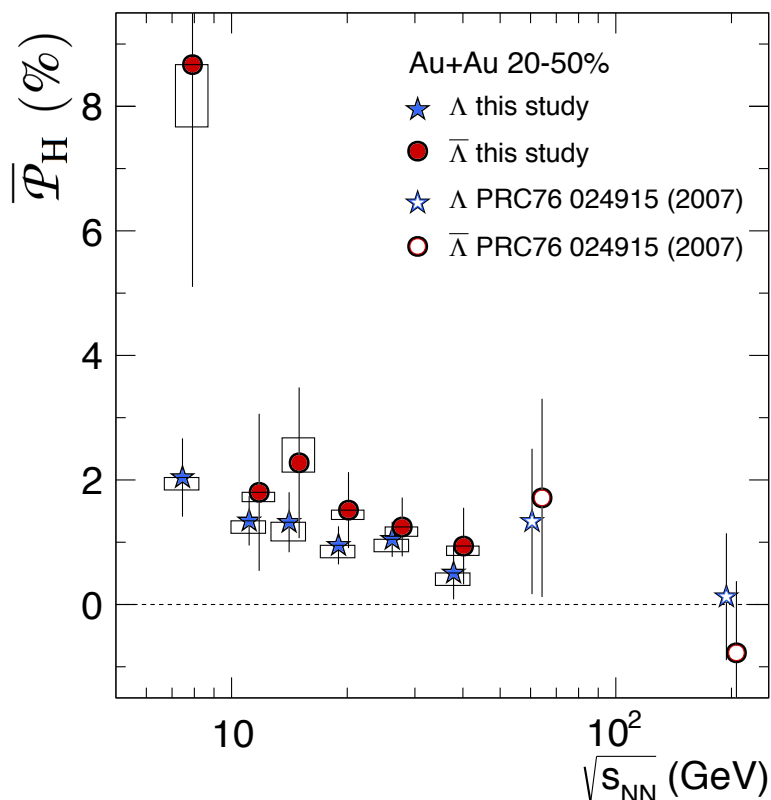
Figure 1.4: (Color online) Average global spin polarization for $\Lambda(\bar{\Lambda})$ hyperons in 20-50% centrality Au + Au collisions as a function of collision energy [90].

the decrease in the collision energy which naturally makes the low- and mid-energy reactions of special interest. The differences between particle and antiparticle polarization may be explainable by their interaction with the initial electromagnetic fields supposedly generated in early stages, however, they are not yet quantitatively described theoretically.

This measurement has opened up new directions in the studies of QGP [91, 98–105], providing opportunities to gain new physics insights such as chiral dynamics of strongly-interacting and deconfined matter [106, 107]. New phenomena such as chiral vortical effect [108–118], due to vortical structure of QGP, analogous to the chiral magnetic effect [87, 88, 119–127] generated huge interests.

Apart from global vorticity along the direction of the total angular momentum, namely the y-component, the matter produced in the heavy-ion collisions may also exhibit local vortical structures which can lead to non-vanishing values of other components of polarization. Of particular interest is the *longitudinal polarization*, meaning the component of polarization along the beam direction (z-axis), as it probes the vorticity of the velocity field generated in the transverse plane, see Fig. 1.5. Indeed, the measurements of $\Lambda(\bar{\Lambda})$ longitudinal polarization [130] confirm this reasoning. Figure 1.6 shows the cosine of the polar angle of the daughter particle in the rest frame of its parent particle that is averaged over all $\Lambda(\bar{\Lambda})$ particles. One may notice the quadrupole dependence of the longitudinal polarization which matches the one for longitudinal vorticity resulting from the elliptic
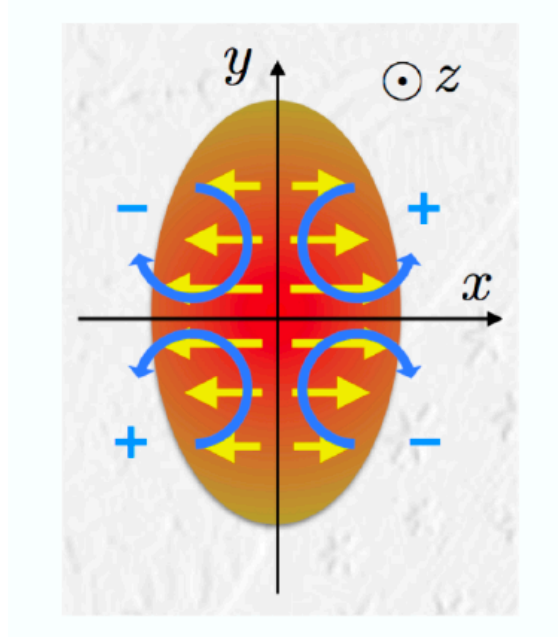
Figure 1.5: (Color online) Schematic view of the flow structure in the transverse plane which may generate longitudinal polarization [128, 129].
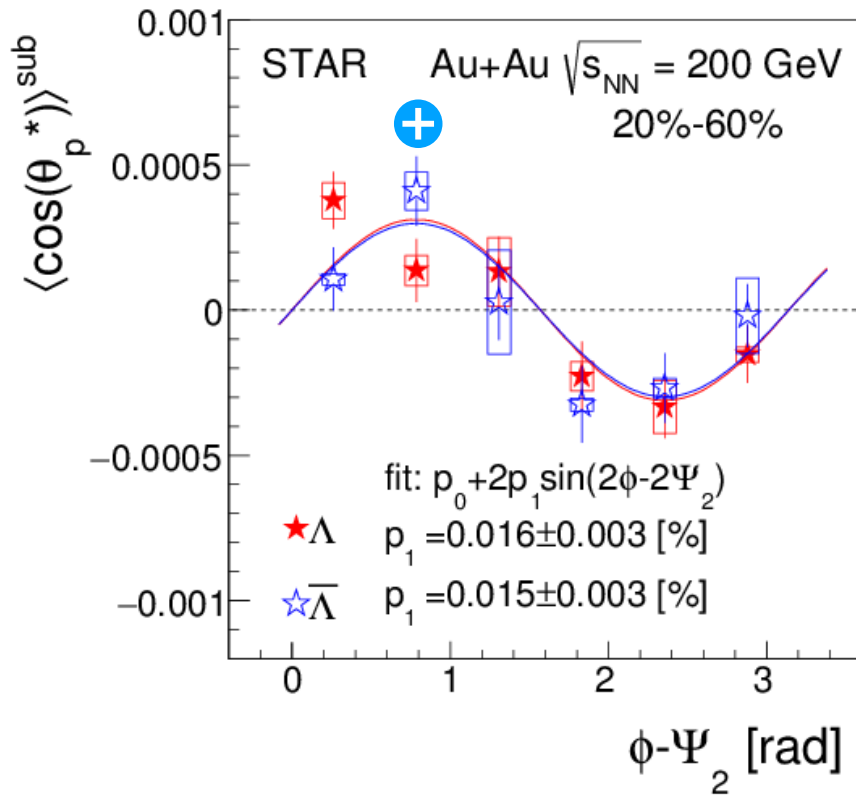
Figure 1.6: (Color online) Cosine of the polar angle of the proton in the rest frame of the parent $\Lambda(\bar{\Lambda})$ that is averaged over all $\Lambda(\bar{\Lambda})$ particles as a function of azimuthal angle (ϕ) relative to second-order event plane (ψ) [130]. Note the correlation with flow structure in Fig. 1.5 represented by "+" sign.

flow structure in Fig. 1.5. While theoretical calculations based on transport models [131] confirm observed signal, hydrodynamic models using spin-vorticity coupling did not predict it correctly [128, 132, 133]. Note that due to symmetry longitudinal component of averaged polarization is supposed to be zero.

Spin polarization [12] of the $\Lambda(\bar{\Lambda})$ hyperons has also been observed in the lowest [137] and the highest energies [138, 139] which became the subject of intense investigations [140–144].

1.3 Relativistic hydrodynamics

If due to initial multi-particle scattering, thermalization can be achieved locally in the early stages of heavy-ion collisions and the interaction among quarks and gluons is strong enough to maintain local thermodynamic equilibrium (LTE), then the space-time evolution of the strongly-interacting matter can be described by hydrodynamic principles [54, 55, 145–153].

Contrary to microscopic quantum field theory (QFT), hydrodynamics is an effective theory defined at a length scale larger than the mean free path of microscopic particles, but smaller than the system size. Such scale differences can be argued if the microscopic and the macroscopic length scales associated with the system are sufficiently separated. Generically a hydrodynamic model describes the space-time evolution of macroscopic thermodynamic variables, such as local energy density, pressure, temperature, fluid-flow velocity, etc. In fluid or hydrodynamic description the system is expected to be continuous. If we neglect any non-equilibrium effects then every fluid cell (infinitesimal volume element) is assumed to be in LTE throughout its evolution. This implies, that each fluid element must be large enough (compared to the microscopic scales) to properly define the thermodynamic variables including the notion of thermal equilibrium, and, at the same time, must be small enough to ensure the continuum limit. Although relativistic hydrodynamics is an effective approach, detailed knowledge of the microscopic dynamics enters it through the equation of state (EoS) relating pressure, energy density, and net baryon density.

Hydrodynamic models have been used to describe collective dynamics of different physical systems including cosmological and astrophysical plasma [154], the strongly-interacting plasma produced in heavy-ion collision experiments, etc. Relativistic hydrodynamics has been extensively studied to model the bulk evolution of the strongly-interacting medium produced in relativistic heavy-ion collisions and turned out to be successful in describing multiple collective phenomena. Both ideal, as well as dissipative frameworks, have been developed to explain the observed hadron spectra in experiments. Considering its successes it is fair to say that the hydrodynamic framework along with the description of the initial state and the prescription for hadronization constitutes the 'standard model' of heavy-ion collision physics.

In this Thesis, we will not discuss dissipative phenomena, explicitly, but a few comments on dissipative hydrodynamics are in order here. Although the relativistic generalization of the ideal hydrodynamic framework is rather straightforward, the generalization of dissipative non-relativistic hydrodynamics for a relativistic system is a non-trivial task and it is a timely research topic in high-energy physics. A relativistic generalization of Navier-Stokes (NS) theory was proposed by Eckart [155] and Landau [156] independently. Eckart's and Landau's theories are also known as first-order theories of dissipative hydrodynamics as the dissipative current can be expressed as a first-order gradient of the fundamental fluid vari-

---

[12]Study of spin physics and vorticity in the context of relativistic heavy-ion collisions may also help in clear understanding of spin-orbit coupling in the field of spintronics [134–136].

ables, *i.e.* temperature, chemical potential (associated with any global conserved charge), and fluid four-velocity. However, the relativistic NS frameworks as given by Eckart and Landau are plagued with acausality and instability problems [157, 158]. The reason for the acausality is that in the NS formalism, the dissipative currents are linearly proportional to gradients of temperature, chemical potential, and velocity giving rise to parabolic differential equations which do not preserve causality which, in turn, can be the source of instability. The second-order generalization of the NS framework as put forward in various studies solves the problem of acausality by introducing a 'time delay' between the gradients of the primary fluid-dynamical variables and resulting dissipative currents. In such a theory, apart from temperature, chemical potential, and fluid four-velocity one also has to consider various dissipative quantities as dynamic variables satisfying evolution equations describing their relaxation towards the NS limit. In this improved framework, the hydrodynamic equations are generically hyperbolic preserving causality. A more detailed discussion on the development of second-order dissipative hydrodynamics can be found in Refs. [150, 159, 160]

In the present work, we focus on the perfect-fluid hydrodynamic framework and its possible generalization to include the space-time evolution of spin degrees of freedom. Therefore, we first discuss briefly the salient features of standard perfect-fluid hydrodynamics without spin for completeness. The details of perfect-fluid hydrodynamics with spin will be discussed in subsequent chapters of this Thesis.

1.3.1 Kinetic-theory-wise formulation of hydrodynamics

A covariant hydrodynamic theory can be formulated using the macroscopic conservation laws. On the macroscopic level, a many-particle system can be expressed in terms of currents such as the energy-momentum tensor, number current associated with any conserved quantity, etc. Using the single-particle distribution function ($f(x,p)$) we can write the energy-momentum tensor ($T^{\mu\nu}$), and number current (N^μ) in the following manner,

$$T^{\mu\nu} = \int \mathrm{dP}\, p^\mu p^\nu\, f(x,p)\,, \tag{1.1}$$

$$N^\mu = \int \mathrm{dP}\, p^\mu\, f(x,p)\,, \tag{1.2}$$

where $\mathrm{dP} = d^3p/((2\pi)^3 E_p)$ is the momentum integration measure with $E_p = \sqrt{\boldsymbol{p}^2 + m^2}$ denoting the on-shell particle energy. It can easily be proved that the momentum integration measure dP is a Lorentz-invariant quantity and the distribution function $f(x,p)$ transforms as a Lorentz scalar. Physically, the components T^{00}, T^{0i}, T^{i0}, and T^{ij} can be interpreted as the energy density, energy flow, momentum density, and momentum flow, respectively. Similarly, N^0 is the particle number density, and N^i is the particle number current. In relativistic kinetic theory, N^μ and $T^{\mu\nu}$ can be considered as the first and the second moment in momentum space of the distribution function [161, 162]. It should be emphasized that to define the energy-momentum tensor (1.1) one implicitly assumes that the system is dilute such that the interaction energy among different particles can be neglected as compared to their kinetic energy.

Equations (1.1) and (1.2) can be generalized to a multi-component system in a straight-

forward way [161],

$$T^{\mu\nu} = \sum_{k=1}^{N} \int \frac{d^3p_k}{(2\pi)^3 p_k^0} \, p_k^\mu p_k^\nu \, f_k(x, p_k) \,, \tag{1.3}$$

$$N^\mu = \sum_{k=1}^{N} \int \frac{d^3p_k}{(2\pi)^3 p_k^0} \, p_k^\mu \, f_k(x, p_k) \,. \tag{1.4}$$

Here $k = 1, 2, \ldots, N$ denotes different particle component of the system, *e.g.*, if we consider a hadronic medium then k runs over particle species. A priori the conservation of $T^{\mu\nu}$ and N^μ is not evident from Eqs. (1.1) and (1.2). Conservation of these macroscopic currents can be obtained using the evolution equation for the distribution function within the framework of relativistic kinetic theory. Assuming only binary collisions along with the hypothesis of molecular chaos, the kinetic equations determining dynamics of distribution functions $f_k(x, p_k)$ can be expressed as,

$$p_k^\mu \partial_\mu f_k(x, p_k) = \frac{1}{2} \sum_{i,j,l=1}^{N} \int \frac{d^3p_l}{(2\pi)^3 p_l^0} \frac{d^3p_i}{(2\pi)^3 p_i^0} \frac{d^3p_j}{(2\pi)^3 p_j^0} (f_i f_j W_{ij \to kl} - f_k f_l W_{kl \to ij}) \,. \tag{1.5}$$

From the above equation, one can identify the collision term for the process $kl \to ij$,

$$\mathcal{C}_{kl} \equiv \frac{1}{2} \sum_{i,j=1}^{N} \int \frac{d^3p_l}{(2\pi)^3 p_l^0} \frac{d^3p_i}{(2\pi)^3 p_i^0} \frac{d^3p_j}{(2\pi)^3 p_j^0} (f_i f_j W_{ij \to kl} - f_k f_l W_{kl \to ij}) \,, \tag{1.6}$$

where $W_{kl \to ij}$ is the transition rate for the collision process $kl \to ij$ which includes both elastic and inelastic scattering processes. The factor of $1/2$ in the front takes into account the identical particles in the final state. By the virtue of conservation of energy and momentum in microscopic collisions, the collision term $\mathcal{C}_{kl}$ satisfies the following relations [161],

$$\sum_{k,l=1}^{N} \int \frac{d^3p_k}{(2\pi)^3 p_k^0} \, \mathcal{C}_{kl}(x, p_k) = 0 \,, \tag{1.7}$$

$$\sum_{k,l=1}^{N} \int \frac{d^3p_k}{(2\pi)^3 p_k^0} \, p_k^\mu \, \mathcal{C}_{kl}(x, p_k) = 0 \,. \tag{1.8}$$

Once we identify the properties of the collision terms, the conservation of the number current can be obtained in a straightforward way,

$$\partial_\mu N^\mu = \sum_{k=1}^{N} \int \frac{d^3p_k}{(2\pi)^3 p_k^0} p_k^\mu \partial_\mu f_k(x, p_k) = \sum_{k,l=1}^{N} \int \frac{d^3p_k}{(2\pi)^3 p_k^0} \, \mathcal{C}_{kl}(x, p_k) = 0 \,. \tag{1.9}$$

Similarly, the conservation of the energy-momentum tensor is expressed as

$$\partial_\mu T^{\mu\nu} = \sum_{k=1}^{N} \int \frac{d^3p_k}{(2\pi)^3 p_k^0} p_k^\mu p_k^\nu \partial_\mu f_k(x, p_k) = \sum_{k,l=1}^{N} \int \frac{d^3p_k}{(2\pi)^3 p_k^0} p_k^\nu \, \mathcal{C}_{kl}(x, p_k) = 0 \,.$$

In general, $T^{\mu\nu}$ and N^μ can be decomposed into ideal and dissipative parts. Since this Thesis is based particularly on the perfect-fluid hydrodynamics, we discuss the latter without

spin as a warm-up. The energy-momentum tensor and the number current for a perfect-fluid (single component) can be expressed as,

$$T_{\text{eq}}^{\mu\nu} = \int \mathrm{dP} \, p^{\mu} p^{\nu} f_{\text{eq}}(x, p) \,, \tag{1.10}$$

$$N_{\text{eq}}^{\mu} = \int \mathrm{dP} \, p^{\mu} f_{\text{eq}}(x, p) \,, \tag{1.11}$$

where $f_{\text{eq}}(x, p)$ is the distribution function in local equilibrium, hence, the suffix 'eq'. An ideal fluid is defined assuming that all fluid elements must be locally exactly in thermodynamic equilibrium. Therefore, we can define the local temperature $T(x)$, chemical potential $\mu(x)$, and fluid four-velocity $U^{\mu}(x)$ (normalized as $U^{\mu} U_{\mu} = 1$). Now our task is to write the conserved energy-momentum tensor and number current in terms of T, μ and U^{μ}. As $T_{\text{eq}}^{\mu\nu}$ is symmetric in its indices, it can be decomposed in terms of U^{μ} and $g^{\mu\nu}$ whereas N_{eq}^{μ} can be expressed only in terms of U^{μ} as [147, 163],

$$T_{\text{eq}}^{\mu\nu} = c_1 \, U^{\mu} U^{\nu} + c_2 \, g^{\mu\nu} \,, \qquad N_{\text{eq}}^{\mu} = c_3 \, U^{\mu} \,. \tag{1.12}$$

The coefficients c_1, c_2, c_3 can be uniquely determined by considering the expression of the energy-momentum tensor in the local rest frame (LRF) of the fluid element where $U^{\mu} = (1, 0, 0, 0)$. In the LRF there is no flow of energy and the momentum flux is isotropic. Moreover, in this frame, there is no particle three current. Therefore, LRF characterizes a static equilibrium. It can be easily observed that, in LRF, the energy-momentum tensor, and number four-current take the following forms [147, 163]

$$T_{\text{LRF}}^{\mu\nu} = \begin{pmatrix} \mathcal{E} & 0 & 0 & 0 \\ 0 & \mathcal{P} & 0 & 0 \\ 0 & 0 & \mathcal{P} & 0 \\ 0 & 0 & 0 & \mathcal{P} \end{pmatrix} \,, \qquad N_{\text{LRF}}^{\mu} = \begin{pmatrix} \mathcal{N} \\ 0 \\ 0 \\ 0 \end{pmatrix} \,, \tag{1.13}$$

respectively, where $\mathcal{E}$, $\mathcal{P}$, and $\mathcal{N}$ is the energy density, pressure and number density, respectively. Equations (1.12) and (1.13) allow us to identify the coefficients c_1, c_2, and c_3 as,

$$c_1 = \mathcal{E} + \mathcal{P} \,, \qquad c_2 = -\mathcal{P} \,, \qquad c_3 = \mathcal{N} \,. \tag{1.14}$$

Therefore, the conserved currents of the perfect fluid (1.12) can be written as,

$$T_{\text{eq}}^{\mu\nu} = (\mathcal{E} + \mathcal{P}) \, U^{\mu} U^{\nu} - \mathcal{P} g^{\mu\nu} \,, \qquad N_{\text{eq}}^{\mu} = \mathcal{N} U^{\mu} \,. \tag{1.15}$$

Using Eqs. (1.10), (1.11), and (1.15) one can obtain the energy density, pressure and number density in terms of the equilibrium distribution function as

$$\mathcal{E} = \int \mathrm{dP} \, (U \cdot p)^2 \, f_{\text{eq}}(x, p) \,, \tag{1.16}$$

$$\mathcal{P} = \frac{1}{3} \int \mathrm{dP} \, \left((U \cdot p)^2 - m^2 \right) \, f_{\text{eq}}(x, p) \,, \tag{1.17}$$

$$\mathcal{N} = \int \mathrm{dP} \, (U \cdot p) \, f_{\text{eq}}(x, p) \,. \tag{1.18}$$

Note that, $\mathcal{E}$, $\mathcal{P}$, and $\mathcal{N}$ are local functions of T, μ, and U^{μ}. The space-time evolution of these quantities is governed by the conservation laws

$$\partial_{\mu} T_{\text{eq}}^{\mu\nu} = 0 \,, \qquad \partial_{\mu} N_{\text{eq}}^{\mu} = 0 \,. \tag{1.19}$$

It is a common practice to split the conservation equation of the energy-momentum tensor into two parts, one along the direction of U^μ and another orthogonal to U^μ. Therefore, taking the projection of conservation law of energy-momentum tensor parallel and orthogonal to the fluid four-velocity together with the conservation of particle four-current, we find the equations of motion of the perfect-fluid hydrodynamics

$$U_\nu \partial_\mu T_{\text{eq}}^{\mu\nu} \equiv U^\mu \partial_\mu \mathcal{E} + (\mathcal{E} + \mathcal{P}) \partial_\mu U^\mu = 0, \tag{1.20}$$

$$\Delta^\alpha{}_\nu \partial_\mu T_{\text{eq}}^{\mu\nu} \equiv (\mathcal{E} + \mathcal{P}) U^\mu \partial_\mu U^\alpha - \Delta^{\alpha\beta} \partial_\beta \mathcal{P} = 0, \tag{1.21}$$

$$\partial_\mu N_{\text{eq}}^\mu \equiv U^\mu \partial_\mu \mathcal{N} + \mathcal{N} \partial_\mu U^\mu = 0, \tag{1.22}$$

where $\Delta^{\mu\nu} = g^{\mu\nu} - (U^\mu U^\nu)/U \cdot U$ is the spatial projection operator orthogonal to U. It is important to emphasize that the conservation of the energy-momentum tensor and number four-current provide five evolution equations for six unknowns $\mathcal{E}, \mathcal{P}, \mathcal{N}$, and three independent components of U^μ (note normalization constraint of U). Therefore, to close the system of equations we need an EoS relating different state variables, *i.e.* $\mathcal{P} = \mathcal{P}(\mathcal{E}, \mathcal{N})$. Once the EoS is properly defined, ideal hydrodynamic equations can be used to obtain the space-time evolution of energy density, pressure, number density, and fluid four-velocity.

1.4 Theoretical efforts to explain spin polarization

Spin polarization is one of the most interesting properties of the QGP measured recently, allowing to probe its quantum properties directly. With the arrival of spin polarization data, discussed in Sec. 1.2, it became necessary to develop theoretical models for the qualitative and quantitative interpretation of the data. This in turn gives a hope on better understanding of the vorticity as well as spin dynamics in the QGP. This thesis focuses on this particular problem.

The first formal understanding of the spin polarization phenomena came from the 'spin-thermal models'. These models assume that a large orbital angular momentum created in the non-central collisions induces vorticity in the QGP, which, if the spin is thermalized together with other degrees of freedom, gives rise to the spin polarization of the particles due to the so-called *spin-vorticity coupling*, with the vorticity quantified by the so-called *thermal vorticity*, $\varpi_{\mu\nu} = -(1/2)(\partial_\mu \beta_\nu - \partial_\nu \beta_\mu)$ [97] where $\beta_\mu = U_\mu/T$.

Based on these assumptions several hydrodynamic and transport models have been used to study the global polarization and the azimuthal angle dependence of the longitudinal spin polarization in heavy-ion collisions [97, 132, 164–176]. These models are successful in describing the center of mass-energy dependence of the global polarization measurements, see Fig. 1.4. Within a hydrodynamic framework, addressing the spin-vorticity coupling is straightforward as gradients of the flow can be obtained naturally. On the other hand, transport models which describe microscopic particle dynamics can also be used to obtain flow gradients by considering suitable coarse-graining procedures.

The 'spin-thermal' models which explain the global polarization data within the systematic uncertainty range, fail to explain the azimuthal angle dependence of longitudinal polarization shown in Fig. 1.6. In fact, theoretical model prediction is opposite (having opposite sign) to the data, see Refs. [128, 131–133, 177]. This disagreement may indicate that the assumptions of local thermodynamic equilibrium for spin degrees of freedom may not be fully satisfied under those extreme conditions or spin polarization may not be solely determined by the thermal vorticity in equilibrium. A possible explanation of this puzzle was proposed recently by including the *thermal shear* component, $\xi_{\mu\nu} = (1/2)(\partial_\mu \beta_\nu + \partial_\nu \beta_\mu)$,

along with the thermal vorticity component [178–183], however, enforcing strong assumptions such as neglecting temperature-gradients at the freeze-out which may only be true for the high-energy collisions or correcting the masses of the particles of interest.

The lack of theoretical understanding of the longitudinal spin polarization motivates us to consider new hydrodynamic and kinetic theory approaches where spin polarization is an independent dynamical variable, not necessarily respecting the spin-vorticity coupling. The development of such approaches is currently under intense investigation, see Sec. 1.6.

In this Thesis, we will discuss one such approach where the spin degrees of freedom are incorporated into standard relativistic perfect-fluid hydrodynamics treating spin as a dynamical quantity like other standard hydrodynamic variables such as temperature and baryon chemical potential and use this formalism to study various physical systems.

1.5   Pseudogauge transformation

Before diving into the details of hydrodynamics with spin, we would first like to convey that treating spin as a dynamical quantity requires extra care, meaning that, in addition to the conservation of energy-momentum tensor, we also need to include the evolution of the spin through the conservation of total angular momentum.

More specifically, from the knowledge of QFT [184, 185], it is known that, for a system with spin, total angular momentum tensor ($\hat{J}^{\lambda,\mu\nu}$) consist of both the orbital ($\hat{L}^{\lambda,\mu\nu}$) and spin ($\hat{S}^{\lambda,\mu\nu}$) contributions, namely

$$\hat{J}^{\lambda,\mu\nu} \;=\; \hat{L}^{\lambda,\mu\nu} \;+\; \hat{S}^{\lambda,\mu\nu} \;=\; x^\mu \hat{T}^{\lambda\nu} - x^\nu \hat{T}^{\lambda\mu} \;+\; \hat{S}^{\lambda,\mu\nu} \,, \tag{1.23}$$

which, with the help of total angular momentum conservation [161, 185],

$$\partial_\lambda \hat{J}^{\lambda,\mu\nu} \;=\; \partial_\lambda \hat{L}^{\lambda,\mu\nu} + \partial_\lambda \hat{S}^{\lambda,\mu\nu} \;=\; \hat{T}^{\mu\nu} - \hat{T}^{\nu\mu} + \partial_\lambda \hat{S}^{\lambda,\mu\nu} \;=\; 0 \,, \tag{1.24}$$

leads to

$$\partial_\lambda \hat{S}^{\lambda,\mu\nu} \;=\; \hat{T}^{\nu\mu} - \hat{T}^{\mu\nu} \,. \tag{1.25}$$

From the above relation, one may conclude that, although the total angular momentum is conserved, neither the spin tensor nor the orbital angular momentum tensor is separately conserved. Physically it means that orbital angular momentum can be transformed to spin angular momentum and vice versa (spin-orbit coupling). However, the forms of the energy-momentum tensor $T^{\mu\nu}$ and spin tensor $S^{\lambda\mu\nu}$ in Eq. (1.25) are not uniquely defined by Noether's theorem. One can, in principle, construct various forms of the energy-momentum tensor and the spin tensor through the so-called *pseudogauge transformation* [100, 186–188] such that the total energy, momentum, and angular momentum are preserved.

In particular, Eq (1.25) holds for the system of massive spin-1/2 fermions where we use the Dirac Lagrangian for the free fields [13]

$$\mathcal{L}_D(x) \;=\; \frac{i}{2} \, \bar{\psi}(x) \overleftrightarrow{\slashed{\partial}} \psi(x) - m \, \bar{\psi}(x) \, \psi(x) \,, \tag{1.26}$$

with ψ and $\bar{\psi} \equiv \psi^\dagger \gamma^0$ being the Dirac field operator and its adjoint, respectively, and Noether theorem to arrive at [184]

$$\partial_\mu \hat{T}^{\mu\nu}_{\mathrm{Can}} \;=\; 0 \,, \qquad \partial_\lambda \hat{J}^{\lambda,\mu\nu}_{\mathrm{Can}} \;=\; 0 \,, \tag{1.27}$$

$$\partial_\lambda \hat{S}^{\lambda,\mu\nu}_{\mathrm{Can}} \;=\; \hat{T}^{\nu\mu}_{\mathrm{Can}} - \hat{T}^{\mu\nu}_{\mathrm{Can}} \,. \tag{1.28}$$

---

[13]$\slashed{\partial}$ represents the Feynman slashed notation with $\slashed{\partial} = \gamma^\mu \partial_\mu$ and $\overleftrightarrow{\slashed{\partial}} \equiv \overrightarrow{\slashed{\partial}} - \overleftarrow{\slashed{\partial}}$.

Here, by the label 'Can' we denote canonical procedure of obtaining the currents. One can check that the resulting energy-momentum tensor

$$\hat{T}^{\mu\nu}_{\mathrm{Can}} = \frac{i}{2}\,\bar{\psi}\,\gamma^{\mu}\,\overleftrightarrow{\partial}^{\nu}\,\psi - g^{\mu\nu}\mathcal{L}_D\,, \qquad (1.29)$$

is asymmetric, whereas the spin tensor $\hat{S}^{\lambda,\mu\nu}_{\mathrm{Can}}$ is defined as [14]

$$\hat{S}^{\lambda,\mu\nu}_{\mathrm{Can}} = \frac{i}{8}\,\bar{\psi}\left\{\gamma^{\lambda},\left[\gamma^{\mu},\gamma^{\nu}\right]\right\}\psi = -\frac{1}{2}\,\epsilon^{\lambda\mu\nu\alpha}\,\bar{\psi}\,\gamma_{\alpha}\,\gamma_5\,\psi\,, \qquad (1.30)$$

where we adopt the convention $\epsilon^{0123} = 1$ and γ_5 matrix is defined in terms of the other Dirac gamma matrices, $\gamma_5 \equiv \gamma^5 = i\,\gamma^0\,\gamma^1\,\gamma^2\,\gamma^3$.

One may construct a new pair of 'improved' energy-momentum and spin tensors in such a way that the improved energy-momentum tensor is symmetric, and, as a result, the improved spin tensor is separately conserved. The new pair of tensors may be obtained from the canonical one by means of the pseudogauge transformation [91, 100, 161, 187]

$$\begin{aligned}
\hat{T}^{\mu\nu} &= \hat{T}^{\mu\nu}_{\mathrm{Can}} + \frac{1}{2}\partial_{\lambda}(\hat{\Pi}^{\lambda,\mu\nu} + \hat{\Pi}^{\nu,\mu\lambda} + \hat{\Pi}^{\mu,\nu\lambda})\,, \\
\hat{S}^{\lambda,\mu\nu} &= \hat{S}^{\lambda,\mu\nu}_{\mathrm{Can}} - \hat{\Pi}^{\lambda,\mu\nu} + \partial_{\rho}\hat{\Upsilon}^{\mu\nu,\lambda\rho}\,,
\end{aligned} \qquad (1.31)$$

where the super-potentials $\hat{\Pi}^{\lambda,\mu\nu}$ and $\hat{\Upsilon}^{\mu\nu,\lambda\rho}$ satisfy

$$\hat{\Pi}^{\lambda,\mu\nu} = -\hat{\Pi}^{\lambda,\nu\mu}\,, \qquad \hat{\Upsilon}^{\mu\nu,\lambda\rho} = -\hat{\Upsilon}^{\nu\mu,\lambda\rho} = -\hat{\Upsilon}^{\mu\nu,\rho\lambda}\,. \qquad (1.32)$$

In principle, one may have several different choices of $\hat{\Pi}$ and $\hat{\Upsilon}$, nevertheless the improved tensors do not change the total four-momentum and total angular momentum and Eqs. (1.27) are still valid with these improved tensors.

We mention some well-explored pseudogauge choices relevant for theoretical modeling of the medium produced in heavy-ion collisions:

- The first trivial choice is $\hat{\Pi}^{\lambda,\mu\nu} = \hat{\Upsilon}^{\mu\nu,\lambda\rho} = 0$. This gives back the canonical currents, Eqs. (1.29) and (1.30).

- Another choice is the well-known Belinfante–Rosenfeld (BR) pesudogauge [189–191] where $\hat{\Pi}^{\lambda,\mu\nu} = \hat{S}^{\lambda,\mu\nu}_{\mathrm{Can}}$ and $\hat{\Upsilon}^{\mu\nu,\lambda\rho} = 0$. In this case, energy-momentum tensor and spin tensor become [188]

$$\hat{T}^{\mu\nu}_{\mathrm{BR}} = \frac{i}{2}\bar{\psi}\gamma^{\mu}\overleftrightarrow{\partial}^{\nu}\psi - \frac{i}{16}\partial_{\lambda}\left(\bar{\psi}\left\{\gamma^{\lambda},\left[\gamma^{\mu},\gamma^{\nu}\right]\right\}\psi\right)\,, \qquad \hat{S}^{\lambda,\mu\nu}_{\mathrm{BR}} = 0\,, \qquad (1.33)$$

respectively. The above tensors are particularly important from the point of view of General Relativity (GR). Since in GR, the symmetric energy-momentum tensor is considered to be the source of the gravitational field, its canonical form cannot be used [187]. Symmetric energy-momentum tensor is also natural in GR as it can be obtained using the variation of the Einstein-Hilbert action with respect to the spacetime metric. However, the formalism of GR based on the Einstein-Hilbert action is not suitable to capture the spin dynamics.

---

[14]Here, $\{A, B\} = AB + BA$ and $[A, B] = AB - BA$.

- The third choice is Hilgevoord–Wouthuysen (HW) form of the pseudogauge [100, 192, 193] where $\hat{\Pi}^{\lambda,\mu\nu} = M^{[\mu\nu]\lambda} - g^{\lambda[\mu}M_\rho{}^{\nu]\rho}$ with $M^{\lambda\mu\nu} \equiv \frac{i}{4m}\bar{\psi}\sigma^{\mu\nu}\overleftrightarrow{\partial}^\lambda\psi$ and $\hat{\Upsilon}^{\mu\nu,\lambda\rho} = -\frac{1}{8m}\bar{\psi}(\sigma^{\mu\nu}\sigma^{\lambda\rho} + \sigma^{\lambda\rho}\sigma^{\mu\nu})\psi$, which yields

$$\hat{T}^{\mu\nu}_{\text{HW}} = \hat{T}^{\mu\nu}_{\text{Can}} + \frac{i}{2m}\left(\partial^\nu\bar{\psi}\sigma^{\mu\beta}\partial_\beta\psi + \partial_\alpha\bar{\psi}\sigma^{\alpha\mu}\partial^\nu\psi\right) - \frac{i}{4m}g^{\mu\nu}\partial_\lambda\left(\bar{\psi}\sigma^{\lambda\alpha}\overleftrightarrow{\partial}_\alpha\psi\right),$$

$$\hat{S}^{\lambda,\mu\nu}_{\text{HW}} = \hat{S}^{\lambda,\mu\nu}_{\text{Can}} - \frac{1}{4m}\left(\bar{\psi}\sigma^{\mu\nu}\sigma^{\lambda\rho}\partial_\rho\psi + \partial_\rho\bar{\psi}\sigma^{\lambda\rho}\sigma^{\mu\nu}\psi\right). \tag{1.34}$$

- Finally we come to de Groot–van Leeuwen–van Weert (GLW) pseudogauge [91, 161] where $\hat{\Pi}^{\lambda,\mu\nu} = \frac{i}{4m}\bar{\psi}(\sigma^{\lambda\mu}\overleftrightarrow{\partial}^\nu - \sigma^{\lambda\nu}\overleftrightarrow{\partial}^\mu)\psi$ and $\hat{\Upsilon}^{\mu\nu,\lambda\rho} = 0$, which give

$$\hat{T}^{\mu\nu}_{\text{GLW}} = -\frac{1}{4m}\bar{\psi}\overleftrightarrow{\partial}^\mu\overleftrightarrow{\partial}^\nu\psi,$$

$$\hat{S}^{\lambda,\mu\nu}_{\text{GLW}} = \bar{\psi}\left[\frac{\sigma^{\mu\nu}}{4} - \frac{1}{8m}\left(\gamma^\mu\overleftrightarrow{\partial}^\nu - \gamma^\nu\overleftrightarrow{\partial}^\mu\right)\right]\gamma^\lambda\psi + \text{h.c}, \tag{1.35}$$

where $\sigma^{\mu\nu} = (i/2)[\gamma^\mu, \gamma^\nu]$ is the Dirac spin operator. HW and GLW pseudogauges provide symmetric energy-momentum tensors, and therefore, one may obtain conserved spin tensors [15].

1.6 Objective of the Thesis

Different pseudogauge choices can give rise to different hydrodynamic frameworks for spin-polarized media. Although these frameworks can be formulated from equivalent (through pseudogauge) sets of the energy-momentum and the spin tensors, the resulting dynamical evolution of spin may not be equivalent, particularly in the local thermal equilibrium, as, in particular, densities of the hydrodynamic quantities change. This can be observed in the following manner. In the case of BR pseudogauge, the energy-momentum tensor is symmetric and there is no explicit presence of spin, hence, there is no independent evolution of the spin degree of freedom. Nevertheless, in this case, one can still completely determine the polarization as the latter is bound to the evolution of velocity gradients. This reasoning has been used in 'spin-thermal' framework of Refs. [97, 179] where spin polarization arises through spin-vorticity coupling.

On the other hand, the canonical energy-momentum tensor is asymmetric, hence the spin tensor is not separately conserved. Finally, in the case of GLW and HW, the energy-momentum tensor is symmetric by construction making the spin tensor conserved independently. These pseudogauges can be used to formulate hydrodynamics with spin. The constitutive relations and the hydrodynamic equations can be different in these frameworks, therefore, *a priori*, it is not evident whether these frameworks can be considered equivalent and well-defined as a boundary value problem, particularly as a set of partial differential equations with some initial conditions. Note that, in the context of hyperon polarization observed in the heavy-ion collision experiments, physical implications of the pseudogauge transformation of the energy-momentum tensor and the spin tensor have been extensively discussed [91, 100, 187, 194, 196, 197].

As relativistic hydrodynamics is a classical theory, the natural starting point for a proper formulation of hydrodynamics with spin is to define the energy-momentum and

---

[15] Some more forms of pseudogauge and its details can be found in Refs. [100, 187, 194, 195].

the spin currents as ensemble averages of their respective normal-ordered QFT operators, namely

$$T^{\mu\nu} \; = \; \langle : \hat{T}^{\mu\nu} : \rangle \,, \qquad S^{\lambda,\mu\nu} \; = \; \langle : \hat{S}^{\lambda,\mu\nu} : \rangle \,. \tag{1.36}$$

In the framework of hydrodynamics with spin, in addition to the conservation of energy-momentum, we also need to incorporate conservation of total angular momentum

$$\partial_\mu T^{\mu\nu} \; = \; 0 \,, \qquad \partial_\lambda S^{\lambda,\mu\nu} \; = \; T^{\nu\mu} - T^{\mu\nu} \,. \tag{1.37}$$

The evolution of the spin tensor will introduce six additional dynamical equations in addition to the standard hydrodynamic ones.

Having stated different intricacies and conceptual difficulties arising when developing hydrodynamics with spin, in the following we consider the GLW definition of the energy-momentum tensor and the spin tensor. One of the important features of this pseudogauge, as mentioned earlier, is that the spin tensor is separately conserved because the energy-momentum tensor is symmetric, see Eq. (1.37). Therefore, various components of the energy-momentum tensor and the spin tensor evolve separately, making this framework much simpler to handle mathematically as well as numerically [16].

The first proposition of *relativistic hydrodynamics with spin* as a dynamical quantity [17] was made in 2017 by W. Florkowski *et.al.* in Ref. [231] using the kinetic theory approach. This formalism [231–234] was further extended to derive the constitutive relations for the net baryon density, the energy-momentum tensor, and the spin tensor [235, 236] using the Wigner function formalism [161, 198, 237, 238] and semi-classical expansion method [239–243] based on the GLW pseudogauge. Numerical modelling of the spin polarization was then investigated in Refs. [244–248] using different hydrodynamic backgrounds. Further extensions to include dissipative effects using relaxation time approximation were performed in Refs. [249–252], for a recent review see Ref. [91]. Keeping the experimental results [90, 96] in mind, the spin polarization effects in Refs. [231, 232, 235] were considered small, leading to decoupling of background dynamics (energy, momentum and baryon number) from the spin dynamics. Moreover in this framework, the spin polarization is assumed to appear in zeroth-order in the semi-classical expansion of the Wigner function satisfying quantum kinetic equations. The crucial aspect of such a kinetic theory is the presence of a second-rank antisymmetric spin chemical potential in the equilibrium distribution function which plays a role of an extra Lagrange multiplier (more precisely six Lagrange multipliers) responsible for angular momentum conservation in the relativistic regime. This is the striking difference between this framework and the "spin-thermal models", as generically, the spin chemical potential is not necessarily related to the thermal vorticity appearing in the spin-thermal models. Recently, propagation properties of the components of spin polarization tensor have also been investigated [253] through the method of linear mode analysis [224, 254–258].

---

[16]We note that use of HW pseudogauge is also possible and it leads to equivalent hydrodynamic framework as long as we consider only local collisions between the particles. Otherwise, these two frameworks are different, see Refs. [198, 199] for the details of the framework based on HW pseudogauge considering non-local collisions.

[17]Many alternative approaches incorporating spin into hydrodynamics were also developed. They used effective theory [197, 200–203], entropy-current analysis [204–209], statistical operator method [210], non-local collisions [198, 199, 211–216], chiral kinetic theory [211, 217–220], methods of holography [197, 221–225], anomalous (with triangle anomaly) hydrodynamics [108, 226], the Lagrangian method [227, 228], and perturbative scattering techniques [229, 230].

This Thesis focuses on the developments of relativistic perfect-fluid hydrodynamics with spin based on the GLW pseudogauge and modelling of the dynamics of spin-polarized matter using this framework; for the specific list of publications on which this Thesis is based see Sec. 1.8.

1.7 Overview of the Thesis

- The quantum kinetic-theory formulation of relativistic perfect-fluid hydrodynamics with spin from the collisionless transport equation for the Wigner function for spin-half fermions using GLW pseudogauge (1.35) and assuming a small spin polarization limit was developed in Ref. [235]. As this pseudogauge makes the energy-momentum tensor symmetric, the spin tensor is conserved independently, leading to the decoupling of the orbital angular momentum from spin angular momentum.

  However, as shown in Refs. [198, 199], the non-local collisions at the microscopic scale, which were neglected in Ref. [235], may give rise to coupling between the spin and orbital parts of the total angular momentum through antisymmetric parts of the energy-momentum tensor, see Eq. (1.25). Hence, to address vorticity sourcing of polarization, it is necessary to include such collisional effects in the formalism. This extension of the framework of Ref. [235] is presented in **Chapter 2**. It provides a pedagogical introduction to the Wigner function formalism for spin-½ massive particles and the semi-classical expansion method, followed by the derivation of the Boltzmann-like spin-kinetic equations using the equations of motion for the components of the Wigner function. For this derivation, we do not assume any specific constraints on the collision terms and consider that the spin polarization effects can appear at both the zeroth ($\hbar^0$) and first ($\hbar^1$) order in $\hbar$. The physical meaning of this assumption is that the spin polarization effects can have both classical and quantum origins, respectively.

- **Chapter 3** briefly reviews the formalism of perfect-fluid relativistic hydrodynamics with spin presented in Ref. [235]. The assumption that the system is in the local equilibrium state, makes the collision terms vanish which corresponds to the zeroth-order of the semi-classical expansion. Such a system can be described by the equilibrium Wigner function, expressed in terms of the Dirac spinors. Due to the spinor representation of the Wigner function, using the Clifford algebra, the Wigner function can be decomposed into irreducible components which transform in specific ways under the Lorentz transformation. Interestingly, these irreducible components can be used to derive the relations constituting the perfect-fluid hydrodynamics with spin.

  In this chapter we explicitly calculate these components, using an ansatz for the spin-dependent phase-space distribution function, which are subsequently used to derive the conservation laws for the net baryon current, energy-momentum tensor, and spin tensor based on the GLW pseudogauge. These conservation laws are used in the following chapters to study the dynamics of spin polarization of $\Lambda(\bar{\Lambda})$ hyperons.

  An alternative approach to formulating our framework is based on the classical description of spin [91]. It is compelling to observe that the constitutive relations for the net baryon current, energy-momentum tensor, and spin tensor obtained this way in the small spin polarization limit match the relations derived using the above-mentioned Wigner function approach. The results mentioned in this chapter form the basis for the later parts of the Thesis.

- In **Chapter 3**, the spin tensor was derived, for simplicity, using classical Boltzmann statistics. However, to study the polarization of particles obeying quantum statistics, the spin tensor needs to be generalized. This is done in **Chapter 4**. Using wave propagation analysis, this extended spin tensor is used to study the behavior of the

spin polarization components after they are perturbed in the longitudinal direction and to derive the dispersion relation of spin wave velocity. Then we obtain spin wave velocity in two special cases of distribution: Maxwell-Jüttner and Fermi-Dirac. We observe that, for the Fermi-Dirac gas, the spin wave velocity is related to sound velocity in the degenerate limit.

- Using the spin hydrodynamic formalism developed in **Chapter 3**, one may determine the spacetime evolution of the thermodynamic and hydrodynamic parameters. However, these are not suitable to be compared with the experimental spin polarization measurements. To make such a comparison feasible we have to calculate the spin polarization of particles at the freeze-out surface. For this purpose, in **Chapter 5** we provide the details required to compute the momentum-dependent and momentum-averaged mean spin polarization per particle using Pauli-Lubański four-vector. These expressions are then used in **Chapter 6** to numerically model the spin polarization of $\Lambda(\bar{\Lambda})$ hyperons.

- **Chapter 6** starts with the derivation of the equations of motion for the conservation laws of net baryon current, energy-momentum tensor, and spin tensor presented in **Chapter 3** which are then used to study the spin polarization dynamics of the systems respecting certain spacetime symmetries.

  We begin our study with the Bjorken model which is commonly employed in the phenomenology of heavy-ion collisions. We determine the time evolution of temperature, baryon chemical potential, and spin components and calculate mean spin polarization at the freeze-out. In the following sections, we relax the symmetry of boost-invariance, keeping homogeneity in the transverse plane in order to capture some non-trivial dynamics of realistic systems produced in the low- and mid-energy heavy-ion collisions. Our spin polarization results for the non-boost-invariant case qualitatively agree with other model calculations and experimental data.

- As electromagnetic fields may be present in the early stages of relativistic collisions of heavy-ions, they may have some effects on the physical observables. In particular, it is suggested that the splitting of Λ and $\bar{\Lambda}$ spin polarization seen in experiments may have a source in the interaction of the produced polarized matter with electromagnetic fields. To find how these fields affect the evolution of spin polarization within our framework, we incorporate them into our formalism. **Chapter 7** studies the background and spin dynamics in the presence of an external electric field for Bjorken-expanding matter and finds that its presence may play a significant role in spin polarization evolution.

- **Chapter 8** discusses the dynamics of a longitudinally boost-invariant system with inhomogeneous expansion in the transverse direction which respects the so-called Gubser conformal symmetry, assuming that the system is cylindrically-symmetric with respect to the beam direction. Using Gubser's prescription we find transformation rules that the conservation laws, derived in **Chapter 3**, must respect to be conformally invariant. We find that, while the energy-momentum tensor and net baryon current preserve conformal symmetry, the spin tensor breaks it explicitly. However, this breaking does not spoil the conformal invariance of the background as the background and spin dynamics are decoupled due to the assumption of small spin polarization. This allows us to find approximate novel solutions for the spin.

- **Chapter 9** closes the Thesis with a brief summary.

1.8 Publications

On which this Thesis is based

e-prints

D1: Arpan Das, Wojciech Florkowski, Avdhesh Kumar, Radoslaw Ryblewski, and Rajeev Singh, *Semi-classical kinetic theory for massive spin-half fermions with leading-order spin effects*, arXiv: 2203.15562 [259].

D2: Victor E. Ambrus, Radoslaw Ryblewski, and Rajeev Singh, *Spin waves in spin hydrodynamics*, arXiv: 2202.03952. Accepted in Physical Review D. [253].

Peer-reviewed journal publications

D3: Wojciech Florkowski, Radoslaw Ryblewski, Rajeev Singh, and Gabriel Sophys, *Spin polarization dynamics in the non-boost-invariant background*, Phys.Rev.D 105 (2022) 5, 054007 [247].

D4: Rajeev Singh, Masoud Shokri, and Radoslaw Ryblewski, *Spin polarization dynamics in the Bjorken-expanding resistive MHD background*, Phys.Rev.D 103 (2021) 9, 094034 [246].

D5: Rajeev Singh, Gabriel Sophys, and Radoslaw Ryblewski, *Spin polarization dynamics in the Gubser-expanding background*, Phys.Rev.D 103 (2021) 7, 074024 [245].

D6: Wojciech Florkowski, Avdhesh Kumar, Radoslaw Ryblewski, and Rajeev Singh, *Spin polarization evolution in a boost invariant hydrodynamical background*, Phys.Rev.C 99 (2019) 4, 044910 [244].

Conference proceedings

D7: Rajeev Singh, *Conformal Transformations of Conservation Equations in Spin Hydrodynamics*, Acta Phys.Polon.B 52 (2021) 8, 1081 [260].

D8: Rajeev Singh, *Hydrodynamics formalism with Spin dynamics*, Acta Phys.Polon.Supp. 14 (2021) 461 [261].

D9: Rajeev Singh, *Formalism of hydrodynamics with spin degrees of freedom*, PoS LHCP2020 (2021) 236 [262].

D10: Radoslaw Ryblewski and Rajeev Singh, *Relativistic hydrodynamics for spin-polarized media*, Acta Phys.Polon.B 51 (2020) 1537 [263].

D11: Rajeev Singh, *Boost-invariant description of polarization within hydrodynamics with spin*, Acta Phys.Polon.Supp. 13 (2020) 931 [264].

Other publications during PhD studies

e-prints

O1: Rajeev Singh, Masoud Shokri, and S.M.A. Tabatabaee Mehr, *Relativistic magnetohydrodynamics with spin*, arXiv: 2202.11504 [248].

Peer-reviewed journal publications

O2: Arpan Das, Wojciech Florkowski, Radoslaw Ryblewski, and Rajeev Singh, *Quantum baryon number fluctuations in subsystems of a hot and dense relativistic gas of fermions*, Acta Phys.Pol.B 53, 7-A5 (2022) [265].

O3: Arpan Das, Wojciech Florkowski, Radoslaw Ryblewski, and Rajeev Singh, *Pseudo-gauge dependence of quantum fluctuations of the energy in a hot relativistic gas of fermions*, Phys.Rev.D 103 (2021) 9, L091502 [266].

O4: Arpan Das, Wojciech Florkowski, Radoslaw Ryblewski, and Rajeev Singh, *Quantum Fluctuations of Energy in Subsystems of a Hot Relativistic Gas*, Acta Phys.Polon. B 52 (2021) 12, 1395 [267].

Conference proceedings

O5: Rajeev Singh, *A compact formula for the quantum fluctuations of energy*, Rev.Mex.Fis.Suppl. 3 (2022) 3, 0308115 [268].

O6: Rajeev Singh, *Quantum fluctuations of baryon number density*, J.Phys.Conf.Ser. 2105 (2021) 15, 012006 [269].

O7: Rajeev Singh, *Mathematical expressions for quantum fluctuations of energy for different energy-momentum tensors*, PoS LHCP2021 (2021) 161 [270].

2

KINETIC THEORY FOR DIRAC FERMIONS

*"Mathematics reveals its secrets
only to those who approach it
with pure love, for its own beauty."*
– ARCHIMEDES

Hydrodynamics, being a macroscopic, long-wavelength limit of the theory describing systems near equilibrium, follows directly from the continuity equations of conserved quantities, such as energy, momentum, and charge, supplemented by the second law of thermodynamics and the equation of state. However, the spacetime evolution of the dissipative quantities rests upon the specifics of how the system approaches thermal distribution and requires a correct and explicit description of the processes within the underlying microscopic theory, such as kinetic theory [161, 271, 272].

Properties of a many-body system depend, in particular, on the details of particle interactions (collisions) and external forces (constraints). To describe the system dynamics near equilibrium, we need to express these quantities in the language of macroscopic state variables, such as temperature, charge density, and fluid velocity. Within the classical relativistic kinetic theory, this description can be formulated using the single-particle distribution function $f(x, k)$ that describes the mean number of particles with four-momentum k at space-time position x. Specific form of $f(x, k)$ follows from the kinetic (transport) equation which describes its phase-space evolution. Conserved quantities can then be evaluated through the moments of $f(x, k)$ in momentum space, see Section 1.3 for more details on the introductory level.

However, for the description of the quantum mechanical systems the classical distribution function, due to Heisenberg's uncertainty principle, is not properly defined [273]. Instead, we use the Wigner function which represents the quantum analog of the classical distribution function. Wigner function is a quasi-probability distribution function that, unlike the classical distribution function, may also give rise to negative probabilities that disappear in the classical limit. However, at the leading order of spatial gradients, the Wigner function can be related to the classical distribution [274]. Densities of macroscopic quantities can be then obtained from the Wigner function after integrating over the momentum variable k [240].

With the motivation of explaining spin polarization of $\Lambda (\bar{\Lambda})$ hyperons in mind [90, 275], the authors of Ref. [235] formulated a framework of relativistic hydrodynamics with spin using the collisionless transport equation for the Wigner function with the assumption of small spin polarization. This assumption derives its motivation from the actual magnitude

of the hyperon spin polarization observed in the experiments [90, 275]. The developed formalism is based on the specific form of the energy-momentum tensor and the spin tensor resulting from GLW pseudogauge [161], see Sec. 1.5. The spin tensor in this framework is conserved independently due to the symmetric form of the energy-momentum tensor. Thus the evolution of spin polarization is governed only by the conservation of spin tensor.

However, in general, antisymmetric parts of the energy-momentum tensor, due to non-local collisions of particles, may not vanish which allows the coupling between the spin angular momentum and orbital angular momentum (even though energy-momentum tensor and total angular momentum are conserved separately). A general framework of relativistic hydrodynamics with spin starting from the microscopic quantum kinetic theory and considering both local and non-local collisions may allow having such an interaction [198,211–214]. This spin-orbit interaction can give rise to the dissipative phenomena [1] [204] which were not taken into account in Ref. [235].

In this chapter, we study such a case by extending the analysis done in Ref. [235] to include local and non-local collisions between particles in a way proposed in Refs. [198,199]. After discussing the details on the Wigner function approach and semi-classical expansion we derive equations of motion for the components of the Wigner function. Our work generalizes the results of Refs. [198, 199] [2] and considers that spin effects may have their origin at both the classical and quantum levels (zeroth and first-order in $\hbar$). This means that both the zeroth and the first-order axial-vector components of the Wigner function, in our approach, are non-vanishing. We then derive the general form of a Boltzmann-like spin-kinetic equation that may serve as a starting point in formulating a general formalism of relativistic hydrodynamics with spin. Details of this chapter are based on the Ref. [D1].

2.1 Covariant Wigner function and its transport equation

Let us start by introducing the definition of the Wigner function [3] for spin-$^1/_2$ particles having mass m (Dirac fermions) as [4] [161, 237, 240]

$$W_{\alpha\beta}(x,k) \;=\; \int \frac{d^4y}{(2\pi\hbar)^4} \; e^{-\frac{i}{\hbar}k\cdot y} \langle : \bar{\psi}_\beta(x_+)\psi_\alpha(x_-) : \rangle. \tag{2.1}$$

Here ψ and $\bar{\psi} \equiv \psi^\dagger \gamma^0$ are the Dirac field operator and its adjoint, respectively, whereas $x_+ = x + y/2$ and $x_- = x - y/2$ denote two spacetime points with x as the center position and y as the relative position. In Eq. (2.1), $\langle : Q_W : \rangle$ means ensemble (statistical) average of the normal ordered quantity Q_W.

The Dirac equation for the system of spin-$^1/_2$ particles with interactions is defined

---

[1] In the context of non-relativistic spin hydrodynamic formalism, see Refs. [135, 276, 277].
[2] The authors of Refs. [198,199] assumed that spin effects arise at the level of $\hbar$, hence, they only consider the first-order axial-vector component non-vanishing making spin a dissipative effect.
[3] This chapter deals with the semi-classical expansion of the Wigner function that can also be interpreted as an expansion in $\hbar$. Thus we put $\hbar$ explicitly in the definition of the Wigner function. Although, in this work, we use Wigner function formalism for massive spin-$^1/_2$ particles, this method can also be used to develop respective kinetic theory for chiral fermions [111, 220, 278–281].
[4] Note that α and β in Eq. (2.1) represent the spinor indices.

as [5] [161]

$$\left(i\,\hbar\,\slashed{\partial} - m\right)\psi(x) \;=\; \hbar\,\rho(x) \;=\; -\frac{\partial \mathcal{L}_I}{\partial \bar{\psi}}\,, \tag{2.2}$$

where $\mathcal{L}_I(x)$ is the interaction Lagrangian density [6]. Using the total Lagrangian density

$$\mathcal{L}(x) = \mathcal{L}_D(x) + \mathcal{L}_I(x)$$

with

$$\mathcal{L}_D(x) \;=\; \frac{i\hbar}{2}\bar{\psi}(x)\overleftrightarrow{\slashed{\partial}}\psi(x) - m\bar{\psi}(x)\psi(x)\,, \tag{2.3}$$

being the Lagrangian density for the free field and $\overleftrightarrow{\slashed{\partial}} \equiv \overrightarrow{\slashed{\partial}} - \overleftarrow{\slashed{\partial}}$, the following transport equation can be derived [161, 237],

$$\left(i\hbar\frac{\slashed{\partial}}{2} + \slashed{k} - m\right) W(x,k) \;=\; \hbar\,\mathcal{C}\left[W(x,k)\right]\,, \tag{2.4}$$

with

$$\mathcal{C}_{\alpha\beta}\left[W(x,k)\right] \;\equiv\; \int \frac{d^4y}{(2\pi\hbar)^4} e^{-\frac{i}{\hbar}k\cdot y}\langle :\rho_\alpha(x_-)\bar{\psi}_\beta(x_+): \rangle\,, \tag{2.5}$$

being the collision kernel which vanishes in the global equilibrium [7].

As the Wigner function is a 4×4 complex matrix, it is difficult to provide some physical insights about the dynamics of the Wigner function and its components by working directly with Eq. (2.1). Instead, it is more convenient to perform the decomposition of Eq. (2.1) in terms of 16 independent generators of the Clifford algebra as follows [184] [8]

$$W(x,k) = \frac{1}{4}\left[\mathbf{1}\,F(x,k) + i\,\gamma^5\,P(x,k) + \gamma^\mu\,V_\mu(x,k) + \gamma^5\,\gamma^\mu\,A_\mu(x,k) + \Sigma^{\mu\nu}\,S_{\mu\nu}(x,k)\right], \tag{2.6}$$

where $\Sigma^{\mu\nu} \equiv (1/2)\sigma^{\mu\nu} \equiv (i/4)[\gamma^\mu,\gamma^\nu]$ is the Dirac spin operator and $F(x,k)$, $P(x,k)$, $V_\mu(x,k)$, $A_\mu(x,k)$, and $S_{\mu\nu}(x,k)$ are the 16 independent components of the Wigner function. To obtain the latter we first need to multiply the Wigner function $W(x,k)$ by the matrices: $\Gamma_X \in \{\mathbf{1}, -i\gamma_5, \gamma^\mu, \gamma^\mu\gamma_5, 2\Sigma^{\mu\nu}\}$ where $X \in \{F, P, V, A, S\}$, respectively, and then calculate its trace. Using the decomposition (2.6) along with the conjugation relation

$$W(x,k) \;=\; \gamma_0\,W(x,k)^\dagger\,\gamma_0\,, \tag{2.7}$$

(which is also followed by the Clifford algebra generators), it can be observed that the Wigner function components are real.

Under Lorentz transformations the components F, P, V_μ, A_μ, and $S_{\mu\nu}$ transform as a scalar, pseudo-scalar, vector, axial-vector, and an antisymmetric tensor, respectively [240].

---

[5]$\slashed{\partial}$ represents the Feynman slashed notation with $\slashed{\partial} = \gamma^\mu\partial_\mu$. Note that $\hbar$ is always present with the gradient, hence $\hbar$ expansion is effectively a gradient expansion.

[6]We assume that $\mathcal{L}_I(x)$ does not contain derivatives of the fields.

[7]In this thesis, the collision term describes the non-equilibrium system giving rise to the quantum corrections to the zeroth-order Wigner function. These corrections appear beyond zeroth-order in $\hbar$ ($\hbar^0$).

[8]The Clifford (geometric) algebra decomposition is a widely used expansion method, for instance, to derive the transport equations for abelian plasmas [240, 242], the quark-gluon plasma [239, 282], chiral models [243], and spin polarization [91, 198, 199, 235, 281, 283–287].

Moreover, F and P can be interpreted as the mass and pseudo-scalar condensate, respectively, whereas, fermion number current density and the polarization density can be represented by V_μ and A_μ, respectively. Finally, we can interpret the six independent components of $S_{\mu\nu}$ as electric (S_{0i}) and magnetic (S_{ij}) dipole moments.

Using Eq. (2.6) in Eq. (2.4) gives a set of coupled equations of motion for the Wigner function coefficients F, P, V^μ, A^μ, and $S^{\mu\nu}$, where the real parts of these equations are

$$k^\mu V_\mu - m\,F \;=\; \hbar\,\mathcal{D}_F\,, \tag{2.8}$$

$$-\frac{\hbar}{2}\,\partial^\mu A_\mu - m\,P \;=\; \hbar\,\mathcal{D}_P\,, \tag{2.9}$$

$$k_\mu F - \frac{\hbar}{2}\,\partial^\nu S_{\nu\mu} - m\,V_\mu \;=\; \hbar\,\mathcal{D}_{V,\mu}\,, \tag{2.10}$$

$$\frac{\hbar}{2}\,\partial_\mu P - k^\beta \overset{\star}{\tilde{S}}_{\mu\beta} - m\,A_\mu \;=\; \hbar\,\mathcal{D}_{A,\mu}\,, \tag{2.11}$$

$$\hbar\,\partial_{[\mu}V_{\nu]} - \epsilon_{\mu\nu\alpha\beta}k^\alpha A^\beta - m\,S_{\mu\nu} \;=\; \hbar\,\mathcal{D}_{S,\mu\nu}\,, \tag{2.12}$$

whereas the imaginary parts read [9]

$$\frac{\hbar}{2}\,\partial^\mu V_\mu \;=\; \hbar\,\mathcal{C}_F\,, \tag{2.13}$$

$$k^\mu A_\mu \;=\; \hbar\,\mathcal{C}_P\,, \tag{2.14}$$

$$\frac{\hbar}{2}\,\partial_\mu F + k^\nu S_{\nu\mu} \;=\; \hbar\,\mathcal{C}_{V,\mu}\,, \tag{2.15}$$

$$-k_\mu P - \frac{\hbar}{2}\,\partial^\beta \overset{\star}{\tilde{S}}_{\mu\beta} \;=\; \hbar\,\mathcal{C}_{A,\mu}\,, \tag{2.16}$$

$$-2\,k_{[\mu}V_{\nu]} - \frac{\hbar}{2}\,\epsilon_{\mu\nu\alpha\beta}\partial^\alpha A^\beta \;=\; \hbar\,\mathcal{C}_{S,\mu\nu}\,. \tag{2.17}$$

The quantities $\mathcal{D}_X$ and $\mathcal{C}_X$ denote the collision terms for the real parts and the imaginary parts of the kinetic equations, respectively, that can be evaluated using

$$\mathcal{D}_X \;=\; \Re\,\mathrm{Tr}\big[\Gamma_X \mathcal{C}[W(x,k)]\big] \quad \text{and} \quad \mathcal{C}_X \;=\; \Im\,\mathrm{Tr}\big[\Gamma_X \mathcal{C}[W(x,k)]\big]\,.$$

2.2   Semi-classical expansion

As one can observe that Eqs. (2.8)–(2.17) are coupled which makes them rather difficult to interpret physically. However, this complexity can be decreased after using the method of semi-classical expansion in $\hbar$ where the terms with zeroth power in $\hbar$ match with the classical terms and higher order terms in $\hbar$ can be interpreted as the quantum corrections [273]. In the $\hbar$ expansion method Eqs. (2.8)–(2.17) give rise to a set of coupled hierarchical equations at different orders of $\hbar$. This can be achieved by expanding components of the Wigner function and the collision terms in powers of $\hbar$ as $X = \sum_n \hbar^n X^{(n)}$, $\mathcal{C}_X = \sum_n \hbar^n \mathcal{C}_X^{(n)}$, and $\mathcal{D}_X = \sum_n \hbar^n \mathcal{D}_X^{(n)}$. In the following we expand Eqs. (2.8)–(2.17) up to second-order in $\hbar$.

---

[9]One should note here that Eq. (2.13) has $\hbar$ on both sides of the equation. Thus, one may also consider this equation at the zeroth-order by removing $\hbar$ from both sides. However, we consider it to be at the first-order keeping $\hbar$ [240].

2.2.1 Zeroth order

Below are the real parts of the equations of motion (2.8)–(2.17) in the zeroth-order in $\hbar$ [240]

$$k^\mu V_\mu^{(0)} - m F^{(0)} = 0 \,, \tag{2.18}$$

$$m P^{(0)} = 0 \,, \tag{2.19}$$

$$k_\mu F^{(0)} - m V_\mu^{(0)} = 0 \,, \tag{2.20}$$

$$k^\beta \overset{\star}{S}_{\mu\beta}^{(0)} + m A_\mu^{(0)} = 0 \,, \tag{2.21}$$

$$\epsilon_{\mu\nu\alpha\beta} k^\alpha A^{\beta(0)} + m S_{\mu\nu}^{(0)} = 0 \,. \tag{2.22}$$

Eq. (2.19) tells that zeroth-order pseudo-scalar component $P^{(0)}$ always vanishes for massive spin-half particles [235, 240, 288].

The imaginary parts in the zeroth-order of $\hbar$ are

$$k^\mu A_\mu^{(0)} = 0 \,, \tag{2.23}$$

$$k^\nu S_{\nu\mu}^{(0)} = 0 \,, \tag{2.24}$$

$$k_\mu P^{(0)} = 0 \,, \tag{2.25}$$

$$k_{[\mu} V_{\nu]}^{(0)} = 0 \,. \tag{2.26}$$

If one looks closely the Eqs. (2.18)–(2.26), it can be observed that all the Wigner function components can be written in terms of $F^{(0)}$ and $A_\mu^{(0)}$. Thus, we can safely assume these components as the basic independent ones [10] , provided the orthogonality condition (2.23) of $A_\mu^{(0)}$ is fulfilled [240].

2.2.2 First order

Reals parts of the equations (2.8)–(2.17) in the first-order in $\hbar$ are

$$k^\mu V_\mu^{(1)} - m F^{(1)} = \mathcal{D}_F^{(0)} \,, \tag{2.27}$$

$$-\frac{1}{2} \partial^\mu A_\mu^{(0)} - m P^{(1)} = \mathcal{D}_P^{(0)} \,, \tag{2.28}$$

$$k_\mu F^{(1)} - \frac{1}{2} \partial^\nu S_{\nu\mu}^{(0)} - m V_\mu^{(1)} = \mathcal{D}_{V,\mu}^{(0)} \,, \tag{2.29}$$

$$\frac{1}{2} \partial_\mu P^{(0)} - k^\beta \overset{\star}{S}_{\mu\beta}^{(1)} - m A_\mu^{(1)} = \mathcal{D}_{A,\mu}^{(0)} \,, \tag{2.30}$$

$$\partial_{[\mu} V_{\nu]}^{(0)} - \epsilon_{\mu\nu\alpha\beta} k^\alpha A^{\beta(1)} - m S_{\mu\nu}^{(1)} = \mathcal{D}_{S,\mu\nu}^{(0)} \,, \tag{2.31}$$

---

[10]This assumption is only true for the kinetic theory of massive spin-1/2 particles and is not valid for the case of massless particles [220, 281].

whereas the imaginary parts give

$$\frac{1}{2}\partial^\mu V_\mu^{(0)} = \mathcal{C}_F^{(0)}, \qquad (2.32)$$

$$k^\mu A_\mu^{(1)} = \mathcal{C}_P^{(0)}, \qquad (2.33)$$

$$\frac{1}{2}\partial_\mu F^{(0)} + k^\nu S_{\nu\mu}^{(1)} = \mathcal{C}_{V,\mu}^{(0)}, \qquad (2.34)$$

$$-k_\mu P^{(1)} - \frac{1}{2}\partial^\beta \overset{\star}{S}_{\mu\beta}^{(0)} = \mathcal{C}_{A,\mu}^{(0)}, \qquad (2.35)$$

$$-2\,k_{[\mu} V_{\nu]}^{(1)} - \frac{1}{2}\epsilon_{\mu\nu\alpha\beta}\partial^\alpha A^{\beta(0)} = \mathcal{C}_{S,\mu\nu}^{(0)}. \qquad (2.36)$$

While going from the zeroth-order to the first-order, we observe from Eq. (2.33) that the presence of collisions prevent the first-order axial-vector coefficient $A^{(1)}$ to be orthogonal to k, cf. Eq. (2.23).

2.2.3 Second order

It is necessary to go to the second-order equations of motion for the derivation of the kinetic equations for the first-order Wigner function components. In this case the real parts yield

$$k^\mu V_\mu^{(2)} - mF^{(2)} = \mathcal{D}_F^{(1)}, \qquad (2.37)$$

$$-\frac{1}{2}\partial^\mu A_\mu^{(1)} - mP^{(2)} = \mathcal{D}_P^{(1)}, \qquad (2.38)$$

$$k_\mu F^{(2)} - \frac{1}{2}\partial^\nu S_{\nu\mu}^{(1)} - mV_\mu^{(2)} = \mathcal{D}_{V,\mu}^{(1)}, \qquad (2.39)$$

$$\frac{1}{2}\partial_\mu P^{(1)} - k^\beta \overset{\star}{S}_{\mu\beta}^{(2)} - mA_\mu^{(2)} = \mathcal{D}_{A,\mu}^{(1)}, \qquad (2.40)$$

$$\partial_{[\mu} V_{\nu]}^{(1)} - \epsilon_{\mu\nu\alpha\beta}k^\alpha A^{\beta(2)} - mS_{\mu\nu}^{(2)} = \mathcal{D}_{S,\mu\nu}^{(1)}, \qquad (2.41)$$

while the imaginary parts give

$$\frac{1}{2}\partial^\mu V_\mu^{(1)} = \mathcal{C}_F^{(1)}, \qquad (2.42)$$

$$k^\mu A_\mu^{(2)} = \mathcal{C}_P^{(1)}, \qquad (2.43)$$

$$\frac{1}{2}\partial_\mu F^{(1)} + k^\nu S_{\nu\mu}^{(2)} = \mathcal{C}_{V,\mu}^{(1)}, \qquad (2.44)$$

$$-k_\mu P^{(2)} - \frac{1}{2}\partial^\beta \overset{\star}{S}_{\mu\beta}^{(1)} = \mathcal{C}_{A,\mu}^{(1)}, \qquad (2.45)$$

$$-2\,k_{[\mu} V_{\nu]}^{(2)} - \frac{1}{2}\epsilon_{\mu\nu\alpha\beta}\partial^\alpha A^{\beta(1)} = \mathcal{C}_{S,\mu\nu}^{(1)}. \qquad (2.46)$$

2.3 Mass-shell conditions

In order to describe the physical system, the components of the Wigner function must satisfy the mass-shell conditions. We shall derive below the conditions to be satisfied by the zeroth and first-order components of the Wigner function.

2.3.1 Zeroth order

Eq. (2.19), as mentioned before, depicts that the zeroth-order pseudo-scalar component always satisfies

$$P^{(0)} = 0 \,,$$

whereas Eq. (2.20) gives an important relation between the zeroth-order vector coefficient $V_\mu^{(0)}$ and the zeroth-order scalar coefficient $F^{(0)}$ [235, 240, 288]

$$V_\mu^{(0)} = \frac{k_\mu}{m} F^{(0)} \,. \tag{2.47}$$

Multiplying Eq. (2.26) with k^μ and then using Eqs. (2.18) and (2.20), we arrive at the constraint equation for the zeroth-order vector coefficient

$$k^2 V_\mu^{(0)} = m^2 V_\mu^{(0)} \,. \tag{2.48}$$

Similarly, plugging Eq. (2.47) in Eq. (2.18) we obtain constraint equation for the zeroth-order scalar coefficient [288]

$$k^2 F^{(0)} = m^2 F^{(0)} \,. \tag{2.49}$$

Within the framework of quantum kinetic theory [289], the axial-vector coefficient A^μ [198, 286] holds an important place as spin polarization effects appear through A^μ. In the current chapter, for generality, we assume that the spin polarization effects can appear at, both, the zeroth and the first-order in $\hbar$ [11]. Thus, non-zero $A_{(0)}^\mu$ implies non-vanishing zeroth-order tensor coefficient $S_{\mu\nu}^{(0)}$ through the relation [235, 240]

$$S_{\mu\nu}^{(0)} = -\frac{1}{m} \epsilon_{\mu\nu\alpha\beta} k^\alpha A_{(0)}^\beta \,, \tag{2.50}$$

(see Eq. (2.22)), whereas the dual form of $S_{\mu\nu}^{(0)}$ is

$$\overset{\star}{S}_{(0)}^{\mu\nu} = \frac{1}{m} \left(k^\mu A_{(0)}^\nu - k^\nu A_{(0)}^\mu \right) \,. \tag{2.51}$$

The above relation is crucial to obtain the constraint equation for $A_\mu^{(0)}$. We first put Eq. (2.51) in Eq. (2.21) and then employ Eq. (2.23) to get [288]

$$k^2 A_\mu^{(0)} = m^2 A_\mu^{(0)} \,. \tag{2.52}$$

In a similar way, substituting Eq. (2.50) in Eq. (2.22), and then plugging Eq. (2.24) we arrive at the constraint equation for $S_{\mu\nu}^{(0)}$

$$k^2 S_{\mu\nu}^{(0)} = m^2 S_{\mu\nu}^{(0)} \,. \tag{2.53}$$

Form the discussion above, we observe that all the zeroth-order coefficients of the Wigner function need to fulfill the on-shell condition ($k^2 = m^2$) for a non-trivial solution with k being the kinetic momentum. We find that the Eqs. (2.47), (2.50) and (2.51) not only satisfy Eqs. (2.18)–(2.26) provided Eq. (2.23) is fulfilled, but also can be expressed in terms

---

[11]Our assumption is more general in contrast to Refs. [198, 199]. Refs. [198, 199] consider that spin is a dissipative effect coming from first-order in $\hbar$, hence, they assume $A_{(0)}^\mu = 0$, whereas we consider that spin polarization can have both classical and quantum counterparts.

of independent components $F^{(0)}$ and $A_\nu^{(0)}$ [235, 240] whose on-shell conditions, (2.49) and (2.52), give rise to [288]

$$F^{(0)} \;=\; \delta(k^2 - m^2)\mathcal{F}^{(0)}, \qquad A_\mu^{(0)} \;=\; \delta(k^2 - m^2)\mathcal{A}_\mu^{(0)}. \tag{2.54}$$

$\mathcal{F}^{(0)}$ and $\mathcal{A}_\mu^{(0)}$ are scalar and axial-vector functions, respectively, which are non-singular at $k^2 = m^2$.

2.3.2 First order

The first-order forms of the pseudo-scalar, vector and tensor coefficients can be obtained from Eqs. (2.28), (2.29) and (2.31), respectively, as

$$P^{(1)} \;=\; -\frac{1}{2m}\left[\partial^\mu A_\mu^{(0)} + 2\,\mathcal{D}_P^{(0)}\right], \tag{2.55}$$

$$V_\mu^{(1)} \;=\; \frac{1}{m}\left[k_\mu F^{(1)} - \frac{1}{2}\,\partial^\nu S_{\nu\mu}^{(0)} - \mathcal{D}_{V,\mu}^{(0)}\right], \tag{2.56}$$

$$S_{\mu\nu}^{(1)} \;=\; \frac{1}{m}\left[\partial_{[\mu} V_{\nu]}^{(0)} - \epsilon_{\mu\nu\alpha\beta} k^\alpha A_{(1)}^\beta - \mathcal{D}_{S,\mu\nu}^{(0)}\right], \tag{2.57}$$

with the dual of $S_{\mu\nu}^{(1)}$ written as,

$$\overset{\star}{S}{}_{\mu\beta}^{(1)} \;=\; \frac{1}{m}\left[\frac{1}{2}\epsilon_{\mu\beta\sigma\rho}\partial^{[\sigma} V_{(0)}^{\rho]} + 2\,k_{[\mu} A_{\beta]}^{(1)} - \frac{1}{2}\epsilon_{\mu\beta\sigma\rho}\,\mathcal{D}_{S(0)}^{\sigma\rho}\right]. \tag{2.58}$$

To obtain the constraint condition for first-order axial-vector coefficient, we first put Eqs. (2.19) and (2.58) in Eq. (2.30) and then use Eqs. (2.33) and (2.47) to arrive at

$$(k^2 - m^2)A_\mu^{(1)} \;=\; k_\mu \mathcal{C}_P^{(0)} - \frac{1}{2}\epsilon_{\mu\beta\sigma\rho} k^\beta\,\mathcal{D}_{S(0)}^{\sigma\rho} + m\,\mathcal{D}_{A,\mu}^{(0)}. \tag{2.59}$$

Multiplying Eq. (2.29) with k^μ and then using Eqs. (2.27) and (2.50) gives the constraint equation of the first-order scalar coefficient

$$\left(k^2 - m^2\right) F^{(1)} \;=\; k^\mu \mathcal{D}_{V,\mu}^{(0)} + m\,\mathcal{D}_F^{(0)}. \tag{2.60}$$

Contracting Eq. (2.36) with k_μ and then using Eqs. (2.22), (2.27) and (2.29) we arrive at the constraint equation for first-order vector coefficient

$$\left(k^2 - m^2\right) V_{(1)}^\rho \;=\; m\,\mathcal{D}_{V(0)}^\rho + k^\rho\,\mathcal{D}_{F(0)} - k_\lambda\,\mathcal{C}_{S(0)}^{\lambda\rho}. \tag{2.61}$$

To obtain the constraint equation for first-order pseudo-scalar coefficient we proceed as follows: we first multiply Eq. (2.35) by k_ρ and Eq. (2.28) by m, and then subtract the resulting equations. Subsequently we use this equation in Eq. (2.21) to get

$$(k^2 - m^2)P^{(1)} \;=\; -k_\rho \mathcal{C}_{A(0)}^\rho + m\,\mathcal{D}_P^{(0)}. \tag{2.62}$$

Combining Eqs. (2.19), (2.30) and (2.31) and performing some algebraic manipulations we obtain

$$2m\,\partial^{[\rho} V_{(0)}^{\lambda]} - \epsilon^{\alpha\rho\lambda\sigma}\epsilon_{\alpha\gamma\delta\beta} k_\sigma k^\beta S_{(1)}^{\gamma\delta} + 2\epsilon^{\rho\lambda\sigma\alpha} k_\sigma \mathcal{D}_{A,\alpha}^{(0)} - 2m^2 S_{(1)}^{\rho\lambda} \;=\; 2m\mathcal{D}_{S(0)}^{\rho\lambda}. \tag{2.63}$$

Contracting the Levi-Civita tensors [12] in Eq. (2.63) and then using Eqs. (2.34) and (2.20) one obtains the constraint equation for first-order tensor coefficient $S_{(1)}^{\rho\lambda}$

$$\left(k^2 - m^2\right) S_{(1)}^{\rho\lambda} = 2\, k^{[\rho} \mathcal{C}_{V(0)}^{\lambda]} + m\, \mathcal{D}_{S(0)}^{\rho\lambda} - \epsilon^{\rho\lambda\sigma\alpha}\, k_\sigma \mathcal{D}_{A,\alpha}^{(0)}. \tag{2.64}$$

From Eqs. (2.59)–(2.62) and (2.64), one can observe that, in the absence of collisions, all the first-order coefficients remain on-shell.

2.4 General kinetic equation

In this section we will obtain the general Boltzmann-like kinetic equation which can be used for the formulation of a general spin hydrodynamic formalism. For that purpose we start with formulating the kinetic equations for the Wigner function components at the zeroth and first-order in $\hbar$.

Using Eqs. (2.32) and (2.47) the kinetic equation for the zeroth-order scalar coefficient is expressed as

$$k^\mu \partial_\mu F^{(0)} = 2\, m\, \mathcal{C}_F^{(0)}, \tag{2.65}$$

whereas combining Eqs. (2.42) and (2.56) we arrive at the kinetic equation for the first-order scalar coefficient

$$k^\mu \partial_\mu F^{(1)} = 2\, m\, \mathcal{C}_F^{(1)} + \partial^\mu \mathcal{D}_{V,\mu}^{(0)}. \tag{2.66}$$

Similarly, the kinetic equation for the zeroth-order axial-vector coefficient can be obtained by combining Eqs. (2.28), (2.35) and (2.51)

$$k^\beta \partial_\beta A_\mu^{(0)} = 2\, m\, \mathcal{C}_{A,\mu}^{(0)} - 2\, k_\mu \mathcal{D}_P^{(0)}, \tag{2.67}$$

while using Eqs. (2.38) and (2.58) in Eq. (2.45) we obtain the kinetic equation for the first-order axial-vector coefficient

$$k^\beta \partial_\beta A_\mu^{(1)} = 2\, m\, \mathcal{C}_{A,\mu}^{(1)} - 2\, k_\mu \mathcal{D}_P^{(1)} - \frac{1}{2} \epsilon_{\mu\beta\gamma\delta}\, \partial^\beta \mathcal{D}_{S(0)}^{\gamma\delta}. \tag{2.68}$$

At this point it is important to highlight again the difference of the assumptions and considerations taken in Refs. [198, 199] and this work, where we consider the most general structure of the equations without any assumptions on the collision terms:

- In this work we have assumed that both zeroth $(A_\mu^{(0)})$ and first-order $(A_\mu^{(1)})$ axial-vector components are non-zero, which means that spin polarization effects can appear at both the classical $(\hbar^0)$ and quantum level $(\hbar^1)$, which is fundamentally different from the considerations in Refs. [198, 199] where they consider that spin effects arise at order $\hbar$, thus considering only first-order axial-vector component non-vanishing.

- Moreover, Refs. [198, 199] assumed zeroth-order collision terms corresponding to pseudo-scalar, axial-vector, and tensor components vanishing, i.e., $\mathcal{C}_P^{(0)} = 0$, $\mathcal{C}_A^{\mu(0)} = 0$, $\mathcal{C}_S^{\mu\nu(0)} = 0$, $\mathcal{D}_P^{(0)} = 0$, $\mathcal{D}_A^{\mu(0)} = 0$, and $\mathcal{D}_S^{\mu\nu(0)} = 0$. These assumptions may also have some effect on the mass-shell conditions of the Wigner function components.

  However, we put no constraints on the collision terms, hence they are, in general, all non-vanishing, leading to $P^{(1)} \neq 0$, $(k^2 - m^2)A_\mu^{(1)} \neq 0$, and $k^\mu A_\mu = \mathcal{O}(\hbar)$.

---

[12] $\epsilon^{\mu\lambda\gamma\delta}\epsilon_{\nu\alpha\beta\delta} = \left[-g^\mu{}_\nu g^\lambda{}_\alpha g^\gamma{}_\beta + g^\mu{}_\nu g^\lambda{}_\beta g^\gamma{}_\alpha + g^\mu{}_\alpha g^\lambda{}_\nu g^\gamma{}_\beta - g^\mu{}_\alpha g^\lambda{}_\beta g^\gamma{}_\nu - g^\mu{}_\beta g^\lambda{}_\nu g^\gamma{}_\alpha + g^\mu{}_\beta g^\lambda{}_\alpha g^\gamma{}_\nu \right].$

We use Eqs. (2.65) and (2.66) to obtain the kinetic equation for the scalar coefficient

$$k^\mu \partial_\mu \tilde{F} \;=\; 2\,m\,\tilde{\mathcal{C}}_F \,, \tag{2.69}$$

where we introduced the following notation

$$
\begin{aligned}
\tilde{F} &= F^{(0)} + \hbar\, F^{(1)} \,, \\
\tilde{\mathcal{C}}_F &= \mathcal{C}_F^{(0)} + \hbar \left(\mathcal{C}_F^{(1)} + \frac{1}{2m} \partial^\mu \mathcal{D}_{V,\mu}^{(0)} \right) .
\end{aligned}
\tag{2.70}
$$

Using Eqs. (2.67) and (2.68), we arrive at the analogous kinetic equation for axial-vector component

$$k^\beta \partial_\beta \tilde{A}_\mu \;=\; 2\,m\,\tilde{\mathcal{C}}_{A,\mu} \,, \tag{2.71}$$

where we used

$$
\begin{aligned}
\tilde{A}_\mu &= A_\mu^{(0)} + \hbar\, A_\mu^{(1)} \,, \\
\tilde{\mathcal{C}}_{A,\mu} &= \mathcal{C}_{A,\mu}^{(0)} + \hbar\, \mathcal{C}_{A,\mu}^{(1)} - \frac{k_\mu}{m} \left(\mathcal{D}_P^{(0)} + \hbar \mathcal{D}_P^{(1)} \right) - \frac{\hbar}{4m} \epsilon_{\mu\beta\gamma\delta}\, \partial^\beta \mathcal{D}_{S(0)}^{\gamma\delta} \,.
\end{aligned}
\tag{2.72}
$$

We now define single-particle distribution function extended to spin phase-space as [91, 198, 290–292]

$$\mathfrak{f}(x,k,s) \;=\; \frac{1}{2} \left(\tilde{F}(x,k) - s \cdot \tilde{A}(x,k) \right) , \tag{2.73}$$

where s^α denotes the spin four-vector. The above relation will allow us to connect the quantum description of spin to a classical description which, then, can be used for developing hydrodynamical equations. It also incorporates the dynamics of the kinetic equations (2.69) and (2.71) into one Boltzmann-like equation, see Eq. (2.81), which may lead to a more general interpretation of the conservation laws.

Performing the proper averages in the spin space it is possible to invert Eq. (2.73) to get the scalar and axial vector components of the Wigner function. Namely, we can write

$$\tilde{F}(x,k) \;=\; \int \mathrm{dS}(k)\, \mathfrak{f}(x,k,s), \qquad \tilde{A}^\mu(x,k) \;=\; \int \mathrm{dS}(k)\, s^\mu\, \mathfrak{f}(x,k,s) \,, \tag{2.74}$$

with the covariant spin measure defined as [198, 199]

$$\int \mathrm{dS}(k) \;\equiv\; \frac{1}{\pi} \sqrt{\frac{k^2}{3}} \int d^4 s\, \delta(s \cdot s + 3)\, \delta(k \cdot s) \,. \tag{2.75}$$

Note that the spin measure is consists of two delta functions which are responsible for the normalization of s and orthogonal condition between k and s. The factor outside the integral takes care of the following normalization

$$\int \mathrm{dS}(k) \;=\; 2 \,, \tag{2.76}$$

which takes into account the spin degeneracy for the spin-1/2 particles. Using Eq. (2.76) and other identities for the spin measure [198, 199]

$$\int \mathrm{dS}(k)\, s^\mu s^\nu \;=\; -2 \left(g^{\mu\nu} - \frac{k^\mu k^\nu}{k^2} \right), \qquad \int \mathrm{dS}(k)\, s^\mu \;=\; 0 \,, \tag{2.77}$$

we can verify the relation between $\tilde{F}(x,k)$ and $\mathfrak{f}(x,k,s)$ in Eq. (2.74). To establish the relation between $\tilde{A}^\mu(x,k)$ and $\mathfrak{f}(x,k,s)$ we proceed as follows: using Eq. (2.73) in Eq. (2.74) we have

$$\int dS(k)\, s^\mu\, \mathfrak{f}(x,k,s) \;=\; \tilde{A}^\mu(x,k) - \frac{k^\mu}{k^2}\left(k\cdot\tilde{A}\right),\qquad(2.78)$$

where, using Eqs. (2.23) and (2.33), we find that $k\cdot\tilde{A} = \hbar\,\mathcal{C}_P^{(0)}$. On the other hand, using Eqs. (2.11) and (2.14) one gets

$$k^\mu\partial_\mu P \;=\; 2\,m\,\mathcal{C}_P + 2\,k^\mu\,\mathcal{D}_{A,\mu},\qquad(2.79)$$

which, in the zeroth-order, gives

$$m\,\mathcal{C}_P^{(0)} + k^\mu\mathcal{D}_{A,\mu}^{(0)} \;=\; 0.\qquad(2.80)$$

Above we have used the knowledge that $P^{(0)} = 0$. Since $\mathcal{D}_{A,\mu}^{(0)}$ is an axial-vector under the Lorentz transformation, it can be written as $\mathcal{D}_{A,\mu}^{(0)} = s_\mu\,\delta A$, with δA being a scalar function. Using the orthogonality condition $k\cdot s = 0$ and Eqs. (2.75) and (2.80), we obtain $\mathcal{C}_P^{(0)} = 0$ [13]. To summarize, Eqs. (2.74) give the correct relations [14] between the Wigner function components and the distribution function $\mathfrak{f}(x,k,s)$.

Combining Eqs. (2.69), (2.71) and (2.73) we get the general Boltzmann equation as follows

$$k^\mu\partial_\mu\mathfrak{f}(x,k,s) \;=\; m\,\mathfrak{C}(\mathfrak{f}) \;=\; m\left(\tilde{\mathcal{C}}_F - s\cdot\tilde{\mathcal{C}}_A\right),\qquad(2.81)$$

where $\mathfrak{C}(\mathfrak{f})$ is the collision term. Quasiparticle approximation allows us to write $\mathfrak{f}(x,k,s)$ as $\mathfrak{f}(x,k,s) = m\delta(k^2 - M^2)f(x,k,s)$ where $\delta(k^2 - M^2)$ represents the on-shell singularity for the quasiparticle having mass M [15] with the non-singular function $f(x,k,s)$ [161,198].

We would like to emphasize here that the Eq. (2.81) is a general kinetic equation considering spin effects both at the zeroth and first-order in $\hbar$ that may serve as a starting point in formulating a general framework for relativistic hydrodynamics with spin.

---

[13]Another possibility to obtain relation between $\tilde{A}^\mu(x,k)$ and $\mathfrak{f}(x,k,s)$ in Eq. (2.74) is to define Eq. (2.73) with only the components of $\tilde{A}^\mu$ which are orthogonal to k^μ, i.e. $(g^{\mu\nu} - k^\mu k^\nu/k^2)\tilde{A}_\nu$. This actually does not change Eq. (2.73), since s^μ is orthogonal to k^μ, so the parallel components vanish and we obtain the second relation in Eq. (2.74). (Thanks to Nora Weickgenannt for pointing this out.)

[14]These relations are important as macroscopic currents such as energy-momentum and spin tensors are expressed in terms of the Wigner function components [91, 100].

[15]M includes quantum corrections to the particle mass m, however these corrections do not contribute to the Boltzmann equation [198,199].

3

FORMULATION OF PERFECT-FLUID HYDRO-DYNAMICS WITH SPIN

"You see, one thing is,
I can live with doubt,
and uncertainty, and not knowing.
I think it's much more interesting to live,
not knowing, than to have answers which might be wrong."

– RICHARD FEYNMAN

In the previous chapter, we have derived equations of motion for the Wigner function components in the presence of collisions which, using the semi-classical expansion, led us to the general kinetic equation for the distribution function in the phase-space extended to spin. Using such a quantum kinetic theory approach one can in principle obtain a general dissipative spin hydrodynamic equations.

In this chapter, we develop perfect-fluid hydrodynamics for a spin-polarized system of Dirac fermions in equilibrium using the GLW framework and assuming that the collisional kernels are vanishing completely, which is a natural expectation for equilibrium. This can be achieved by explicitly calculating the equilibrium Wigner function [1] using an ansatz for the spin-dependent phase-space distribution functions for spin-$1/2$ particles. Various hydrodynamic currents, *e.g.* the energy-momentum tensor, net baryon current, spin-tensor, etc. can be obtained by expressing them in terms of different components of the Wigner function in the Clifford algebra basis. Conservation laws of these currents lead us to the formulation of hydrodynamic equations of interest [235].

Subsequently, we show that such spin-hydrodynamic equations can also be obtained starting from the classical transport theory in the phase-space extended to spin. In Ref. [91] such a framework has been obtained using the spin-dependent equilibrium distribution function where one inherently considers the classical description of spin. Interestingly, the constitutive relations for the net baryon current, energy-momentum tensor, and spin tensor match in these two cases [235]. The same results from the two completely independent approaches put the GLW framework on a firm mathematical footing.

---

[1]Equilibrium means the leading (or zeroth) order in $\hbar$.

3.1 Wigner function approach

In this section, employing an ansatz for a phase-space distribution function in the spin representation, we construct the equilibrium Wigner function which we subsequently use to derive the conservation laws for net baryon current, energy-momentum tensor, and spin tensor, constituting perfect-fluid hydrodynamics with spin.

3.1.1 Equilibrium Wigner function

Let us start with the transport equation for the Wigner function (2.4), and assume that the system reaches equilibrium state. In such a situation, the collision kernel on the right-hand side of Eq. (2.4) is expected to vanish, meaning that the rest energy of the particles dominates over the mean interaction energy. In this case the respective transport equation takes the form [2]

$$\left(i\hbar\frac{\slashed{\partial}}{2} + \slashed{k} - m\right) W_{\text{eq}}(x,k) = 0, \tag{3.1}$$

where we introduced the label "eq" to indicate the equilibrium form of the respective Wigner function. Moreover, in the case of global equilibrium one may expect the microscopic non-uniformities in the system to vanish, allowing the gradient term in Eq. (3.1) to be neglected. From the discussion in Section 2.2 we know that this situation corresponds to the zeroth-order of the semi-classical expansion, where the momenta of the particles satisfy the mass-shell condition.

As shown by de Groot, van Leeuwen, and van Weert (GLW) [161] the restrictions discussed above are satisfied by the Wigner function of the form

$$W_{\text{eq}}(x,k) = W_{\text{eq}}^{+}(x,k) + W_{\text{eq}}^{-}(x,k),$$

with the particle and antiparticle contributions given by,

$$W_{\text{eq}}^{+}(x,k) = \frac{1}{2}\sum_{r,s}\int \mathrm{dP}\,\delta^{(4)}(k-p)\,\mathcal{U}^{r}(p)\,\bar{\mathcal{U}}^{s}(p)\,f_{rs}^{+}(x,p), \tag{3.2}$$

$$W_{\text{eq}}^{-}(x,k) = -\frac{1}{2}\sum_{r,s}\int \mathrm{dP}\,\delta^{(4)}(k+p)\,\mathcal{V}^{s}(p)\,\bar{\mathcal{V}}^{r}(p)\,f_{rs}^{-}(x,p), \tag{3.3}$$

respectively [3] . Here, $\mathrm{dP} = d^3p/((2\pi)^3 E_p)$ is the invariant momentum integration measure with $E_p = \sqrt{\boldsymbol{p}^2 + m^2}$ denoting the on-shell particle energy, $\mathcal{U}_r(p)$ and $\mathcal{V}_r(p)$ denote the Dirac bispinors with the normalizations $\bar{\mathcal{U}}_r(p)\mathcal{U}_s(p) = 2m\,\delta_{rs}$ and $\bar{\mathcal{V}}_r(p)\mathcal{V}_s(p) = -2m\,\delta_{rs}$ while indices r and s represent the spin states.

For the equilibrium Wigner function $W_{\text{eq}}(x,k)$ to satisfy the conjugation relation (2.7), the phase-space distribution functions $f_{rs}^{\pm}(x,p)$ have to be Hermitian matrices. They can be written as [164]

$$\left[f^{+}(x,p)\right]_{rs} \equiv f_{rs}^{+}(x,p) = \frac{1}{2\,m}\,\bar{\mathcal{U}}_r(p)\,X^{+}\,\mathcal{U}_s(p),$$

$$\left[f^{-}(x,p)\right]_{rs} \equiv f_{rs}^{-}(x,p) = -\frac{1}{2\,m}\,\bar{\mathcal{V}}_s(p)\,X^{-}\,\mathcal{V}_r(p). \tag{3.4}$$

---

[2]From the transport equation for the Wigner function one may notice that the gradient expansion is effectively a $\hbar$ expansion.

[3]Note the Dirac delta functions in the equilibrium Wigner function definitions, suggesting that these definitions describe classical motion, *i.e.*, particle energy is always on the mass shell.

In Eq. (3.4), $X^{\pm}$ are 4×4 matrices defined as the products of the Maxwell-Jüttner distributions [293] [4] and matrices $M^{\pm}$ [231]

$$M^{\pm} = \exp\left[\pm\frac{1}{2}\,\omega_{\mu\nu}(x)\,\Sigma^{\mu\nu}\right], \qquad (3.5)$$

namely,

$$X^{\pm} = \exp\left[\pm\xi(x) - \beta_{\mu}(x)\,p^{\mu}\right]\,M^{\pm}. \qquad (3.6)$$

The quantity $\beta^{\mu}(x)$ is the ratio of the fluid four-velocity $U^{\mu}(x)$ [5] and the local temperature $T(x)$, $\beta^{\mu} = U^{\mu}/T$, and $\xi(x)$ is the ratio of the baryon chemical potential $\mu_B(x)$ and the temperature, $\xi = \mu_B/T$ [6]. The rank-two antisymmetric tensor $\omega^{\mu\nu}(x)$, also known as the spin polarization tensor [7], introduces into the theory, apart from the standard ones, six extra Lagrange multipliers, which, given $\omega^{\mu\nu}(x)$ being to conjugated to the Dirac spin operator $\Sigma^{\mu\nu} = (i/4)\left[\gamma^{\mu}, \gamma^{\nu}\right]$ (generators of Lorentz transformation of spinors), are responsible for angular momentum conservation in the system. One should stress here that the quantity $\omega^{\mu\nu}(x)$ in Eq. (3.5) is, assumed to be, in general, different from the thermal vorticity, $\varpi_{\mu\nu} = -(1/2)(\partial_{\mu}\beta_{\nu} - \partial_{\nu}\beta_{\mu})$ originally used in Ref. [164], allowing us to construct the closed [8] perfect-fluid hydrodynamic framework based on the conservation equations.

As shown in Ref. [231] expressions Eq. (3.5) can be put into the form

$$M^{\pm} = \frac{1}{2}\left[2\cosh(\zeta) \pm \frac{\sinh(\zeta)}{\zeta}\,\omega_{\mu\nu}\Sigma^{\mu\nu}\right], \qquad (3.7)$$

where the quantity

$$\zeta = \frac{1}{2\sqrt{2}}\sqrt{\omega_{\mu\nu}\omega^{\mu\nu}}, \qquad (3.8)$$

is assumed to be real [9].

In this Thesis, following experimental observations of small values of polarization, we consider the limit $\omega_{\mu\nu} \ll 1$ (in other words, $\zeta \to 0$), where Eq. (3.7) reduces to

$$M^{\pm} = 1 \pm \frac{1}{2}\,\omega_{\mu\nu}\,\Sigma^{\mu\nu}.$$

---

[4]Note that for simplicity, instead of Fermi-Dirac statistics used in Ref. [164], herein we consider the classical Boltzmann statistics.

[5]Due to normalization condition, $U \cdot U = 1$, the four-velocity vector has only three independent components. Hence, one may write $U^{\mu}(x) = \gamma(1, \boldsymbol{v})$ where $\boldsymbol{v}$ is the three-velocity and $\gamma = 1/\sqrt{1 - v^2}$ is the Lorentz factor.

[6]Note that for $\Lambda(\bar{\Lambda})$ hyperon, $\mu_B = 3\mu_Q$, with μ_Q being the quark chemical potential [54].

[7]Note that in literature instead of $\omega_{\mu\nu}$ one often uses the tensor $\Omega_{\mu\nu} = T\omega_{\mu\nu}$, which, by analogy to the baryon chemical potential, $\mu_B = T\xi$, is called the spin chemical potential.

[8]By closed, we have in mind that the number of conservation equations matches the number of Lagrange multipliers.

[9]In Refs. [231, 232] it was shown that the thermodynamic consistency requires the spin polarization tensor to satisfy the following constraints

$$\omega^{\mu\nu}\omega_{\mu\nu} \geq 0, \qquad \overset{\star}{\omega}{}^{\mu\nu}\omega_{\mu\nu} = 0. \qquad (3.9)$$

Violating above conditions may result in imaginary ζ which leads to the negative values of the thermodynamic quantities. However, one should notice that such constraints are not necessary in the small polarization limit $\omega_{\mu\nu} \ll 1$ in which case one can directly Taylor expand Eq. (3.5).

However, in order to keep our discussion general, in what follows, we use Eq. (3.7), considering the small polarization limit only in the final formulas.

Putting Eqs. (3.4) in Eq. (3.2) and Eq. (3.3), we find

$$
W_{\text{eq}}^{\pm}(x,k) \;=\; \frac{1}{4m} \int d\text{P}\, \delta^{(4)}(k \mp p)(\slashed{p} \pm m) X^{\pm}(\slashed{p} \pm m)\,, \tag{3.10}
$$

respectively. With the help of Eq. (3.7) we can further rewrite the above equation as

$$
\begin{aligned}
W_{\text{eq}}^{\pm}(x,k) \;=\; & \frac{1}{4m} \int d\text{P}\, e^{-\beta \cdot p \pm \xi}\, \delta^{(4)}(k \mp p) \\
& \times \left[2\,m(m \pm \slashed{p})\cosh(\zeta) \pm \frac{\sinh(\zeta)}{2\zeta}\, \omega_{\mu\nu}(\slashed{p} \pm m)\Sigma^{\mu\nu}(\slashed{p} \pm m) \right].
\end{aligned} \tag{3.11}
$$

It is instructive to decompose the Wigner function (3.11) using the Clifford algebra expansion in analogous way as in Eq. (2.6) to obtain equilibrium Wigner function components. In this case one obtains [235]

$$
F_{\text{eq}}^{\pm}(x,k) \;=\; \text{tr}\,[W_{\text{eq}}^{\pm}(x,k)] \;=\; 2\,m\cosh(\zeta) \int d\text{P}\; e^{-\beta \cdot p \pm \xi}\, \delta^{(4)}(k \mp p)\,, \tag{3.12}
$$

$$
P_{\text{eq}}^{\pm}(x,k) \;=\; -i\,\text{tr}\,[\gamma^5 W_{\text{eq}}^{\pm}(x,k)] \;=\; 0\,, \tag{3.13}
$$

$$
V_{\text{eq},\mu}^{\pm}(x,k) \;=\; \text{tr}\,[\gamma_\mu W_{\text{eq}}^{\pm}(x,k)] \;=\; \pm 2\cosh(\zeta) \int d\text{P}\, e^{-\beta \cdot p \pm \xi}\, \delta^{(4)}(k \mp p)\, p_\mu\,, \tag{3.14}
$$

$$
A_{\text{eq},\mu}^{\pm}(x,k) \;=\; \text{tr}\,[\gamma_\mu \gamma^5 W_{\text{eq}}^{\pm}(x,k)] \;=\; -\frac{\sinh(\zeta)}{\zeta} \int d\text{P}\, e^{-\beta \cdot p \pm \xi}\, \delta^{(4)}(k \mp p)\, \overset{\star}{\omega}_{\mu\nu}\, p^\nu\,, \tag{3.15}
$$

$$
\begin{aligned}
S_{\text{eq},\mu\nu}^{\pm}(x,k) \;=\; 2\,\text{tr}\,[\Sigma_{\mu\nu} W_{\text{eq}}^{\pm}(x,k)] \;=\; & \pm \frac{\sinh(\zeta)}{m\,\zeta} \int d\text{P}\, e^{-\beta \cdot p \pm \xi}\, \delta^{(4)}(k \mp p) \\
& \times \left[(p_\mu \omega_{\nu\alpha} - p_\nu \omega_{\mu\alpha})\, p^\alpha + m^2 \omega_{\mu\nu} \right].
\end{aligned} \tag{3.16}
$$

One can easily check that, for arbitrary form of the fields ξ, β, and $\omega_{\mu\nu}$, the coefficient functions defined in Eqs. (3.12)–(3.16) satisfy the following constraints

$$
k^\mu V_{\text{eq},\mu}^{\pm}(x,k) \;=\; m\,F_{\text{eq}}^{\pm}(x,k)\,, \qquad k_\mu F_{\text{eq}}^{\pm}(x,k) \;=\; m\,V_{\text{eq},\mu}^{\pm}(x,k)\,, \tag{3.17}
$$

$$
P_{\text{eq}}^{\pm}(x,k) \;=\; 0\,, \qquad k^\mu A_{\text{eq},\mu}^{\pm}(x,k) \;=\; 0\,, \qquad k^\mu S_{\text{eq},\mu\nu}^{\pm}(x,k) \;=\; 0\,, \tag{3.18}
$$

$$
k^\beta \overset{\star}{S}_{\text{eq},\mu\beta}^{\pm}(x,k) + m\,A_{\text{eq},\mu}^{\pm}(x,k) \;=\; 0\,, \qquad \epsilon_{\mu\nu\alpha\beta}\, k^\alpha A_{\text{eq}}^{\pm\,\beta}(x,k) + m\,S_{\text{eq},\mu\nu}^{\pm}(x,k) \;=\; 0. \tag{3.19}
$$

From Eqs. (3.17)–(3.19) we can notice that the equilibrium coefficient functions follow constraints of the same form as the ones satisfied by the zeroth-order components of Wigner function, c.f. Eqs. (2.18)–(2.26). It suggests that the equilibrium Wigner functions (3.11) are the good candidates for the zeroth-order Wigner function components, allowing us to write [235]

$$
\begin{aligned}
F^{(0)} \;=\; F_{\text{eq}}\,, \qquad P^{(0)} \;=\; 0\,, \qquad V_\mu^{(0)} \;=\; V_{\text{eq},\mu}\,, \\
A_\mu^{(0)} \;=\; A_{\text{eq},\mu}\,, \qquad S_{\mu\nu}^{(0)} \;=\; S_{\text{eq},\mu\nu}\,.
\end{aligned} \tag{3.20}
$$

In the following sections, these components will serve as a starting point to construct the perfect-fluid hydrodynamics with spin formalism for spin-polarized particles.

3.1.2 Conservation laws

In the absence of collisions, the zeroth-order scalar and axial-vector coefficients of the Wigner function defined by Eqs. (3.20) satisfy kinetic equations (2.65) and (2.67) found at the first-order of the semi-classical expansion [10], with the vanishing collision kernels, $\mathcal{C}_\mathcal{X} = \mathcal{D}_\mathcal{X} = 0$, supplemented with the constraint (2.23). Hence, we have

$$k^\mu \partial_\mu F_{\text{eq}}(x, k) \;=\; 0\,, \qquad k^\mu \partial_\mu A_{\text{eq}}^\nu(x, k) \;=\; 0\,, \qquad k_\nu\, A_{\text{eq}}^\nu(x, k) \;=\; 0\,, \qquad (3.21)$$

where kinetic momentum k is supposed to be on the mass shell. First-order contributions to other coefficients of Wigner function can be written as

$$
\begin{aligned}
P^{(1)} &= -\frac{1}{2m}\, \partial^\mu A_{\text{eq},\mu}\,, \\
V_\mu^{(1)} &= -\frac{1}{2m}\, \partial^\nu S_{\text{eq},\nu\mu}\,, \\
S_{\mu\nu}^{(1)} &= \frac{1}{2m}\, (\partial_\mu V_{\text{eq},\nu} - \partial_\nu V_{\text{eq},\mu})\,.
\end{aligned}
\qquad (3.22)
$$

Similarly to the treatment of spinless particles [235, 272, 294], left-hand sides of collisionless Boltzmann-like kinetic equations (3.21) are satisfied exactly in the global equilibrium. In this case, using (3.12) and (3.15), one can show that Eqs. (3.21) are satisfied if β^α is a Killing field fulfilling $\partial_\alpha \beta_\beta + \partial_\beta \beta_\alpha = 0$, and ξ and $\omega_{\alpha\beta}$ are constants. One should stress here that $\omega_{\mu\nu}$ is not necessarily equal to thermal vorticity $\varpi_{\mu\nu}$, although both are constant in the global equilibrium. The difference between $\omega_{\mu\nu}$ and $\varpi_{\mu\nu}$ in global equilibrium is understood on general grounds for conservative systems provided energy-momentum tensor is asymmetric and spin tensor does not vanish [235]. As a matter of fact, the presence of non-local collisions may make the energy-momentum tensor asymmetric giving rise to the spin-orbit coupling which in global equilibrium results in $\varpi_{\mu\nu} = \omega_{\mu\nu}$ [198, 199] [D1].

In local equilibrium, only certain moments (integrals) in momentum space of Eqs. (3.21) are satisfied. In particular, following the standard hydrodynamic treatment of relativistic rarefied spinless gases [235, 272, 294], one may show that the zeroth and first moments of the transport equations (3.21) (related to collisional invariants of baryon charge and four-momentum, respectively), lead to the net baryon current and energy-momentum tensor conservation laws. However, for spin polarized particles considered in this Thesis, the precise form of the collisional kernel is so far unknown, hence it is unclear which type of the moment one should consider to impose the angular momentum conservation in the collisions. Hence, in the following sections we will follow somewhat different methodology. We will use a so-called phenomenological approach to formulate conservation law for currents defined by the moments of the Wigner function. In particular, we will formulate the conservation equation for the spin current (the spin part of the total angular momentum rank-three tensor) which, as it was shown in Ref. [235], agrees with a certain moment of the equation for the axial coefficient of the equilibrium Wigner function.

3.1.2.1 Net baryon current

Equilibrium Wigner function, $W_{\text{eq}}(x, k)$, allows us to write the macroscopic form of net baryon current, with particle $(W_{\text{eq}}^+(x, k))$ and antiparticle $(W_{\text{eq}}^-(x, k))$ contributions, as a

---

[10] Following Eqs. (2.33), (2.66) and (2.68), we observe that the zeroth-order and first-order coefficients decouple in the absence of particle interactions, hence, in the following, we can safely assume $F^{(1)}(x, k) = A_\mu^{(1)}(x, k) = 0$.

momentum integral [161]

$$
\begin{aligned}
N^\alpha(x) &= \langle : \bar\psi \, \gamma^\alpha \, \psi : \rangle \,, \\
&= \operatorname{tr} \int d^4k \, \gamma^\alpha \, \left(W_{\mathrm{eq}}^+(x,k) - W_{\mathrm{eq}}^-(x,k) \right) \\
&= \int d^4k \, \left(V_{\mathrm{eq}}^{+,\alpha}(x,k) - V_{\mathrm{eq}}^{-,\alpha}(x,k) \right) \,,
\end{aligned}
\tag{3.23}
$$

where the right hand side of the first line depicts the ensemble (statistical) average of the, normal-ordered, microscopic net baryon current, whereas tr (trace), in the second line, provides the expectation value (in other words, statistical average) of the microscopic quantity.

Using Eq. (3.17) in Eq. (3.23) one gets

$$
N^\alpha(x) = \frac{1}{m} \int d^4k \, k^\alpha \left(F_{\mathrm{eq}}^+(x,k) - F_{\mathrm{eq}}^-(x,k) \right) .
\tag{3.24}
$$

Substituting Eq. (3.12) into Eq. (3.24) we obtain the net baryon current as [91, 231, 235]

$$
\begin{aligned}
N^\alpha(x) &= \frac{1}{m} \int d^4k \, k^\alpha \left(F_{\mathrm{eq}}^+(x,k) - F_{\mathrm{eq}}^-(x,k) \right) \\
&= 4\cosh(\zeta)\sinh(\xi) \int \mathrm{dP}\, p^\alpha \, e^{-\beta\cdot p} \\
&= \mathcal{N} \, U^\alpha \,.
\end{aligned}
\tag{3.25}
$$

The quantity $\mathcal{N}$ in the above equation represents the net baryon density written as

$$
\mathcal{N} = 4\cosh(\zeta)\sinh(\xi)\,\mathcal{N}_{(0)}(T)\,,
\tag{3.26}
$$

where $\mathcal{N}_{(0)}(T)$ is the number density of spinless and neutral classical massive particles for an ideal relativistic Boltzmann gas defined as [54, 91, 235]

$$
\mathcal{N}_{(0)}(T) = \int \mathrm{dP}\,(U \cdot p)\, e^{-\beta\cdot p} = \frac{1}{2\pi^2} T^3 z^2 K_2(z)\,.
\tag{3.27}
$$

Here, z is defined as the ratio of the particle mass m and the temperature T, $z \equiv m/T$ [11], and K_n denotes the modified Bessel function of the second kind [295]

$$
K_n(z) = \frac{z^n}{(2n+1)!!} \int_1^\infty dx \, (x^2-1)^{n-1/2} \, e^{-xz} \,.
\tag{3.28}
$$

One can observe that the factor $\sinh(\xi) = \left(e^\xi - e^{-\xi}\right)/2$ in Eq. (3.26) denotes the presence of both particles and antiparticles in the system, and the quantity $\cosh(\zeta) = \left(e^\zeta + e^{-\zeta}\right)/2$ represents the presence of both spin-up and spin-down particles.

Since the baryon current must be conserved, we write

$$
\partial_\alpha N^\alpha(x) = 0 \,.
\tag{3.29}
$$

---

[11] The variable 'z' can also be interpreted as a controlling parameter for temperature, meaning that, for the fixed mass, temperature can be varied in order to go from relativistic (high temperature) limit to non-relativistic (low temperature) limit.

3.1.2.2 Energy-momentum tensor

Similarly to the definition of the net baryon current, using Eq. (1.35), we can also define the macroscopic (non-interacting) energy-momentum tensor by taking trace of the second moment of the equilibrium Wigner function for particle and antiparticle as, see page 116 in Ref. [161]

$$
\begin{aligned}
T_{\mathrm{GLW}}^{\mu\nu}(x) &= \langle : \hat{T}_{\mathrm{GLW}}^{\mu\nu} : \rangle , \\
&= \frac{1}{m} \operatorname{tr} \int d^4 k \, k^\mu k^\nu \left(W_{\mathrm{eq}}^+(x,k) + W_{\mathrm{eq}}^-(x,k) \right) , \\
&= \frac{1}{m} \int d^4 k \, k^\mu k^\nu \left(F_{\mathrm{eq}}^+(x,k) + F_{\mathrm{eq}}^-(x,k) \right) .
\end{aligned}
\tag{3.30}
$$

where we use the assumption that $F^{(1)}(x,k) = 0$. Using Eq. (3.12) in Eq. (3.30) we obtain the perfect-fluid form of the energy-momentum tensor as [91, 231, 235]

$$
\begin{aligned}
T_{\mathrm{GLW}}^{\mu\nu}(x) &= \frac{1}{m} \int d^4 k \, k^\mu k^\nu \left(F_{\mathrm{eq}}^+(x,k) + F_{\mathrm{eq}}^-(x,k) \right) , \tag{3.31} \\
&= 4 \cosh(\zeta) \cosh(\xi) \int \mathrm{dP} \, p^\mu p^\nu e^{-\beta \cdot p} , \\
&= (\mathcal{E} + \mathcal{P}) \, U^\mu U^\nu - \mathcal{P} \, g^{\mu\nu} , \tag{3.32}
\end{aligned}
$$

where the energy density ($\mathcal{E}$) and pressure ($\mathcal{P}$) are, respectively, given as

$$
\mathcal{E} = 4 \cosh(\zeta) \cosh(\xi) \, \mathcal{E}_{(0)}(T) , \qquad \mathcal{P} = 4 \cosh(\zeta) \cosh(\xi) \, \mathcal{P}_{(0)}(T) . \tag{3.33}
$$

Similarly to the number density, we define the energy density ($\mathcal{E}_{(0)}(T)$) and pressure ($\mathcal{P}_{(0)}(T)$) for Boltzmann gas as [54, 91, 235]

$$
\mathcal{E}_{(0)}(T) = \int \mathrm{dP} \, (U \cdot p)^2 e^{-\beta \cdot p} = \frac{1}{2\pi^2} T^4 \, z^2 \left[z K_1(z) + 3 K_2(z) \right] , \tag{3.34}
$$

$$
\mathcal{P}_{(0)}(T) = -\frac{1}{3} \int \mathrm{dP} \left[p \cdot p - (U \cdot p)^2 \right] e^{-\beta \cdot p} = \frac{1}{2\pi^2} T^4 \, z^2 \, K_2(z) , \tag{3.35}
$$

respectively. From Eq. (3.35) and Eq. (3.27), we notice that,

$$
\mathcal{P}_{(0)}(T) = T \mathcal{N}_{(0)}(T) , \tag{3.36}
$$

which is the equation of state (EoS) for the ideal relativistic Boltzmann statistics. Again, since we assume the energy-momentum tensor to be conserved, we write

$$
\partial_\alpha T_{\mathrm{GLW}}^{\alpha\beta}(x) = 0 . \tag{3.37}
$$

3.1.2.3 Spin tensor

The GLW form of the spin tensor is defined as the momentum average of the microscopic spin density (1.35) [161] [12]

$$
\begin{aligned}
S_{\mathrm{GLW}}^{\alpha,\beta\gamma} &= \langle : \hat{S}_{\mathrm{GLW}}^{\alpha,\beta\gamma} : \rangle , \\
&= \frac{\hbar}{4} \int d^4 k \, \operatorname{tr}\left[\left(\{ \sigma^{\beta\gamma}, \gamma^\alpha \} + \frac{2i}{m} \left(\gamma^{[\beta} k^{\gamma]} \gamma^\alpha - \gamma^\alpha \gamma^{[\beta} k^{\gamma]} \right) \right) \right. \\
&\quad \times \left. \left(W_{\mathrm{eq}}^+(x,k) + W_{\mathrm{eq}}^-(x,k) \right) \right] .
\end{aligned}
\tag{3.38}
$$

---

[12]Note that we explicitly placed the Planck constant $\hbar$ in Eq. (3.38) due to dimensional reason. Here $\{A, B\} = AB + BA$ and $A^{[\mu} B^{\nu]} = \frac{1}{2}[A^\mu B^\nu - A^\nu B^\mu]$.

Putting particle and antiparticle contributions from Eq. (3.11) in Eq. (3.38), performing the trace and carrying out the momentum integration we get

$$S_{\text{GLW}}^{\alpha,\beta\gamma} = \frac{\mathcal{C}}{m^2} \int \mathrm{dP}\, e^{-\beta \cdot p} p^\alpha \left(m^2 \omega^{\beta\gamma} + 2\, p^\mu p^{[\beta} \omega^{\gamma]}{}_\mu \right) = S_{\text{PH}}^{\alpha,\beta\gamma} + S_\Delta^{\alpha,\beta\gamma}, \qquad (3.39)$$

where we identify [231, 235]

$$S_{\text{PH}}^{\alpha,\beta\gamma} = \mathcal{C}\,\mathcal{N}_{(0)} U^\alpha \omega^{\beta\gamma}, \qquad (3.40)$$

$$S_\Delta^{\alpha,\beta\gamma} = \mathcal{C}\left[\mathcal{A}_{(0)}\, U^\alpha U^\delta U^{[\beta} \omega^{\gamma]}{}_\delta + \mathcal{B}_{(0)} \left(U^{[\beta} \Delta^{\alpha\delta} \omega^{\gamma]}{}_\delta + U^\alpha \Delta^{\delta[\beta} \omega^{\gamma]}{}_\delta + U^\delta \Delta^{\alpha[\beta} \omega^{\gamma]}{}_\delta \right) \right], (3.41)$$

with the thermodynamic coefficients expressed as

$$\mathcal{B}_{(0)} = -\frac{2}{z^2} \frac{\mathcal{E}_{(0)} + \mathcal{P}_{(0)}}{T}, \qquad \mathcal{A}_{(0)} = 2\mathcal{N}_{(0)} - 3\mathcal{B}_{(0)}. \qquad (3.42)$$

Here, we introduce $\mathcal{C} \equiv \hbar \cosh(\xi) \sinh(\zeta)/\zeta$ [13] and $\Delta^{\mu\nu} = g^{\mu\nu} - (U^\mu U^\nu)/(U \cdot U)$ which is the operator projecting onto the plane orthogonal to U^μ. One may interpret $S_\Delta^{\alpha,\beta\gamma}$ as the correction to the phenomenological part ($S_{\text{PH}}^{\alpha,\beta\gamma}$).

We can write the spin tensor (3.39) in a more compact way as [D3, D6]

$$S_{\text{GLW}}^{\alpha,\beta\gamma} = U^\alpha \left(\mathcal{A}_1 \omega^{\beta\gamma} + \mathcal{A}_2 U^{[\beta} \omega^{\gamma]}{}_\delta U^\delta \right) + \mathcal{A}_3 \left(U^{[\beta} \omega^{\gamma]\alpha} + g^{\alpha[\beta} \omega^{\gamma]}{}_\delta U^\delta \right), \qquad (3.43)$$

with the thermodynamic coefficients having the forms

$$\mathcal{A}_1 = \mathcal{C} \left(\mathcal{N}_{(0)} - \mathcal{B}_{(0)} \right), \qquad \mathcal{A}_2 = \mathcal{C} \left(\mathcal{A}_{(0)} - 3\mathcal{B}_{(0)} \right), \qquad \mathcal{A}_3 = \mathcal{C}\,\mathcal{B}_{(0)}. \qquad (3.44)$$

Since the energy-momentum tensor (3.32) is completely symmetric, the conservation of total angular momentum [161, 185],

$$\partial_\alpha J^{\alpha,\beta\gamma} = T_{\text{GLW}}^{\beta\gamma} - T_{\text{GLW}}^{\gamma\beta} + \partial_\alpha S_{\text{GLW}}^{\alpha,\beta\gamma} = 0, \qquad (3.45)$$

implies that the spin tensor is independently conserved [235],

$$\partial_\alpha S_{\text{GLW}}^{\alpha,\beta\gamma}(x) = T_{\text{GLW}}^{\gamma\beta} - T_{\text{GLW}}^{\beta\gamma} = 0. \qquad (3.46)$$

Equations (3.29), (3.37), and (3.46), represent closed set of evolution equations constituting the formulation of perfect-fluid hydrodynamics with spin. Note that in all above conservation laws, the small polarization limit ($\omega_{\alpha\beta} \ll 1$), which we consider throughout the remaining parts of the thesis, is implemented by $\zeta \to 0$. Taking this limit prevents the coupling between the dynamics of perfect-fluid background, represented through the energy-momentum and baryon number conservation laws, and spin. Thus, the evolution of spin polarization is determined solely through the conservation of total angular momentum (in practice, conservation of spin tensor) [14].

---

[13]Note that $\mathcal{C}$ is not related to the collisional kernels discussed in the previous chapter.

[14]Note that the spin tensor (3.39) diverges in the $m \to 0$ limit, breaking conformal symmetry explicitly, however, one may obtain approximate solutions for spin treating mass as a very small parameter. See Chapter 8 for extensive discussions on this matter.

3.2 Classical approach

In this section we present a complementary method to derive the constitutive relations for the net baryon current (3.25), energy-momentum tensor (3.32), and spin tensor (3.39) using an approach based on the classical single-particle distribution function in a phase space extended to spin. Such a distribution function may arise from the quantum kinetic considerations as discussed in Section 2.4.

3.2.1 Spin-dependent distribution function in equilibrium

We consider classical single-particle distribution function for particles and antiparticles in a phase space consisting of space-time position (x^μ), four-momentum (p^μ), and spin (s^μ). Identifying the collisional invariants of the local Boltzmann equation one finds [91],

$$f_{\text{eq}}^{\pm}(x,p,s) \;=\; \exp\left(-\beta(x)\cdot p \pm \xi(x)\right) \exp\left\{ \frac{1}{2}\omega_{\mu\nu}(x)s^{\mu\nu} \right\}, \tag{3.47}$$

where $s^{\mu\nu} = (1/m)\epsilon^{\mu\nu\alpha\beta}p_\alpha s_\beta$ is the internal angular momentum tensor [184, 296]. In Eq. (3.47) the tensor $\omega_{\mu\nu}$ plays the role of the spin polarization tensor, encountered in the quantum statistical approach (3.5), and arises due to the spin angular momentum conservation considered herein.

   Equation (3.47) gives the distribution function in terms of position x and momentum p coordinates only, once averaged over spin,

$$\int \mathrm{dS}\, f_{\text{eq}}^{\pm}(x,p,s) \;=\; f_{\text{eq}}^{\pm}(x,p), \tag{3.48}$$

where the spin integration measure dS is defined as follows [15] [91].

$$\mathrm{dS} \;=\; \frac{m}{\pi\mathfrak{s}}\,\mathrm{d}^4 s\,\delta(s\cdot s + \mathfrak{s}^2)\,\delta(p\cdot s). \tag{3.49}$$

Here, unlike in Eq. (2.75), p is the on-shell kinetic four-momentum of the particle. For spin-half particles the length of the spin vector is given by $\mathfrak{s}^2 = \frac{1}{2}\left(1+\frac{1}{2}\right) = \frac{3}{4}$, which can also be related to the respective value of the Casimir operator.

   In the remaining part of this section we provide definitions of the conserved currents in terms of the moments of the distribution function (3.47), which ought to satisfy macroscopic balance equations describing conservation laws.

3.2.2 Net baryon current

The net baryon current in equilibrium can be obtained using the formula [91]

$$N^\mu(x) \;=\; \int \mathrm{dP}\,\mathrm{dS}\, p^\mu \left[f_{\text{eq}}^{+}(x,p,s) - f_{\text{eq}}^{-}(x,p,s) \right]. \tag{3.50}$$

Putting the equilibrium function (3.47) in Eq. (3.50) leads to

$$N^\mu(x) \;=\; 2\sinh(\xi) \int \mathrm{dP}\, p^\mu e^{-p\cdot\beta} \int \mathrm{dS}\, \exp\left(\frac{1}{2}\omega_{\alpha\beta}\, s^{\alpha\beta} \right). \tag{3.51}$$

---

[15]Note that in the spin measure (3.49) we choose a different normalization of the spin four-vector as compared to (2.75) defined in Chapter 2. We note that the choice of the normalization convention in the spin measure definition does not affect our results, up to an overall constant factor.

In our approach we consider the case of small values of the spin polarization tensor $\omega_{\mu\nu}$, which allows us to expand the last exponential term up to the first-order in ω. Proceeding this way we get

$$N^\mu \;=\; 2\sinh(\xi)\int dP\, p^\mu\, e^{-p\cdot\beta}\int dS\left(1+\frac{1}{2}\omega_{\alpha\beta}s^{\alpha\beta}\right), \tag{3.52}$$

which, after performing the spin and momentum integration, yields [91]

$$N^\mu \;=\; \mathcal{N}\, U^\mu. \tag{3.53}$$

The resulting net baryon current matches exactly the one derived using the Wigner function approach, in the small polarization limit, see Eq. (3.25) in Sec. 3.1.2.1.

3.2.3 Energy-momentum tensor

The symmetric energy-momentum tensor is defined by the following average [91],

$$T^{\mu\nu} \;=\; \int dP\, dS\, p^\mu p^\nu\left[f_{\text{eq}}^+(x,p,s)+f_{\text{eq}}^-(x,p,s)\right], \tag{3.54}$$

Substituting the distribution function (3.47) in Eq. (3.54) we obtain

$$T^{\mu\nu} \;=\; 2\cosh(\xi)\int dP\, p^\mu p^\nu\, e^{-p\cdot\beta}\int dS\exp\left(\frac{1}{2}\omega_{\alpha\beta}s^{\alpha\beta}\right), \tag{3.55}$$

where, again, employing the small polarization limit and performing the integrations, leads to the same formula as the one obtained in Sec. 3.1.2.2, see Eq. (3.32).

3.2.4 Spin tensor

Spin tensor is defined as follows [91]

$$S^{\lambda,\mu\nu} \;=\; \int dP\, dS\, p^\lambda s^{\mu\nu}\left[f_{\text{eq}}^+(x,p,s)+f_{\text{eq}}^-(x,p,s)\right], \tag{3.56}$$

$$=\; 2\cosh(\xi)\int dP\, p^\lambda\exp\left(-p\cdot\beta\right)\int dS\, s^{\mu\nu}\exp\left(\frac{1}{2}\omega_{\alpha\beta}s^{\alpha\beta}\right), \tag{3.57}$$

where, in the second line, we substituted the distribution function from Eq. (3.47). Performing the integral over the spin in Eq. (3.57), to the first order in $\omega_{\mu\nu}$, gives

$$\int dS\, s^{\mu\nu}\exp\left(\frac{1}{2}\omega_{\alpha\beta}s^{\alpha\beta}\right) \;=\; \int dS\, s^{\mu\nu}\left(1+\frac{1}{2}\omega_{\alpha\beta}s^{\alpha\beta}\right)$$

$$=\; \frac{2}{3m^2}\,\mathfrak{s}^2\left(m^2\omega^{\mu\nu}+2p^\alpha p^{[\mu}\omega^{\nu]}{}_\alpha\right). \tag{3.58}$$

Putting Eq. (3.58) back in Eq. (3.57) we obtain

$$S^{\lambda,\mu\nu} \;=\; \frac{4}{3\,m^2}\,\mathfrak{s}^2\cosh(\xi)\int dP\, p^\lambda\, e^{-p\cdot\beta}\left(m^2\omega^{\mu\nu}+2\,p^\alpha\, p^{[\mu}\omega^{\nu]}{}_\alpha\right), \tag{3.59}$$

which after doing momentum integration leads to [91, 235]

$$S^{\lambda,\mu\nu} \;=\; \mathcal{C}\left(\mathcal{N}_0(T)U^\lambda\omega^{\mu\nu}+S_\Delta^{\lambda,\mu\nu}\right). \tag{3.60}$$

The above result agrees with the spin tensor $S_{\text{GLW}}^{\lambda,\mu\nu}$ derived in Sec. 3.1.2.3, see Eq. (3.39).

For the forthcoming discussions it is useful to consider the spin tensor (3.39) in the large mass ($z \gg 1$ or $m \gg T$) regime, which is equivalent to neglecting the relativistic corrections in Eq. (3.39). This is particularly interesting in the context of low-energy heavy-ion experiments where the mass of the particles (Λ hyperons) is much higher than the system's temperature. Within this limit the thermodynamic coefficient $\mathcal{B}_{(0)} \sim -T^3 e^{-z}\sqrt{z}$ is small compared to $\mathcal{N}_{(0)} \sim T^3 e^{-z} z^{3/2}$ and thus can be neglected. Therefore, Eq. (3.39) takes the form [D3] [232]

$$S_{z \gg 1}^{\alpha,\beta\gamma} \;=\; \cosh(\xi)\,\mathcal{N}_{(0)}\,U^{\alpha}\left[\omega^{\beta\gamma} + 2\,U^{\delta}\,U^{[\beta}\omega^{\gamma]}{}_{\delta}\right]. \tag{3.61}$$

4

PROPAGATION PROPERTIES OF SPIN POLARIZATION

"All truths are easy to understand
once they are discovered.
The point is to discover them."
– GALILEO GALILEI

In this chapter, we study the propagation properties of the spin polarization components of spin hydrodynamics developed in the previous chapter through linear perturbation analysis. The idea behind this analysis is to observe the behavior of the spin components and their dependence on the thermodynamic parameters after they are perturbed in the longitudinal direction. We find that the longitudinal spin components do not propagate, however, the transverse spin components propagate in an analogous way to electromagnetic waves. Material presented here may be found in Refs. [D2] and [D3].

4.1 Properties and parameterizations of the spin polarization tensor

As the spin polarization tensor $\omega_{\mu\nu}$ is a second-rank antisymmetric tensor it is convenient to decompose it with respect to fluid four-velocity U^μ in terms of two electric-like (κ^μ) and magnetic-like (ω^μ) four-vectors as follows [1] [231]

$$\omega_{\mu\nu} = \kappa_\mu U_\nu - \kappa_\nu U_\mu + \epsilon_{\mu\nu\alpha\beta} U^\alpha \omega^\beta \,, \tag{4.1}$$

with the following properties arising from it:

- Components of four-vectors κ^μ and ω^μ parallel to U^μ have no contribution to the right-hand side of Eq. (4.1). Hence, κ^μ and ω^μ satisfy the following constraints

$$\kappa \cdot U = 0 \,, \qquad \omega \cdot U = 0 \,. \tag{4.2}$$

---

[1]We use terms "electric-like" and "magnetic-like" with respect to four-vectors κ^μ and ω^μ to highlight their similarity to the components present in analogous decomposition of the Faraday tensor in electromagnetism [297]

$$F_{\mu\nu} = E_\mu U_\nu - E_\nu U_\mu + \epsilon_{\mu\nu\alpha\beta} U^\alpha B^\beta \,.$$

- One can obtain κ_μ and ω_μ from $\omega_{\mu\nu}$ using the relations

$$\kappa_\mu = \omega_{\mu\alpha} U^\alpha, \qquad \omega_\mu = \frac{1}{2}\epsilon_{\mu\alpha\beta\gamma}\, \omega^{\alpha\beta}\, U^\gamma\,. \qquad (4.3)$$

- Each of the four-vectors, κ^μ and ω^μ, have three independent components. Hence, they together constitute same number of independent components as $\omega_{\mu\nu}$.

For mathematical convenience we introduce a basis $I \in \{U, X, Y, Z\}$ formed by a set of mutually orthogonal four-vectors: U, X, Y, and Z satisfying the following normalization conditions

$$U \cdot U = 1, \qquad X \cdot X = Y \cdot Y = Z \cdot Z = -1\,. \qquad (4.4)$$

The four-vectors X, Y and Z span the space transverse to U and may be obtained by canonical boost transformation with four-velocity U of the local-rest-frame (LRF) forms [298–300]

$$X^\alpha_{\mathrm{LRF}} = \left(0, 1, 0, 0\right), \qquad Y^\alpha_{\mathrm{LRF}} = \left(0, 0, 1, 0\right), \qquad Z^\alpha_{\mathrm{LRF}} = \left(0, 0, 0, 1\right)\,. \qquad (4.5)$$

Using the four-vector basis, κ^μ and ω^μ can be decomposed in terms of Lorentz-scalar spin coefficients $C_{\boldsymbol{\kappa}} = (C_{\kappa X}, C_{\kappa Y}, C_{\kappa Z})$ and $C_{\boldsymbol{\omega}} = (C_{\omega X}, C_{\omega Y}, C_{\omega Z})$ [2] as follows

$$\kappa^\alpha = C_{\kappa X}X^\alpha + C_{\kappa Y}Y^\alpha + C_{\kappa Z}Z^\alpha\,, \qquad \omega^\alpha = C_{\omega X}X^\alpha + C_{\omega Y}Y^\alpha + C_{\omega Z}Z^\alpha\,. \qquad (4.6)$$

Decompositions (4.6) allow us to rewrite the spin polarization tensor Eq. (4.1) in the form

$$\begin{aligned}
\omega_{\alpha\beta} &= 2\left(C_{\kappa X}X_{[\alpha}U_{\beta]} + C_{\kappa Y}Y_{[\alpha}U_{\beta]} + C_{\kappa Z}Z_{[\alpha}U_{\beta]}\right) \\
&+ \epsilon_{\alpha\beta\gamma\delta}\,U^\gamma\left(C_{\omega X}X^\delta + C_{\omega Y}Y^\delta + C_{\omega Z}Z^\delta\right)\,.
\end{aligned} \qquad (4.7)$$

In the laboratory (LAB) frame one can have different parameterization [3] of the spin polarization tensor consisting of electric-like, $\boldsymbol{e} = (e^1, e^2, e^3)$, and magnetic-like, $\boldsymbol{b} = (b^1, b^2, b^3)$, components as [232]

$$\omega_{\alpha\beta} = \begin{bmatrix} 0 & e^1 & e^2 & e^3 \\ -e^1 & 0 & -b^3 & b^2 \\ -e^2 & b^3 & 0 & -b^1 \\ -e^3 & -b^2 & b^1 & 0 \end{bmatrix}\,. \qquad (4.8)$$

4.2 Spin tensor for general statistics

The spin tensor in Eq. (3.60) has been derived using the equilibrium distribution function (3.47) for the Maxwell-Jüttner (MJ) statistics. In what follows, we extend the spin tensor to other statistics so that we can study the polarization of other species of particles produced in the experiments. For that purpose, we first extend the definition of the distribution function (3.47).

Let us start by considering the general distribution function

$$f^\sigma_{\mathrm{eq}} \equiv f^\sigma_{\mathrm{eq}}(y_\sigma)\,, \qquad (4.9)$$

---

[2]Note that, all the spin components are dimensionless and are functions of spacetime coordinates.
[3]We followed the sign conventions of Ref. [297].

with

$$y_\sigma \;=\; y_{\sigma;0} + y_{\rm spin}\,, \qquad y_{\sigma;0} \;=\; \beta p\cdot U - \sigma\,\xi\,, \qquad y_{\rm spin} \;=\; -\frac{1}{2}\omega^{\mu\nu}s_{\mu\nu}\,, \tag{4.10}$$

where β is the inverse of temperature and $\sigma = +1(-1)$ represent particles (antiparticles).

Assuming $y_{\rm spin} \ll y_{\sigma;0}$ we have

$$f^\sigma_{\rm eq}(y_\sigma) \;=\; f^\sigma_{\rm eq}(y_{\sigma;0}) + f^{\sigma\prime}_{\rm eq}(y_{\sigma;0})y_{\rm spin} + \dots\,, \tag{4.11}$$

where the derivative is done at vanishing spin polarization

$$f^{\prime\sigma}_{\rm eq}(y_{\sigma;0}) \;=\; -\sigma\left(\frac{\partial f^\sigma_{\rm eq}}{\partial\xi}\right)_\beta \;=\; \frac{1}{p\cdot U}\left(\frac{\partial f^\sigma_{\rm eq}}{\partial\beta}\right)_\xi. \tag{4.12}$$

Thus the spin tensor (3.59) can be written for an arbitrary statistics as

$$S^{\lambda,\mu\nu} \;=\; -\frac{2\mathfrak{s}^2}{3m^2}\sum_{\sigma=\pm}\int {\rm dP}\,p^\lambda f^{\prime\sigma}_{\rm eq}\left(m^2\omega^{\mu\nu}+2p^\alpha p^{[\mu}\omega^{\nu]}{}_\alpha\right)\,, \tag{4.13}$$

where we can write the integral of $p^\lambda f^{\sigma\prime}_{\rm eq}$ as

$$2\sum_{\sigma=\pm}\int {\rm dP}\,p^\lambda f^{\sigma\prime}_{\rm eq} \;=\; a_1\,U^\lambda\,, \qquad \text{with} \qquad a_1 \;=\; -\left(\frac{\partial\mathcal{N}}{\partial\xi}\right)_\beta. \tag{4.14}$$

Factor 2 appears due to spin degeneracy.

Furthermore, the integral of $p^\lambda p^\alpha p^\mu f^{\prime\sigma}_{\rm eq}$ can be decomposed as

$$2\sum_{\sigma=\pm}\int {\rm dP}\,f^{\sigma\prime}_{\rm eq}\,p^\lambda p^\alpha p^\mu \;=\; a_2\,U^\lambda U^\alpha U^\mu + b_2(U^\lambda\Delta^{\alpha\mu} + U^\alpha\Delta^{\lambda\mu} + U^\mu\Delta^{\lambda\alpha})\,, \tag{4.15}$$

where thermodynamic coefficients a_2 and b_2 can be evaluated by contracting the above expression with $U_\lambda U_\alpha U_\mu$ and $U_\lambda g_{\alpha\mu}$. In this way one gets

$$a_2 \;=\; \left(\frac{\partial\mathcal{E}}{\partial\beta}\right)_\xi\,, \qquad a_2 + 3b_2 \;=\; -m^2\left(\frac{\partial\mathcal{N}}{\partial\xi}\right)_\beta\,, \tag{4.16}$$

respectively.

Using Eqs. (4.14) and (4.15) in Eq. (4.13) and comparing with Eq. (3.60) shows that $a_1 = -(3/\mathfrak{s}^2)(\mathcal{A}_1 + \mathcal{A}_3)$, $a_2 = (3m^2/2\mathfrak{s}^2)(\mathcal{A}_3 - 2\mathcal{A}_1)$, and $b_2 = -(3m^2/2\mathfrak{s}^2)\mathcal{A}_3$. Hence, one can have yet another decomposition of Eqs. (3.40) and (3.41) as

$$S^{\alpha,\beta\gamma}_{\rm PH} \;=\; (\mathcal{A}_1 + \mathcal{A}_3)U^\alpha\omega^{\beta\gamma}\,, \tag{4.17}$$

$$S^{\alpha,\beta\gamma}_{\Delta} \;=\; (2\mathcal{A}_1 - \mathcal{A}_3)\,U^\alpha U^\delta U^{[\beta}\omega^{\gamma]}{}_\delta + \mathcal{A}_3\left(\Delta^{\alpha\delta}U^{[\beta}\omega^{\gamma]}{}_\delta + U^\alpha\Delta^{\delta[\beta}\omega^{\gamma]}{}_\delta + U^\delta\Delta^{\alpha[\beta}\omega^{\gamma]}{}_\delta\right)\,, \tag{4.18}$$

where $\mathcal{A}_1$ and $\mathcal{A}_3$ for general statistics are

$$\mathcal{A}_1 \;=\; \frac{\mathfrak{s}^2}{9}\left[\left(\frac{\partial\mathcal{N}}{\partial\xi}\right)_\beta - \frac{2}{m^2}\left(\frac{\partial\mathcal{E}}{\partial\beta}\right)_\xi\right]\,, \qquad \mathcal{A}_3 \;=\; \frac{2\mathfrak{s}^2}{9}\left[\left(\frac{\partial\mathcal{N}}{\partial\xi}\right)_\beta + \frac{1}{m^2}\left(\frac{\partial\mathcal{E}}{\partial\beta}\right)_\xi\right]. \tag{4.19}$$

One can check that above equations reduce to Eqs. (3.44) for MJ statistics.

69

4.3   Dispersion relation of spin wave velocity

As mentioned in Chapter 3, due to the assumption of small polarization, conservation laws for net baryon current (3.29) as well as for energy and momentum (3.37) are independent of the spin dynamics [91,235], hence, may be treated as a a perfect-fluid background for the latter. As a result, the analysis of propagation of perturbations at the level of background will lead to a widely known spectrum of sound waves where the sound speed is defined as [154, 162, 254, 255]

$$c_s^2 \;=\; \left(\frac{\partial \mathcal{P}}{\partial \mathcal{E}}\right)_{\mathcal{N}} + \frac{\mathcal{N}}{\mathcal{E} + \mathcal{P}}\left(\frac{\partial \mathcal{P}}{\partial \mathcal{N}}\right)_{\mathcal{E}}, \tag{4.20}$$

In consequence, the propagation of perturbations at the level of spin tensor conservation law can be studied independently.

We will start with the spin tensor decomposition, derived for the general statistics, shown in Eqs. (4.17) and (4.18) along with the thermodynamic coefficients (4.19). At the level of spin tensor, background fluid is at rest, hence $U^\mu = g^{t\mu}$. In addition, we also consider that the system is homogeneous in the transverse plane. Due to the small polarization limit considered we can also assume that the background fluid can be unpolarized. Therefore, Eqs. (4.17) and (4.18) reduce to

$$\begin{aligned} S_{\rm PH}^{\alpha,\mu\nu} &= (\mathcal{A}_1 + \mathcal{A}_3)\, g^{t\alpha}\, \omega^{\mu\nu}, \\ S_{\Delta}^{\alpha,\mu\nu} &= 2\,(\mathcal{A}_1 - 2\mathcal{A}_3)\, g^{t\alpha}\, g^{t[\mu}\omega^{\nu]t} + \mathcal{A}_3\left(g^{t[\mu}\omega^{\nu]\alpha} + g^{\alpha[\mu}\omega^{\nu]t} - g^{t\alpha}\omega^{\mu\nu}\right), \end{aligned} \tag{4.21}$$

and their divergence read

$$\begin{aligned} \partial_\alpha S_{\rm PH}^{\alpha,\mu\nu} &= (\mathcal{A}_1 + \mathcal{A}_3)\, \partial_t\omega^{\mu\nu}, \\ \partial_\alpha S_{\Delta}^{\alpha,\mu\nu} &= (2\mathcal{A}_1 - 3\mathcal{A}_3)\, g^{t[\mu}\,\partial_t\omega^{\nu]t} + \mathcal{A}_3\left(\partial^{[\mu}\omega^{\nu]t} - \partial_t\omega^{\mu\nu} + g^{t[\mu}\partial_z\omega^{\nu]z}\right). \end{aligned} \tag{4.22}$$

Considering cases such as $\{\mu = 0, \nu = i\}$ and $\{\mu = i, \nu = j\}$, and using the fact that $S_{\rm GLW}^{\alpha,\beta\gamma} = S_{\rm PH}^{\alpha,\beta\gamma} + S_{\Delta}^{\alpha,\beta\gamma}$, see Eq. (3.39), we obtain

$$\begin{aligned} \partial_\alpha S_{\rm GLW}^{\alpha,ti} &= \partial_\alpha S_{\rm PH}^{\alpha,ti} + \partial_\alpha S_{\Delta}^{\alpha,ti} = \mathcal{A}_3\left(\partial_t\omega^{ti} + \frac{1}{2}\partial_z\omega^{iz}\right), \\ \partial_\alpha S_{\rm GLW}^{\alpha,ij} &= \partial_\alpha S_{\rm PH}^{\alpha,ij} + \partial_\alpha S_{\Delta}^{\alpha,ij} = \mathcal{A}_1\,\partial_t\omega^{ij} + \mathcal{A}_3\,\partial^{[i}\omega^{j]t}. \end{aligned} \tag{4.23}$$

Using Eq. (4.7) one can write the spin polarization tensor in the fluid rest frame as

$$\omega^{ti} \;=\; -C_{\kappa i}, \qquad \omega^{ij} \;=\; -\epsilon^{tijk}C_{\omega k}, \tag{4.24}$$

and the conservation law for spin, $\partial_\alpha S_{\rm GLW}^{\alpha,\beta\gamma}(x) = 0$, gives

$$\begin{aligned} \partial_t C_{\kappa X} - \frac{1}{2}\partial_z C_{\omega Y} &= 0, & \partial_t C_{\omega Y} + \frac{\mathcal{A}_3}{2\mathcal{A}_1}\partial_z C_{\kappa X} &= 0, \\ \partial_t C_{\kappa Y} + \frac{1}{2}\partial_z C_{\omega X} &= 0, & \partial_t C_{\omega X} - \frac{\mathcal{A}_3}{2\mathcal{A}_1}\partial_z C_{\kappa Y} &= 0. \end{aligned} \tag{4.25}$$

Since $\partial_t C_{\kappa Z} = \partial_t C_{\omega Z} = 0$, we find that the longitudinal spin components do not propagate. Hence, the spin degrees of freedom propagate as transverse waves analogous to electromagnetic waves [253, 297].

All four transverse spin components follow the same wave-like equation as

$$\left(\partial_t^2 - c_{\text{spin}}^2 \partial_z^2\right) C_{\kappa X} = 0, \qquad \left(\partial_t^2 - c_{\text{spin}}^2 \partial_z^2\right) C_{\kappa Y} = 0,$$
$$\left(\partial_t^2 - c_{\text{spin}}^2 \partial_z^2\right) C_{\omega X} = 0, \qquad \left(\partial_t^2 - c_{\text{spin}}^2 \partial_z^2\right) C_{\omega Y} = 0, \tag{4.26}$$

where the c_{spin} is the speed of the spin wave expressed as

$$c_{\text{spin}}^2 = -\frac{1}{4}\frac{\mathcal{A}_3}{\mathcal{A}_1} = \frac{1}{4}\frac{(\partial\mathcal{E}/\partial T)_\xi - z^2 (\partial\mathcal{N}/\partial\xi)_T}{(\partial\mathcal{E}/\partial T)_\xi + \frac{z^2}{2}(\partial\mathcal{N}/\partial\xi)_T}, \tag{4.27}$$

which in the high temperature ($z \to 0$) limit gives $c_{\text{spin}} = 1/2$. We emphasize that the relation for c_{spin} in Eq. (4.27) holds true for an arbitrary statistics.

4.3.1 The case of Maxwell-Jüttner distribution

We now move on to find the form of Eq. (4.27) for Maxwell-Jüttner (MJ) statistics. In this case the distribution reads

$$f_{\text{eq}}^\sigma = \frac{g_s}{(2\pi)^3} e^{-\beta U \cdot p + \sigma\xi}, \tag{4.28}$$

with $g_s = 2$ representing the spin degeneracy. The net baryon current (N^μ) and energy-momentum tensor ($T^{\mu\nu}$) can be evaluated in the following way

$$N^\mu = \sum_\sigma \sigma \int \text{dP}\, p^\mu f_{\text{eq}}^\sigma, \qquad T^{\mu\nu} = \sum_\sigma \int \text{dP}\, p^\mu p^\nu f_{\text{eq}}^\sigma. \tag{4.29}$$

Above equations reproduce the relations given in Eqs. (3.53) and (3.55), respectively. The derivatives of net baryon density ($\mathcal{N}$) and energy density ($\mathcal{E}$) with respect to ξ and β give, respectively

$$\left(\frac{\partial\mathcal{N}}{\partial\xi}\right)_\beta = \frac{2m^2 T}{\pi^2}\cosh(\xi)\, K_2(z),$$
$$\left(\frac{\partial\mathcal{E}}{\partial\beta}\right)_\xi = -\frac{2m^3 T^2}{\pi^2}\cosh(\xi)\, [zK_2(z) + 3K_3(z)]. \tag{4.30}$$

Thus, $\mathcal{A}_1$ and $\mathcal{A}_3$ in Eq. (4.19) for the MJ statistics are

$$\mathcal{A}_1 = \frac{4\mathfrak{s}^2 m T^2}{3\pi^2}\cosh(\xi)\left[K_3(z) + \frac{z}{2}K_2(z)\right],$$
$$\mathcal{A}_3 = -\frac{4\mathfrak{s}^2 m T^2}{3\pi^2}\cosh(\xi)\, K_3(z), \tag{4.31}$$

in agreement with Eqs. (3.44) where $\mathfrak{s}^2 = 3/4$. Substituting the above equations in Eq. (4.27) gives c_{spin}^2 for (ideal) MJ gas

$$c_{\text{spin}}^2\Big|_{\text{MJ}} = -\frac{1}{4}\frac{\mathcal{A}_3}{\mathcal{A}_1} = \frac{1}{4}\left[\frac{K_3(z)}{K_3(z) + \frac{z}{2}K_2(z)}\right], \tag{4.32}$$

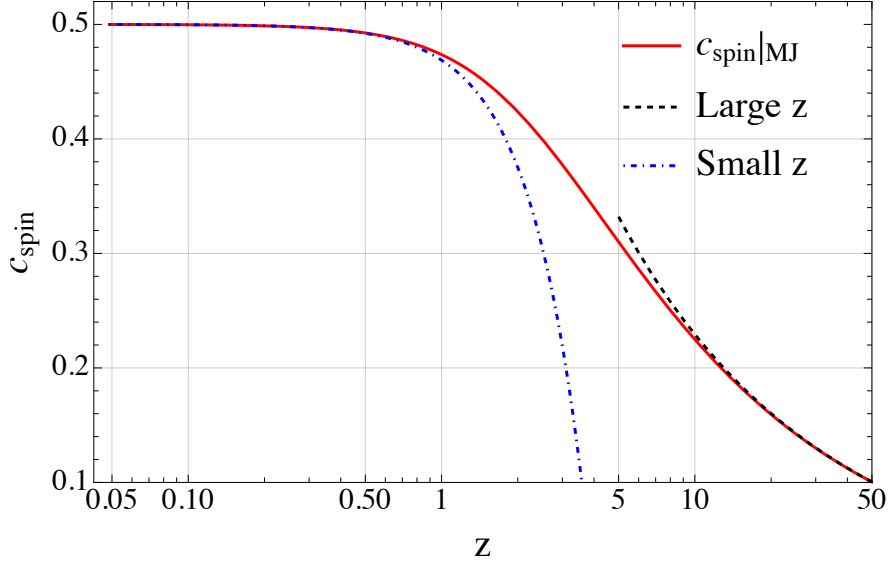which depends only on the parameter $z = m/T$, see Fig. 4.1.

Figure 4.1: (Color online) The speed of the spin wave c_{spin} for MJ statistics as a function of $z = m/T$ together with their respective asymptotic forms.

4.3.1.1 Asymptotic limit

To understand the asymptotic behavior of $c_{\mathrm{spin}}\big|_{\mathrm{MJ}}$, it is useful to discuss its asymptotic properties for the non-relativistic ($z \gg 1$) and ultra-relativistic ($z \ll 1$) cases.

The modified Bessel functions can be expanded in the following way for large values of z [295]

$$
K_\nu(z) = \sqrt{\frac{\pi}{2z}} e^{-z} \sum_{k=0}^{\infty} \frac{a_k(\nu)}{z^k}, \qquad \text{with} \qquad a_k(\nu) = \frac{\left(\frac{1}{2} - \nu\right)_k \left(\frac{1}{2} + \nu\right)_k}{(-2)^k k!}. \tag{4.33}
$$

Thus,

$$
\begin{aligned}
K_2(z) &= \sqrt{\frac{\pi}{2z}} e^{-z} \left(1 + \frac{15}{8z} + \frac{105}{128z^2} + \dots\right), \\
K_3(z) &= \sqrt{\frac{\pi}{2z}} e^{-z} \left(1 + \frac{35}{8z} + \frac{945}{128z^2} + \dots\right).
\end{aligned} \tag{4.34}
$$

Using Eqs. (4.34) in Eq. (4.32) we obtain $c_{\mathrm{spin}}\big|_{\mathrm{MJ}}$ for large values of z

$$
c_{\mathrm{spin}}\Big|_{\mathrm{MJ}(z\gg1)} \simeq \frac{1}{\sqrt{2z}}. \tag{4.35}
$$

Similarly, the modified Bessel functions of the second kind $K_n(z)$ can be expanded for small values of z as [295]

$$
\begin{aligned}
K_n(z) &= \frac{1}{2}\left(\frac{z}{2}\right)^{-n} \sum_{k=0}^{n-1} \frac{(n-k-1)!}{k!} \left(-\frac{z^2}{4}\right)^k + (-1)^{n+1} \ln\left(\frac{z}{2}\right) I_n(z) \\
&+ \frac{(-1)^n}{2}\left(\frac{z}{2}\right)^n \sum_{k=0}^{\infty} [\psi(k+1) + \psi(n+k+1)] \frac{(z^2/4)^k}{k!(n+k)!},
\end{aligned} \tag{4.36}
$$

with $\psi(z) = \Gamma'(z)/\Gamma(z)$ being the digamma function, whereas $I_n(z)$ are the modified Bessel functions of the first kind

$$I_n(z) = \left(\frac{z}{2}\right)^n \sum_{k=0}^{\infty} \frac{(z^2/4)^k}{k!(n+k)!}. \tag{4.37}$$

Leading order terms of $K_2(z)$ and $K_3(z)$ come from the first term of Eq. (4.36),

$$K_2(z) = \frac{2}{z^2} - \frac{1}{2} + O(z^2), \qquad K_3(z) = \frac{8}{z^3} - \frac{1}{z} + O(z), \tag{4.38}$$

which, after using in Eq. (4.32), gives $c_{\text{spin}}\big|_{\text{MJ}}$ for small values of z

$$c_{\text{spin}}\big|_{\text{MJ}(z \ll 1)} = \frac{1}{2}\left[1 - \frac{z^2}{16} + O(z^4)\right]. \tag{4.39}$$

Figure 4.1 shows the comparison between the exact $c_{\text{spin}}\big|_{\text{MJ}}$ (4.32) and its asymptotic expressions (4.35) and (4.39). It can be observed, as expected, that at $z = 0$ the magnitude of $c_{\text{spin}} = 1/2$ which eventually vanishes for large values of z.

4.3.2 The case of Fermi-Dirac distribution

Fermi-Dirac (FD) gas is modelled using the distribution [301, 302]

$$f_{\text{eq}}^{\sigma} = \frac{g_s}{8\,\pi^3} \frac{1}{e^{(\beta p \cdot U - \sigma\xi)} + 1}. \tag{4.40}$$

In this case the net baryon density $\mathcal{N}$, energy density $\mathcal{E}$, and pressure $\mathcal{P}$ are evaluated, respectively, as [303]

$$\begin{pmatrix} \mathcal{N} \\ \mathcal{E} \\ \mathcal{P} \end{pmatrix} = \frac{1}{\pi^2} \sum_{\sigma} \int_m^{\infty} dE\, p \begin{pmatrix} \sigma E \\ E^2 \\ \frac{1}{3}p^2 \end{pmatrix} \frac{1}{e^{(\beta E - \sigma\xi)} + 1}, \tag{4.41}$$

where p is the momentum of the particle. For $\xi < z = \beta m$ we can expand Fermi-Dirac factor $[e^{(\beta E - \sigma\xi)} + 1]^{-1}$ as

$$\frac{1}{e^{(\beta E - \sigma\xi)} + 1} = \sum_{\ell=1}^{\infty} (-1)^{\ell+1} e^{-(\ell\beta E - \ell\sigma\xi)}, \tag{4.42}$$

which then allows $\mathcal{N}$ and $\mathcal{E}$ to have the forms

$$\mathcal{N} = \frac{2m^2 T}{\pi^2} \sum_{\ell=1}^{\infty} \frac{(-1)^{\ell+1}}{\ell} \sinh(\ell\xi)\, K_2(\ell z),$$

$$\mathcal{E} = \frac{2m^2 T^2}{\pi^2} \sum_{\ell=1}^{\infty} \frac{(-1)^{\ell+1}}{\ell^2} \cosh(\ell\xi)\, [\ell z K_1(\ell z) + 3K_2(\ell z)], \tag{4.43}$$

respectively. Putting $\ell = 1$ in Eq. (4.43) gives the results for the MJ statistics given in Eqs. (3.26) and (3.33). The derivatives of $\mathcal{E}$ with respect to β, and of $\mathcal{N}$ with respect to ξ are

$$\left(\frac{\partial \mathcal{E}}{\partial \beta}\right)_{\xi} = -\frac{1}{\pi^2 \beta} \sum_{\sigma} \int_m^{\infty} dE\, E^2 \frac{3p + \frac{E^2}{p}}{e^{(\beta E - \sigma\xi)} + 1},$$

$$\left(\frac{\partial \mathcal{N}}{\partial \xi}\right)_{\beta} = \frac{1}{\pi^2 \beta} \sum_{\sigma} \int_m^{\infty} dE \frac{p + \frac{E^2}{p}}{e^{(\beta E - \sigma\xi)} + 1}. \tag{4.44}$$

However, for the case when $|\xi| < z$, the above integrals can be calculated using Eq. (4.42) allowing $\mathcal{A}_1$ and $\mathcal{A}_3$ to take the forms

$$
\mathcal{A}_1 = \frac{4\mathfrak{s}^2 m T^2}{3\pi^2} \sum_{\ell=1}^{\infty} \frac{(-1)^{\ell+1}}{\ell} \cosh(\ell\xi) \left[K_3(\ell z) + \frac{\ell z}{2} K_2(\ell z) \right] ,
$$

$$
\mathcal{A}_3 = -\frac{4\mathfrak{s}^2 m T^2}{3\pi^2} \sum_{\ell=1}^{\infty} \frac{(-1)^{\ell+1}}{\ell} \cosh(\ell\xi) \, K_3(\ell z) . \tag{4.45}
$$

These results reduce to Eqs. (4.31) for $\ell = 1$. Therefore, for FD gas c_{spin}^2 becomes [4]

$$
\left. c_{\text{spin}}^2 \right|_{\text{FD}} = -\frac{1}{4} \frac{\mathcal{A}_3}{\mathcal{A}_1} = \frac{1}{4} \frac{\sum_{\ell=1}^{\infty} \frac{(-1)^{\ell+1}}{\ell} \cosh(\ell\xi) K_3(\ell z)}{\sum_{\ell=1}^{\infty} \frac{(-1)^{\ell+1}}{\ell} \cosh(\ell\xi) \left[K_3(\ell z) + \frac{\ell z}{2} K_2(\ell z) \right]} . \tag{4.46}
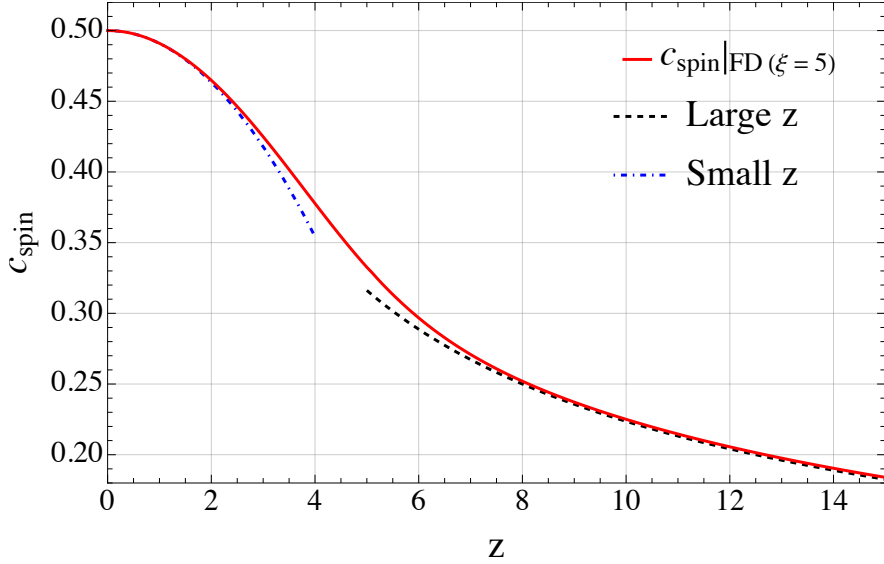$$

Figure 4.2: (Color online) The speed of the spin wave c_{spin} for FD statistics as a function of $z = m/T$ together with their respective asymptotic forms.

4.3.2.1 Asymptotic limit

Now let us derive the non-relativistic and relativistic limits for $\left. c_{\text{spin}} \right|_{\text{FD}}$. In the non-relativistic limit we use large z expansion (4.34) where the terms with $\ell > 1$ are replaced by $K_n(\ell z) \sim e^{-\ell z}/\sqrt{\ell z}$. Thus for large z values the expression of $\left. c_{\text{spin}} \right|_{\text{FD}(z \gg 1)}$ agrees with $\left. c_{\text{spin}} \right|_{\text{MJ}(z \gg 1)}$, see Eq. (4.35).

In the relativistic limit we use Eq. (4.38). Using the notation $S_n = \sum_{\ell=1}^{\infty} \frac{(-1)^{\ell+1}}{\ell^n} \cosh(\ell\xi)$, the coefficients $\mathcal{A}_1$ and $\mathcal{A}_3$ can be expressed as

$$
\mathcal{A}_1 = \frac{32\mathfrak{s}^2 T^4}{3\pi^2 m^2} \left[S_4 + O(z^4) \right] , \qquad \mathcal{A}_3 = -\frac{32\mathfrak{s}^2 T^4}{3\pi^2 m^2} \left[S_4 - \frac{z^2}{8} S_2 + O(z^4) \right] . \tag{4.47}
$$

---

[4]Eq. (4.46) is true for $|\xi| < z$. For $|\xi| > z$, it diverges and then the asymptotic expression in Eq. (4.48), obtained in the following section, must be used.

Now using $S_4 = (7\pi^4 + 30\pi^2\xi^2 + 15\xi^4)/720$ and $S_2 = (\pi^2 + 3\xi^2)/12$, we obtain c_{spin}^2 for the relativistic case as

$$
\begin{aligned}
\left. c_{\mathrm{spin}}^2 \right|_{\mathrm{FD}(z \ll 1)} &= \frac{1}{4}\left[1 - \frac{z^2}{8}\frac{S_2}{S_4} + O(z^4)\right] \\
&= \frac{1}{4}\left[1 - \frac{15z^2}{2}\frac{\pi^2 + 3\,\xi^2}{7\,\pi^4 + 30\,\pi^2\,\xi^2 + 15\,\xi^4} + O(z^4)\right].
\end{aligned}
\tag{4.48}
$$

Figure 4.2 shows the comparison between the exact $\left. c_{\mathrm{spin}} \right|_{\mathrm{FD}}$ (4.46) and its asymptotic expressions (4.35) and (4.48). Here, also at $z = 0$, $c_{\mathrm{spin}} = 1/2$ which vanishes for large z.
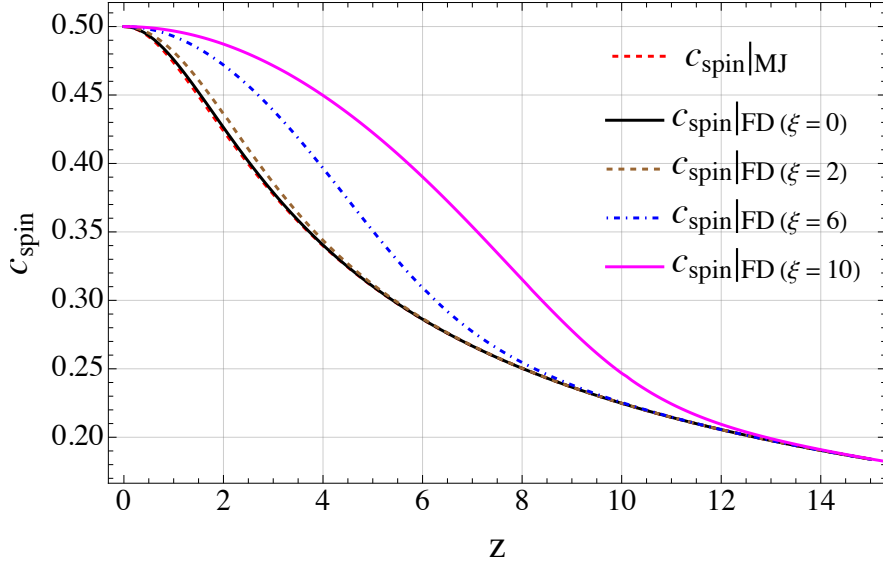

Figure 4.3: (Color online) Comparison between $\left. c_{\mathrm{spin}} \right|_{\mathrm{MJ}}$ and $\left. c_{\mathrm{spin}} \right|_{\mathrm{FD}}$ for various values of ξ. The MJ results are obtained using Eq. (4.32), while the FD results are obtained using Eqs. (4.46) and (4.48) when $z > |\xi|$ and $z < |\xi|$, respectively.

Figure 4.3 shows the comparison between the exact expressions of $\left. c_{\mathrm{spin}} \right|_{\mathrm{MJ}}$ and $\left. c_{\mathrm{spin}} \right|_{\mathrm{FD}}$ for different values of ξ. In summary it is observed that c_{spin} is monotonically decreasing with z from 0 to $\frac{1}{2}$ where the lower bound is for low temperature limit (non-relativistic limit) while the upper bound is for high temperatures.

4.3.2.2 Degenerate limit

An another interesting case which is relevant for the FD statistics is the degenerate limit, i.e. low temperature and high baryon density regime ($T \to 0$ and $\mu_B > m$), in which we have

$$
\mathcal{N} = \frac{p_F^3}{3\pi^2}, \qquad \mathcal{E} = \frac{1}{8\pi^2}\left[p_F\,\mu_B\,(p_F^2 + \mu_B^2) + m^4\ln\left(\frac{m}{p_F + \mu_B}\right)\right],
\tag{4.49}
$$

with $p_F = \sqrt{\mu_B^2 - m^2}$. In this case $\mathcal{E} \equiv \mathcal{E}(\mu_B)$, and the derivatives of $\mathcal{E}$ and $\mathcal{N}$ with respect to β and ξ, respectively, are

$$
\begin{aligned}
\left(\frac{\partial \mathcal{E}}{\partial \beta}\right)_\xi &= -\frac{\mu_B}{\beta}\frac{\partial \mathcal{E}}{\partial \mu_B} = -\frac{\mu_B^3\sqrt{\mu_B^2 - m^2}}{\pi^2\beta}, \\
\left(\frac{\partial \mathcal{N}}{\partial \xi}\right)_\beta &= \frac{\mu_B\sqrt{\mu_B^2 - m^2}}{\pi^2\beta} = -\frac{1}{\mu_B^2}\left(\frac{\partial \mathcal{E}}{\partial \beta}\right)_\xi.
\end{aligned}
\tag{4.50}
$$

Hence, using above equations in Eq. (4.27) leads to the expression of c_{spin} in the degenerate limit

$$\left. c_{\text{spin}}^2 \right|_{\text{FD(deg)}} = \frac{1}{4}\left(\frac{\xi^2 - z^2}{\xi^2 + z^2/2} \right) , \tag{4.51}$$

which is valid when $\xi \gg z$ or in other words $\mu_B \gg m$. Moreover, for the degenerate gas the expression of pressure can be written as

$$\mathcal{P} = \frac{1}{24\pi^2}\left[p_F\,\mu_B\,\left(5\,p_F^2 - 3\,\mu_B^2 \right) - 3\,m^4 \ln \frac{m}{p_F + \mu_B} \right] , \tag{4.52}$$

which gives us the expression for the sound speed

$$\left. c_s^2 \right|_{\text{deg}} = \frac{\partial \mathcal{P}}{\partial \mathcal{E}} = \frac{1}{3}\left(\frac{\xi^2 - z^2}{\xi^2} \right) . \tag{4.53}$$

Interestingly, we can establish a relationship between the spin wave velocity (4.51) and the sound velocity (4.53) for the degenerate FD gas as

$$\left. c_{\text{spin}}^2 \right|_{\text{FD(deg)}} = \frac{1}{2}\left[\frac{\left. c_s^2 \right|_{\text{deg}}}{1 - \left. c_s^2 \right|_{\text{deg}}} \right] . \tag{4.54}$$

4.4 Linear and circular polarization of spin waves

For Eqs. (4.25) one can obtain the linearly polarized solutions for the components $C_{\boldsymbol{\kappa}}$ and $C_{\boldsymbol{\omega}}$ with C_0 as the real amplitude of the wave

$$
\begin{aligned}
C_{\boldsymbol{\kappa}} &= C_0 \operatorname{Re}\left[e^{-ik\left(c_{\text{spin}}t - z \right)} \right] \left(\hat{\boldsymbol{e}}_1 \cos(\theta) + \hat{\boldsymbol{e}}_2 \sin(\theta) \right) , \\
C_{\boldsymbol{\omega}} &= 2\,c_{\text{spin}}\,C_0 \operatorname{Re}\left[e^{-ik\left(c_{\text{spin}}t - z \right)} \right] \left(\hat{\boldsymbol{e}}_1 \sin(\theta) - \hat{\boldsymbol{e}}_2 \cos(\theta) \right) ,
\end{aligned} \tag{4.55}
$$

where θ is the inclination angle with respect to the x-axis. One can find the relation

$$C_{\boldsymbol{\omega}} = 2\,c_{\text{spin}}\,\hat{\boldsymbol{n}} \times C_{\boldsymbol{\kappa}} , \tag{4.56}$$

with $\hat{\boldsymbol{n}} = \hat{\boldsymbol{e}}_3$ being the direction of the wave propagation. One can observe that the Eq. (4.56) is analogous to $\boldsymbol{H} = c\,\hat{\boldsymbol{n}} \times \boldsymbol{D}$ from electromagnetism [297] with c denoting the speed of light.

Consequently, circularly polarized waves read

$$
\begin{aligned}
C_{\boldsymbol{\kappa};R/L} &= \frac{1}{\sqrt{2}} C_0 \operatorname{Re}\left[e^{-ik\left(c_{\text{spin}}t - z \right)} \left(\hat{\boldsymbol{e}}_1 \cos(\theta) \pm i\hat{\boldsymbol{e}}_2 \sin(\theta) \right) \right] , \\
C_{\boldsymbol{\omega};R/L} &= \sqrt{2}\, C_0\, c_{\text{spin}} \operatorname{Re}\left[e^{-ik\left(c_{\text{spin}}t - z \right)} \left(\hat{\boldsymbol{e}}_1 \sin(\theta) \mp i\hat{\boldsymbol{e}}_2 \cos(\theta) \right) \right] ,
\end{aligned} \tag{4.57}
$$

which also satisfies Eq. (4.56).

5

SPIN POLARIZATION OF EMITTED PARTI-
CLES

In Chapter 3 we formulated the framework of relativistic perfect-fluid hydrodynamics with spin where the evolution of the background parameters is obtained through the conservation of net baryon current (3.29) and energy-momentum tensor (3.37), and the evolution of the spin polarization components is obtained through the conservation of spin tensor (3.46). Starting with certain initial conditions specified at a fixed space-like hypersurface, from the above hydrodynamic equations we may determine the dynamics of the thermodynamic and hydrodynamic fields in the future spacetime region. However, it is known very well, that when the system expands and dilutes, the mean free path of its constituents (particles) increases which gives rise to the decoupling of the particles. Eventually, the interactions are so weak that their momenta and spin get 'frozen'. This process is commonly known as *freeze-out*. Using the values of hydrodynamic fields at the freeze-out we can calculate the mean spin polarization per particle which can be compared with the experimental results.

In this chapter, we present details required to calculate the momentum-dependent and momentum-averaged mean spin polarization that will be used further for the numerical modeling of spin polarization of $\Lambda(\bar{\Lambda})$ hyperons in the subsequent chapters. Parts presented in this chapter may be found in Ref. [D3].

5.1 Pauli-Lubański four-vector

To obtain the information about the spin of individual particles at the freeze-out we need to introduce Pauli-Lubański (PL) four-vector, defined as [304, 305]

$$\Pi_\mu = -\frac{1}{2}\epsilon_{\mu\nu\alpha\beta} J^{\nu\alpha} p^\beta, \qquad (5.1)$$

where p is the particle four-momentum and $J^{\nu\alpha}$ is total angular momentum which can be calculated by averaging the total angular momentum density over the three-dimensional

volume

$$J^{\mu\nu} = \int d\Sigma_\lambda \, J^{\lambda,\mu\nu} \,. \tag{5.2}$$

Decomposing $J^{\nu\alpha}$ in Eq. (5.1) in terms of orbital $(x^\nu p^\alpha - x^\alpha p^\nu)$ and spin $(S^{\nu\alpha})$ parts gives

$$
\begin{aligned}
\Pi_\mu &= -\frac{1}{2}\epsilon_{\mu\nu\alpha\beta} \, (x^\nu p^\alpha - x^\alpha p^\nu + S^{\nu\alpha}) \, p^\beta \,, \\
&= -\frac{1}{2}\epsilon_{\mu\nu\alpha\beta} \, (x^\nu p^\alpha - x^\alpha p^\nu) \, p^\beta - \frac{1}{2}\epsilon_{\mu\nu\alpha\beta} S^{\nu\alpha} \, p^\beta \,, \\
&= -\frac{1}{2}\epsilon_{\mu\nu\alpha\beta} S^{\nu\alpha} \, p^\beta \,,
\end{aligned}
\tag{5.3}
$$

where, due to the presence of Levi-Civita symbol, orbital part vanishes and PL four-vector is linked directly to the spin angular momentum, describing spin states of the particle. Obviously, p in Eq. (5.3) is orthogonal to Π.

5.2 Phase-space density of the Pauli-Lubański four-vector

As the QGP is strongly-coupled we use relativistic hydrodynamics as an effective framework to describe its properties. However, due to expansion the interactions between the fluid constituents gradually cease making the system weakly coupled. The adequate description of the subsequent dynamics of the particles is provided by transport theory. To make this transition possible one is required to provide a prescription to describe the process of transforming the fluid elements to particles at the switching hypersurface Σ. A commonly used approach is the so-called Cooper-Frye formula [306], which is based on the assumption of the continuity of the particle current at Σ, see for instance Ref. [307] for details.

Below we develop a respective freeze-out procedure for the spin of the particles using a similar reasoning to the one of Cooper-Frye approach. Using Eq. (5.1) we first calculate, using the invariant total angular momentum density $(J^{\lambda,\nu\alpha})$, the phase-space density of the PL four-vector in the volume $\Delta\Sigma$ and divide this quantity by the momentum density of all particles and antiparticles produced at the surface $\Delta\Sigma$. This ratio provides the information of average spin polarization per particle at the freeze-out hypersurface.

The phase-space density of PL four-vector in the volume $\Delta\Sigma$ is written as [164, 232]

$$E_p \frac{d\Delta\Pi_\mu(x,p)}{d^3p} = -\frac{1}{2} \, \epsilon_{\mu\nu\alpha\beta} \, \Delta\Sigma_\lambda(x) \, E_p \frac{dJ^{\lambda,\nu\alpha}(x,p)}{d^3p} \frac{p^\beta}{m} \,. \tag{5.4}$$

Here, $J^{\lambda,\nu\alpha} = L^{\lambda,\nu\alpha} + S^{\lambda,\nu\alpha} = x^\nu T^{\lambda\alpha} - x^\alpha T^{\lambda\nu} + S^{\lambda,\nu\alpha}$. Levi-Civita symbol forces the orbital part $(L^{\lambda,\nu\alpha})$ to vanish and we obtain

$$E_p \frac{d\Delta\Pi_\mu(x,p)}{d^3p} = -\frac{1}{2} \, \epsilon_{\mu\nu\alpha\beta} \, \Delta\Sigma_\lambda(x) \, E_p \frac{dS^{\lambda,\nu\alpha}(x,p)}{d^3p} \frac{p^\beta}{m} \,. \tag{5.5}$$

The term $E_p \, dS^{\lambda,\nu\alpha}/d^3p$ on the right hand side of the Eq. (5.5), within the GLW formulation, using Eq. (3.39), can be written as [235]

$$E_p \frac{dS^{\lambda,\nu\alpha}_{\mathrm{GLW}}(x,p)}{d^3p} = \frac{\cosh(\xi)}{(2\pi)^3} \, e^{-\beta\cdot p} p^\lambda \left(\omega^{\nu\alpha} + \frac{2}{m^2} p^{[\nu}\omega^{\alpha]}{}_\delta \, p^\delta \right) \,. \tag{5.6}$$

Note that $\zeta \to 0$ has been assumed herein and $\hbar = 1$. Putting Eq. (5.6) in Eq. (5.5), we get the phase-space density as

$$
\begin{aligned}
E_p \frac{d\Delta\Pi_\mu(x,p)}{d^3p} &= -\frac{\cosh(\xi)}{2m(2\pi)^3}\epsilon_{\mu\nu\alpha\beta}\Delta\Sigma_\lambda p^\lambda e^{-\beta \cdot p}\left(\omega^{\nu\alpha}p^\beta + \frac{2}{m^2}p^{[\nu}\omega^{\alpha]}{}_\delta\, p^\delta p^\beta\right), \\
&= -\frac{\cosh(\xi)}{(2\pi)^3 m}\Delta\Sigma_\lambda p^\lambda e^{-\beta \cdot p}\left(\overset{\star}{\omega}_{\mu\beta}p^\beta + \frac{1}{m^2}\epsilon_{\mu\nu\alpha\beta}p^{[\nu}\omega^{\alpha]}{}_\delta\, p^\delta p^\beta\right).
\end{aligned} \tag{5.7}
$$

In the above equation, the second term in the bracket will vanish due to the Levi-Civita symbol and we also used $\frac{1}{2}\epsilon_{\mu\nu\alpha\beta}\omega^{\nu\alpha} = \overset{\star}{\omega}_{\mu\beta}$. Thus we obtain [1]

$$
E_p \frac{d\overset{*}{\Pi}_\mu(p)}{d^3p} = -\frac{1}{(2\pi)^3 m}\int \cosh(\xi)\,\Delta\Sigma_\lambda\, p^\lambda\, e^{-\beta\cdot p}\left(\overset{\star}{\omega}_{\mu\beta}p^\beta\right)^*, \tag{5.8}
$$

which has to be integrated over volume $\Delta\Sigma_\lambda$ to obtain momentum density of the total value of the PL four-vector. The asterisk $(\ )^*$ indicates that the quantity is boosted to the particle rest frame (PRF) [2] [232, 308].

The four-momentum $p^\alpha = (E_p, p_x, p_y, p_z)$ can be parametrized as

$$
E_p = m_T \cosh(y_p), \quad p_x = p_T \cos(\phi_p), \quad p_y = p_T \sin(\phi_p), \quad p_z = m_T \sinh(y_p), \tag{5.9}
$$

where m_T is the transverse mass, y_p is the momentum rapidity, p_T is the transverse momentum, and ϕ_p is the azimuthal angle. Using trigonometric formulae, from the momentum parameterization (5.9), we can get known relations for p_T and m_T

$$
p_T = \sqrt{p_x^2 + p_y^2}, \qquad m_T = \sqrt{E_p^2 - p_z^2} = \sqrt{m^2 + p_T^2}. \tag{5.10}
$$

5.3   Mean spin polarization per particle

To calculate the average spin polarization per particle we first need to define the total particle number current as [232]

$$
\mathcal{N}^\mu(x) = \int dP\, dS\, p^\mu \left[f_{\text{eq}}^+(x,p,s) + f_{\text{eq}}^-(x,p,s)\right], \tag{5.11}
$$

where using the equilibrium function (3.47), after some algebraic manipulations, in the limit of $\omega_{\alpha\beta} \ll 1$ we get

$$
\begin{aligned}
\mathcal{N}^\mu(x) &= 2\cosh(\xi)\int dP\, p^\mu\, e^{-p\cdot\beta}\int dS\left(1 + \frac{1}{2}\omega_{\alpha\beta}s^{\alpha\beta}\right), \\
&= 4\cosh(\xi)\int dP\, p^\mu\, e^{-p\cdot\beta},
\end{aligned} \tag{5.12}
$$

---

[1] The spin tensor (and total angular momentum) is a charge-conjugation even operator, therefore in thermodynamic equilibrium, thermal effects cannot distinguish between the internal (spin) charge of the particles and the antiparticles. Hence, the direction of the spin polarization vector of particles and antiparticles will be same, which is not the case if we introduce electromagnetic fields in the system.

[2] In the experiments, $\Lambda(\bar{\Lambda})$ hyperon spin polarization is measured in the rest frame of the decaying particle, hence to have a comparison of our results with the experimental data, we must Lorentz transform the quantity $\overset{\star}{\omega}_{\mu\beta}p^\beta$ to the PRF.

where we have used the identities $\int dS = 2$ and $\int dS\, s^{\alpha\beta} = 0$ [91]. Note that, Eq. (5.11) is the total particle current, *i.e.*, sum of the number of particles and antiparticles, which is different from the net baryon current (3.50), that is coming from the subtraction of the number of baryons and number of anti-baryons.

The momentum density of all particles and antiparticles being emitted from the hypersurface can be written as [235]

$$E_p \frac{d\mathcal{N}(p)}{d^3p} \;=\; \frac{4}{(2\pi)^3} \int \cosh(\xi)\, \Delta\Sigma_\lambda\, p^\lambda\, e^{-\beta\cdot p}\,.$$
(5.13)

Then the ratio of the total PL four-vector (5.8) and the momentum density of particles and antiparticles (5.13) gives us the average spin polarization per particle as a function of momentum coordinates defined as

$$\langle\pi_\mu\rangle_p \;=\; \frac{E_p \frac{d\overset{*}{\Pi}_\mu(p)}{d^3p}}{E_p \frac{d\mathcal{N}(p)}{d^3p}}\,.$$
(5.14)

It should be noted that $\langle\pi_\mu\rangle_p\langle\pi^\mu\rangle_p$ is a Lorentz invariant quantity and the time component of $\langle\pi_\mu\rangle_p$ must vanish as in PRF, $\langle\pi_\mu\rangle_p p_*^\mu = \langle\pi_0\rangle_p m = 0$. After integrating over momentum variables we arrive at the momentum averaged spin polarization as

$$\langle\pi_\mu\rangle \;=\; \frac{\int dP\, \langle\pi_\mu\rangle_p\, E_p \frac{d\mathcal{N}(p)}{d^3p}}{\int dP\, E_p \frac{d\mathcal{N}(p)}{d^3p}} \;\equiv\; \frac{\int d^3p\, \frac{d\overset{*}{\Pi}_\mu(p)}{d^3p}}{\int d^3p\, \frac{d\mathcal{N}(p)}{d^3p}}\,.$$
(5.15)

The second equality in Eq. (5.15) is obtained using Eqs. (5.13) and (5.14). Results coming from Eqs. (5.14) and (5.15) will be compared with the experimental data.

6

MODELING OF THE SPIN POLARIZATION DYNAMICS

*"An equation for me has no meaning
unless it expresses a thought of God."*
– SRINIVASA RAMANUJAN

After formulating relativistic perfect-fluid hydrodynamics with spin in Chapter 3, in the present chapter we will make use of it to study the dynamics of transversely homogeneous spin-polarizable matter with boost-invariant and boost-invariance-violating longitudinal (with respect to beam) expansion. For this purpose, we first tensor decompose the equations of motion for the background and spin. Subsequently, we use them to study different physical systems and draw some conclusions for spin polarization observables introduced in Chapter 5.

6.1 Basis-vector decomposition of evolution equations

In this section we tensor decompose conservation laws for background and spin derived in Chapter 3 using the four-vector basis introduced in Section 4.1. Resulting evolution equations will be subsequently used in the following sections to study spin polarization dynamics of systems respecting certain spacetime symmetries. Details of this section are based mainly on Ref. [D3].

6.1.1 (3+1)–dimensional parametrization of the four-vector basis

One can write a general (3+1)–dimensional parametrization of the fluid flow four-vector in Minkowski coordinates (μ) in the following form [298–300]

$$U^\mu \;=\; \Big(U_0 \cosh(\Phi),\, U_x,\, U_y,\, U_0 \sinh(\Phi) \Big), \qquad (6.1)$$

with the quantities U_0, U_x, and U_y defined as

$$U_0 \;=\; \cosh(\theta_\perp)\,, \qquad U_x \;=\; U_\perp \cos(\varphi)\,, \qquad U_y \;=\; U_\perp \sin(\varphi)\,, \qquad (6.2)$$

respectively. Here, $\Phi, \theta_\perp, \varphi$ are functions of τ, x, y, η in the Milne coordinate system, where $\tau = \sqrt{t^2 - z^2}$ is the longitudinal proper time and $\eta = \frac{1}{2} \ln\left[(t+z)/(t-z)\right]$ is the space-time

81

rapidity. We adopt convention where the longitudinal fluid rapidity $\Phi = \vartheta(\tau, x, y, \eta) + \eta$ with ϑ denoting the deviation of longitudinal fluid rapidity from the boot-invariant one; we will come back to the discussion of the boot-invariant expansion in Section 6.2. Our choice makes the parametrization (6.1) convenient for describing systems rapidly evolving along the longitudinal (z) direction. Such a situation takes place in ultra-relativistic heavy-ion collision experiments, where the particle production in central rapidity (also known as midrapidity) region is approximately boost-invariant along z (beam) direction [309], meaning $\vartheta \approx 0$.

Using trigonometric relations we find that $U_0 = \sqrt{1 + U_x^2 + U_y^2}$ and $U_\perp = \sqrt{U_x^2 + U_y^2} = \sinh(\theta_\perp)$. The remaining three basis vectors which span the space transverse to U have the form

$$
\begin{aligned}
X^\mu &= \left(U_\perp \cosh(\Phi), \, \frac{U_0 U_x}{U_\perp}, \, \frac{U_0 U_y}{U_\perp}, \, U_\perp \sinh(\Phi) \right), \\
Y^\mu &= \left(0, \, -\frac{U_y}{U_\perp}, \, \frac{U_x}{U_\perp}, \, 0 \right), \\
Z^\mu &= \left(\sinh(\Phi), \, 0, \, 0, \, \cosh(\Phi) \right),
\end{aligned}
\tag{6.3}
$$

which, as mentioned in Chapter 4, result from canonical boost transformation $\Lambda^\mu_\nu(U^\lambda)$ (with U given in (6.1)) applied to LRF forms (4.5).

Before moving ahead, it is also convenient to introduce some notation for the directional derivatives and divergences of the basis vectors, which will turn out handy in subsequent sections. In particular, directional derivatives for the flow U^α (6.1) and space-like basis vectors X^α, Y^α and Z^α (6.3) are denoted as

$$
\begin{aligned}
U^\alpha \partial_\alpha &= U \cdot \partial \equiv (\overset{\bullet}{}), & X^\alpha \partial_\alpha &= X \cdot \partial \equiv (\overset{\blacksquare}{}), \\
Y^\alpha \partial_\alpha &= Y \cdot \partial \equiv (\overset{\square}{}), & Z^\alpha \partial_\alpha &= Z \cdot \partial \equiv (\overset{\circ}{}),
\end{aligned}
\tag{6.4}
$$

while the divergences of the basis vectors are written as

$$
\begin{aligned}
\partial_\alpha U^\alpha &= \partial \cdot U \equiv \theta_U, & \partial_\alpha X^\alpha &= \partial \cdot X \equiv \theta_X, \\
\partial_\alpha Y^\alpha &= \partial \cdot Y \equiv \theta_Y, & \partial_\alpha Z^\alpha &= \partial \cdot Z \equiv \theta_Z.
\end{aligned}
\tag{6.5}
$$

Derivatives with respect to the Cartesian coordinates, t, x, y, and z, used above, are related to the ones with respect to Milne coordinates through the following matrix equation [D6]

$$
\begin{bmatrix} \partial_t \\ \partial_x \\ \partial_y \\ \partial_z \end{bmatrix}
=
\begin{bmatrix}
\cosh(\eta) & 0 & 0 & -\sinh(\eta) \\
0 & 1 & 0 & 0 \\
0 & 0 & 1 & 0 \\
-\sinh(\eta) & 0 & 0 & \cosh(\eta)
\end{bmatrix}
\begin{bmatrix} \partial_\tau \\ \partial_x \\ \partial_y \\ \frac{1}{\tau}\partial_\eta \end{bmatrix}.
\tag{6.6}
$$

6.1.2 Perfect-fluid background

6.1.2.1 Net baryon density conservation

Substituting expression for the net baryon current, see Eq. (3.25), in the net baryon density conservation law $\partial_\alpha N^\alpha(x) = 0$, see Eq. (3.29), we obtain the following equation of motion

$$
U^\alpha \partial_\alpha \mathcal{N} + \mathcal{N} \partial_\alpha U^\alpha = \overset{\bullet}{\mathcal{N}} + \mathcal{N} \theta_U = 0,
\tag{6.7}
$$

where we used the notation listed in Eqs. (6.4) and (6.5). The net baryon density $\mathcal{N}$ is expressed by Eq. (3.26), and, in general, depends on T, μ_B and m (recall that in the small polarization limit, which we will consider henceforth, we take $\zeta \to 0$).

6.1.2.2 Energy and linear momentum conservation

Contracting energy and linear momentum conservation law, $\partial_\alpha T_{\text{GLW}}^{\alpha\beta}(x) = 0$, see Eq. (3.37), with fluid four-vector U_β and then using perfect-fluid form of energy-momentum tensor $(T_{\text{GLW}}^{\alpha\beta}(x) = (\mathcal{E} + \mathcal{P})U^\alpha U^\beta - \mathcal{P} g^{\alpha\beta})$, see Eq. (3.32), we obtain

$$U^\alpha \partial_\alpha \mathcal{E} + (\mathcal{E} + \mathcal{P})\, \partial_\alpha U^\alpha \;=\; \overset{\bullet}{\mathcal{E}} + (\mathcal{E} + \mathcal{P})\, \theta_U \;=\; 0\,, \tag{6.8}$$

where the energy density $\mathcal{E}$ and pressure $\mathcal{P}$ are given by Eqs. (3.33). The implicit relation between equilibrium thermodynamic quantities $(\mathcal{N}, \mathcal{E}, \mathcal{P})$ expressed by their dependence on T, μ_B and m, defines equation of state for the system and employs the small polarization limit. It is equivalent to keeping terms in above equations of leading order in $\omega_{\mu\nu}$ or equivalently setting the limit $\zeta \to 0$. Effectively, it removes ω from the energy-momentum and net-baryon density conservation laws and makes the background insensitive to the polarization dynamics.

Equation (6.8) has to be supplemented with its transverse counterpart; contracting Eq. (3.37) with the transverse projector $(\Delta^\mu_{\ \beta} = g^\mu_{\ \beta} - \frac{U^\mu U_\beta}{U \cdot U})$ and using Eq. (3.32) gives a set of three additional equations of motion

$$(\mathcal{E} + \mathcal{P})\, U^\beta \partial_\beta U^\alpha - \Delta^{\alpha\beta} \partial_\beta \mathcal{P} \;=\; (\mathcal{E} + \mathcal{P})\, \overset{\bullet}{U^\alpha} - \left(\partial^\alpha - U^\alpha U^\beta \partial_\beta\right) \mathcal{P} \;=\; 0\,, \tag{6.9}$$

which, by taking non-relativistic limit, may be interpreted as a relativistic generalization of the Euler equation [147]. In subsequent sections, we will solve five partial differential equations given by Eqs. (6.7)–(6.9) for five unknowns, T, μ_B, and three independent components of U^μ, in order to determine collective background on top of which we will study the dynamics of spin polarization. One should stress here, that, in practice, the small polarization limit makes Eqs. (6.7)–(6.9) to represent state of the art formulation of relativistic perfect-fluid hydrodynamics for baryon-charged fluids [307].

6.1.3 Collective dynamics of spin polarization

As discussed in Chapter 4, due to the antisymmetry of the spin polarization tensor ω, it is convenient to work with its parametrization (4.1) in terms of electric-like and magnetic-like components, $C_{\boldsymbol{\kappa}}$ and $C_{\boldsymbol{\omega}}$, which behave as scalars under Lorentz boosts and rotations. To derive equations of motion for the components $C_{\boldsymbol{\kappa}}$ and $C_{\boldsymbol{\omega}}$, we will use the form of the spin tensor given by Eq. (3.43) with the general spin polarization tensor decomposition (4.7) in the angular momentum conservation law (3.46). The final equations of motion will be then obtained by projecting (3.46) on the basis tensors: $U_\beta X_\gamma$, $U_\beta Y_\gamma$, $U_\beta Z_\gamma$, $Y_\beta Z_\gamma$, $X_\beta Z_\gamma$ and $X_\beta Y_\gamma$.

The spin tensor (3.43) may be expressed in terms of basis four-vectors I, by contracting it with all their possible combinations. This leads to its following form

$$S_{\text{GLW}}^{\alpha,\beta\gamma} \;=\; \sum_{i=x,y,z} S_{\alpha_i}^{\alpha,\beta\gamma} + S_{\beta_i}^{\alpha,\beta\gamma}\,, \tag{6.10}$$

where

$$S_{\alpha_x}^{\alpha,\beta\gamma} = 2\,\alpha_{x1}\,U^\alpha\,U^{[\beta}X^{\gamma]} + \alpha_{x2}\,Y^\alpha\,Y^{[\beta}X^{\gamma]} + \alpha_{x2}\,Z^\alpha\,Z^{[\beta}X^{\gamma]}\,, \tag{6.11}$$

$$S_{\alpha_y}^{\alpha,\beta\gamma} = 2\,\alpha_{y1}\,U^\alpha\,U^{[\beta}Y^{\gamma]} + \alpha_{y2}\,X^\alpha\,X^{[\beta}Y^{\gamma]} + \alpha_{y2}\,Z^\alpha\,Z^{[\beta}Y^{\gamma]}\,, \tag{6.12}$$

$$S_{\alpha_z}^{\alpha,\beta\gamma} = 2\,\alpha_{z1}\,U^\alpha\,U^{[\beta}Z^{\gamma]} + \alpha_{z2}\,X^\alpha\,X^{[\beta}Z^{\gamma]} + \alpha_{z2}\,Y^\alpha\,Y^{[\beta}Z^{\gamma]}\,, \tag{6.13}$$

$$S_{\beta_x}^{\alpha,\beta\gamma} = 2\,\beta_{x1}\Big(Y^\alpha\,U^{[\beta}Z^{\gamma]} + Z^\alpha\,Y^{[\beta}U^{\gamma]}\Big) - 2\,\beta_{x2}\,U^\alpha\,Y^{[\beta}Z^{\gamma]}\,, \tag{6.14}$$

$$S_{\beta_y}^{\alpha,\beta\gamma} = 2\,\beta_{y1}\Big(Z^\alpha\,U^{[\beta}X^{\gamma]} + X^\alpha\,Z^{[\beta}U^{\gamma]}\Big) - 2\,\beta_{y2}\,U^\alpha\,Z^{[\beta}X^{\gamma]}\,, \tag{6.15}$$

$$S_{\beta_z}^{\alpha,\beta\gamma} = 2\,\beta_{z1}\Big(X^\alpha\,U^{[\beta}Y^{\gamma]} + Y^\alpha\,X^{[\beta}U^{\gamma]}\Big) - 2\,\beta_{z2}\,U^\alpha\,X^{[\beta}Y^{\gamma]}\,, \tag{6.16}$$

and the coefficients α and β are defined as

$$\alpha_{i1} = -\Big(\mathcal{A}_1 - \frac{\mathcal{A}_2}{2} - \mathcal{A}_3\Big)C_{\kappa i}\,, \qquad \alpha_{i2} = -\mathcal{A}_3\,C_{\kappa i}\,,$$

$$\beta_{i1} = \frac{\mathcal{A}_3}{2}C_{\omega i}\,, \qquad \beta_{i2} = \mathcal{A}_1\,C_{\omega i}\,, \tag{6.17}$$

where, in the small polarization limit ($\zeta \to 0$),

$$\mathcal{A}_1 = \cosh{(\xi)}(\mathcal{N}_{(0)} - \mathcal{B}_{(0)})\,, \quad \mathcal{A}_2 = \cosh{(\xi)}(\mathcal{A}_{(0)} - 3\mathcal{B}_{(0)})\,, \ \text{and} \ \mathcal{A}_3 = \cosh{(\xi)}\,\mathcal{B}_{(0)}\,,$$

see Eqs. (3.44).

The divergence of Eq. (6.10) can be expressed as a sum

$$\partial_\alpha S_{\text{GLW}}^{\alpha,\beta\gamma} = \partial_\alpha S_{\alpha_x}^{\alpha,\beta\gamma} + \partial_\alpha S_{\alpha_y}^{\alpha,\beta\gamma} + \partial_\alpha S_{\alpha_z}^{\alpha,\beta\gamma} + \partial_\alpha S_{\beta_x}^{\alpha,\beta\gamma} + \partial_\alpha S_{\beta_y}^{\alpha,\beta\gamma} + \partial_\alpha S_{\beta_z}^{\alpha,\beta\gamma} = 0\,, \tag{6.18}$$

where the subsequent summands

$$\partial_\alpha S_{\alpha_x}^{\alpha,\beta\gamma} = 2\,\overset{\bullet}{\alpha_{x1}}U^{[\beta}X^{\gamma]} + \overset{\square}{\alpha_{x2}}Y^{[\beta}X^{\gamma]} + \overset{\circ}{\alpha_{x2}}Z^{[\beta}X^{\gamma]} + 2\,\alpha_{x1}\Big[\theta_U\,U^{[\beta}X^{\gamma]} + \overset{\bullet}{U}{}^{[\beta}X^{\gamma]} + U^{[\beta}\overset{\bullet}{X}{}^{\gamma]}\Big]$$
$$+ \alpha_{x2}\Big[\theta_Y\,Y^{[\beta}X^{\gamma]} + \theta_Z\,Z^{[\beta}X^{\gamma]} + \overset{\square}{Y}{}^{[\beta}X^{\gamma]} + Y^{[\beta}\overset{\square}{X}{}^{\gamma]} + \overset{\circ}{Z}{}^{[\beta}X^{\gamma]} + Z^{[\beta}\overset{\circ}{X}{}^{\gamma]}\Big]\,, \tag{6.19}$$

$$\partial_\alpha S_{\alpha_y}^{\alpha,\beta\gamma} = 2\,\overset{\bullet}{\alpha_{y1}}U^{[\beta}Y^{\gamma]} + \overset{\blacksquare}{\alpha_{y2}}X^{[\beta}Y^{\gamma]} + \overset{\circ}{\alpha_{y2}}Z^{[\beta}Y^{\gamma]} + 2\,\alpha_{y1}\Big[\theta_U\,U^{[\beta}Y^{\gamma]} + \overset{\bullet}{U}{}^{[\beta}Y^{\gamma]} + U^{[\beta}\overset{\bullet}{Y}{}^{\gamma]}\Big]$$
$$+ \alpha_{y2}\Big[\overset{\blacksquare}{X}{}^{[\beta}Y^{\gamma]} + X^{[\beta}\overset{\blacksquare}{Y}{}^{\gamma]} + \overset{\circ}{Z}{}^{[\beta}Y^{\gamma]} + Z^{[\beta}\overset{\circ}{Y}{}^{\gamma]} + \theta_X\,X^{[\beta}Y^{\gamma]} + \theta_Z\,Z^{[\beta}Y^{\gamma]}\Big]\,, \tag{6.20}$$

$$\partial_\alpha S_{\alpha_z}^{\alpha,\beta\gamma} = 2\,\overset{\bullet}{\alpha_{z1}}\,U^{[\beta}Z^{\gamma]} + \overset{\blacksquare}{\alpha_{z2}}\,X^{[\beta}Z^{\gamma]} + \overset{\square}{\alpha_{z2}}\,Y^{[\beta}Z^{\gamma]} + 2\,\alpha_{z1}\Big[\theta_U\,U^{[\beta}Z^{\gamma]} + \overset{\bullet}{U}{}^{[\beta}Z^{\gamma]} + U^{[\beta}\overset{\bullet}{Z}{}^{\gamma]}\Big]$$
$$+ \alpha_{z2}\Big[\overset{\blacksquare}{X}{}^{[\beta}Z^{\gamma]} + X^{[\beta}\overset{\blacksquare}{Z}{}^{\gamma]} + \overset{\square}{Y}{}^{[\beta}Z^{\gamma]} + Y^{[\beta}\overset{\square}{Z}{}^{\gamma]} + \theta_X\,X^{[\beta}Z^{\gamma]} + \theta_Y\,Y^{[\beta}Z^{\gamma]}\Big]\,, \tag{6.21}$$

$$\partial_\alpha S_{\beta_x}^{\alpha,\beta\gamma} = 2\Big[\overset{\square}{\beta_{x1}}\,U^{[\beta}Z^{\gamma]} + \overset{\circ}{\beta_{x1}}\,Y^{[\beta}U^{\gamma]} + \beta_{x1}\Big(\theta_Y\,U^{[\beta}Z^{\gamma]} + \theta_Z\,Y^{[\beta}U^{\gamma]}\Big) - \overset{\bullet}{\beta_{x2}}\,Y^{[\beta}Z^{\gamma]}$$
$$- \beta_{x2}\theta_U\,Y^{[\beta}Z^{\gamma]}\Big] + 2\,\beta_{x1}\Big[\overset{\square}{U}{}^{[\beta}Z^{\gamma]} + \overset{\circ}{Y}{}^{[\beta}U^{\gamma]} + U^{[\beta}\overset{\square}{Z}{}^{\gamma]} + Y^{[\beta}\overset{\circ}{U}{}^{\gamma]}\Big]$$
$$- 2\,\beta_{x2}\Big(\overset{\bullet}{Y}{}^{[\beta}Z^{\gamma]} + Y^{[\beta}\overset{\bullet}{Z}{}^{\gamma]}\Big)\,, \tag{6.22}$$

84

$$\partial_\alpha S^{\alpha,\beta\gamma}_{\beta_y} = 2\Big[\overset{\circ}{\beta}_{y1}\, U^{[\beta}X^{\gamma]} + \overset{\blacksquare}{\beta}_{y1}\, Z^{[\beta}U^{\gamma]} + \beta_{y1}\Big(\theta_Z\, U^{[\beta}X^{\gamma]} + \theta_X\, Z^{[\beta}U^{\gamma]}\Big) - \overset{\bullet}{\beta}_{y2}\, Z^{[\beta}X^{\gamma]}$$
$$-\ \beta_{y2}\theta_U\, Z^{[\beta}X^{\gamma]}\Big] + 2\,\beta_{y1}\Big[\overset{\circ}{U}{}^{[\beta}X^{\gamma]} + \overset{\blacksquare}{Z}{}^{[\beta}U^{\gamma]} + U^{[\beta}\overset{\circ}{X}{}^{\gamma]} + Z^{[\beta}\overset{\blacksquare}{U}{}^{\gamma]}\Big]$$
$$-\ 2\,\beta_{y2}\Big(\overset{\bullet}{Z}{}^{[\beta}X^{\gamma]} + Z^{[\beta}\overset{\bullet}{X}{}^{\gamma]}\Big)\,, \tag{6.23}$$

$$\partial_\alpha S^{\alpha,\beta\gamma}_{\beta_z} = 2\Big[\overset{\blacksquare}{\beta}_{z1}\, U^{[\beta}Y^{\gamma]} + \overset{\square}{\beta}_{z1}\, X^{[\beta}U^{\gamma]} + \beta_{z1}\Big(\theta_X\, U^{[\beta}Y^{\gamma]} + \theta_Y\, X^{[\beta}U^{\gamma]}\Big) - \overset{\bullet}{\beta}_{z2}\, X^{[\beta}Y^{\gamma]}$$
$$-\ \beta_{z2}\theta_U\, X^{[\beta}Y^{\gamma]}\Big] + 2\,\beta_{z1}\Big[\overset{\blacksquare}{U}{}^{[\beta}Y^{\gamma]} + \overset{\square}{X}{}^{[\beta}U^{\gamma]} + U^{[\beta}\overset{\blacksquare}{Y}{}^{\gamma]} + X^{[\beta}\overset{\square}{U}{}^{\gamma]}\Big]$$
$$-\ 2\,\beta_{z2}\Big(\overset{\bullet}{X}{}^{[\beta}Y^{\gamma]} + X^{[\beta}\overset{\bullet}{Y}{}^{\gamma]}\Big)\,, \tag{6.24}$$

were obtained from Eqs. (6.11)–(6.16), respectively.

Finally, to derive the evolution equations for the spin polarization components C (recall that α's and β's depend explicitly on C's), we contract the partial differential equation (6.18) with $U_\beta X_\gamma$, $U_\beta Y_\gamma$, $U_\beta Z_\gamma$, $Y_\beta Z_\gamma$, $X_\beta Z_\gamma$, and $X_\beta Y_\gamma$, and obtain

$$\overset{\bullet}{\alpha}_{x1} + \alpha_{x1}\theta_U + \frac{\alpha_{x2}}{2}\Big(U\overset{\square}{Y} + U\overset{\circ}{Z}\Big) - \frac{\alpha_{y2}}{2}U\overset{\blacksquare}{Y} - \alpha_{y1}X\overset{\bullet}{Y} - \frac{\alpha_{z2}}{2}U\overset{\blacksquare}{Z} - \alpha_{z1}X\overset{\bullet}{Z} - \beta_{x1}\Big(X\overset{\square}{Z} - X\overset{\circ}{Y}\Big)$$
$$+\overset{\circ}{\beta}_{y1} + \beta_{y1}\Big(\theta_Z + X\overset{\blacksquare}{Z}\Big) - \beta_{y2}U\overset{\bullet}{Z} - \overset{\circ}{\beta}_{z1} - \beta_{z1}\Big(\theta_Y + X\overset{\blacksquare}{Y}\Big) + \beta_{z2}U\overset{\bullet}{Y} = 0\,, \tag{6.25}$$

$$\overset{\bullet}{\alpha}_{y1} + \alpha_{y1}\theta_U + \frac{\alpha_{y2}}{2}\Big(U\overset{\blacksquare}{X} + U\overset{\circ}{Z}\Big) - \frac{\alpha_{z2}}{2}U\overset{\square}{Z} - \alpha_{z1}Y\overset{\bullet}{Z} - \frac{\alpha_{x2}}{2}U\overset{\square}{X} - \alpha_{x1}Y\overset{\bullet}{X} - \beta_{y1}\Big(Y\overset{\circ}{X} - Y\overset{\blacksquare}{Z}\Big)$$
$$+\overset{\blacksquare}{\beta}_{z1} + \beta_{z1}\Big(\theta_X + Y\overset{\square}{X}\Big) - \beta_{z2}U\overset{\bullet}{X} - \overset{\blacksquare}{\beta}_{x1} - \beta_{x1}\Big(\theta_Z + Y\overset{\square}{Z}\Big) + \beta_{x2}U\overset{\bullet}{Z} = 0\,, \tag{6.26}$$

$$\overset{\bullet}{\alpha}_{z1} + \alpha_{z1}\theta_U + \frac{\alpha_{z2}}{2}\Big(U\overset{\blacksquare}{X} + U\overset{\square}{Y}\Big) - \frac{\alpha_{x2}}{2}U\overset{\circ}{X} - \alpha_{x1}Z\overset{\bullet}{X} - \frac{\alpha_{y2}}{2}U\overset{\circ}{Y} - \alpha_{y1}Z\overset{\bullet}{Y} - \beta_{z1}\Big(Z\overset{\blacksquare}{Y} - Z\overset{\square}{X}\Big)$$
$$+\overset{\square}{\beta}_{x1} + \beta_{x1}\Big(\theta_Y + Z\overset{\circ}{Y}\Big) - \beta_{x2}U\overset{\bullet}{Y} - \overset{\square}{\beta}_{y1} - \beta_{y1}\Big(\theta_X + Z\overset{\circ}{X}\Big) + \beta_{y2}U\overset{\bullet}{X} = 0\,, \tag{6.27}$$

$$\frac{\overset{\circ}{\alpha}_{y2}}{2} + \frac{\alpha_{y2}}{2}\Big(\theta_Z - Z\overset{\blacksquare}{X}\Big) - \alpha_{y1}Z\overset{\bullet}{U} - \frac{\overset{\square}{\alpha}_{z2}}{2} - \frac{\alpha_{z2}}{2}\Big(\theta_Y - Y\overset{\blacksquare}{X}\Big) + \alpha_{z1}Y\overset{\bullet}{U} - \frac{\alpha_{x2}}{2}\Big(Y\overset{\circ}{X} - Z\overset{\square}{X}\Big)$$
$$+\overset{\bullet}{\beta}_{x2} + \beta_{x2}\theta_U + \beta_{x1}\Big(Y\overset{\square}{U} + Z\overset{\circ}{U}\Big) - \beta_{y1}Y\overset{\blacksquare}{U} + \beta_{y2}Y\overset{\bullet}{X} - \beta_{z1}Z\overset{\blacksquare}{U} + \beta_{z2}Z\overset{\bullet}{X} = 0\,, \tag{6.28}$$

$$\frac{\overset{\blacksquare}{\alpha}_{z2}}{2} + \frac{\alpha_{z2}}{2}\Big(\theta_X - X\overset{\square}{Y}\Big) - \alpha_{z1}X\overset{\bullet}{U} - \frac{\overset{\circ}{\alpha}_{x2}}{2} - \frac{\alpha_{x2}}{2}\Big(\theta_Z - Z\overset{\square}{Y}\Big) + \alpha_{x1}Z\overset{\bullet}{U} - \frac{\alpha_{y2}}{2}\Big(Z\overset{\blacksquare}{Y} - X\overset{\circ}{Y}\Big)$$
$$+\overset{\bullet}{\beta}_{y2} + \beta_{y2}\theta_U + \beta_{y1}\Big(Z\overset{\circ}{U} + X\overset{\blacksquare}{U}\Big) - \beta_{z1}Z\overset{\square}{U} + \beta_{z2}Z\overset{\bullet}{Y} - \beta_{x1}X\overset{\square}{U} + \beta_{x2}X\overset{\bullet}{Y} = 0\,, \tag{6.29}$$

$$\frac{\overset{\square}{\alpha}_{x2}}{2} + \frac{\alpha_{x2}}{2}\Big(\theta_Y - Y\overset{\circ}{Z}\Big) - \alpha_{x1}Y\overset{\bullet}{U} - \frac{\overset{\blacksquare}{\alpha}_{y2}}{2} - \frac{\alpha_{y2}}{2}\Big(\theta_X - X\overset{\circ}{Z}\Big) + \alpha_{y1}X\overset{\bullet}{U} - \frac{\alpha_{z2}}{2}\Big(X\overset{\square}{Z} - Y\overset{\blacksquare}{Z}\Big)$$
$$+\overset{\bullet}{\beta}_{z2} + \beta_{z2}\theta_U + \beta_{z1}\Big(X\overset{\blacksquare}{U} + Y\overset{\square}{U}\Big) - \beta_{x1}X\overset{\circ}{U} + \beta_{x2}X\overset{\bullet}{Z} - \beta_{y1}Y\overset{\circ}{U} + \beta_{y2}Y\overset{\bullet}{Z} = 0\,, \tag{6.30}$$

respectively.

As, in general, Eqs. (6.25)–(6.30) are quite complex, they need to be solved numerically to determine the dynamics of C_κ and C_ω. Moreover, one may observe, that the evolution of the background enters Eqs. (6.25)–(6.30) solely through the thermodynamic factors $\mathcal{A}_1$–$\mathcal{A}_3$ and the flow vectors I, and can be entirely determined in advance; we will often exploit this property hereafter. Finally, as we will see in the following sections, while, in general, all spin components are entangled with each other, see Eqs. (6.25)–(6.30), in simple physics situations the dynamics of some components decouples from others, providing opportunity to get some insights on their collective properties more easily.

In subsequent sections we will study a number of special physics situations advocated by phenomenological observations, whose complexity will change with the change of symmetry constraints imposed on the system.

6.2 Boost-invariant and transversely homogeneous background

Experimental measurements show that in heavy-ion collisions, at top energies, the matter produced in the central (midrapidity) region exhibits invariance with respect to Lorentz boosts along the beam direction [309]. Moreover, as it takes finite time for the hydrodynamic gradients to build up, the transverse expansion of the system in the vicinity of the beam axis [1] may be treated initially as invariant with respect to translations in the transverse plane. These two approximate symmetries, namely boost-invariance and transverse homogeneity, (together with the $\eta \to -\eta$ parity symmetry) constitute the so-called Bjorken symmetry [2]. This symmetry is employed commonly in the phenomenology of heavy-ion collisions due to its advantage of decreasing dimensionality and reducing number of independent parameters required to describe the dynamics of the system. In particular, one can show that all thermodynamic variables are Lorentz scalars which are functions of longitudinal proper time (τ) only, while the flow pattern is completely fixed by symmetry. Indeed, in this case the basis four-vectors (6.1) and (6.3) take the forms

$$
\begin{aligned}
U^\alpha &= (\cosh(\eta),\, 0,\, 0,\, \sinh(\eta))\,, & Z^\alpha &= (\sinh(\eta),\, 0,\, 0,\, \cosh(\eta))\,, \\
X^\alpha &= (0,\, 1,\, 0,\, 0)\,, & Y^\alpha &= (0,\, 0,\, 1,\, 0)\,.
\end{aligned}
\tag{6.31}
$$

Moreover, directional derivatives (6.4) and the divergences (6.5) take the forms $U \cdot \partial = \partial_\tau$, $Z \cdot \partial = \frac{1}{\tau}\partial_\eta$, $X \cdot \partial = \partial_x$, $Y \cdot \partial = \partial_y$, and

$$
\partial \cdot U = \frac{1}{\tau}\,,
\tag{6.32}
$$

respectively. One can also check that $\partial \cdot X = \partial \cdot Y = \partial \cdot Z = 0$.

In the remaining part of Section 6.2 we will make use of the above expressions to study polarization dynamics of Bjorken-expanding matter. The material discussed here is partially based on Ref. [D6].

---

[1] By vicinity we mean that the distances from the z axis are much smaller than the root-mean-square radius of the hard-sphere nuclear overlap region.

[2] The concept of boost-invariance was first discussed by R.P. Feynman in 1969 within the context of hadron production at high energies [310]. In 1983 J.D. Bjorken implemented boost-invariance along with homogeneity in the transverse direction (now known as Bjorken symmetry) into the equations of hydrodynamics and estimated the values of initial energy densities in the collisions [311].

6.2.1   Hydrodynamic evolution

One can check that, due to the symmetries imposed, the relativistic Euler equation (6.9) is trivially satisfied. On the other hand, the energy equation (6.8) takes the form

$$\frac{\partial \mathcal{E}}{\partial \tau} + \frac{\mathcal{E} + \mathcal{P}}{\tau} = 0. \tag{6.33}$$

For baryon-charged matter Eq. (6.33) has to be supplemented with the conservation law for net baryon density (6.7), which for Bjorken-expanding matter becomes

$$\frac{\partial \mathcal{N}}{\partial \tau} + \frac{\mathcal{N}}{\tau} = 0, \tag{6.34}$$

and has the solution

$$\mathcal{N} = \frac{\tau_0}{\tau} \mathcal{N}_0, \tag{6.35}$$

where $\mathcal{N}_0$ is the initial net baryon density at the initial proper time τ_0, $\mathcal{N}_0 = \mathcal{N}(\tau_0)$.

We solve numerically Eqs. (6.34) and (6.33) choosing the conditions aiming at mimicking the situation encountered in high-energy heavy-ion collisions, where the temperature is much higher than the baryon chemical potential. In such a case, we consider the initial baryon chemical potential and the initial temperature as $\mu_{B0} = \mu_B(\tau_0) = 0.05\,\text{GeV}$ and $T_0 = T(\tau_0) = 0.5\,\text{GeV}$, respectively, with $\tau_0 = 1$ fm/c. For simplicity, we consider the system of Λ hyperons and choose the particle mass as $m = m_\Lambda = 1.116$ GeV [312]. The resulting evolution of the temperature (T), baryon chemical potential (μ_B), and the ratio of baryon chemical potential over temperature (ξ) as a function of τ is shown in Figs. 6.1. One can notice that, both, the temperature and baryon chemical potential, decrease with τ for massive $(m = m_\Lambda)$ as well as massless $(m \to 0)$ case. In the $m \to 0$ limit, T and μ_B follow the analytical solutions $T_0 \, (\tau_0/\tau)^{1/3}$ and $\mu_{B_0} \, (\tau_0/\tau)^{1/3}$, respectively, resulting in a constant ξ. In the massive case, the latter increases with τ as expected

$$\xi = \sinh^{-1}\left[\frac{\tau_0}{\tau} \frac{\mathcal{N}_{(0)}(\tau_0)}{\mathcal{N}_{(0)}} \sinh(\xi_0)\right], \tag{6.36}$$

where ξ_0 and $\mathcal{N}_{(0)}(\tau_0)$ are the values of the parameters at τ_0.

Due to restrictive character of Bjorken expansion the evolution equations for spin components (6.25)–(6.30) take the following simple form

$$\begin{aligned}
\overset{\bullet}{\alpha}_{x1} &= -\alpha_{x1}\,\theta_U - \frac{\alpha_{x2}}{2}\, U\overset{\circ}{Z}\,, \\
\overset{\bullet}{\alpha}_{y1} &= -\alpha_{y1}\,\theta_U - \frac{\alpha_{y2}}{2}\, U\overset{\circ}{Z}\,, \\
\overset{\bullet}{\alpha}_{z1} &= -\alpha_{z1}\,\theta_U\,, \\
\overset{\bullet}{\beta}_{x2} &= -\beta_{x2}\,\theta_U - \beta_{x1}\, Z\overset{\circ}{U}\,, \\
\overset{\bullet}{\beta}_{y2} &= -\beta_{y2}\,\theta_U - \beta_{y1}\, Z\overset{\circ}{U}\,, \\
\overset{\bullet}{\beta}_{z2} &= -\beta_{z2}\,\theta_U\,,
\end{aligned} \tag{6.37}$$

where one can check that $U\overset{\circ}{Z} = -Z\overset{\circ}{U} = 1/\tau$. As we observe from Eqs. (6.37), Bjorken symmetries prevent the spin components to couple with each other.
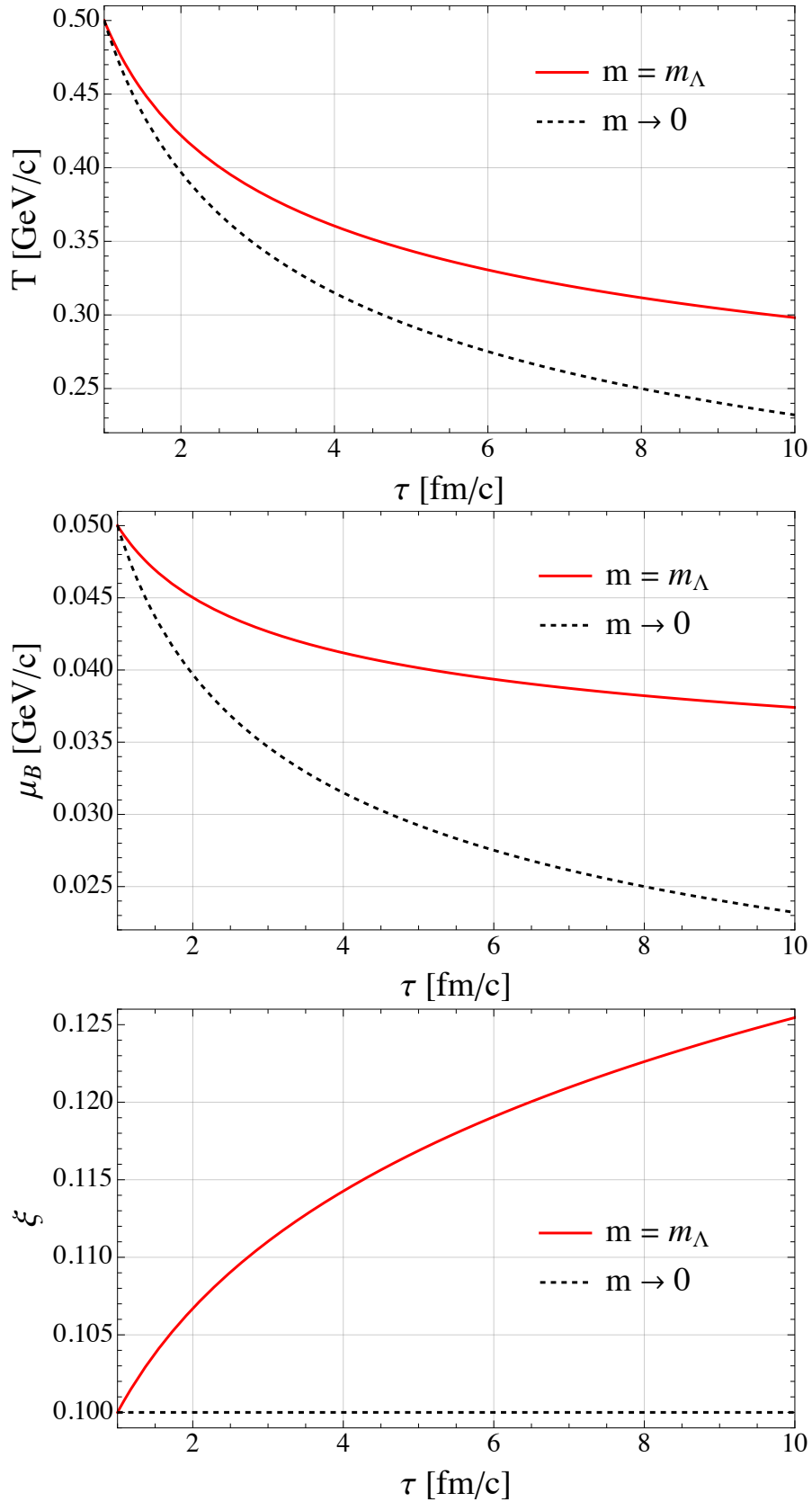
Figure 6.1: (Color online) Evolution of T (top panel), μ_B (middle panel), and $\xi = \mu_B/T$ (lower panel) as a function of τ for Bjorken background along with their respective massless case.
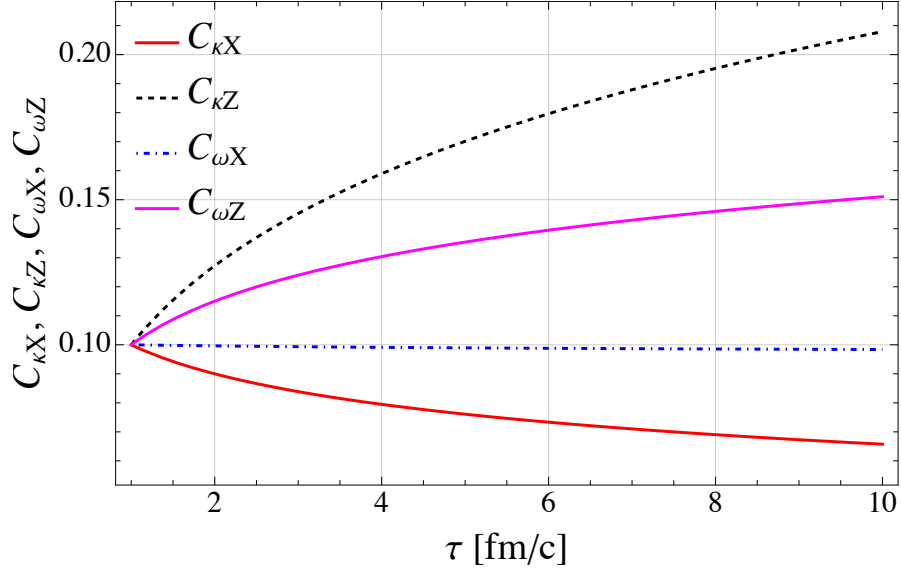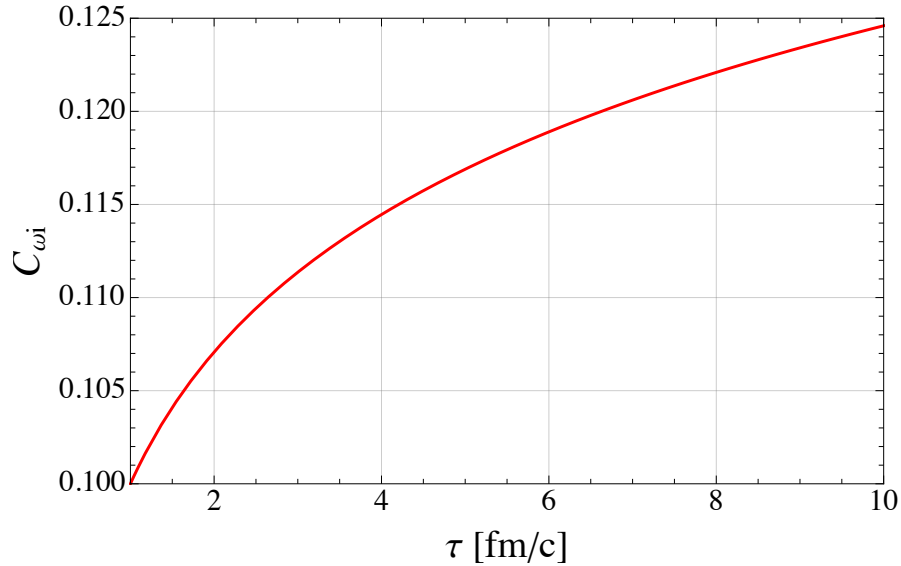
Figure 6.2: (Color online) Time evolution of spin components.

Figure 6.3: (Color online) Evolution of $C_{\omega i}$ components in the $z \gg 1$ limit.

In Fig. 6.2 we show the evolution of the spin polarization components as a function of τ obtained by solving Eqs. (6.37) numerically. The initial value of all the components are chosen arbitrarily to be 0.1 [3]. Transverse components $C_{\kappa X}$ and $C_{\omega X}$ decrease with τ whereas the longitudinal components $C_{\kappa Z}$ and $C_{\omega Z}$ show opposite behavior. Due to the rotational invariance, the transverse components $C_{\kappa X}$ and $C_{\kappa Y}$ (as well as $C_{\omega X}$ and $C_{\omega Y}$) follow the same differential equations, hence we refrain to show $C_{\kappa Y}$ and $C_{\omega Y}$ evolution in Fig. 6.2. We checked that the qualitative behavior of all the spin components does not change significantly with the change in the initial values of thermodynamic parameters such as T_0 or μ_{B0}. Interestingly, in the large mass regime ($z \gg 1$), see the discussion in Section 3.2.4, the quantity $\mathcal{B}_0$ can be neglected making only β_{i2} remain non-vanishing. As a result, Eqs. (6.37) allow to determine only the dynamics of magnetic-like components

---

[3]We kept the initial value for all the spin components same in order to observe their relative behavior with respect to each other, as well as much smaller than 1 to respect the assumed small polarization limit.

$(C_{\omega X}, C_{\omega Y}, C_{\omega Z})$, which follow the same dynamics given by equations

$$\overset{\bullet}{\beta}_{i2} = -\beta_{i2}\,\theta_U\,. \tag{6.38}$$

Above equations have monotonically increasing solution

$$C_{\omega i} \;=\; C_{\omega i}^0\,\frac{\tau_0}{\tau}\,\frac{\cosh(\xi_0)}{\cosh(\xi)}\,\frac{\mathcal{N}_{(0)}(\tau_0)}{\mathcal{N}_{(0)}}\,, \tag{6.39}$$

where $C_{\omega i}^0$, ξ_0 and $\mathcal{N}_{(0)}(\tau_0)$ are the values of the parameters at τ_0. The solution (6.39) is presented in Fig. 6.3. It shows that the qualitative behavior of $C_{\omega Z}$ component remains same as in Fig. 6.2, whereas the behavior of $C_{\omega X}$ and $C_{\omega Y}$ becomes opposite in the $z \gg 1$ limit.

6.2.2 Angular momentum of a boost-invariant firecylinder

Solutions obtained in the previous section acquire intuitive interpretation when one considers spin and orbital contributions to total angular momentum $J_{\text{FC}}^{\mu\nu} = L_{\text{FC}}^{\mu\nu} + S_{\text{FC}}^{\mu\nu}$ at the hypersurface of fixed longitudinal proper time we call a *firecylinder* (FC). Using the fact that the total angular momentum is conserved, see Eq. (3.45), this will help us with initialization of the spin components in numerical simulations. For this purpose, let us
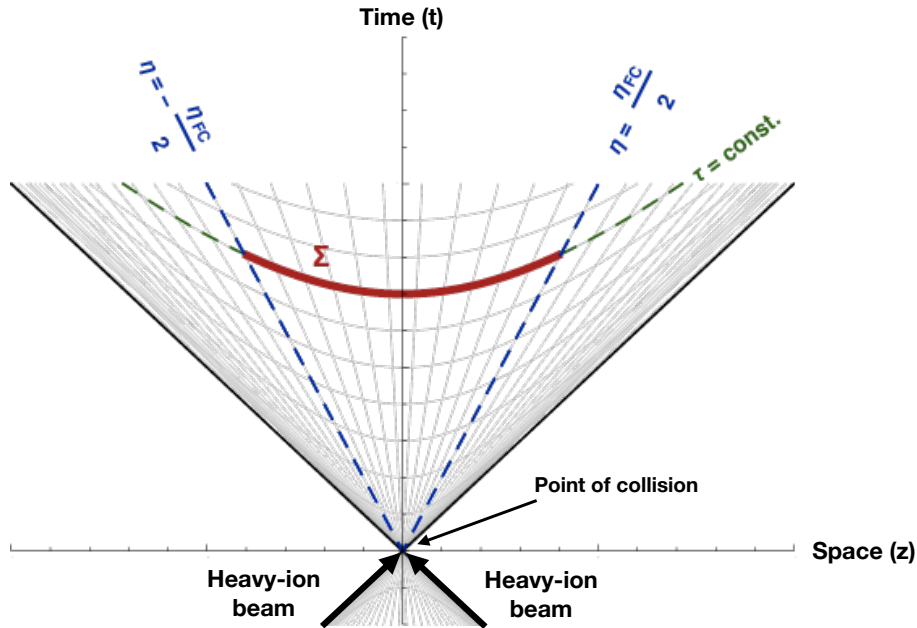

Figure 6.4: (Color online) Schematic diagram of the boost-invariant firecylinder with Σ denoting the hypersurface.

consider a boost-invariant three-dimensional hypersurface defined by $\tau = \tau_{\text{FC}} = \text{const.}$ and contained within the spacetime region defined by conditions $-\eta_{\text{FC}}/2 \leq \eta \leq \eta_{\text{FC}}/2$ and $(x^2 + y^2)^{1/2} \leq R_{\text{FC}}$, with constant radius R_{FC}, see Fig. 6.4. The respective hypersurface element is defined as

$$\Delta\Sigma_\mu \;=\; \tau_{\text{FC}}\,U_\mu\,dx\,dy\,d\eta\,, \tag{6.40}$$

with the flow vector given by Eq. (6.31).

The orbital contribution for the GLW pseudogauge can be calculated as follows

$$
\begin{aligned}
L_{\mathrm{FC}}^{\mu\nu} &= \int \Delta\Sigma_\lambda \, L^{\lambda,\mu\nu} = \int \Delta\Sigma_\lambda \left(x^\mu \, T_{\mathrm{GLW}}^{\lambda\nu} - x^\nu \, T_{\mathrm{GLW}}^{\lambda\mu} \right) , \\
&= \int \tau_{\mathrm{FC}} \, U_\lambda \, dx \, dy \, d\eta \left(x^\mu \, T_{\mathrm{GLW}}^{\lambda\nu} - x^\nu \, T_{\mathrm{GLW}}^{\lambda\mu} \right) , \\
&= \tau_{\mathrm{FC}} \, \pi \, R_{\mathrm{FC}}^2 \int\limits_{-\eta_{\mathrm{FC}}/2}^{\eta_{\mathrm{FC}}/2} \mathcal{E} \, d\eta \left(x^\mu \, U^\nu - x^\nu \, U^\mu \right) ,
\end{aligned}
\tag{6.41}
$$

where, in the last line, we used the fact that U^μ is the eigenvector of the energy-momentum tensor with $\mathcal{E}$ as an eigenvalue,

$$
T_{\mathrm{GLW}}^{\lambda\nu} \, U_\lambda = \mathcal{E} \, U^\nu .
\tag{6.42}
$$

Putting the value of U^μ from Eq. (6.31) in Eq. (6.41) we find that $L_{\mathrm{FC}}^{\mu\nu} = 0$. Hence, the orbital part does not contribute to the total angular momentum for Bjorken-expanding matter.

The respective contribution from the spin part can be calculated as

$$
\begin{aligned}
S_{\mathrm{FC}}^{\mu\nu} &= \int \Delta\Sigma_\lambda \, S_{\mathrm{GLW}}^{\lambda,\mu\nu} = \tau_{\mathrm{FC}} \int dx \, dy \int\limits_{-\eta_{\mathrm{FC}}/2}^{\eta_{\mathrm{FC}}/2} d\eta \, U_\lambda \, S_{\mathrm{GLW}}^{\lambda,\mu\nu} , \\
&= \tau_{\mathrm{FC}} \, \pi \, R_{\mathrm{FC}}^2 \int\limits_{-\eta_{\mathrm{FC}}/2}^{\eta_{\mathrm{FC}}/2} d\eta \, U_\lambda \, S_{\mathrm{GLW}}^{\lambda,\mu\nu} .
\end{aligned}
\tag{6.43}
$$

Using in Eq. (6.43) the relation $U_\lambda \, S_{\mathrm{GLW}}^{\lambda,\mu\nu} = \mathcal{A}_3 \left(\kappa^\mu \, U^\nu - \kappa^\nu \, U^\mu \right) + \mathcal{A}_1 \, \epsilon^{\mu\nu\beta\gamma} \, U_\beta \, \omega_\gamma$, see Eq. (3.43), and integrating over η the spin angular momentum tensor takes the form

$$
S_{\mathrm{FC}}^{\mu\nu} = -S_{\mathrm{FC}}^{\nu\mu} = \begin{bmatrix} 0 & S_{\mathrm{FC}}^{01} & S_{\mathrm{FC}}^{02} & S_{\mathrm{FC}}^{03} \\ -S_{\mathrm{FC}}^{01} & 0 & S_{\mathrm{FC}}^{12} & S_{\mathrm{FC}}^{13} \\ -S_{\mathrm{FC}}^{02} & -S_{\mathrm{FC}}^{12} & 0 & S_{\mathrm{FC}}^{23} \\ -S_{\mathrm{FC}}^{03} & -S_{\mathrm{FC}}^{13} & -S_{\mathrm{FC}}^{23} & 0 \end{bmatrix} ,
\tag{6.44}
$$

with its components expressed by

$$
\begin{aligned}
S_{01}^{\mathrm{FC}} &= -S_{\mathrm{FC}}^{01} = 2\pi R_{\mathrm{FC}}^2 \, \tau_{\mathrm{FC}} \, \mathcal{A}_3 \, C_{\kappa X} \sinh(\eta_{\mathrm{FC}}/2) , \\
S_{02}^{\mathrm{FC}} &= -S_{\mathrm{FC}}^{02} = 2\pi R_{\mathrm{FC}}^2 \, \tau_{\mathrm{FC}} \, \mathcal{A}_3 \, C_{\kappa Y} \sinh(\eta_{\mathrm{FC}}/2) , \\
S_{03}^{\mathrm{FC}} &= -S_{\mathrm{FC}}^{03} = \pi R_{\mathrm{FC}}^2 \, \tau_{\mathrm{FC}} \, \mathcal{A}_3 \, C_{\kappa Z} \, \eta_{\mathrm{FC}} , \\
S_{23}^{\mathrm{FC}} &= S_{\mathrm{FC}}^{23} = -2\pi R_{\mathrm{FC}}^2 \, \tau_{\mathrm{FC}} \, \mathcal{A}_1 \, C_{\omega X} \sinh(\eta_{\mathrm{FC}}/2) , \\
S_{13}^{\mathrm{FC}} &= S_{\mathrm{FC}}^{13} = 2\pi R_{\mathrm{FC}}^2 \, \tau_{\mathrm{FC}} \, \mathcal{A}_1 \, C_{\omega Y} \sinh(\eta_{\mathrm{FC}}/2) , \\
S_{12}^{\mathrm{FC}} &= S_{\mathrm{FC}}^{12} = -\pi R_{\mathrm{FC}}^2 \, \tau_{\mathrm{FC}} \, \mathcal{A}_1 \, C_{\omega Z} \, \eta_{\mathrm{FC}} .
\end{aligned}
\tag{6.45}
$$

We observe that in the boost-invariant and transversely homogeneous system different spin components C are directly related to different components of spin angular momentum tensor $S_{\mathrm{FC}}^{\mu\nu}$, which, due to $L_{\mathrm{FC}}^{\mu\nu} = 0$, are conserved during the evolution.

At this point, it is important to emphasize the physics picture for the spin polarization evolution we have in mind, which will be followed in the analyses presented in the current chapter. We assume, that during the initial stage of the non-central relativistic heavy-ion collision, the total angular momentum (J) consists of only orbital angular momentum (L), the direction of which is perpendicular to the reaction ($x - z$) plane *i.e.* along the $-y$ axis [90, 130, 275, 313], see Fig. 1.2.

This derives its motivation from the experimental measurements of the spin polarization of $\Lambda(\bar{\Lambda})$ hyperons where the average direction of the spin is along $-y$-axis. After the collision some fraction of the orbital angular momentum is transferred, due to initial scatterings, to the initial spin angular momentum (S) [314] which is, on average, along the same direction as the original total angular momentum

$$J_{\text{initial}} = L_{\text{initial}} = L_{\text{final}} + S_{\text{final}}. \tag{6.46}$$

This is reflected by the non-vanishing xz component of spin angular momentum [315]. One may notice from Eq. (6.45) that the spin component $C_{\omega Y}$ is directly linked to the xz component of the spin angular momentum (S_{13}^{FC}). Hence, the situation discussed here can be reproduced in the numerical simulation of Bjorken-expanding system by assuming non-vanishing and positive component $C_{\omega Y}(\tau_{\text{FC}} = \tau_0)$ and keeping all the other spin components zero.

6.2.3 Spin polarization at freeze-out

Having the collective dynamics of the system determined in previous sections, we now use it to calculate the spin polarization of particles emitted from the fluid at the freeze-out. Due to simplifications resulting from the Bjorken symmetries, the phase-space density of the PL four-vector (5.8) as well as the momentum density of all particles (5.13) can be calculated analytically allowing us to write the following expressions of average spin polarization (5.14) as a function of particle momentum, in PRF,

$$\langle \pi_\mu \rangle_p = \frac{1}{8m} \begin{bmatrix} 0 \\ \chi \, C_{\omega X} \, m_T{}^2 - 2 \, C_{\kappa Z} \, p_y - \left(\frac{p_x \, p_z}{E_p + m} \right) [\chi \, (C_{\kappa X} \, p_y - C_{\kappa Y} \, p_x) + 2 \, C_{\omega Z}] \\ - \frac{1}{E_p + m} (\chi \, p_x \, E_p \, (C_{\omega X} p_x + C_{\omega Y} p_y)) \\ \chi \, C_{\omega Y} \, m_T{}^2 + 2 \, C_{\kappa Z} \, p_x - \left(\frac{p_y \, p_z}{E_p + m} \right) [\chi \, (C_{\kappa X} \, p_y - C_{\kappa Y} \, p_x) + 2 \, C_{\omega Z}] \\ - \frac{1}{E_p + m} (\chi \, p_y \, E_p \, (C_{\omega X} p_x + C_{\omega Y} p_y)) \\ \left(\frac{m \, E_p + m_T{}^2}{E_p + m} \right) [\chi \, (C_{\kappa X} \, p_y - C_{\kappa Y} \, p_x) + 2 \, C_{\omega Z}] + \frac{\chi \, m \, p_z (C_{\omega X} \, p_x + C_{\omega Y} \, p_y)}{E_p + m} \end{bmatrix} \tag{6.47}$$

where $\chi = (K_0 (\hat{m}_T) + K_2 (\hat{m}_T)) / (m_T K_1 (\hat{m}_T))$ and $\hat{m}_T$ is the ratio of the transverse mass over temperature, $\hat{m}_T = m_T / T$. Note that the time component of $\langle \pi_\mu \rangle_p$ vanishes. Indeed, since $\langle \pi_\mu \rangle_p \langle \pi^\mu \rangle_p$ is a Lorentz-invariant quantity, one can write $\langle \pi_\mu \rangle_p p_*^\mu = \langle \pi_0 \rangle_p m = 0$. Using the numerical results of the thermodynamic parameters from Eqs. (6.33) and (6.34), and the spin components from Eqs. (6.37), from Eq. (6.47) we can obtain x, y, and z components of $\langle \pi_\mu \rangle_p$ as a function of p_x and p_y at midrapidity ($y_p = 0$). In Figs. 6.5 we show plots for $\langle \pi_x \rangle_p$ (top panel) and $\langle \pi_y \rangle_p$ (bottom panel) at midrapidity (one can check that at midrapidity, $\langle \pi_z \rangle_p$ vanishes). The component $\langle \pi_y \rangle_p$ has negative magnitude
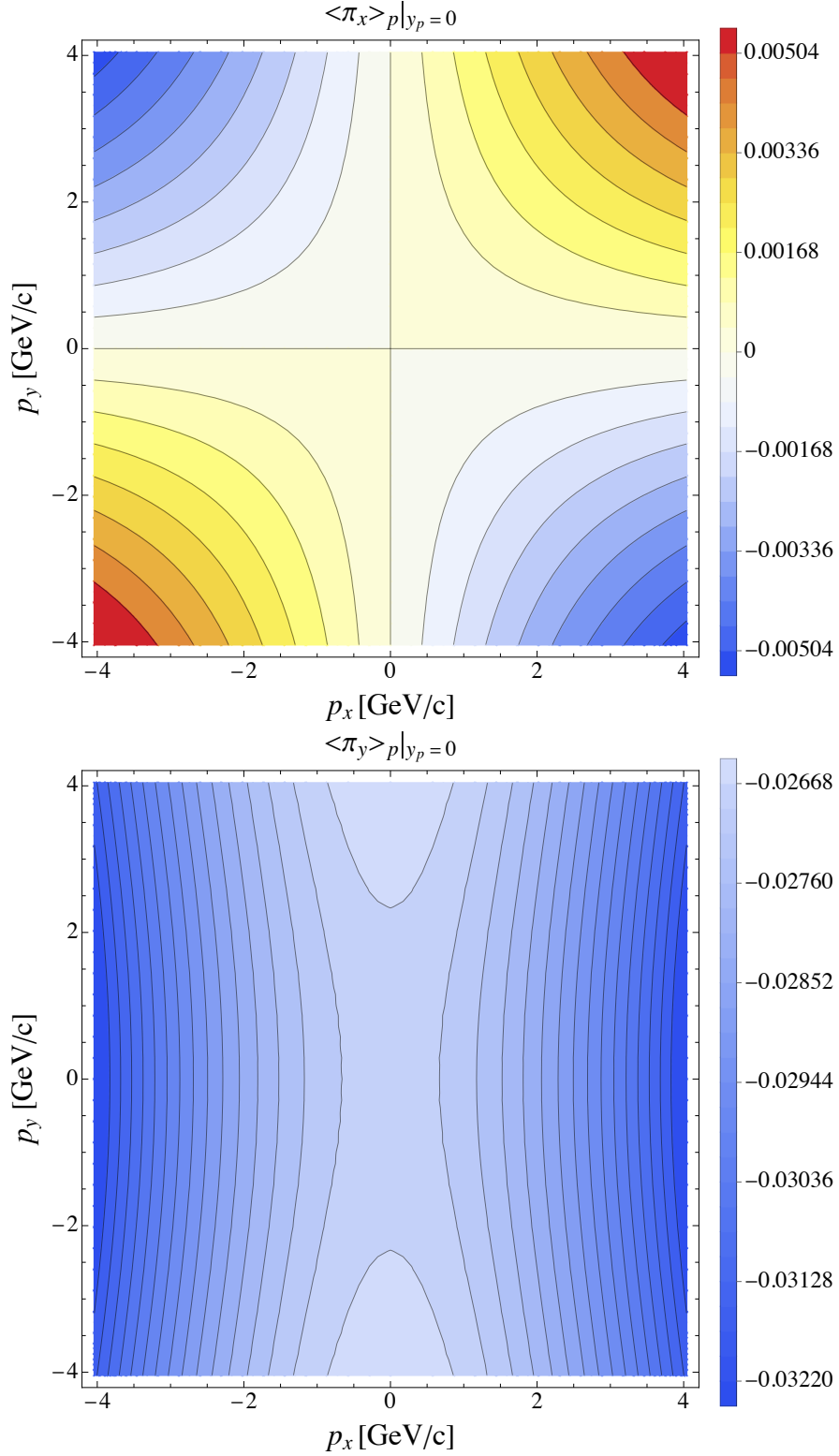
Figure 6.5: (Color online) The x component (top panel) and y component (bottom panel) of the mean spin polarization per particle at midrapidity as a function of p_x and p_y for the Bjorken-expanding matter.

reflecting the initial direction of the spin in the system, whereas the component $\langle \pi_x \rangle_p$ exhibits a quadrupole structure depicting non-trivial momentum dependence of Eq. (6.47).

We note that the results presented here do not reproduce the experimentally observed

polarization measurements, which is primarily due to the symmetries involved in the Bjorken expansion. In particular, our results do not capture the quadrupole structure of the longitudinal spin polarization $\langle \pi_z \rangle_p$ at midrapidity [130], which is expected to arise due to the flow gradients in the transverse plane (anisotropic flow resulting from the elliptic deformation of the system) [129]. Obviously, such mechanism may be addressed only in the framework which relaxes assumption of transverse homogeneity [4].

6.3 Non-boost-invariant and transversely homogeneous background

The experimental results from the STAR Collaboration clearly show the decrease of the amplitude of global polarization as a function of center-of-mass energy, with its values approaching zero at top RHIC and LHC energies, see Fig. 1.4. This makes the low- and mid-energy collisions most interesting from the point of view of polarization phenomenology. On the other hand, the Bjorken model is known of being too restrictive on its assumptions in this region. In this section we try to, partially, address this issue. In what follows, we extend the study done in Section 6.2 by relaxing the symmetry of boost-invariance while keeping assumption of homogeneity of the system in the transverse plane. Details of the study presented in this section may be found in Ref. [D3].

6.3.1 Four-vector basis and spin polarization components

By relaxing the boost-invariance of the produced matter in the beam direction we need to account for possible flow gradients which may build up along the beam direction. This is done by introducing a deviation in the flow-vector (6.31) in the following way

$$U^\alpha \;=\; (\cosh(\Phi),\, 0,\, 0,\, \sinh(\Phi))\,, \tag{6.48}$$

where, as mentioned before, $\Phi = \vartheta(\tau, \eta) + \eta$, and we kept transverse components zero due to homogeneity in $x - y$ plane. The remaining basis vectors, see Eqs. (6.3), take the forms

$$X^\alpha \;=\; (0, 1, 0, 0)\,, \qquad Y^\alpha \;=\; (0, 0, 1, 0)\,, \qquad Z^\alpha \;=\; (\sinh(\Phi),\, 0,\, 0,\, \cosh(\Phi))\,. \tag{6.49}$$

The directional derivatives (6.4) and the divergences (6.5) read

$$U \cdot \partial \;=\; \cosh(\vartheta)\,\partial_\tau + \frac{\sinh(\vartheta)}{\tau}\partial_\eta\,, \qquad Z \cdot \partial \;=\; \sinh(\vartheta)\,\partial_\tau + \frac{\cosh(\vartheta)}{\tau}\partial_\eta\,,$$
$$X \cdot \partial \;=\; \partial_x\,, \qquad Y \cdot \partial \;=\; \partial_y\,, \tag{6.50}$$
$$\partial_\alpha U^\alpha \;=\; \frac{\cosh(\vartheta)}{\tau} + \overset{\circ}{\vartheta}\,, \qquad \partial_\alpha Z^\alpha \;=\; \frac{\sinh(\vartheta)}{\tau} + \overset{\bullet}{\vartheta}\,, \tag{6.51}$$

respectively. Since all the scalar functions must depend now on τ and η, one has $\partial \cdot X = \partial \cdot Y = 0$.

---

[4] We note that in the spin-thermal based models quadrupole structure in the longitudinal spin polarization component, comes, albeit with an opposite sign, from the imposed coupling between vorticity and polarization [132].

6.3.2 Background dynamics

In the case of the non-boost-invariant expansion, equations resulting from baryon density conservation and energy-momentum conservation, (6.7) and (6.8)–(6.9), respectively, are used together with the expressions listed in Section 6.3.1. However, unlike in the case of Bjorken expansion, see Section 6.2.1, this time the relativistic Euler equation (6.9) has one non-trivial (z) component,

$$\left(\mathcal{E} + \mathcal{P}\right) U^\beta \partial_\beta \sinh(\Phi) - \left(\partial^z - \sinh(\Phi) U^\beta \partial_\beta\right) \mathcal{P} \;=\; 0\,. \tag{6.52}$$

As a result, we are left with three partial differential equations in $\tau - \eta$ space to be solved for temperature, baryon chemical potential, and longitudinal fluid rapidity correction.
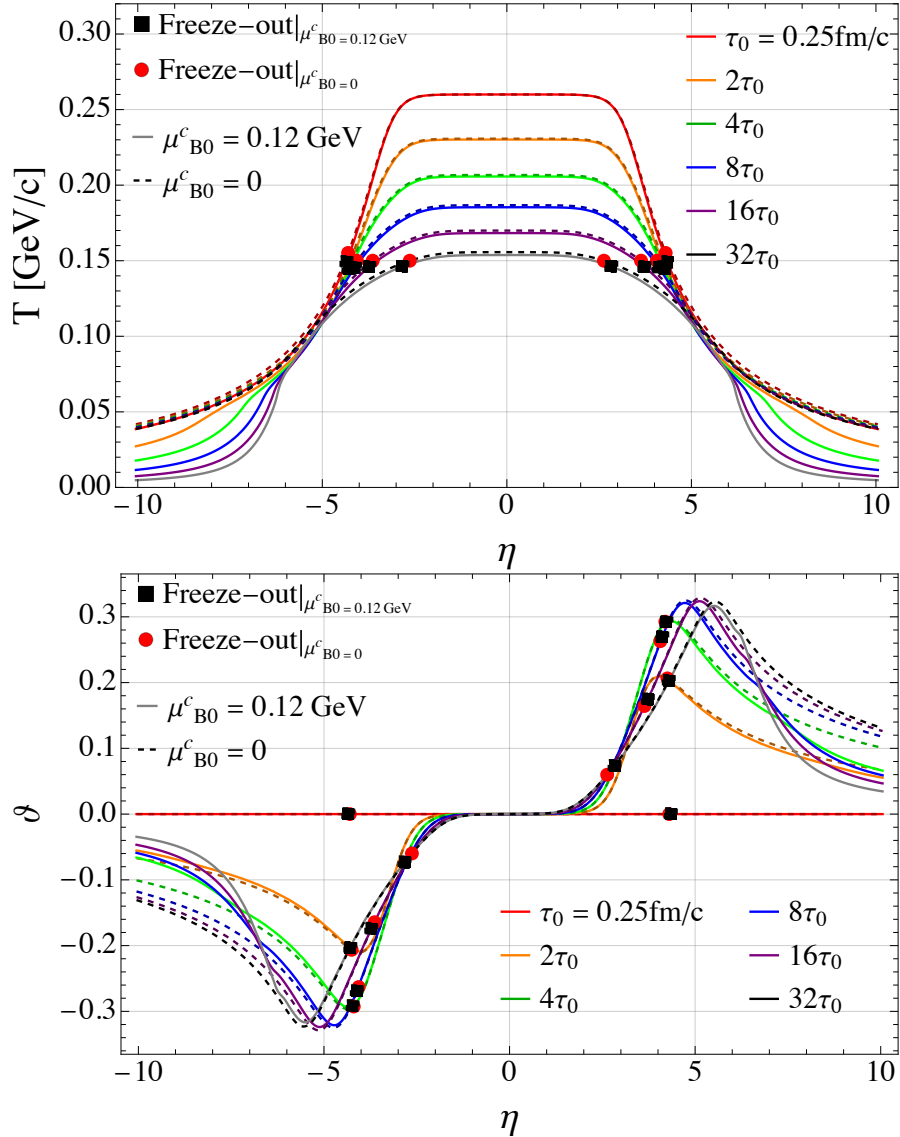

Figure 6.6: (Color online) Temperature (top panel) and fluid rapidity (bottom panel) evolution in η at various τ. Solid and dashed lines represent non-vanishing and vanishing baryon chemical potential, respectively. The black and red symbols denote freeze-out points at different times.

To model the non-trivial rapidity dependence of the initial energy density $\mathcal{E}_0(\eta) =$

$\mathcal{E}(\tau_0, \eta)$ deposited in the collision we introduce the profile

$$
\mathcal{E}_0(\eta) \;=\; \frac{\mathcal{E}_0^c}{2}\left[\Theta(\eta)\Big(\tanh(a - \eta\,b) + 1\Big) \;+\; \Theta(-\eta)\Big(\tanh(a + \eta\,b) + 1\Big)\right], \quad (6.53)
$$

with $a = 6.2$, $b = 1.9$, and Θ denoting the Heaviside step function [316]. Here, $\mathcal{E}_0^c = \mathcal{E}(T_0^c, \mu_{B0}^c)$ is the initial energy density at the center ($\eta = 0$) calculated from Eq. (3.33) at the initial central temperature T_0^c and baryon chemical potential μ_{B0}^c (note that we assume $\zeta \to 0$ herein). In numerical simulations we use $T_0^c = T(\tau_0, \eta = 0) = 0.26$ GeV. In the case of baryon chemical potential profile we consider $\mu_{B0}(\eta) = \mu_{B0}^c = \text{const.}$ with two possibilities: either we choose vanishing baryon chemical potential $\mu_{B0}^c = 0$ (resembling conditions present at the high-energy experiments), or we pick $\mu_{B0}^c = 0.12$ GeV (to address possible effects coming from baryon chemical potential present at lower energies). Throughout we assume the initial longitudinal flow profile to have the Bjorken form $\Phi_0(\eta) = \eta$.

Figure 6.6 shows the evolution for T (top panel) and ϑ (bottom panel) as a function of space-time rapidity for different longitudinal proper times τ with initial $\tau_0 = 0.25$ fm/c. The dashed lines represent $\mu_{B0}^c = 0$ and solid lines denote $\mu_{B0}^c = 0.12$ GeV. We find that the temperature evolution is η-even similar to the evolution of baryon chemical potential, see Fig. 6.7, while the evolution of the fluid rapidity is η-odd. At midrapidity ($\eta = 0$), temperature decreases in τ, similarly to the Bjorken case, see Fig. 6.1. Moreover, we observe that at large $|\eta|$ the energy density gradients lead to the buildup of fluid velocity gradients. One may also notice the steep decay in T and ϑ evolution at $\eta \approx \pm 5$ in the case of non-zero baryon chemical potential. Up to this effect, the baryon chemical potential has no significant effect on the evolution of the background parameters.
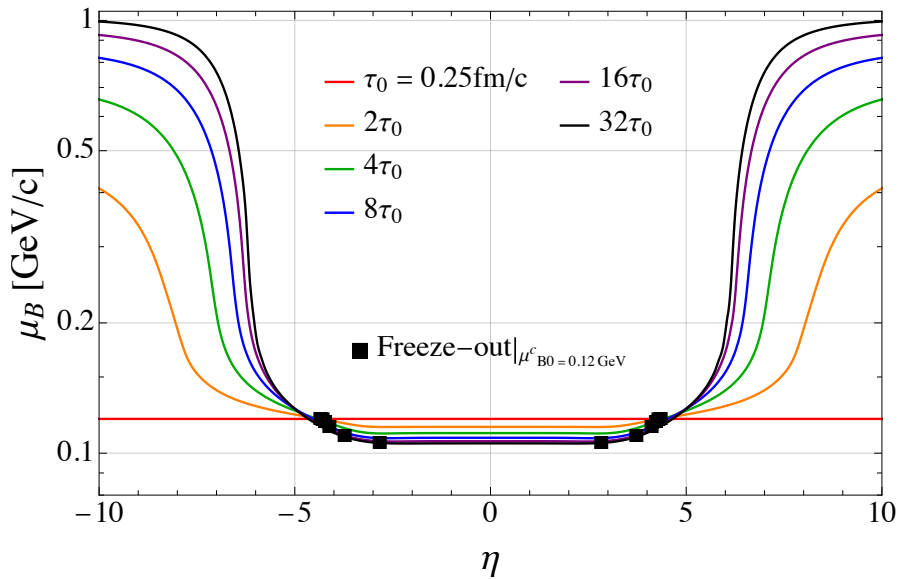

Figure 6.7: (Color online) Baryon chemical potential evolution in η at various τ.

6.3.3   Spin dynamics

The dynamics in the spin sector follows from Eqs. (6.25)–(6.30) which in the boost-invariance-breaking case reduce to

$$\overset{\bullet}{\alpha}_{x1} + \overset{\circ}{\beta}_{y1} = -\alpha_{x1}\,\theta_U - \frac{\alpha_{x2}\,U\overset{\circ}{Z}}{2} - \beta_{y1}\,\theta_Z + \beta_{y2}\,U\overset{\bullet}{Z}\,, \tag{6.54}$$

$$\overset{\bullet}{\alpha}_{y1} - \overset{\circ}{\beta}_{x1} = -\alpha_{y1}\,\theta_U - \frac{\alpha_{y2}\,U\overset{\circ}{Z}}{2} + \beta_{x1}\,\theta_Z - \beta_{x2}\,U\overset{\bullet}{Z}\,, \tag{6.55}$$

$$\overset{\bullet}{\alpha}_{z1} = -\alpha_{z1}\,\theta_U\,, \tag{6.56}$$

$$\frac{\overset{\circ}{\alpha}_{y2}}{2} + \overset{\bullet}{\beta}_{x2} = -\frac{\alpha_{y2}\,\theta_Z}{2} + \alpha_{y1}\,Z\overset{\bullet}{U} - \beta_{x2}\,\theta_U - \beta_{x1}\,Z\overset{\circ}{U}\,, \tag{6.57}$$

$$\frac{\overset{\circ}{\alpha}_{x2}}{2} - \overset{\bullet}{\beta}_{y2} = -\frac{\alpha_{x2}\,\theta_Z}{2} + \alpha_{x1}\,Z\overset{\bullet}{U} + \beta_{y2}\,\theta_U + \beta_{y1}\,Z\overset{\circ}{U}\,, \tag{6.58}$$

$$\overset{\bullet}{\beta}_{z2} = -\beta_{z2}\,\theta_U\,, \tag{6.59}$$

where

$$U\overset{\circ}{Z} = -Z\overset{\circ}{U} = \cosh(\vartheta)\,(1 + \partial\vartheta/\partial\eta)\,/\tau + \sinh(\vartheta)\,\partial\vartheta/\partial\tau\,,$$

and

$$U\overset{\bullet}{Z} = -Z\overset{\bullet}{U} = \sinh(\vartheta)\,(1 + \partial\vartheta/\partial\eta)\,/\tau + \cosh(\vartheta)\,\partial\vartheta/\partial\tau\,.$$

Note that, in contrast to the case of Bjorken expansion, in the present case some spin components in the above equations are coupled, cf. Eqs. (6.37). In particular, from Eqs. (6.54) and (6.58) one observes that this is the case for $C_{\kappa X}$ and $C_{\omega Y}$. Similarly, the coupling concerns $C_{\kappa Y}$ and $C_{\omega X}$, which is evident from Eqs. (6.55) and (6.57). This does not apply to longitudinal spin components $C_{\kappa Z}$ and $C_{\omega Z}$ which evolve independently from others.

In the numerical simulations, we follow the initialization scheme of the spin components C which results from the physical considerations discussed in Section 6.2.2. Since at the initial time $\vartheta_0(\eta) = 0$ (representing Bjorken flow profile), the non-vanishing y-component of the spin angular momentum at the initial time is related to the component $C_{\omega Y}$ and it requires $C_{\omega Y}$ to be symmetric in η, see Appendix A for more details. Hence, it is enough, at the initial time, if we choose

$$C^0_{\omega Y}(\eta) = C_{\omega Y}(\tau_0, \eta) = \frac{d}{\cosh(\eta)}\,, \tag{6.60}$$

where $d = 0.1$, and keep all other spin components zero to obtain the y-component of $S^{\mu\nu}_{\text{FC}}$.

With the help of the following relations between the parameterizations (4.7) and (4.8) of the spin polarization tensor,

$$
\begin{aligned}
C_{\kappa X} &= e^1\cosh(\Phi) - b^2\sinh(\Phi)\,, & e^1 &= C_{\kappa X}\cosh(\Phi) + C_{\omega Y}\sinh(\Phi)\,, & (6.61)\\
C_{\kappa Y} &= e^2\cosh(\Phi) + b^1\sinh(\Phi)\,, & e^2 &= C_{\kappa Y}\cosh(\Phi) - C_{\omega X}\sinh(\Phi)\,, & (6.62)\\
C_{\kappa Z} &= e^3\,, & & & (6.63)\\
C_{\omega X} &= b^1\cosh(\Phi) + e^2\sinh(\Phi)\,, & b^1 &= C_{\omega X}\cosh(\Phi) - C_{\kappa Y}\sinh(\Phi)\,, & (6.64)\\
C_{\omega Y} &= b^2\cosh(\Phi) - e^1\sinh(\Phi)\,, & b^2 &= C_{\kappa X}\sinh(\Phi) + C_{\omega Y}\cosh(\Phi)\,, & (6.65)\\
C_{\omega Z} &= b^3\,, & & & (6.66)
\end{aligned}
$$

the respective initial LAB frame spin components e^1 and b^2 are initialized as

$$e_0^1(\eta) \;=\; e^1(\tau_0, \eta) \;=\; d \tanh(\eta), \qquad b_0^2(\eta) \;=\; b^2(\tau_0, \eta) = d. \qquad (6.67)$$

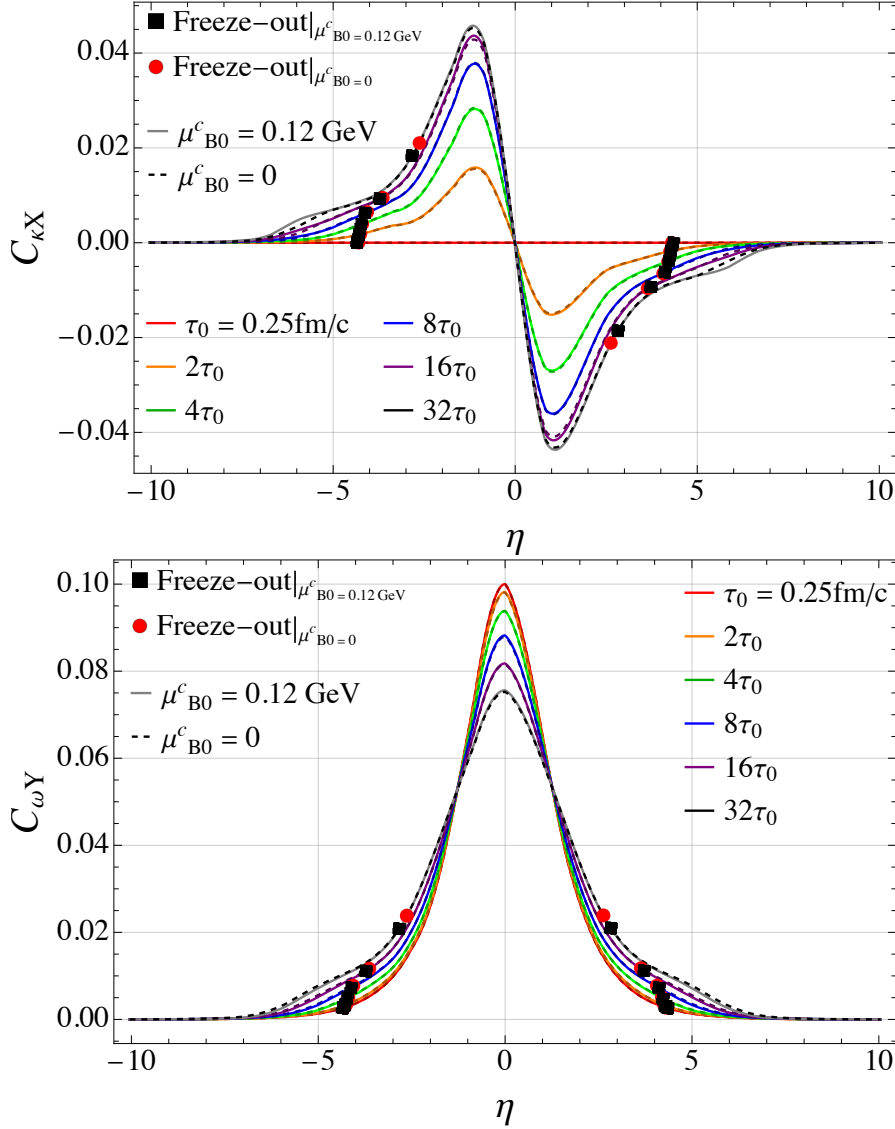In Fig. 6.8 we present results of numerical simulations for spin components $C_{\kappa X}$ and $C_{\omega Y}$.

Figure 6.8: (Color online) Evolution of the coefficients $C_{\kappa X}$ (top panel) and $C_{\omega Y}$ (bottom panel). Solid and dashed lines represent non-vanishing and vanishing baryon chemical potential, respectively.

As discussed above, although initially chosen to be zero, $C_{\kappa X}$ component undergoes non-trivial evolution due to its coupling to $C_{\omega Y}$ through Eqs. (6.54) and (6.58) (obviously, all other spin components remain zero). The symmetry in η of $C_{\kappa X}$ and $C_{\omega Y}$ remains intact throughout the evolution, which is governed by the evolution equations (6.54) and (6.58), along with the initial condition (6.60). One can observe effects of background evolution on spin, appearing in spin equations of motion through the thermodynamic coefficients (6.17). Similarly to temperature, see Fig. 6.6, the coefficient $C_{\omega Y}$ also decreases in time, at the center, reproducing the Bjorken behavior observed in Fig. 6.2. However, at the edges ($\eta \approx \pm 5$), as the system enters the large mass limit regime, the spin dynamics gets reversed

which means that the magnitude of $C_{\omega Y}$ starts to increase with τ. This is also the case for the spin components in the Bjorken expansion, see Fig. 6.3. In Fig. 6.8 we also observe that the presence of homogeneous non-zero, but small, baryon chemical potential is almost irrelevant for spin dynamics, which is understood since baryon chemical potential enters only through $\cosh(\xi)$ in the thermodynamic coefficients (6.17).

6.3.4 Spin polarization at freeze-out

After exploring the collective dynamics of the spin polarization components, we calculate the average spin polarization of the particles emitted at the freeze-out to assess implications of the dynamics for the measured observables. As the freeze-out times (τ_{FO}) depend on the space-time rapidity of the fluid cells, see black and red symbols in Fig. 6.6, in the current analysis, first we need to define the freeze-out hypersurface (Σ_μ) appearing in the phase-space density of the PL four-vector (5.8) accordingly. In consequence, the resulting factor $\Delta\Sigma \cdot p$ is

$$\Delta\Sigma \cdot p \;\; = \;\; m_T \left[\tau_{\text{FO}}(\eta) \cosh\left(y_p - \eta\right) - \tau'_{\text{FO}}(\eta) \sinh\left(y_p - \eta\right) \right] dx\, dy\, d\eta, \qquad (6.68)$$

while the thermal factor has the form

$$\beta \cdot p \;\; = \;\; \frac{U \cdot p}{T} \;\; = \;\; \frac{m_T}{T} \cosh\left(y_p - \Phi\right). \qquad (6.69)$$

Furthermore, the product of the dual polarization tensor $\overset{\star}{\omega}_{\mu\beta}$ with p^β is

$$\overset{\star}{\omega}_{\mu\beta} p^\beta \;\; = \;\; \begin{bmatrix} \left(C_{\kappa X} p_y - C_{\kappa Y} p_x\right) \sinh(\Phi) + \left(C_{\omega X} p_x + C_{\omega Y} p_y\right) \cosh(\Phi) + C_{\omega Z} m_T \sinh\left(y_p\right) \\[2mm] -C_{\kappa Y} m_T \sinh\left(y_p - \Phi\right) - C_{\omega X} m_T \cosh\left(y_p - \Phi\right) + C_{\kappa Z} p_y \\[2mm] C_{\kappa X} m_T \sinh\left(y_p - \Phi\right) - C_{\omega Y} m_T \cosh\left(y_p - \Phi\right) - C_{\kappa Z} p_x \\[2mm] -\left(C_{\kappa X} p_y - C_{\kappa Y} p_x\right) \cosh(\Phi) - \left(C_{\omega X} p_x + C_{\omega Y} p_y\right) \sinh(\Phi) - C_{\omega Z} m_T \cosh\left(y_p\right) \end{bmatrix}, \qquad (6.70)$$

which after Lorentz transformation to the PRF becomes

$$\left(\overset{\star}{\omega}_{\mu\beta} p^\beta\right)^* \;\; = \;\; \begin{bmatrix} 0 \\[2mm] m\,\alpha_p p_x p_y \left[C_{\kappa X} \sinh(\Phi) + C_{\omega Y} \cosh(\Phi)\right] \\[2mm] \begin{aligned} & m\,\alpha_p p_y^2 \left[C_{\kappa X} \sinh(\Phi) + C_{\omega Y} \cosh(\Phi)\right] \\ & - m_T \left[C_{\kappa X} \sinh\left(\Phi - y_p\right) + C_{\omega Y} \cosh\left(\Phi - y_p\right)\right] \end{aligned} \\[2mm] -m\,\alpha_p p_y \left[m_T \left(C_{\kappa X} \cosh\left(\Phi - y_p\right) + C_{\omega Y} \sinh\left(\Phi - y_p\right) \right) + m \left(C_{\kappa X} \cosh(\Phi) + C_{\omega Y} \sinh(\Phi) \right) \right] \end{bmatrix}, \qquad (6.71)$$

where $\alpha_p \equiv 1/(m^2 + m E_p)$ [232]. Note that in the above equation we have kept only $C_{\kappa X}$ and $C_{\omega Y}$ as these are the ones non-vanishing for the current numerical analysis.

Putting Eq. (6.71) in Eq. (5.14) we calculate the average spin polarization per particle as a function of momentum coordinates. The results of this procedure for the case of

vanishing baryon chemical potential at midrapidity and forward rapidity are shown in Figs. 6.9–6.11. As we have shown above, see Fig. 6.8, the non-vanishing baryon chemical potential has very little effect on the spin dynamics. We verified that the same applies to momentum dependent polarization, hence we restrain from showing these results here.

Figure 6.9 shows the $\langle \pi_x \rangle_p$ component of the mean polarization vector which has quadrupole structure with the sign changing sequentially through the subsequent quadrants. Similar results were found in the case with Bjorken expansion, see Fig. 6.5 (top panel). One can notice that this quadrupole structure is arising because of the $p_x p_y$ term in the x component of $(\overset{\star}{\omega}_{\mu\beta} p^\beta)^*$, see Eq. (6.71). One observes that the magnitude of this component decreases with rapidity.

The y component of polarization vector $\langle \pi_y \rangle_p$, shown in Fig. 6.10, is negative, depicting the direction of the spin angular momentum assumed in the initialization of the hydrodynamic equations. Its magnitude decreases with increasing rapidity and eventually becomes independent of ϕ_p.

From the experimental point of view the most interesting is the polarization measured along the beam (z) direction, i.e. longitudinal spin polarization [130, 139] which is still awaiting clear explanation. This component is given by the quantity $\langle \pi_z \rangle_p$. Using symmetry arguments in Eqs. (5.8) and (6.71), one can immediately obtain important information about the $\langle \pi_z \rangle_p$ quantity. Note that the symmetric integration range in η, makes only the contribution of η-even integrands relevant. Thus, due to the assumption of $C_{\kappa X}$ and $C_{\omega Y}$ being odd and even function of η, respectively, makes $\langle \pi_z \rangle_p$ vanish at midrapidity ($y_p = 0$). On the other hand, at forward rapidity we observe non-trivial longitudinal polarization pattern, see Fig. 6.11. We note that, similarly to the Bjorken expansion case, the results shown here do not reproduce the quadrupole structure of the longitudinal spin polarization seen in the experiments primarily due to the homogeneity in the transverse plane.

From the experimental viewpoint, apart from calculating multiple-differential spin polarization vector it is useful to consider integrated $\langle \pi_\mu \rangle$ components (note missing index p). In particular, in order to get the spin polarization $\langle \pi_\mu \rangle$ we integrate Eq. (5.14) over momentum coordinates.

We find that the initialization of the parameters that we adopted and the symmetry properties of the spin polarization components allow only y component of $\langle \pi_\mu \rangle$ to be non-vanishing (and negative).

Figure 6.12 (top panel) shows the behavior of the global polarization as a function of rapidity. At midrapidity the magnitude of $\langle \pi_y \rangle$ component is maximal and then it decreases in forward rapidities indicating that most of the hyperon polarization is coming from the midrapidity region. This behaviour is qualitatively similar to other models [170] and is a subject of future experiments [317]. One can notice that the magnitude of $\langle \pi_y \rangle$ at $y_p = 0$ is qualitatively similar to the one obtained in the global polarization measurements [90], see Fig. 1.4.

We also study the relation between the final polarization ($\langle \pi_y \rangle$) and the initial value of the spin component (b_0^2) at midrapidity and forward rapidity, which we show in Fig. 6.12 (bottom panel). We observe that $\langle \pi_y \rangle$ depends linearly on b_0^2 for, both, vanishing and non-vanishing baryon chemical potential. Notice that, for $b_0^2 = 0.1$, as considered in the current analysis, the magnitude of $\langle \pi_y \rangle$ is about 1.6% ($y_p = 0$) as depicted also in the top panel of Fig. 6.12, however, interestingly for $b_0^2 = 0.3$, magnitude of $\langle \pi_y \rangle$ is about 5% at midrapidity which, qualitatively, agrees with the magnitude of spin polarization of Λ hyperons observed in the low-energy heavy-ion collisions [137].

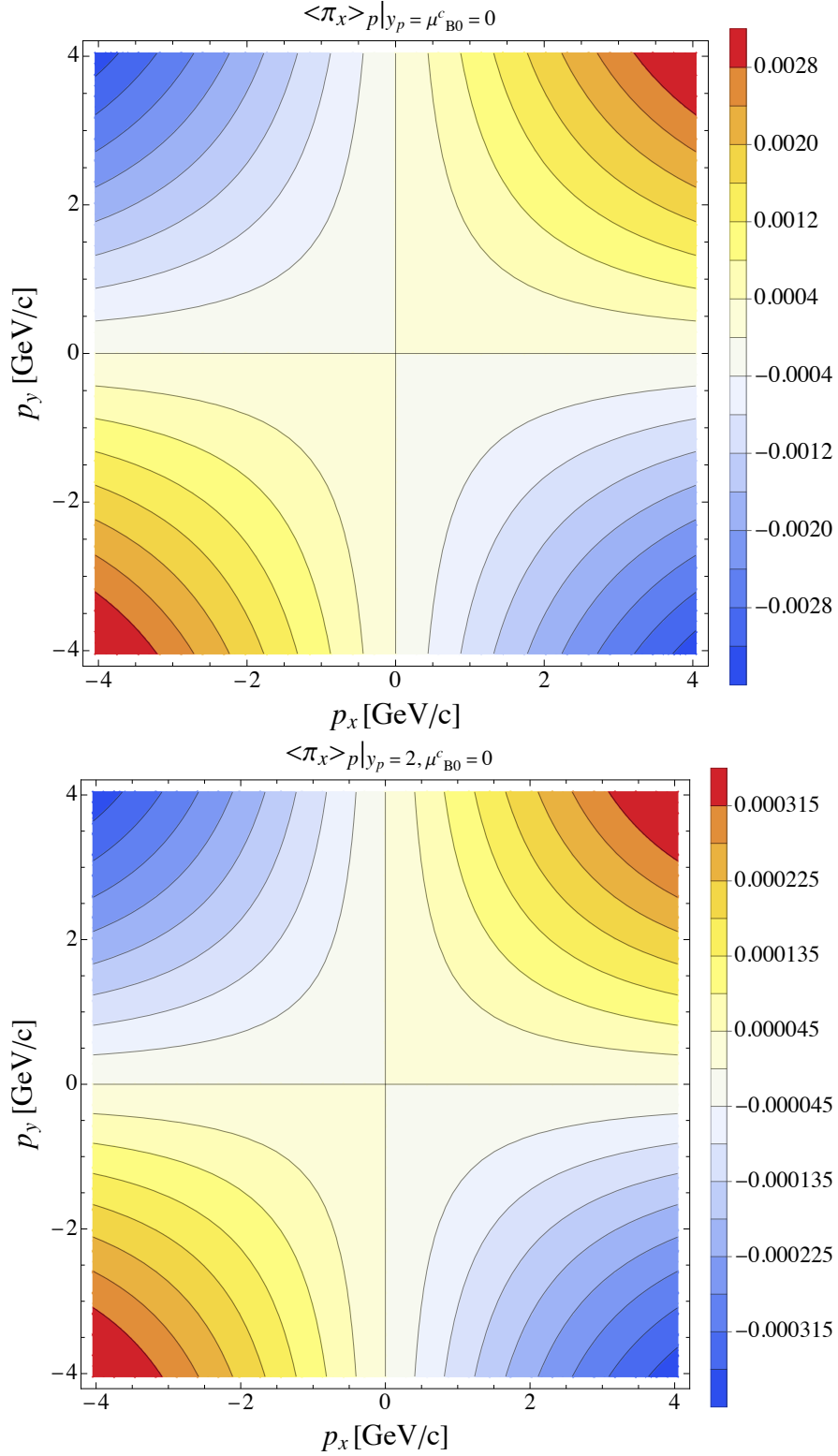It is also interesting to find how spin polarization behaves with respect to transverse mo-

Figure 6.9: (Color online) The x component of the mean spin polarization per particle (5.14) at midrapidity (top panel) and forward rapidity (bottom panel) as a function of p_x and p_y for the non-boost invariant system with vanishing baryon chemical potential.

mentum (p_T) and azimuthal angle (ϕ_p). This may provide important information about the dynamics of spin polarization in the transverse-momentum plane. Integrating Eq. (5.14) over transverse momentum and azimuthal angle gives global polarization as a function of
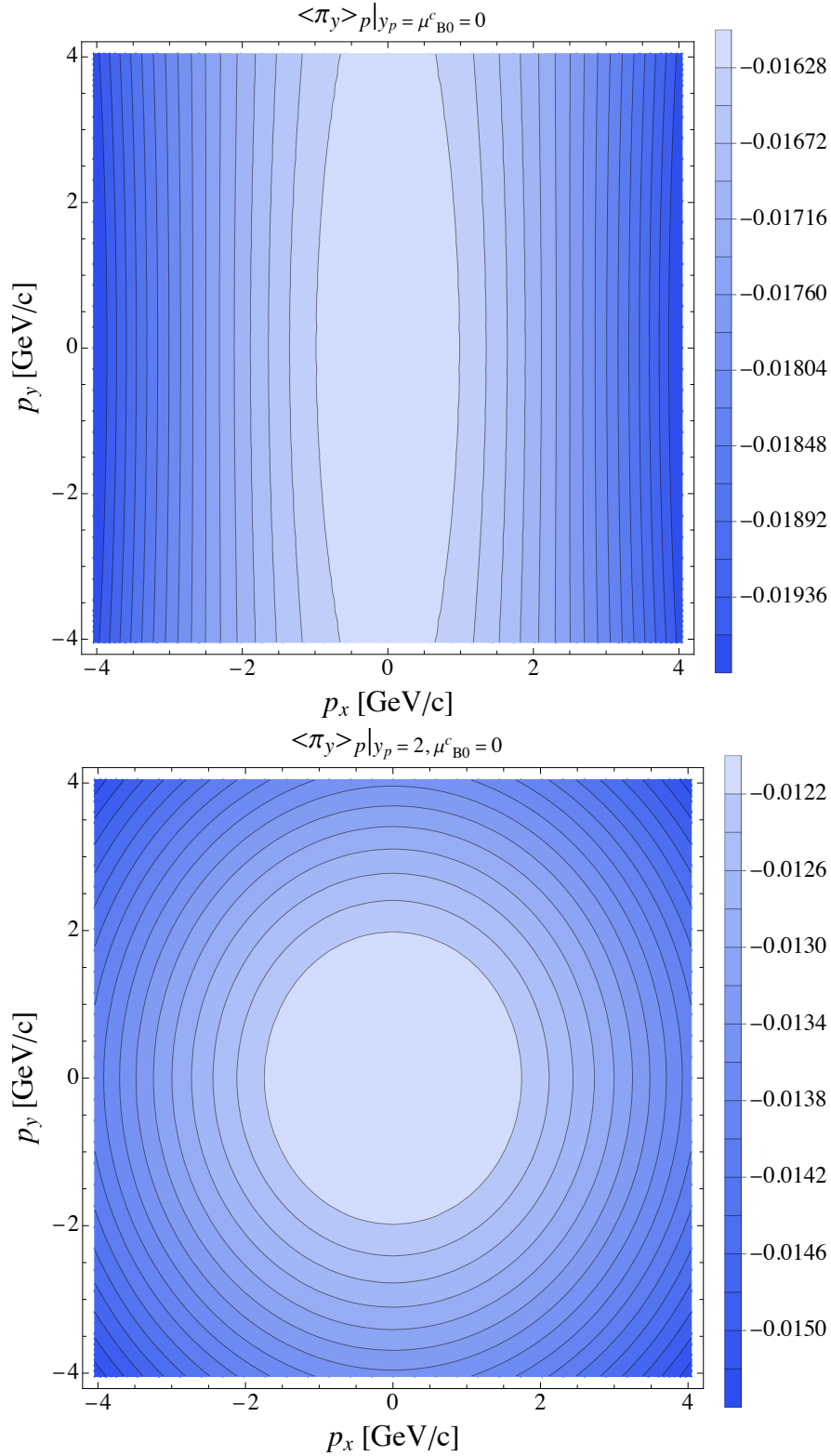
Figure 6.10: (Color online) Same as Fig. 6.9 but for y-component.

ϕ_p and p_T, respectively which can be calculated as follows [181]

$$\langle \pi_\mu(\phi_p) \rangle = \frac{\int p_T \, dp_T \, E_p \frac{d\Pi^*_\mu(p)}{d^3 p}}{\int d\phi_p \, p_T \, dp_T \, E_p \frac{d\mathcal{N}(p)}{d^3 p}} , \qquad \langle \pi_\mu(p_T) \rangle = \frac{\frac{1}{2\pi} \int d\phi_p \, \sin(2\phi_p) \, E_p \frac{d\Pi^*_\mu(p)}{d^3 p}}{\int d\phi_p \, E_p \frac{d\mathcal{N}(p)}{d^3 p}} . \quad (6.72)$$

102
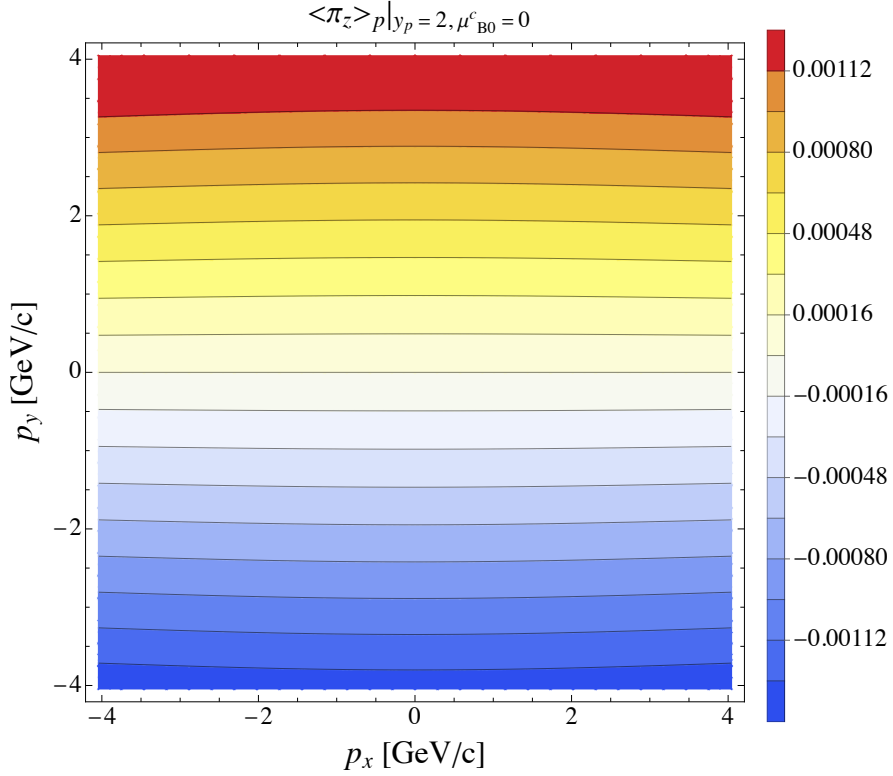
Figure 6.11: (Color online) The z component of the mean spin polarization per particle (5.14) at forward rapidity as a function of p_x and p_y for the non-boost invariant background with vanishing baryon chemical potential.

Figure 6.13 shows the behavior of $\langle \pi_y \rangle$ with respect to p_T (top panel) and ϕ_p (bottom panel). The p_T dependence is found to be strong as compared to other models [170] and the experiments [96] which may be because we assume non-zero initial spin polarization which then evolves in time. On the other hand, if p_T dependence is weak then it probably means that polarization is arising due to spin-orbit coupling which is not present in the current formulation of our framework. The behaviour of ϕ_p dependence of polarization is more pronounced at midrapidity which, within the range of $0 < \phi_p < \pi/2$, is qualitatively similar to the polarization behavior in the experiments [96, 170]. In general, we find that the effect of non-zero baryon chemical potential on $\langle \pi_y \rangle$ is small, and has opposite effect in forward rapidity and midrapidity.
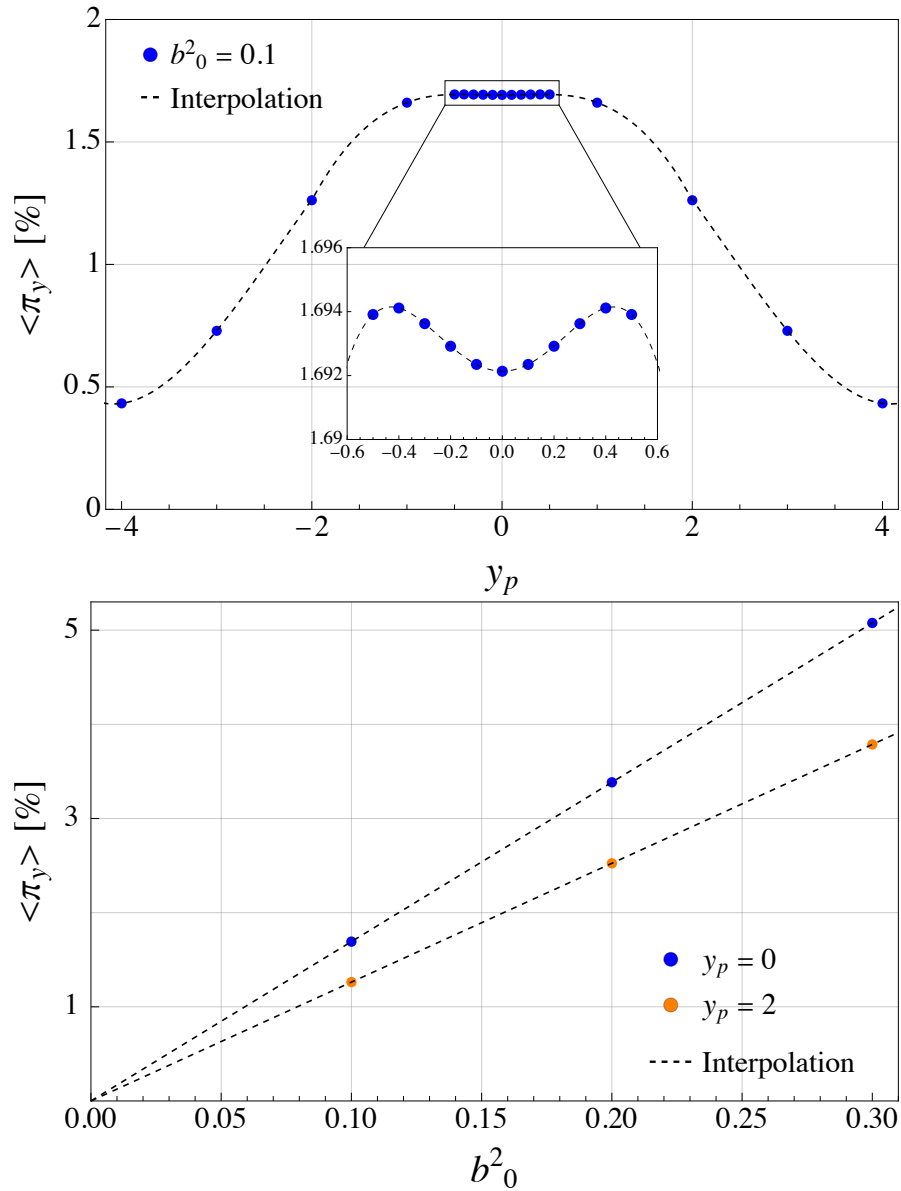
Figure 6.12: (Color online) Global spin polarization, $\langle \pi_y \rangle$, as a function of rapidity (top panel) and spin coefficient b_0^2 (bottom panel).
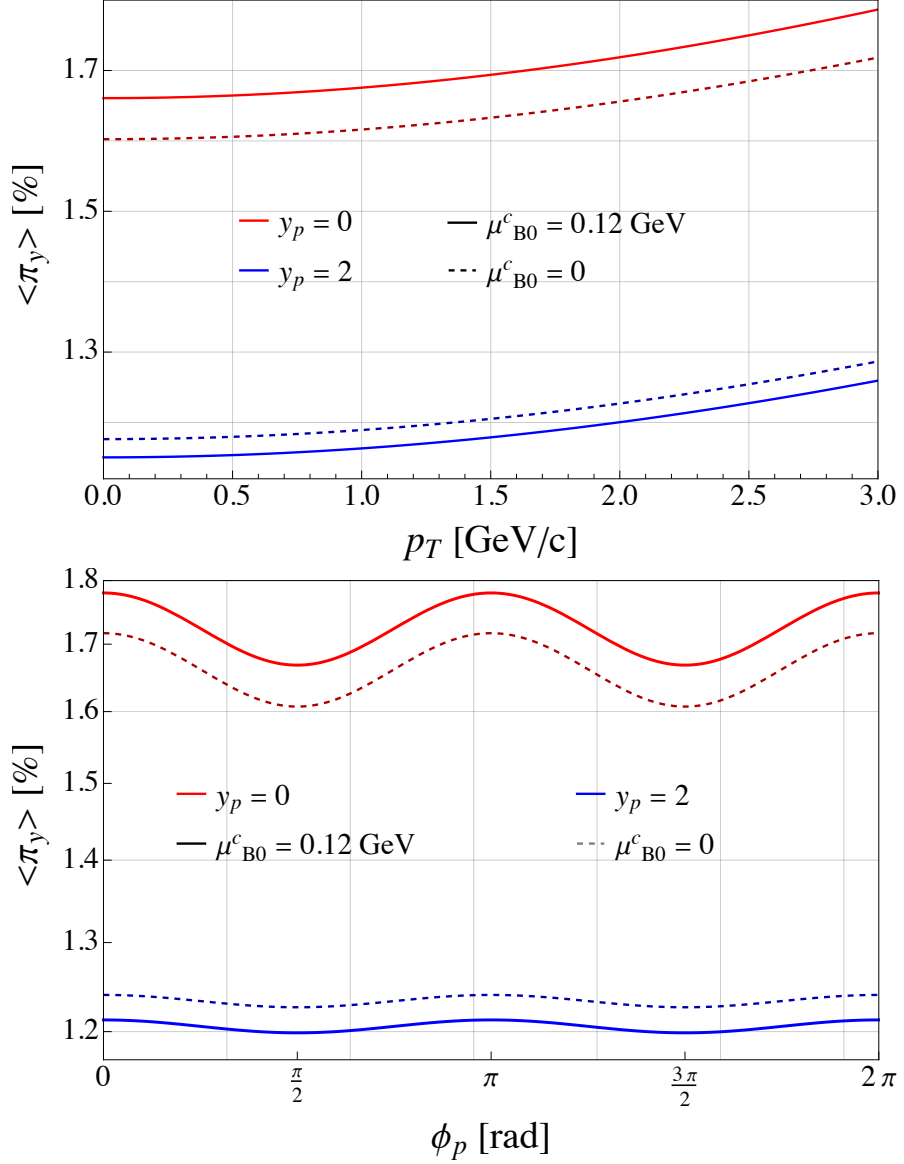
Figure 6.13: (Color online) Component $\langle \pi_y \rangle$ of momentum averaged polarization (5.15) as a function of p_T (top panel) and ϕ_p (bottom panel) with dashed and solid lines representing vanishing and non-vanishing baryon chemical potential, respectively.

7

Bjorken-expanding spin-polarized system in external electric field

In the heavy-ion collisions, it is expected that large electromagnetic fields are produced [119, 318, 319] with the strength of the order of $eE/m_\pi^2 \sim eB/m_\pi^2 \sim \mathcal{O}(1)$ where m_π is the mass of the pion and e is the electric charge. Understanding the dynamics of the EM fields is still one of the key goals in the physics of heavy-ion collisions, for recent studies see Refs. [320–329]. These fields may have an effect on the behavior of spin polarization of particles, for instance, the splitting of Λ and $\bar{\Lambda}$ global polarization, see Fig. 1.4, which is still an open question. Thus, in this section we incorporate electric field into our formalism and study its effects on the evolution of the spin components in the Bjorken-expanding background. Details of this chapter may be found in Ref. [D4].

7.1 Stationary solution to the Boltzmann–Vlasov equation

For the sake of simplicity, we consider the fluid in equilibrium that, at the microscopic scale, is composed of quark-like quasi-particles of N_f flavors which can be described by Boltzmann-Vlasov (BV) equation. With this assumption we are not taking into consideration any direct interaction (coupling) between spin and EM fields. In Ref. [286], a (stationary) solution to the BV equation was presented as the zeroth-order expansion in $\hbar$ where modified chemical potential allows electric field to be non-vanishing in equilibrium [330]. It is possible that in the event-by-event averaging [318] electric field may vanishes, however, its effects on the thermodynamics may survive. We first obtain the modification of the equilibrium hydrodynamic variables, using the stationary solution to the BV equation, which are then inserted into the equations of magnetohydrodynamics (MHD) along with solutions of Maxwell equations derived for the case of Bjorken flow [324]. Subsequently, we obtain the evolution of temperature and chemical potential and plug them into the conservation law for spin to find the evolution of spin components. We observe that the dynamics of the temperature and chemical potential is affected by the Joule heating (JH)

term and modified thermodynamic parameters at the macroscopic and microscopic level, respectively [1].

Due to the presence of EM fields, we use the stationary solution to the Boltzmann–Vlasov (BV) equation [161] where the relativistic collisionless BV equation takes the form

$$p^\mu \, \partial_\mu f_i^\pm \pm q_i \, F^{\mu\nu} \, p_\nu \, \partial_\mu^p \, f_i^\pm \;=\; 0 \,, \tag{7.1}$$

where $i = 1, \ldots, N_f$ represents quark flavor number, and $q_i(-q_i)$ denotes the (anti)particle electric charge for each ith flavor. The field strength tensor $F_{\mu\nu}$ can be written in terms of gauge field A_μ [2] as

$$F_{\mu\nu} \;=\; \partial_\mu A_\nu - \partial_\nu A_\mu \,. \tag{7.2}$$

One can also decompose $F_{\mu\nu}$ in terms of electric (E_μ) and magnetic (B_μ) components as [331]

$$F_{\mu\nu} \;=\; E_\mu U_\nu - E_\nu U_\mu + \epsilon_{\mu\nu\alpha\beta} U^\alpha B^\beta, \tag{7.3}$$

where

$$E^\mu \;\equiv\; F^{\mu\nu} U_\nu \,, \qquad B^\mu \;\equiv\; \frac{1}{2} \epsilon^{\mu\nu\alpha\beta} F_{\nu\alpha} U_\beta \,. \tag{7.4}$$

The equilibrium distribution function (3.47) for the system with non-interacting quark-like quasi-particles with spin, having same baryon number but different electric charges, becomes

$$f_{\text{eq},i}^\pm(x,p,s) \;=\; f_{\text{eq},i}^\pm(x,p) \exp\left[\frac{1}{2}\omega_{\mu\nu}(x)s^{\mu\nu}\right] \,, \tag{7.5}$$

where

$$f_{\text{eq},i}^\pm(x,p) \;=\; \exp\left[-\beta^\mu \left(p_\mu \pm q_i A_\mu\right) \pm \frac{\xi(x)}{3}\right] \,, \tag{7.6}$$

is the stationary solution to Eq. (7.1). Note that, we have divided ξ by the number of quarks (3) present in a baryon to get the quark chemical potential $(\mu_B/3)$. Thus, $\xi/3 = \mu_B/(3\,T) = \mu_Q/T$ where μ_Q is the quark chemical potential.

Putting Eq. (7.6) into Eq. (7.1) gives

$$\frac{1}{2}p^\mu p^\nu \, \pounds_\beta \, g_{\mu\nu} \pm q_i \, p^\mu \, \pounds_\beta \, A_\mu \;=\; 0 \,, \tag{7.7}$$

where $\pounds_\beta X$ is the Lie derivative of a tensor X with respect to β [332]

$$\pounds_\beta A_\mu \;=\; \beta^\nu \partial_\nu A_\mu + A_\nu \partial_\mu \beta^\nu \,, \qquad \pounds_\beta g_{\mu\nu} \;=\; \partial_\mu \beta_\nu + \partial_\nu \beta_\mu \,. \tag{7.8}$$

In the global equilibrium Eq. (7.7) is satisfied, thus we get

$$\pounds_\beta \, g_{\mu\nu} \;=\; 0 \,, \qquad \pounds_\beta \, A_\mu \;=\; 0 \,, \tag{7.9}$$

where, using Eq. (7.8), one gets

$$\begin{aligned}
\pounds_\beta A_\nu \;&=\; \beta^\mu \left(\partial_\mu A_\nu - \partial_\nu A_\mu\right) + \beta^\mu \partial_\nu A_\mu + A_\mu \partial_\nu \beta^\mu \,, \\
&=\; \beta^\mu F_{\mu\nu} + \partial_\nu \left(\beta \cdot A\right) \;=\; 0 \,.
\end{aligned} \tag{7.10}$$

---

[1]Our approach is sometimes dubbed a strong electric field regime [330].

[2]Note that A_μ, defined here, have completely different meaning than the definition of axial-vector component of the Wigner function used in the previous chapters.

Using Eq. (7.3) in Eq. (7.10) we obtain

$$\frac{E_\mu}{T} = \partial_\mu \left(\beta \cdot A \right).$$ (7.11)

Assuming E_μ and T being slowly varying functions at the microscopic scale, the integral of above equation gives

$$\beta \cdot A = \frac{E_\mu}{T} \int dx^\mu,$$ (7.12)

up to a gauge transformation. This is immersed in the quark chemical potential [333]. Thus, Eq. (7.5) is expressed, in the small polarization limit ($\omega_{\mu\nu} \ll 1$), as

$$f^\pm_{\text{eq},i}(x,p,s) = f^\pm_{\text{eq},i}(x,p) \left[1 + \frac{1}{2} \omega_{\mu\nu}(x) s^{\mu\nu} \right],$$ (7.13)

with

$$f^\pm_{\text{eq},i}(x,p) = \exp \left(\pm \xi_i - \beta^\mu p_\mu \right), \qquad \text{where} \qquad \xi_i = \xi - q_i \frac{E_\mu}{T} \int dx^\mu.$$ (7.14)

The interpretation of Eq. (7.14) is that, though the event-by-event average of the electric field vanishes, its traces in the distribution function may survive [318].

7.2 Baryon and electric charges

In this study the fluid has two charge currents: net baryon current (N^α) and electric charge current (J^α). The net baryon current is defined as

$$N^\alpha = \sum_i^{N_f} \int dP \, dS \, p^\alpha \left[f^+_{\text{eq},i}(x,p,s) - f^-_{\text{eq},i}(x,p,s) \right],$$ (7.15)

which reduces, after plugging Eq. (7.13), to

$$N^\alpha = \sum_i^{N_f} \mathcal{N}_i U^\alpha,$$ (7.16)

with

$$\mathcal{N}_i = 4 \sinh(\xi_i) \mathcal{N}_{(0),i}(T), \qquad \text{and} \qquad \mathcal{N}_{(0),i}(T) = \frac{T^3}{2\pi^2} z_i^2 K_2(z_i),$$ (7.17)

where $z_i \equiv m_i/T$ is the ratio between i^{th} flavor mass and temperature.

The inhomogeneous Maxwell equation

$$\partial_\mu F^{\mu\nu} = J^\nu = \rho_e U^\nu + \Delta^{\nu\rho} J_\rho,$$ (7.18)

with ρ_e being local electric charge density

$$\rho_e = \sum_i^{N_f} \int dP \, dS \, (p \cdot U) \, q_i \left[f^+_{\text{eq},i}(x,p,s) - f^-_{\text{eq},i}(x,p,s) \right] = \sum_i^{N_f} q_i \mathcal{N}_i,$$ (7.19)

implies electric current conservation. Since we assume Bjorken–expanding resistive MHD, this requires electric neutrality [324]. In this case, it is possible for the fluid to have a net baryon density $\mathcal{N}$, and vanishing electric charge density ρ_e [3]. Away from equilibrium, the (dissipative) electric current reads

$$J^\mu = \sigma_e E^\mu, \tag{7.20}$$

with σ_e being the electric conductivity which, in general, can depend on T and μ_B.

7.3 Energy-momentum conservation

The energy-momentum tensor of the fluid is defined, in equilibrium, as

$$T^{\mu\nu} = \sum_i^{N_f} \int \mathrm{dP}\,\mathrm{dS}\; p^\mu p^\nu \left[f^+_{\mathrm{eq},i}(x,p,s) + f^-_{\mathrm{eq},i}(x,p,s) \right]. \tag{7.21}$$

After plugging Eq. (7.13) in the above equation we obtain

$$\partial_\mu T^{\mu\nu} = F^{\nu\rho} J_\rho, \tag{7.22}$$

where $T^{\mu\nu}$ has the same form as Eq. (3.32) with the energy density and pressure expressed as

$$\mathcal{E} = 4 \sum_i^{N_f} \cosh(\xi_i)\,\mathcal{E}_{(0),i}(T), \qquad \mathcal{P} = 4 \sum_i^{N_f} \cosh(\xi_i)\,\mathcal{P}_{(0),i}(T), \tag{7.23}$$

respectively. In above equations

$$\mathcal{E}_{(0),i}(T) = \frac{1}{2\pi^2} T^4 z_i^2 \Big[z_i K_1(z_i) + 3 K_2(z_i) \Big], \qquad \mathcal{P}_{(0),i}(T) = T \mathcal{N}_{(0),i}(T). \tag{7.24}$$

7.4 Entropy conservation

It is important to comment on the conservation of entropy in the presence of external electric field in the global equilibrium. The definition of the entropy current is written as [91, 161]

$$
\begin{aligned}
H^\mu &= -\sum_i^{N_f} \int \mathrm{dP}\,\mathrm{dS}\, p^\mu \Big\{ f^+_{\mathrm{eq},i}(x,p,s) \left[\ln f^+_{\mathrm{eq},i}(x,p,s) - 1 \right] \\
&\quad + f^-_{\mathrm{eq},i}(x,p,s) \left[\ln f^-_{\mathrm{eq},i}(x,p,s) - 1 \right] \Big\}.
\end{aligned}
\tag{7.25}
$$

Putting Eq. (7.5) in Eq. (7.25), after some straightforward calculations we have

$$H^\mu = \mathcal{P}\beta^\mu + \beta_\alpha T^{\mu\alpha} - \sum_i^{N_f} \xi_i(x) N_i^\mu, \tag{7.26}$$

---

[3]This kind of setup, although greatly simplified, may hold at later stages of the evolution of the QGP.

whereas, in the global equilibrium, using Eq. (7.22) we obtain

$$
\begin{aligned}
\partial_\mu H^\mu &= \partial_\mu \left(\mathcal{P}\beta^\mu + \beta_\alpha T^{\mu\alpha} - \sum_i^{N_f} \xi_i(x) N_i^\mu \right) \\
&= \beta_\alpha \partial_\mu T^{\mu\alpha} - \sum_i^{N_f} N_i^\mu \partial_\mu \xi_i(x) \\
&= \beta_\alpha F^{\alpha\beta} J_\beta - \sum_i^{N_f} N_i^\mu \partial_\mu \xi_i(x) \\
&= -\sum_i^{N_f} N_i^\mu \partial_\mu \left(\xi_i(x) + q_i E_\mu \right) = -\mathcal{N} T \beta^\mu \partial_\mu \xi = -\mathcal{N} T \pounds_\beta \xi = 0 \,. \quad (7.27)
\end{aligned}
$$

Hence, we can safely say that electric field does not produce entropy in global equilibrium with the condition that chemical potential follows Eq. (7.14). We emphasize that Eq. (7.25) also includes terms of spin polarization tensor ($\omega_{\mu\nu}$), however, those contributions come at quadratic order which we do not consider in our analysis.

The current study assumes resistive MHD equations where the source of dissipation is the electrical conductivity. For out of equilibrium system the divergence of entropy reads

$$
\partial_\mu H^\mu = \frac{\sigma_e}{T} E^2 \,, \qquad \text{where} \qquad E \equiv \sqrt{-E^\mu E_\mu} \,. \quad (7.28)
$$

7.5 Background dynamics

The form of the net baryon density conservation (6.34) and the energy equation (6.33) in the presence of the external electric field and Bjorken expansion become

$$
\frac{\partial \mathcal{N}}{\partial \tau} + \frac{\mathcal{N}}{\tau} = 0 \,, \qquad \frac{\partial \mathcal{E}}{\partial \tau} + \frac{\mathcal{E} + \mathcal{P}}{\tau} = \sigma_e E^2 \,, \quad (7.29)
$$

respectively. Along with the above equations, we must also solve the Maxwell equations to obtain the evolution of the EM fields, which, in general, is quite difficult. Nevertheless, here we assume maximally boost-invariant or non-rotating solution as [324]

$$
B^\mu = B_0 \frac{\tau_0}{\tau} Y^\mu \,, \qquad E^\mu = \ell E_0 \frac{\tau_0}{\tau} e^{-\sigma_e(\tau-\tau_0)} Y^\mu \,, \quad (7.30)
$$

with E_0 and B_0 being the electric and magnetic field values at the initial proper time τ_0, respectively. The variable $\ell \equiv \frac{\boldsymbol{B} \cdot \boldsymbol{E}}{BE} = \pm 1$ represents the parallel ($+1$) and anti-parallel (-1) field configurations.

One obtains solution (7.30) to the resistive MHD equations as follows. Bjorken symmetries prevent magnetic field to exist in the longitudinal (z) direction together with E_z component and electric charge density ρ_e [326], hence allowing electric and magnetic fields to be non-vanishing only in the transverse ($x-y$) plane. Moreover, electric and magnetic fields can only be parallel 0 ($\ell = +1$) or antiparallel π ($\ell = -1$) to each other in order to preserve the Bjorken flow. We also consider that the direction of the fields is boost-

invariant. This allows us to obtain the solution (7.30) from the Maxwell's equations [4]. Using Eq. (7.30) in Eq. (7.14) we have

$$\xi_i = \xi - \ell\, q_i\, R_{\mathrm{RMS}} \frac{E_0}{T} \left(\frac{\tau_0}{\tau}\right) \mathrm{e}^{-\sigma_e(\tau - \tau_0)}, \tag{7.31}$$

with R_{RMS} being the nucleon root-mean-square charge radius.

Another important point is of charge neutrality which is not satisfied at the initial time. However, considering ρ_e at the initial time for $N_f = 3$, charge neutrality forces the initial number densities to follow

$$2\mathcal{N}_u(\tau_0) - \mathcal{N}_d(\tau_0) - \mathcal{N}_s(\tau_0) = 0, \tag{7.32}$$

which, in realistic situations, is not satisfied by the fluid evolution. For our analysis, local electric charge density takes very small values within a fraction of a Fermi, hence can be neglected and neutrality is achieved approximately.

For the numerical modelling of the background, we initialize the parameters at the initial proper time $\tau_0 = 1\,\mathrm{fm}$ as

$$T_0 = 0.6\,\mathrm{GeV}, \qquad \mu_{B0} = 0.05\,\mathrm{GeV}, \tag{7.33}$$

which corresponds to $\sqrt{s_{\mathrm{NN}}} = 200\,\mathrm{GeV}$ collision energy [334]. We use the masses of constituent quarks such as up, down and strange at Λ's mass scale for $N_f = 3$ [335]

$$m_u = m_d = 0.382\,\mathrm{GeV}, \qquad m_s = 0.537\,\mathrm{GeV}, \tag{7.34}$$

whereas $R_{\mathrm{RMS}} = 4.3\,\mathrm{fm}$ [336]. The electrical conductivity follows the relation up to second order in $\xi = \mu_B/T$ as [337]

$$\sigma_e(T, \mu_B) = 0.37\, Q_e\, T \left[1 + 0.15\, \left(\frac{\mu_B}{T}\right)^2\right], \tag{7.35}$$

and $Q_e = (6/9)e^2$ is the sum of the square of up $(2e/3)$, down $(-e/3)$, and strange $(-e/3)$ quark electric charges. We also introduce α parameter to employ different initial values of the electric field (E_0) for the analysis

$$\alpha \equiv \ell\, \frac{eE_0}{m_\pi^2}, \tag{7.36}$$

where $eE_0 = m_\pi^2$. α is our only free variable which we can tune to change the value of the initial electric field.

In order to better understand the evolution of temperature and baryon chemical potential, we first write the energy equation in Eq. (7.29) as

$$\tau \frac{d\mathcal{E}}{d\tau} = - \underbrace{w}_{\text{expansion term}} + \overbrace{\tau\, \sigma_e\, E^2}^{\text{Joule heating term}}, \tag{7.37}$$

---

[4] Note that the presence of EM fields can, in general, break the boost-invariance of the system due to a non-vanishing value of the Poynting vector. In the presence of EM field the most general form of the energy-momentum tensor can have terms of the form $U^\mu \epsilon^{\nu\lambda\alpha\beta} E_\lambda B_\alpha U_\beta$, which can be argued to break the boost-invariant flow. Thus to preserve the Bjorken symmetry in the transverse boost-invariant MHD, the direction of the electric field can either be parallel or antiparallel to the direction of the magnetic field.
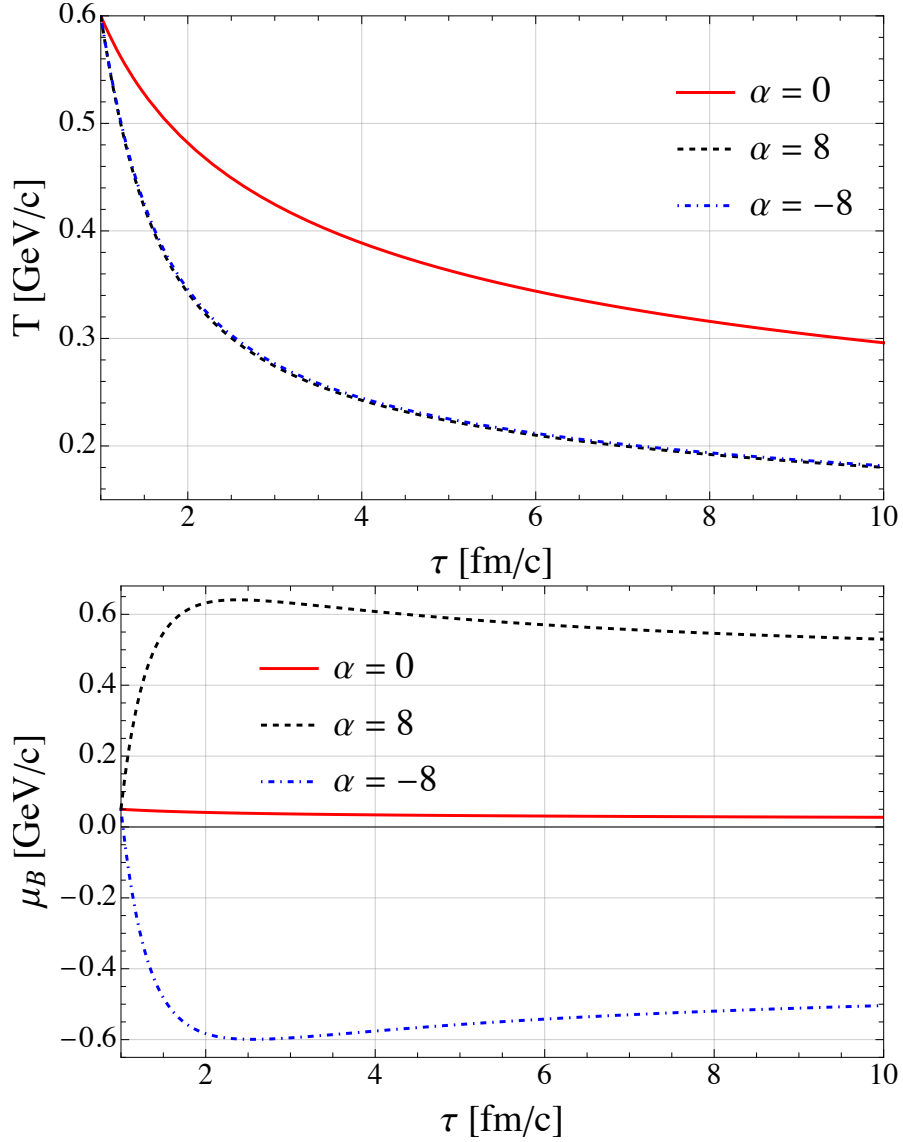
Figure 7.1: (Color online) Evolution of T (top panel) and μ_B (bottom panel) as a function of proper time τ with initial values $T_0 = 0.6$ GeV, and $\mu_{B0} = 0.05$ GeV for Bjorken background in the presence of external electric field. $\alpha = 0$ corresponds no electric field in the system.

with $w = \mathcal{E} + \mathcal{P}$ being the enthalpy density. As observed from Eq. (7.37), the proper-time evolution of the energy density depends on the expansion and JH terms. JH increases the temperature with the increase in the values of E^2 and $\sigma_e \tau$, thus producing heating effect. Equation (7.35) tells us that $\sigma_e \tau$ is a small factor and its increase will decrease the electric field in the hydrodynamic evolution, see Eq. (7.30). However, the JH term can be dominating over the expansion term in the early time for large initial value of electric field, which may induce reheating effect [324]. Nonetheless, in the current setup, fluid evolution gets modified through both JH term and EoS which prevents reheating and increases the enthalpy density. This in turn means that temperature is decreasing due to electric field ($|\alpha| \neq 0$) and makes the fluid elements heavier, which can be seen from Fig. 7.1 (upper panel). The temperature behavior for both negative and positive values of α is almost similar, however, for large values of α it is more pronounced.

Evolution of the baryon chemical potential, as seen from Fig. 7.1 (lower panel), is more sensitive to the presence of the electric field in the system. With the increase in proper time, absolute value of μ_B starts to decrease, specifically at $\tau = 3\,\mathrm{fm}$, because electric field starts to dominate over μ_B, and the sign of μ_B depends on the sign of α.

7.6 Spin dynamics

The spin tensor (3.43) for quark-like quasi-particles takes the form

$$S^{\alpha,\beta\gamma}_{\mathrm{GLW}} = \sum_i^{N_f} \cosh(\xi_i)\left[U^\alpha\left(\mathcal{A}_{1,i}\,\omega^{\beta\gamma} + \mathcal{A}_{2,i}\,U^{[\beta}\,\omega^{\gamma]}{}_\delta\,U^\delta\right) + \mathcal{A}_{3,i}\left(U^{[\beta}\,\omega^{\gamma]\alpha} + g^{\alpha[\beta}\,\omega^{\gamma]}{}_\delta\,U^\delta\right)\right], \tag{7.38}$$

with the thermodynamic coefficients

$$\mathcal{A}_{1,i} = \mathcal{N}_{(0),i} - \mathcal{B}_{(0),i}, \qquad \mathcal{A}_{2,i} = \mathcal{A}_{(0),i} - 3\mathcal{B}_{(0),i}, \qquad \mathcal{A}_{3,i} = \mathcal{B}_{(0),i}. \tag{7.39}$$

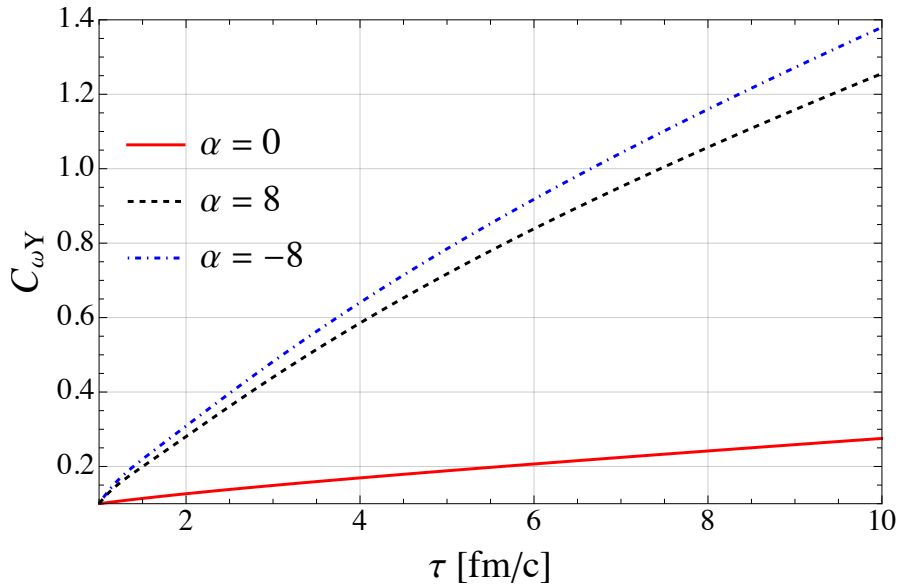We observe that the forms of the spin equations of motion remain the same as Eqs. (6.37)

Figure 7.2: (Color online) Proper-time evolution of spin polarization component $C_{\omega Y}$ with initial value $C_{\omega Y_0} = 0.1$ in the presence of external electric field.

even in the presence of the electric field and find no coupling between the spin components. The evolution of the spin components is qualitatively similar to the Bjorken-expanding system without mean fields, see Sec. 6.2. However, we notice that electric field enhances the spin dynamics as depicted in Fig. 7.2. We only show $C_{\omega Y}$ evolution as this component is relevant keeping in mind the physics situation of heavy-ion collisions, see the discussion in Sec. 6.2.2, and its enhancement suggests that electric field may play an important role in the heavy-ions collision experiments. As the spin component behavior is similar to the Bjorken-expanding matter, we find that the dynamics of mean spin polarization is also qualitatively similar as shown in Figs. 6.5 in Sec. 6.2.3, hence we do not show those plots here.

8

CONFORMAL SYMMETRY OF PERFECT-FLUID HYDRODYNAMICS WITH SPIN

> *"Try not to become a man of success*
> *but rather a man of value."*
> – ALBERT EINSTEIN

In Sections 6.2 and 6.3 we have considered the produced matter to be homogeneous in the direction transverse to the beam and we focused on its dynamics in the longitudinal direction. However, due to the finite size of the colliding nuclei, the dynamics of the produced matter in the transverse plane is inhomogeneous, with energy density strongly decreasing at the radial edge. To address such a possibility, in this section, we consider the simplest nontrivial extension of Bjorken expansion assuming that the system is cylindrically-symmetric with respect to the beam direction. Such conditions arise in perfectly central relativistic collisions of heavy-ions or smaller systems. Although, in general, to study such configuration, it is necessary to perform full numerical simulations, in what follows, we choose a different strategy leading to semi-analytic results. For this purpose, we use a generalization of the Bjorken flow known as Gubser flow [338,339]. The latter introduces the flow component in the transverse direction and can be shown invariant for boost-invariant and cylindrically symmetric systems under conformal symmetry group $SO(3)_q \otimes SO(1,1) \otimes \mathbf{Z}_2$. This special symmetry, known as "Gubser's symmetry", is a generalized version of the Bjorken symmetry $ISO(2) \otimes SO(1,1) \otimes \mathbf{Z}_2$ [1] and has been used in various studies of hydrodynamics [340–348].

In this chapter, we study the dynamics of spin components in the Gubser-expanding perfect-fluid background. For this purpose, we first introduce certain aspects of conformal mapping to the de Sitter space required to make the Gubser's symmetry manifest. We find transformation rules which the conservation laws must follow for the dynamics to respect conformal invariance. While the resulting well-known tracelessness of the energy-momentum tensor is a feasible condition, the additional condition for the spin tensor is not satisfied by the form we use (3.39), thus breaking conformal symmetry explicitly. However, as our formulation prevents any back-reaction from the spin evolution to the perfect-fluid background evolution, the invariance of the background is not spoiled by the conformal

---

[1] $SO(3)_q$ is a special orthogonal rotation group in three dimensions characterized by a length scale q, $SO(1,1)$ is a special orthogonal indefinite group which ensures boost-invariance symmetry in the system and $\mathbf{Z}_2$ symmetry is generated by the reflections in the $r - \phi$ plane. $ISO(2)$ is a Euclidean group with dimension 3 ensuring translational and rotational invariance in the transverse plane. In the limit $q \to 0$, $SO(3)_q$ reduces to $ISO(2)$ and Gubser flow takes the form of Bjorken flow.

symmetry breaking at the level of the spin tensor. This motivates us to find non-trivial approximate solutions for the spin keeping a small but finite mass. The results presented in the current chapter may be found in the Ref. [D5].

8.1 Boost-invariant and cylindrically-symmetric expansion

For boost-invariant and cylindrically-symmetric (with respect to the beam direction) systems respecting Gubser symmetry it is convenient to introduce the polar-Milne coordinates $x^\mu = (\tau, r, \phi, \eta)$ with the line element given as

$$ds^2 = -d\tau^2 + dr^2 + r^2 d\phi^2 + \tau^2 d\eta^2,$$

where τ and η, as defined in Section 6.1.1, are longitudinal proper time and longitudinal spacetime rapidity, while $r = \sqrt{x^2+y^2}$ and $\phi = \tan^{-1}(y/x)$ are the radial distance and the azimuthal angle, respectively, which parameterize the plane transverse to the beam direction.

The four-vector basis for boost-invariant and cylindrically symmetric system can be written in the form (note in LRF, U, X, Y, and Z are the unit vectors in the directions of τ, r, ϕ, and η, respectively)

$$
\begin{aligned}
U^\mu &= (\cosh(\vartheta), \sinh(\vartheta), 0, 0), & X^\mu &= (\sinh(\vartheta), \cosh(\vartheta), 0, 0), \\
Y^\mu &= (0, 0, 1/r, 0), & Z^\mu &= (0, 0, 0, 1/\tau),
\end{aligned}
\tag{8.1}
$$

which follows

$$U \cdot U = -1, \quad X \cdot X = 1, \quad Y \cdot Y = 1, \quad Z \cdot Z = 1, \tag{8.2}$$

and allows polar-hyperbolic metric tensor, $g^{\mu\nu} = \mathrm{diag}(-1, 1, 1/r^2, 1/\tau^2)$ (note opposite signature as compared to previous sections), to be written as

$$g^{\mu\nu} = -U^\mu U^\nu + X^\mu X^\nu + Y^\mu Y^\nu + Z^\mu Z^\nu. \tag{8.3}$$

8.2 Conformal symmetry and conformal mapping to de Sitter space

The invariance of the flow profile with respect to the Gubser's symmetry is manifest if one uses the conformal mapping to the curved (de Sitter) spacetime $dS_3 \otimes R$ defined by three-dimensional de Sitter space and a line. This is performed by Weyl rescaling of the metric

$$ds^2 \;\rightarrow\; \frac{ds^2}{\Omega_{\mathrm{cf}}^2} \;=\; \frac{-d\tau^2 + dr^2 + r^2 d\phi^2}{\tau^2} + d\eta^2, \tag{8.4}$$

where $\Omega_{\mathrm{cf}} = \tau$ is the conformal factor, and the coordinate transformation from polar Milne coordinates to de Sitter coordinates $\hat{\hat{x}}^\mu = (\rho, \theta, \phi, \eta)$ [2] with the help of the relations

$$\sinh(\rho(\tau,r)) = -\frac{1 - (q\tau)^2 + (qr)^2}{2\,q\tau}, \qquad \tan(\theta(\tau,r)) = \frac{2\,qr}{1 + (q\tau)^2 - (qr)^2}. \tag{8.5}$$

---

[2]In the following the quantities with a double hat on top indicate that they are defined in the de Sitter space.

The rescaled line element in the de Sitter space with the metric

$$\hat{\hat{g}}_{\mu\nu} = \mathrm{diag}\left(-1,\, (\cosh(\rho))^2,\, (\cosh(\rho))^2\, (\sin(\theta))^2,\, 1\right),$$

takes the form

$$d\hat{\hat{s}}^2 \;=\; -d\rho^2 + (\cosh(\rho))^2\, (d\theta^2 + (\sin(\theta))^2\, d\phi^2) + d\eta^2. \tag{8.6}$$

From Eq. (8.6) we observe that the Weyl scaling (8.4) along with the change of the coordinates through the relations (8.5) makes the $(SO(3)_q)$ conformal isometry to become a manifest isometry $(SO(3))$ in de Sitter coordinates.

For a system to respect conformal symmetry it is required that (m_A, n_A) tensors transform homogeneously under Weyl rescaling, namely [338, 339, 349–351]

$$A^{\mu_1\ldots\mu_m}_{\nu_1\ldots\nu_n}(x) \;\rightarrow\; e^{(-\varphi(x))\Delta_A} A^{\mu_1\ldots\mu_m}_{\nu_1\ldots\nu_n}(x) \;\equiv\; \Omega_{\mathrm{cf}}^{\Delta_A} A^{\mu_1\ldots\mu_m}_{\nu_1\ldots\nu_n}(x), \tag{8.7}$$

where $\varphi(x)$ depends on the spacetime coordinates, while $\Delta_A = [A] + m_A - n_A$ indicates the conformal weight of A with $[A]$ representing the mass dimension of A, and m_A and n_A are the number of contravariant and covariant indices, respectively, of the quantity A.

Take for example the metric tensor $g_{\mu\nu}$: $g_{\mu\nu}$ is a second-rank $(0,2)$ tensor which is dimensionless, thus $[g_{\mu\nu}] = 0$ with $m_A = 0$ and $n_A = 2$, hence, $\Delta_{g_{\mu\nu}} = -2$, which implies that $g_{\mu\nu}$ transforms homogeneously under Weyl rescaling as [339, 349]

$$g_{\mu\nu} \;\rightarrow\; \Omega_{\mathrm{cf}}^{-2}\, g_{\mu\nu}. \tag{8.8}$$

Similarly, conformal weight of $g^{\mu\nu}$ is $\Delta_{g^{\mu\nu}} = 2$.

With the use of Eq. (8.8) one can obtain the relation between $R^3 \otimes R$ and $dS_3 \otimes R$ as

$$\hat{\hat{g}}_{\mu\nu} \;=\; \frac{1}{\tau^2} \frac{\partial x^\alpha}{\partial \hat{\hat{x}}^\mu} \frac{\partial x^\beta}{\partial \hat{\hat{x}}^\nu}\, g_{\alpha\beta}. \tag{8.9}$$

With the knowledge of $\Delta_{g_{\mu\nu}} = -2$ and fluid flow normalization $U \cdot U = -1$, the conformal weight of contravariant fluid flow vector can be shown to be $\Delta_{U^\mu} = 1$, where the transformation rule is

$$\hat{\hat{U}}_\nu \;=\; \frac{1}{\tau} \frac{\partial x^\mu}{\partial \hat{\hat{x}}^\nu} U_\mu. \tag{8.10}$$

The advantage of going to de Sitter spacetime is that the flow profile (8.1) under (8.10) becomes static

$$\hat{\hat{U}}^\mu \;=\; (1,\, 0,\, 0,\, 0). \tag{8.11}$$

Hence, it respects Gubser's symmetry with the transverse rapidity of the form [338, 339]

$$\vartheta(\tau, r) \;=\; \tanh^{-1}\left(\frac{2\, q\tau\, qr}{1 + (q\tau)^2 + (qr)^2}\right). \tag{8.12}$$

Similarly, other basis vectors (8.1) in the de Sitter spacetime become

$$\hat{\hat{X}}^\mu \;=\; \left(0,\, (\cosh(\rho))^{-1},\, 0,\, 0\right), \qquad \hat{\hat{Y}}^\mu \;=\; \left(0,\, 0,\, (\cosh(\rho)\sin(\theta))^{-1},\, 0\right),$$

$$\hat{\hat{Z}}^\mu \;=\; (0,\, 0,\, 0,\, 1). \tag{8.13}$$

Using basis vectors, the metric $\hat{g}^{\mu\nu}$ reads

$$\hat{g}^{\mu\nu} \;=\; -\hat{U}^\mu\hat{U}^\nu + \hat{X}^\mu\hat{X}^\nu + \hat{Y}^\mu\hat{Y}^\nu + \hat{Z}^\mu\hat{Z}^\nu\,, \qquad (8.14)$$

with its determinant given by

$$\hat{g} \;\equiv\; \det(\hat{g}_{\mu\nu}) \;=\; -(\cosh(\rho))^4\,(\sin(\theta))^2\,. \qquad (8.15)$$

From Eq. (3.33) we find that the mass dimension of the energy density and the pressure is $[\mathcal{E}] \equiv [\mathcal{P}] = 4$, thus their conformal weight is $\Delta_\mathcal{E} = \Delta_\mathcal{P} = 4$. Similarly, for the net baryon density (3.26) one arrives at $[\mathcal{N}] = 3$ with $\Delta_\mathcal{N} = 3$. For the temperature and baryon chemical potential it is easy to observe that their conformal weight is $\Delta_T = \Delta_{\mu_B} = 1$ since their mass dimension is $[T] = [\mu_B] = 1$.

Using the method described above, see Eq. (8.10), transformation rules for other quantities can be found:

$$U_\mu(\tau, r) \;=\; \tau\frac{\partial\hat{\tilde{x}}^\nu}{\partial x^\mu}\,\hat{U}_\nu(\rho)\,,$$

$$T(\tau, r) \;=\; \frac{\hat{\tilde{T}}(\rho)}{\tau}\,, \qquad \mu_B(\tau, r) \;=\; \frac{\hat{\tilde{\mu}}_B(\rho)}{\tau}\,,$$

$$\mathcal{E}(\tau, r) \;=\; \frac{\hat{\tilde{\mathcal{E}}}(\rho)}{\tau^4}\,, \qquad \mathcal{P}(\tau, r) \;=\; \frac{\hat{\tilde{\mathcal{P}}}(\rho)}{\tau^4}\,, \qquad \mathcal{N}(\tau, r) \;=\; \frac{\hat{\tilde{\mathcal{N}}}(\rho)}{\tau^3}\,. \qquad (8.16)$$

For the purpose of the following analysis it is particularly important to find conformal weights of the energy-momentum and the spin tensors. As mentioned before, see Eq. (1.23), total angular momentum has both orbital and spin contributions

$$J^{\lambda,\mu\nu} \;=\; L^{\lambda,\mu\nu} + S^{\lambda,\mu\nu} \;=\; x^\mu T^{\lambda\nu} - x^\nu T^{\lambda\mu} + S^{\lambda,\mu\nu}\,. \qquad (8.17)$$

As the mass dimension of x^μ is $[x^\mu] = -1$, one has $\Delta_{x^\mu} = 0$. From the knowledge of the conformal weights of $\mathcal{E}$ and U^α, and using Eq. (3.32), we find that the conformal weight of the energy-momentum tensor is $\Delta_{T^{\alpha\beta}} = 6$ (note that left-hand side of Eq. (3.32) must have the same conformal weight as each term on the right-hand side). From the reasoning that each term in Eq. (8.17) should have the same conformal weight one can then find that the spin tensor has the conformal weight $\Delta_{S^{\alpha\beta\gamma}} = 6$. Therefore the GLW spin tensor in our formalism should respect $\Delta_{S^{\alpha\beta\gamma}_{\mathrm{GLW}}} = 6$ [3].

In a similar way, using the information of the conformal weights of net baryon density and fluid-flow, we also obtain the conformal weight of the net baryon current (3.25) as $\Delta_{N^\alpha} = 4$. From Eq. (3.40), we find, using the conformal weight of the spin tensor, that the conformal weight of the spin polarization tensor is $\Delta_{\omega^{\alpha\beta}} = 2$ which gives the conformal weights of κ_α and ω_α to be $\Delta_{\kappa^\alpha} = 1$ and $\Delta_{\omega^\alpha} = 1$. Here, we have used the fact that $\epsilon^{\alpha\beta\gamma\delta}$ has no mass dimension and has four contravariant indices resulting in $\Delta_{\epsilon^{\alpha\beta\gamma\delta}} = 4$, see Eq. (4.3). Using the information of how spin polarization tensor transforms under Weyl scaling we find that spin polarization components C_κ and C_ω have conformal weights $\Delta_{C_\kappa} = \Delta_{C_\omega} = 0$, which makes them conformally invariant (note that C_κ and C_ω are dimensionless scalars).

---

[3] Using the information that the conformal weight of the Dirac spinor ψ and Dirac dual spinor $\bar{\psi}$ is $\Delta_\psi = \Delta_{\bar{\psi}} = \frac{3}{2}$ and Dirac Gamma matrix has the conformal weight $\Delta_{\gamma^\mu} = 1$ [352, 353], we can find that the canonical spin tensor (1.30) and the HW spin tensor (1.34) has the same conformal weight as the GLW spin tensor.

To summarise, transformation rules Eq. (8.7) for the net baryon current, the energy-momentum tensor, and the spin tensor for four-dimensional spacetime read

$$N^\alpha \;\to\; \Omega_{\mathrm{cf}}^4\, N^\alpha\,, \qquad T^{\alpha\beta} \;\to\; \Omega_{\mathrm{cf}}^6\, T^{\alpha\beta}\,, \qquad S^{\alpha\beta\gamma} \;\to\; \Omega_{\mathrm{cf}}^6\, S^{\alpha\beta\gamma}\,. \tag{8.18}$$

It can be easily noticed that the transformation rules for the covariant quantities can be found using the information that raising (lowering) the Lorentz index with the metric tensor changes the conformal weight by 2 (-2).

8.3 Conformal invariance of conservation equations

In this section we derive conformal transformation rules for the conservation laws for N^α, $T^{\alpha\beta}$, and $S^{\alpha\beta\gamma}$, which, in curved spacetime, read

$$d_\alpha N^\alpha(x) \;=\; \partial_\alpha N^\alpha + \Gamma^\alpha_{\alpha\beta} N^\beta \;=\; 0\,, \tag{8.19}$$

$$d_\alpha T^{\alpha\beta}(x) \;=\; \partial_\alpha T^{\alpha\beta} + \Gamma^\alpha_{\alpha\lambda} T^{\lambda\beta} + \Gamma^\beta_{\alpha\lambda} T^{\alpha\lambda} \;=\; 0\,, \tag{8.20}$$

$$d_\alpha S^{\alpha\beta\gamma}(x) \;=\; \partial_\alpha S^{\alpha\beta\gamma} + \Gamma^\alpha_{\alpha\lambda} S^{\lambda\beta\gamma} + \Gamma^\beta_{\alpha\lambda} S^{\alpha\lambda\gamma} + \Gamma^\gamma_{\alpha\lambda} S^{\alpha\beta\lambda} \;=\; 0\,, \tag{8.21}$$

with $\Gamma^\nu_{\mu\lambda}$ being the Christoffel symbol defined as [354–356]

$$\Gamma^\nu_{\mu\lambda} \;\equiv\; \Gamma^\nu_{\lambda\mu} \;=\; \frac{1}{2} g^{\nu\sigma}(\partial_\mu g_{\sigma\lambda} + \partial_\lambda g_{\sigma\mu} - \partial_\sigma g_{\mu\lambda})\,. \tag{8.22}$$

Note that d_α in Eqs. (8.19)–(8.21) is the covariant derivative [4], which reduces to partial derivative in flat spacetime.

To obtain conformal transformation of the conservation equations (8.19)–(8.21) we require Christoffel symbols (8.22) to transform accordingly. Using Eq. (8.8) we get [351, 357, 358]

$$
\begin{aligned}
\hat{\hat{\Gamma}}^\nu_{\mu\lambda} \;=\;& \frac{1}{2}\hat{\hat{g}}^{\nu\sigma}\left[\partial_\mu\hat{\hat{g}}_{\sigma\lambda} + \partial_\lambda\hat{\hat{g}}_{\sigma\mu} - \partial_\sigma\hat{\hat{g}}_{\mu\lambda}\right]\,, \\
\;=\;& \frac{1}{2}\Omega^{-2}g^{\nu\sigma}\left[\partial_\mu(\Omega^2 g_{\sigma\lambda}) + \partial_\lambda(\Omega^2 g_{\sigma\mu}) - \partial_\sigma(\Omega^2 g_{\mu\lambda})\right]\,, \\
\;=\;& \frac{e^{2\varphi} g^{\nu\sigma}}{2}\left[\partial_\mu(e^{-2\varphi} g_{\sigma\lambda}) + \partial_\lambda(e^{-2\varphi} g_{\sigma\mu}) - \partial_\sigma(e^{-2\varphi} g_{\mu\lambda})\right]\,, \\
\;=\;& \frac{e^{2\varphi} g^{\nu\sigma}}{2}\Bigg[2e^{-\varphi}\partial_\mu(e^{-\varphi})g_{\sigma\lambda} + e^{-2\varphi}\partial_\mu(g_{\sigma\lambda}) + 2e^{-\varphi}\partial_\lambda(e^{-\varphi})g_{\sigma\mu} + e^{-2\varphi}\partial_\lambda(g_{\sigma\mu}) \\
& -2e^{-\varphi}\partial_\sigma(e^{-\varphi})g_{\mu\lambda} - e^{-2\varphi}\partial_\sigma(g_{\mu\lambda})\Bigg]\,, \\
\;=\;& \frac{g^{\nu\sigma}}{2}\left[\partial_\mu(g_{\sigma\lambda}) + \partial_\lambda(g_{\sigma\mu}) - \partial_\sigma(g_{\mu\lambda}) + 2\,e^{\varphi}\left(\partial_\mu(e^{-\varphi})g_{\sigma\lambda} + \partial_\lambda(e^{-\varphi})g_{\sigma\mu} - \partial_\sigma(e^{-\varphi})g_{\mu\lambda}\right)\right]\,, \\
\;=\;& \Gamma^\nu_{\mu\lambda} + e^{\varphi}\left[\delta^\nu_\lambda\partial_\mu(e^{-\varphi}) + \delta^\nu_\mu\partial_\lambda(e^{-\varphi}) - \partial_\sigma(e^{-\varphi})g^{\nu\sigma}g_{\mu\lambda}\right]\,, \\
\;=\;& \Gamma^\nu_{\mu\lambda} - \delta^\nu_\lambda\partial_\mu\varphi - \delta^\nu_\mu\partial_\lambda\varphi + g^{\nu\sigma}g_{\mu\lambda}\partial_\sigma\varphi\,, \tag{8.23}
\end{aligned}
$$

with δ^β_λ being the Kronecker delta function. However, one may notice that when φ is constant then $\partial_\sigma\varphi = 0$ in Eq. (8.23) which makes $\hat{\hat{\Gamma}}^\nu_{\mu\lambda} = \Gamma^\nu_{\mu\lambda}$.

---

[4]See Appendix B for more information about covariant derivative and Christoffel symbols.

One can easily show that the net baryon current conservation (8.19) is conserved in Minkowski and de Sitter spacetimes which means that it is conformal-frame independent [349–351] resulting in

$$d_\alpha N^\alpha \;=\; \Omega_{\rm cf}^4 \, \hat{\hat{d}}_\alpha \hat{\hat{N}}^\alpha. \tag{8.24}$$

Plugging Eq. (8.23) in Eq. (8.20) we arrive at the conformal transformation of energy and linear momentum conservation [350, 351, 357]

$$d_\alpha T^{\alpha\beta} \;=\; \Omega_{\rm cf}^6 \left[\hat{\hat{d}}_\alpha \hat{\hat{T}}^{\alpha\beta} - \hat{\hat{T}}^\lambda{}_\lambda \, \hat{\hat{g}}^{\beta\delta} \partial_\delta \varphi \right] , \tag{8.25}$$

which indicates that $\hat{\hat{T}}^{\alpha\beta}$ has to be traceless ($\hat{\hat{T}}^\alpha{}_\alpha = 0$) to be conserved in de Sitter spacetime [359–362].

Finally, using Eqs. (8.18) and (8.23) in Eq. (8.21), we obtain the conformal transformation of the spin conservation law

$$d_\alpha S^{\alpha\beta\gamma} \;=\; \Omega_{\rm cf}^6 \left[\hat{\hat{d}}_\alpha \hat{\hat{S}}^{\alpha\beta\gamma} - (\hat{\hat{S}}_\lambda{}^{\lambda\gamma} \, \hat{\hat{g}}^{\beta\sigma} + \hat{\hat{S}}^{\alpha\beta}{}_\alpha \, \hat{\hat{g}}^{\sigma\gamma}) \partial_\sigma \varphi \right] , \tag{8.26}$$

indicating that the spin tensor needs to fulfill the condition $\hat{\hat{S}}_\alpha{}^{\alpha\beta} = 0$ for the spin conservation to be conformally invariant. We also observe from Eqs. (8.24), (8.25), and (8.26) that when φ is constant all the conservation laws automatically become conformally invariant.

8.4 Background dynamics

We will now explore the Gubser-expanding background dynamics which will then be used in the next section to obtain the evolution of the spin polarization components. Using Eqs. (8.16) our results can be transformed back to the Minkowski spacetime.

We find that the GLW energy-momentum tensor (3.32) satisfies the traceless condition only in the conformal limit where energy density (3.33), pressure (3.33), and net baryon density (3.26) are expressed as

$$\hat{\hat{\mathcal{E}}} \;=\; \frac{12}{\pi^2} \cosh(\xi) \, \hat{\hat{T}}^4 , \qquad \hat{\hat{\mathcal{P}}} \;=\; \frac{4}{\pi^2} \cosh(\xi) \, \hat{\hat{T}}^4 , \qquad \hat{\hat{\mathcal{N}}} \;=\; \frac{4}{\pi^2} \sinh(\xi) \, \hat{\hat{T}}^3 , \tag{8.27}$$

respectively. One finds that $\hat{\hat{\mathcal{E}}} = 3\hat{\hat{\mathcal{P}}}$, which makes the energy-momentum traceless, as required in Eq. (8.25). Moreover, we observe that the GLW (3.43) and HW (1.34) definitions of spin tensor do not satisfy the condition of conformal invariance (8.26), which is not the case for canonical spin tensor (1.30).

Since, as before, we assume small spin polarization limit which makes spin dynamics decouple from the background dynamics, in the following we study the dynamics of the spin components on top of the Gubser flow background without spoiling its conformal invariance. Considering evolution of the spin components in the de Sitter coordinates we keep finite mass in the spin tensor (3.43).

The conservation law for net baryon density (6.7) can be written in the de Sitter coordinates as

$$\hat{\hat{U}}^\alpha \partial_\alpha \hat{\hat{\mathcal{N}}} + \hat{\hat{\mathcal{N}}} \partial_\alpha \hat{\hat{U}}^\alpha + \hat{\hat{\mathcal{N}}} \, \hat{\hat{U}}^\alpha \frac{\partial_\alpha \sqrt{-\hat{\hat{g}}}}{\sqrt{-\hat{\hat{g}}}} \;=\; \partial_\rho \hat{\hat{\mathcal{N}}} + 2 \hat{\hat{\mathcal{N}}} \, \tanh(\rho) \;=\; 0 , \tag{8.28}$$

where $\hat{\mathring{g}}$ is the value of the determinant of de Sitter metric (8.15). Similarly, the conservation of energy (6.8) gives

$$\partial_\rho \hat{\mathring{\mathcal{E}}} + 2(\hat{\mathring{\mathcal{E}}} + \hat{\mathring{\mathcal{P}}})\tanh(\rho) = 0\,, \tag{8.29}$$

whereas Euler equation (6.9) is satisfied trivially. The solutions of the above equations of motion can be obtained as [338, 339],

$$\hat{\mathring{\mathcal{E}}} = \hat{\mathring{\mathcal{E}}}_0 \left(\frac{\cosh(\rho_0)}{\cosh(\rho)}\right)^{8/3}\,, \qquad \hat{\mathring{\mathcal{N}}} = \hat{\mathring{\mathcal{N}}}_0 \left(\frac{\cosh(\rho_0)}{\cosh(\rho)}\right)^{2}\,, \tag{8.30}$$

respectively, where $\hat{\mathring{\mathcal{E}}}_0 \equiv \hat{\mathring{\mathcal{E}}}(\rho_0)$ and $\hat{\mathring{\mathcal{N}}}_0 \equiv \hat{\mathring{\mathcal{N}}}(\rho_0)$ are constants of integration at the initial de Sitter time (ρ_0). The respective solutions for temperature and baryon chemical potential in de Sitter space can be obtained using Eqs. (8.27),

$$\hat{\mathring{T}} = \hat{\mathring{T}}_0 \left(\frac{\cosh(\rho_0)}{\cosh(\rho)}\right)^{2/3}\,, \qquad \hat{\mathring{\mu}}_B = \hat{\mathring{\mu}}_{B0} \left(\frac{\cosh(\rho_0)}{\cosh(\rho)}\right)^{2/3}\,, \tag{8.31}$$

where $\hat{\mathring{T}}_0 \equiv \hat{\mathring{T}}(\rho_0)$ and $\hat{\mathring{\mu}}_{B0} \equiv \hat{\mathring{\mu}}_B(\rho_0)$ are the integration constants. This result implies that $\hat{\mathring{\xi}} = \hat{\mathring{\mu}}_B/\hat{\mathring{T}}$ does not depend on ρ [5].
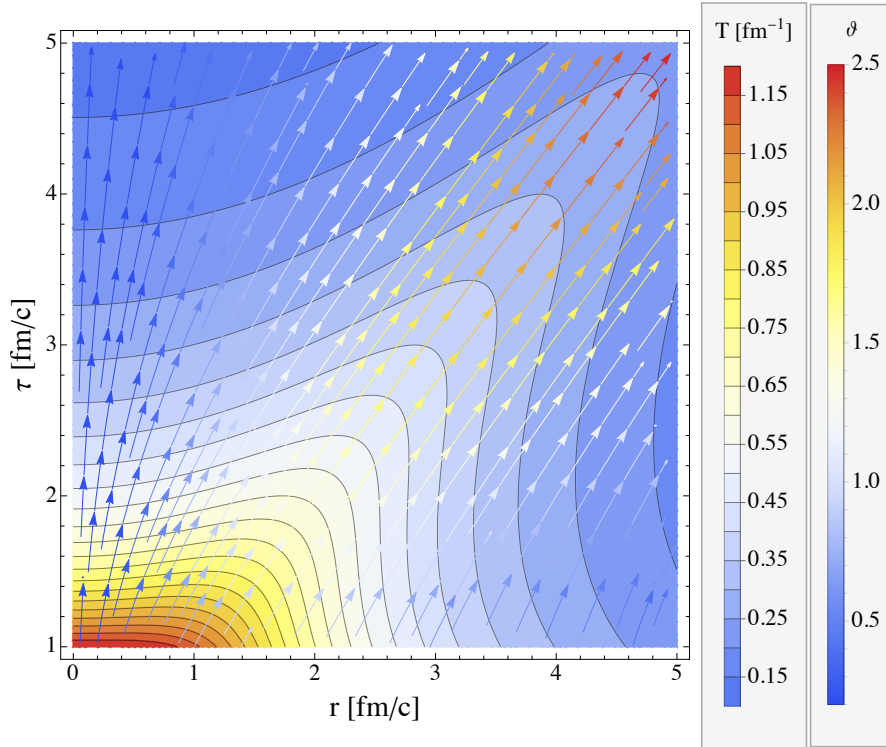
Figure 8.1: (Color online) Temperature (contours) and flow-vector components $(U^\tau, U^r)/\sqrt{(U^\tau)^2 + (U^r)^2}$ (stream lines – the coloring of arrows are indicated by the fluid rapidity ϑ) as functions of longitudinal proper time (τ) and radial distance (r).

Figure 8.1 shows strongly correlated behavior of temperature (8.31) with the flow-vector components $(U^\tau, U^r)/\sqrt{(U^\tau)^2 + (U^r)^2}$ where the initial temperature is $\hat{\mathring{T}}_0 \equiv \hat{\mathring{T}}(\rho_0) = 1.2$ at $\rho_0 = 0$ such that considering $q = 1\,\mathrm{fm}^{-1}$ gives $T(\tau_0 = 1\,\mathrm{fm}, r = 0) = 1.2\,\mathrm{fm}^{-1} = 0.24\,\mathrm{GeV}$ [342].

---

[5] We observe here that the dynamics of the system, due to Gubser symmetry, depends only on ρ [338,339].

8.5 Spin dynamics

In this section we study the evolution of the spin polarization components. For simplicity we continue on using the de Sitter coordinates instead of polar Milne coordinates, although, as we noted above, the considered GLW form of the spin tensor leads to the conformal symmetry breaking.

The spin equations (6.25)–(6.30) reduce, in this case, to

$$\hat{\mathcal{Q}}\,\dot{\hat{C}}_{\kappa X} = -\hat{C}_{\kappa X}\left[\dot{\hat{\mathcal{Q}}} + \frac{5}{2}\hat{\mathcal{Q}}\tanh(\rho)\right],\tag{8.32}$$

$$\hat{\mathcal{Q}}\,\dot{\hat{C}}_{\kappa Y} + \frac{\dot{\hat{\mathcal{Q}}}}{2}\cosh(\rho)\sin(\theta)\,\mathring{\hat{C}}_{\omega Z} = -\hat{C}_{\kappa Y}\left[\dot{\hat{\mathcal{Q}}} + \frac{5}{2}\hat{\mathcal{Q}}\tanh(\rho)\right]$$
$$- \hat{C}_{\omega Z}\frac{\dot{\hat{\mathcal{Q}}}}{2}\cosh(\rho)\cos(\theta),\tag{8.33}$$

$$\hat{\mathcal{Q}}\,\dot{\hat{C}}_{\kappa Z} - \frac{\dot{\hat{\mathcal{Q}}}}{2}\cosh(\rho)\sin(\theta)\,\mathring{\hat{C}}_{\omega Y} = -\hat{C}_{\kappa Z}\left[\dot{\hat{\mathcal{Q}}} + 3\,\hat{\mathcal{Q}}\tanh(\rho)\right]$$
$$+ \hat{C}_{\omega Y}\,\hat{\mathcal{Q}}\cosh(\rho)\cos(\theta),\tag{8.34}$$

$$\left(\hat{\mathcal{Q}} - \hat{\mathcal{R}}\right)\,\dot{\hat{C}}_{\omega X} = -\hat{C}_{\omega X}\left[\dot{\hat{\mathcal{Q}}} - \dot{\hat{\mathcal{R}}} + \left(\frac{9\hat{\mathcal{Q}}}{2} - 4\hat{\mathcal{R}}\right)\tanh(\rho)\right],\tag{8.35}$$

$$\left(\hat{\mathcal{Q}} - \hat{\mathcal{R}}\right)\,\dot{\hat{C}}_{\omega Y} - \frac{\hat{\mathcal{Q}}}{2\sin(\theta)}\frac{1}{(\cosh(\rho))^3}\,\mathring{\hat{C}}_{\kappa Z} = -\hat{C}_{\omega Y}\left[\dot{\hat{\mathcal{Q}}} - \dot{\hat{\mathcal{R}}} + \left(\frac{9\hat{\mathcal{Q}}}{2} - 4\hat{\mathcal{R}}\right)\tanh(\rho)\right],\tag{8.36}$$

$$\left(\hat{\mathcal{Q}} - \hat{\mathcal{R}}\right)\,\dot{\hat{C}}_{\omega Z} + \frac{\hat{\mathcal{Q}}}{2\sin(\theta)}\frac{1}{(\cosh(\rho))^3}\,\mathring{\hat{C}}_{\kappa Y} = -\hat{C}_{\omega Z}\left[\dot{\hat{\mathcal{Q}}} - \dot{\hat{\mathcal{R}}} + \left(5\hat{\mathcal{Q}} - 4\hat{\mathcal{R}}\right)\tanh(\rho)\right]$$
$$- \frac{\hat{\mathcal{Q}}}{2\sin(\theta)}\frac{\cot(\theta)}{(\cosh(\rho))^3}\hat{C}_{\kappa Y},\tag{8.37}$$

where $(\dot{}) \equiv \partial/\partial\rho$, $(\mathring{}) \equiv \partial/\partial\theta$ with $\hat{\mathcal{Q}} = \cosh(\hat{\xi})\,\hat{\mathcal{B}}_{(0)}$ and $\hat{\mathcal{R}} = \cosh(\hat{\xi})\,\hat{\mathcal{N}}_{(0)}$.

In contrast to the Bjorken-expanding system (6.37) where all spin components evolve independently and to the case of non-boost invariant system, see Eqs. (6.54)–(6.59), where the spin components $C_{\kappa X}$, $C_{\omega Y}$ and $C_{\kappa Y}$, $C_{\omega X}$ are coupled with each other, respectively, here we find that $C_{\kappa X}$ and $C_{\omega X}$ evolve independently whereas $C_{\kappa Y}$, $C_{\omega Z}$ and $C_{\kappa Z}$, $C_{\omega Y}$ are coupled with each other, respectively. We observe that these couplings arise due to the breaking of the conformal symmetry in the spin tensor through the dependence of the spin components on the θ coordinate.

For the conformal EoS, the solutions to Eqs. (8.32) and (8.35) can be obtained analytically as

$$\hat{C}_{\kappa X} = \hat{C}^0_{\kappa X}\left(\frac{\cosh(\rho)}{\cosh(\rho_0)}\right)^{5/6}, \qquad \hat{C}_{\omega X} = \hat{C}^0_{\omega X}\left(\frac{\cosh(\rho_0)}{\cosh(\rho)}\right)^{7/6},\tag{8.38}$$

where $\hat{C}^0_{\kappa X} \equiv \hat{C}_{\kappa X}(\rho_0)$ and $\hat{C}^0_{\omega X} \equiv \hat{C}_{\omega X}(\rho_0)$ are the initial values of the spin components. Interestingly, the behavior (concave function of ρ) of $\hat{C}_{\omega X}$ is qualitatively similar to the
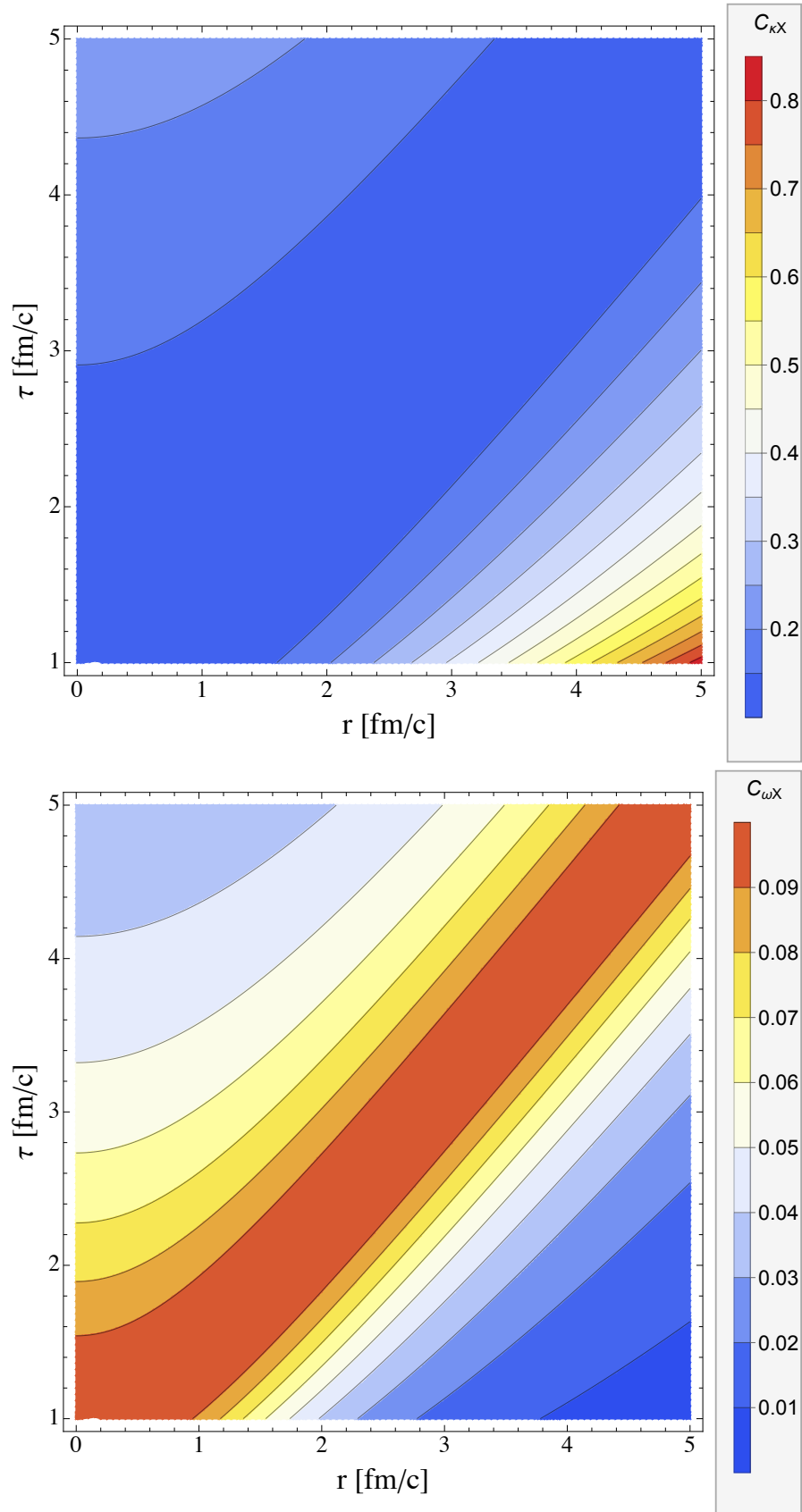
Figure 8.2: (Color online) Dynamics of coefficients $C_{\kappa X}$ (top panel) and $C_{\omega X}$ (bottom panel) in $\tau - r$ plane. Note different color scaling for the two panels.

evolution of temperature and baryon chemical potential (8.31), whereas dynamics of $\hat{\hat{C}}_{\kappa X}$ is given by a convex function of de Sitter time ρ.

Figure 8.2 shows the evolution of $C_{\kappa X}$ (top panel) and $C_{\omega X}$ (bottom panel) in the polar Milne coordinates (τ, r) with the initial values of the spin components as $\hat{\hat{C}}^0_{\kappa X} = \hat{\hat{C}}^0_{\omega X} = 0.1$ implying $C_{\kappa X}(\tau_0 = 1\mathrm{fm}, r = 0) = C_{\omega X}(\tau_0 = 1\mathrm{fm}, r = 0) = 0.1$ and the mass we considered in the calculations is $m = 0.5\,\hat{\hat{T}}_0\,\mathrm{fm}^{-1}$.

The dynamics of the components $\hat{\hat{C}}_{\omega Y}$ and $\hat{\hat{C}}_{\kappa Z}$ is quite complicated due to their coupling through Eqs. (8.34) and (8.36). However, when $\hat{\hat{C}}_{\omega Y}$ is kept initially negligible, then it can be shown that $\hat{\hat{C}}_{\kappa Z}$ is approximately θ-independent

$$\hat{\hat{C}}_{\kappa Z}\big|_{\hat{\hat{C}}_{\omega Y}=0} \approx \hat{\hat{C}}^0_{\kappa Z}\left(\frac{\cosh(\rho)}{\cosh(\rho_0)}\right)^{1/3}, \tag{8.39}$$

where $\hat{\hat{C}}^0_{\kappa Z} \equiv \hat{\hat{C}}_{\kappa Z}(\rho_0)$ and $\hat{\hat{C}}_{\kappa Z}(\rho) \sim 1/\sqrt{\hat{\hat{T}}(\rho)}$.

Furthermore, when $\hat{\hat{C}}_{\omega Y} \neq 0$, one may notice that $\hat{\hat{C}}_{\kappa Z}$ vary slowly with θ and the second term on the left-hand side of Eq. (8.36) can be considered negligible. In this case, the solution to $\hat{\hat{C}}_{\omega Y}$ component takes the form

$$\hat{\hat{C}}_{\omega Y} \approx \hat{\hat{C}}^0_{\omega Y}\left(\frac{\cosh(\rho_0)}{\cosh(\rho)}\right)^{7/6}, \tag{8.40}$$

where $\hat{\hat{C}}^0_{\omega Y}$ is the initial value of $\hat{\hat{C}}_{\omega Y}$ at ρ_0. Numerically, it has checked that $\hat{\hat{C}}_{\omega Y}$ depends weakly on θ and thus approximately proportional to $\hat{\hat{C}}_{\omega X}$.

From Eqs. (8.33) and (8.37) we observe that the solutions for $\hat{\hat{C}}_{\kappa Y}$ and $\hat{\hat{C}}_{\omega Z}$ can be obtained only numerically. Nevertheless some special solutions can be obtained if we assume that θ terms vanish which will make $\hat{\hat{C}}_{\kappa Y}$ and $\hat{\hat{C}}_{\omega Z}$ decouple from each other

$$\hat{\hat{C}}_{\kappa Y} \approx \hat{\hat{C}}^0_{\kappa Y}\left(\frac{\cosh(\rho)}{\cosh(\rho_0)}\right)^{5/6}\csc\theta, \qquad \hat{\hat{C}}_{\omega Z} \approx \hat{\hat{C}}^0_{\omega Z}\left(\frac{\cosh(\rho_0)}{\cosh(\rho)}\right)^{5/3}\csc\theta, \tag{8.41}$$

where $\hat{\hat{C}}^0_{\kappa Y} \equiv \hat{\hat{C}}_{\kappa Y}(\rho_0)$ and $\hat{\hat{C}}^0_{\omega Z} \equiv \hat{\hat{C}}_{\omega Z}(\rho_0)$ and thus $\hat{\hat{C}}_{\kappa Y} \sim \hat{\hat{C}}_{\kappa X}$. All the spin components tend to exhibit the behavior $(\cosh\rho)^c$, with c being positive (or negative) constant.

9

SUMMARY

> *"Begin at the beginning", the King said gravely,*
> *"and go on till you come to the end: then stop."*
> – LEWIS CARROLL, *Alice in Wonderland*

- In this Thesis, we developed a quantum kinetic theory formalism for the Wigner function for spin-$1/2$ massive particles considering local and non-local collisional effects which we used to derive the Boltzmann-like kinetic equation for classical distribution function in phase-space extended to spin. In this process, we assumed no extra constraints on the collisional kernels and considered that the spin polarization may have, both, classical and quantum origins (zeroth and the first-order, in $\hbar$).

- In the case of local equilibrium where the collisional kernels vanish using the developed quantum kinetic theory we derived the perfect-fluid hydrodynamics with spin. We obtained them from the conservation laws for the net baryon current, the energy-momentum tensor, and the spin tensor using GLW definitions of the currents. These relations agree with the conservation equations derived using the classical approach in the small polarization limit.

- We then studied the propagation properties of the spin polarization components using the general form of spin tensor and derived the spin-wave velocity for the Maxwell-Jüttner and Fermi-Dirac statistics. We analyzed the wave spectrum of the spin polarization components and found that only the transverse spin components propagate, as in the case of electromagnetic waves.

- Finally, we studied the space-time evolution of the spin polarization components using the formalism of perfect-fluid hydrodynamics with spin and obtained some novel numerical and analytic results using various hydrodynamic backgrounds and/or external electric field. We found qualitative agreement between our spin polarization results with other models and experimental observations.

A

INTERPRETATION OF SPIN COMPONENTS FOR BOOST-INVARIANCE-BREAKING FLOW

Following the discussions in Sec. 6.2.2 where we calculated orbital and spin contributions to the total angular momentum at the hypersurface of fixed τ, in this appendix, we do the same but for the non-boost-invariant transversely homogeneous system which helps us in the initialization of the spin components in the numerical analysis. Details of the following discussion are provided in the appendix of Ref. [D3].

Considering a similar boost-invariant three-dimensional hypersurface, as depicted in Fig. 6.4, we calculate the orbital contribution to the total angular momentum as

$$L_{\text{FC}}^{\mu\nu} = \int \Delta\Sigma_\lambda \, L^{\lambda,\mu\nu} = \int \Delta\Sigma_\lambda \left(x^\mu \, T_{\text{GLW}}^{\lambda\nu} - x^\nu \, T_{\text{GLW}}^{\lambda\mu} \right), \tag{A.1}$$

with infinitesimal element of the hypersurface $(\Delta\Sigma_\lambda)$ defined as

$$\Delta\Sigma_\mu = \tau_{\text{FC}} \, U_\mu^{\text{B}} \, dx \, dy \, d\eta, \tag{A.2}$$

cf. Eq. (6.40). Note that U_μ^{B} is the same as Bjorken flow in Eq. (6.31), however, to distinguish it from the non-boost-invariant flow (6.48) we have given it the suffix 'B'. Similarly to Eq. (6.41) we find

$$L_{\text{FC}}^{\mu\nu} = \int \Delta\Sigma_\lambda \left(x^\mu \, T_{\text{GLW}}^{\lambda\nu} - x^\nu \, T_{\text{GLW}}^{\lambda\mu} \right), \tag{A.3}$$

$$= \tau_{\text{FC}} \, \pi \, R_{\text{FC}}^2 \int_{-\eta_{\text{FC}}/2}^{\eta_{\text{FC}}/2} d\eta \, U_\lambda^B U^\lambda \left[\left(\mathcal{E} + \mathcal{P} \right) \left(x^\mu U^\nu - x^\nu U^\mu \right) - \mathcal{P} \left(x^\mu U_{\text{B}}^\nu - x^\nu U_{\text{B}}^\mu \right) \right].$$

Using definitions of Bjorken flow (6.31) and non-boost-invariant flow (6.48) we can show that $L_{\text{FC}}^{\mu\nu} = 0$. Thus, there is vanishing contribution from the orbital part to the total angular momentum.

Similarly, we can obtain the contribution from spin angular momentum as

$$S_{\text{FC}}^{\mu\nu} = \int \Delta\Sigma_\lambda \, S_{\text{GLW}}^{\lambda,\mu\nu} = \tau_{\text{FC}} \, \pi \, R_{\text{FC}}^2 \int_{-\eta_{\text{FC}}/2}^{\eta_{\text{FC}}/2} d\eta \, U_\lambda^{\text{B}} \, S_{\text{GLW}}^{\lambda,\mu\nu}, \tag{A.4}$$

where we insert Eqs. (6.31) and (6.48) to calculate the components of $S_{\text{FC}}^{\mu\nu}$. With the assumption that ϑ is η-odd, we obtain the components S_{FC}^{03} and S_{FC}^{12} as

$$
\begin{aligned}
S_{\text{FC}}^{03} &= -\pi R_{\text{FC}}^2 \tau_{\text{FC}} \int d\eta\, \mathcal{A}_3\, C_{\kappa Z} \cosh(\vartheta)\,, \\
S_{\text{FC}}^{12} &= -\pi R_{\text{FC}}^2 \tau_{\text{FC}} \int d\eta\, \mathcal{A}_1\, C_{\omega Z} \cosh(\vartheta)\,,
\end{aligned}
\tag{A.5}
$$

which vanish when both the longitudinal components are arbitrary odd functions of η or zero. These symmetries are also maintained by their equations of motion, see Eqs. (6.56) and (6.59). Furthermore, S_{FC}^{13} and S_{FC}^{01} components

$$
\begin{aligned}
S_{\text{FC}}^{13} &= \pi R_{\text{FC}}^2 \tau_{\text{FC}} \int d\eta\, \mathcal{A}_3 \Bigg[\left(\frac{\mathcal{A}_1}{\mathcal{A}_3} \cosh(\vartheta) \cosh(\Phi) - \frac{1}{2} \sinh(\vartheta) \sinh(\Phi) \right) C_{\omega Y} \\
&\quad + \frac{1}{4} \left(\sinh(\eta) + 3\sinh(\Phi + \vartheta) \right) C_{\kappa X} \Bigg]\,,
\end{aligned}
\tag{A.6}
$$

$$
\begin{aligned}
S_{\text{FC}}^{01} &= -\pi R_{\text{FC}}^2 \tau_{\text{FC}} \int d\eta\, \mathcal{A}_3 \Bigg[\left(\frac{\mathcal{A}_1}{\mathcal{A}_3} \cosh(\vartheta) \sinh(\Phi) - \frac{1}{2} \sinh(\vartheta) \cosh(\Phi) \right) C_{\omega Y} \\
&\quad + \frac{1}{4} \left(\cosh(\eta) + 3\cosh(\Phi + \vartheta) \right) C_{\kappa X} \Bigg]\,,
\end{aligned}
\tag{A.7}
$$

indicate that to have vanishing S_{FC}^{01} and non-vanishing S_{FC}^{13}, it is necessary that $C_{\omega Y}$ is even function of η, whereas $C_{\kappa X}$ can be η-odd or zero. Thus, these conditions permit us to initialize the spin components as Eq. (6.60).

Similar physical arguments can also be put forward for the spin components $C_{\kappa Y}$ and $C_{\omega X}$, however, for our assumed physical situation we can safely put them to zero.

B

COVARIANT DERIVATIVE AND CHRISTOF-FEL SYMBOLS IN DE SITTER COORDINATES

In this appendix we list some important properties of the covariant derivative and the Christoffel symbols in the de Sitter coordinates. Details presented here may be found in the appendix of Ref. [D5].

B.1 The covariant derivative

For a general spacetime curvature, the partial derivative operator is not suitable for calculating derivatives and thus we need to have a more general derivative operator namely covariant derivative which acts on an arbitrary scalar V, rank-1 V^μ and rank-2 $V^{\mu\nu}$ tensors as

$$d_\mu V = \partial_\mu V \,, \tag{B.1}$$
$$d_\mu V_\nu = \partial_\mu V_\nu - \Gamma^\sigma_{\mu\nu} V_\sigma \,, \tag{B.2}$$
$$d_\lambda V_{\mu\nu} = \partial_\lambda V_{\mu\nu} - \Gamma^\sigma_{\lambda\mu} V_{\sigma\nu} - \Gamma^\sigma_{\lambda\nu} V_{\mu\sigma} \,, \tag{B.3}$$
$$d_\mu V^\nu = \partial_\mu V^\nu + \Gamma^\nu_{\mu\sigma} V^\sigma \,, \tag{B.4}$$
$$d_\mu V^\mu = \partial_\mu V^\mu + \Gamma^\mu_{\mu\sigma} V^\sigma \,, \tag{B.5}$$
$$d_\mu V^{\mu\nu} = \partial_\mu V^{\mu\nu} + \Gamma^\mu_{\mu\sigma} V^{\sigma\nu} + \Gamma^\nu_{\mu\sigma} V^{\mu\sigma} \,, \tag{B.6}$$
$$d_\lambda V^{\mu\nu} = \partial_\lambda V^{\mu\nu} + \Gamma^\mu_{\lambda\sigma} V^{\sigma\nu} + \Gamma^\nu_{\lambda\sigma} V^{\mu\sigma} \,. \tag{B.7}$$

B.2 Christoffel symbols in the de Sitter coordinates

Using the definition of Christoffel symbol (8.22) and the de Sitter metric (8.6), the following non-vanishing Christoffel symbols remain

$$\Gamma^\rho_{\theta\theta} = \sinh(\rho)\cosh(\rho) \,, \tag{B.8}$$
$$\Gamma^\rho_{\phi\phi} = (\sin(\theta))^2 \sinh(\rho)\cosh(\rho) \,, \tag{B.9}$$
$$\Gamma^\theta_{\rho\theta} = \Gamma^\theta_{\theta\rho} = \tanh(\rho) \,, \tag{B.10}$$
$$\Gamma^\theta_{\phi\phi} = -\sin(\theta)\cos(\theta) \,, \tag{B.11}$$
$$\Gamma^\phi_{\rho\phi} = \Gamma^\phi_{\phi\rho} = \tanh(\rho) \,, \tag{B.12}$$
$$\Gamma^\phi_{\theta\phi} = \Gamma^\phi_{\phi\theta} = \cot(\theta) \,. \tag{B.13}$$

Bibliography

[1] G. Lemaître, "Un Univers homogène de masse constante et de rayon croissant rendant compte de la vitesse radiale des nébuleuses extra-galactiques," *Annales de la Société Scientifique de Bruxelles* **47** (Jan., 1927) 49–59. 17

[2] J.-P. Luminet, "Editorial note to "A Homogeneous Universe of Constant Mass and Increasing Radius accounting for the Radial Velocity of Extra–Galactic Nebulae" by Georges Lemaître (1927)," *Gen. Rel. Grav.* **45** (2013) 1619–1633, `arXiv:1305.6470` `[physics.hist-ph]`.

[3] A. Friedman, "On the curvature of space," *General Relativity and Gravitation* **31** no. 12, (1999) 1991–2000. `https://doi.org/10.1023/A:1026751225741`. 17

[4] H. Nussbaumer, L. Bieri, and A. Sandage, *Discovering the Expanding Universe.* Cambridge University Press, 2009. 17

[5] K. Lundmark, "The Determination of the Curvature of Space-Time in de Sitter's World," *Monthly Notices of the Royal Astronomical Society* **84** no. 9, (07, 1924) 747–770. 17

[6] H. P. Robertson, "Kinematics and World-Structure. 2," *Astrophys. J.* **83** (1935) 187–201. 17

[7] H. P. Robertson, "Kinematics and World-Structure," *Astrophys. J.* **82** (1935) 284–301.

[8] H. P. Robertson, "Kinematics and World-Structure. 3," *Astrophys. J.* **83** (1936) 257–271.

[9] A. G. Walker, "On Milne's Theory of World-Structure*," *Proceedings of the London Mathematical Society* **s2-42** no. 1, (01, 1937) 90–127. 17

[10] E. Hubble, "A relation between distance and radial velocity among extra-galactic nebulae," *Proceedings of the National Academy of Sciences* **15** no. 3, (1929) 168–173. 17

[11] A. A. Penzias and R. W. Wilson, "A Measurement of excess antenna temperature at 4080-Mc/s," *Astrophys. J.* **142** (1965) 419–421. 17

[12] G. Gamow, "The origin of elements and the separation of galaxies," *Phys. Rev.* **74** (Aug, 1948) 505–506. 17

[13] R. A. Alpher, H. Bethe, and G. Gamow, "The origin of chemical elements," *Phys. Rev.* **73** (Apr, 1948) 803–804. 17

[14] H. R. Schmidt and J. Schukraft, "The Physics of ultrarelativistic heavy ion collisions," *J. Phys. G* **19** (1993) 1705–1796. 17, 20

[15] J. Schukraft and R. Stock, "Toward the Limits of Matter: Ultra-relativistic nuclear collisions at CERN," *Adv. Ser. Direct. High Energy Phys.* **23** (2015) 61–87, `arXiv:1505.06853 [nucl-ex]`. 17, 20

[16] E. W. Kolb and M. S. Turner, *The Early Universe*, vol. 69. CRC Press, 1990. 17

[17] A. D. Linde, "Phase Transitions in Gauge Theories and Cosmology," *Rept. Prog. Phys.* **42** (1979) 389. 17

[18] D. Boyanovsky, H. J. de Vega, and D. J. Schwarz, "Phase transitions in the early and the present universe," *Ann. Rev. Nucl. Part. Sci.* **56** (2006) 441–500, `arXiv:hep-ph/0602002`. 17, 18

[19] H. Satz, *Statistical Mechanics of Quarks and Hadrons: Proceedings of an International Symposium Held at the University of Bielefeld, F.R.G., August 24-31, 1980*. North-Holland, 1981. `https://books.google.pl/books?id=OY8uAAAAIAAJ`. 18

[20] L. D. McLerran, "The Physics of the Quark - Gluon Plasma," *Rev. Mod. Phys.* **58** (1986) 1021–1064. 18

[21] B. V. Jacak and B. Muller, "The exploration of hot nuclear matter," *Science* **337** (2012) 310–314. 18

[22] K. Fukushima and C. Sasaki, "The phase diagram of nuclear and quark matter at high baryon density," *Prog. Part. Nucl. Phys.* **72** (2013) 99–154, `arXiv:1301.6377 [hep-ph]`. 18

[23] D. J. Gross and F. Wilczek, "Ultraviolet Behavior of Nonabelian Gauge Theories," *Phys. Rev. Lett.* **30** (1973) 1343–1346. 18

[24] H. D. Politzer, "Reliable Perturbative Results for Strong Interactions?," *Phys. Rev. Lett.* **30** (1973) 1346–1349. 18

[25] Y. B. Zel'dovich and Y. P. Raizer, *Physics of shock waves and high-temperature hydrodynamic phenomena*. Courier Corporation, 1967. 18

[26] J. R. Oppenheimer and G. M. Volkoff, "On massive neutron cores," *Phys. Rev.* **55** (1939) 374–381. 19

[27] G. Gamow, "Expanding universe and the origin of elements," *Phys. Rev.* **70** (1946) 572–573. 19

[28] Y. B. Zel'dovich, "The equation of state at ultrahigh densities and its relativistic limitations," *Zh. Eksp. Teor. Fiz.* **41** (1961) 1609–1615. 19

[29] F. Karsch and E. Laermann, "Susceptibilities, the specific heat and a cumulant in two flavor QCD," *Phys. Rev. D* **50** (1994) 6954–6962, `arXiv:hep-lat/9406008`. 19

[30] F. Karsch, "Lattice QCD at high temperature and density," *Lect. Notes Phys.* **583** (2002) 209–249, `arXiv:hep-lat/0106019`. 19

[31] L. D. McLerran and B. Svetitsky, "Quark Liberation at High Temperature: A Monte Carlo Study of SU(2) Gauge Theory," *Phys. Rev. D* **24** (1981) 450. 19

[32] P. de Forcrand, "Simulating QCD at finite density," *PoS* **LAT2009** (2009) 010, `arXiv:1005.0539 [hep-lat]`. 19

[33] Y. Nambu and G. Jona-Lasinio, "Dynamical Model of Elementary Particles Based on an Analogy with Superconductivity I," *Phys. Rev.* **122** (1961) 345–358. 19

[34] Y. Nambu and G. Jona-Lasinio, "Dynamical Model of Elementary Particles Based on an Analogy with Superconductivity II," *Phys. Rev.* **124** (1961) 246–254. 19

[35] S. P. Klevansky, "The Nambu-Jona-Lasinio model of quantum chromodynamics," *Rev. Mod. Phys.* **64** (1992) 649–708. 19

[36] M. Buballa, "NJL model analysis of quark matter at large density," *Phys. Rept.* **407** (2005) 205–376, `arXiv:hep-ph/0402234`. 19

[37] C. Ratti, S. Roessner, M. A. Thaler, and W. Weise, "Thermodynamics of the PNJL model," *Eur. Phys. J. C* **49** (2007) 213–217, `arXiv:hep-ph/0609218`. 19

[38] J. C. Collins and M. J. Perry, "Superdense Matter: Neutrons Or Asymptotically Free Quarks?," *Phys. Rev. Lett.* **34** (1975) 1353. 20

[39] R. Hagedorn, "Statistical thermodynamics of strong interactions at high-energies," *Nuovo Cim. Suppl.* **3** (1965) 147–186. 20

[40] N. Cabibbo and G. Parisi, "Exponential Hadronic Spectrum and Quark Liberation," *Phys. Lett. B* **59** (1975) 67–69. 20

[41] E. V. Shuryak, "Quark-Gluon Plasma and Hadronic Production of Leptons, Photons and Psions," *Phys. Lett. B* **78** (1978) 150. 20

[42] E. V. Shuryak, "Quantum Chromodynamics and the Theory of Superdense Matter," *Phys. Rept.* **61** (1980) 71–158. 20

[43] G. F. Chapline, M. H. Johnson, E. Teller, and M. S. Weiss, "Highly excited nuclear matter," *Phys. Rev. D* **8** (1973) 4302–4308. 20

[44] W. Scheid, H. Muller, and W. Greiner, "Nuclear Shock Waves in Heavy-Ion Collisions," *Phys. Rev. Lett.* **32** (1974) 741–745. 20

[45] M. I. Sobel, H. A. Bethe, P. J. Siemens, and J. P. Bondorf, "Shock Waves in Colliding Nuclei," *Nucl. Phys. A* **251** (1975) 502–529. 20

[46] S. Nagamiya and M. Gyulassy, "HIGH-ENERGY NUCLEAR COLLISIONS," *Adv. Nucl. Phys.* **13** (1984) 201–315. 20

[47] R. Stock, "Particle Production in High-Energy Nucleus Nucleus Collisions," *Phys. Rept.* **135** (1986) 259–315. 20

[48] H. Stoecker and W. Greiner, "High-Energy Heavy Ion Collisions: Probing the Equation of State of Highly Excited Hadronic Matter," *Phys. Rept.* **137** (1986) 277–392. 20

[49] R. C. Hwa, ed., *Quark - gluon plasma*. WSP, Singapore, 1990. 20

[50] C. Y. Wong, *Introduction to high-energy heavy ion collisions*. World Scientific, 1995. 20

[51] B. Muller, "Physics and signatures of the quark - gluon plasma," *Rept. Prog. Phys.* **58** (1995) 611–636, arXiv:nucl-th/9410005. 20

[52] K. Yagi, T. Hatsuda, and Y. Miake, "Quark-gluon plasma: From big bang to little bang," *Camb. Monogr. Part. Phys. Nucl. Phys. Cosmol.* **23** (2005) 1–446. 20

[53] R. Vogt, *Ultrarelativistic heavy-ion collisions*. Elsevier, Amsterdam, 2007. 20

[54] W. Florkowski, *Phenomenology of ultra-relativistic heavy-ion collisions*. World Scientific, Singapore, 2010. https://cds.cern.ch/record/1321594. 20, 21, 27, 57, 60, 61

[55] W. Busza, K. Rajagopal, and W. van der Schee, "Heavy Ion Collisions: The Big Picture, and the Big Questions," *Ann. Rev. Nucl. Part. Sci.* **68** (2018) 339–376, arXiv:1802.04801 [hep-ph]. 20, 27

[56] R. Stock, "7 relativistic nucleus-nucleus collisions and the qcd matter phase diagram: Datasheet from landolt-börnstein - group i elementary particles, nuclei and atoms · volume 21a: "theory and experiments" in springermaterials (https://doi.org/10.1007/978-3-540-74203-6_7),". https://materials.springer.com/lb/docs/sm_lbs_978-3-540-74203-6_7. 20

[57] Z.-T. Liang, M. A. Lisa, and X.-N. Wang, "Global Polarization Effect in the Extremely Rapidly Rotating QGP in HIC," *Nucl. Phys. News* **30** no. 2, (2020) 10–16, arXiv:1912.07822 [nucl-th]. 21

[58] **STAR** Collaboration, J. Adams *et al.*, "Experimental and theoretical challenges in the search for the quark gluon plasma: The STAR Collaboration's critical assessment of the evidence from RHIC collisions," *Nucl. Phys. A* **757** (2005) 102–183, arXiv:nucl-ex/0501009. 20

[59] W. Broniowski and W. Florkowski, "Explanation of the RHIC p(T) spectra in a thermal model with expansion," *Phys. Rev. Lett.* **87** (2001) 272302, arXiv:nucl-th/0106050. 21

[60] L. D. Landau, "On the multiparticle production in high-energy collisions," *Izv. Akad. Nauk Ser. Fiz.* **17** (1953) 51–64. 21

[61] W. Broniowski, M. Chojnacki, W. Florkowski, and A. Kisiel, "Uniform Description of Soft Observables in Heavy-Ion Collisions at s(NN)**(1/2) = 200 GeV**2," *Phys. Rev. Lett.* **101** (2008) 022301, arXiv:0801.4361 [nucl-th]. 21

[62] W. Florkowski, "Basic phenomenology for relativistic heavy-ion collisions," *Acta Phys. Polon. B* **45** no. 12, (2014) 2329–2354, arXiv:1410.7904 [nucl-th]. 21

[63] **WA80** Collaboration, R. Albrecht *et al.*, "Limits on the production of direct photons in 200a gev $^{32}s + au$ collisions," *Phys. Rev. Lett.* **76** (May, 1996) 3506–3509. 21

[64] **WA98** Collaboration, M. M. Aggarwal *et al.*, "Observation of direct photons in central 158-A-GeV Pb-208 + Pb-208 collisions," *Phys. Rev. Lett.* **85** (2000) 3595–3599, arXiv:nucl-ex/0006008. 21

[65] T. Matsui and H. Satz, "J/ψ Suppression by Quark-Gluon Plasma Formation," *Phys. Lett. B* **178** (1986) 416–422. 21

[66] N. Brambilla *et al.*, "Heavy Quarkonium: Progress, Puzzles, and Opportunities," *Eur. Phys. J. C* **71** (2011) 1534, arXiv:1010.5827 [hep-ph]. 21

[67] A. Andronic *et al.*, "Heavy-flavour and quarkonium production in the LHC era: from proton–proton to heavy-ion collisions," *Eur. Phys. J. C* **76** no. 3, (2016) 107, arXiv:1506.03981 [nucl-ex]. 21

[68] J. Rafelski and B. Muller, "Strangeness Production in the Quark - Gluon Plasma," *Phys. Rev. Lett.* **48** (1982) 1066. [Erratum: Phys.Rev.Lett. 56, 2334 (1986)]. 22

[69] P. Koch, B. Muller, and J. Rafelski, "Strangeness in Relativistic Heavy Ion Collisions," *Phys. Rept.* **142** (1986) 167–262. 22

[70] M. Marczenko, D. Blaschke, K. Redlich, and C. Sasaki, "Chiral symmetry restoration by parity doubling and the structure of neutron stars," *Phys. Rev. D* **98** no. 10, (2018) 103021, arXiv:1805.06886 [nucl-th]. 22

[71] **WA97** Collaboration, "Transverse mass spectra of strange and multi-strange particles in Pb-Pb collisions at 158 A GeV/c," *Eur. Phys. J. C* **14** (Jan, 2000) 633–641. 16 p. 22

[72] M. Gyulassy and M. Plumer, "Jet Quenching in Dense Matter," *Phys. Lett. B* **243** (1990) 432–438. 22

[73] M. Gyulassy, I. Vitev, X.-N. Wang, and B.-W. Zhang, "Jet quenching and radiative energy loss in dense nuclear matter," arXiv:nucl-th/0302077. 22

[74] **ATLAS** Collaboration, G. Aad *et al.*, "Observation of a Centrality-Dependent Dijet Asymmetry in Lead-Lead Collisions at $\sqrt{s_{NN}} = 2.77$ TeV with the ATLAS Detector at the LHC," *Phys. Rev. Lett.* **105** (2010) 252303, arXiv:1011.6182 [hep-ex]. 22

[75] **CMS** Collaboration, S. Chatrchyan *et al.*, "Observation and studies of jet quenching in PbPb collisions at nucleon-nucleon center-of-mass energy = 2.76 TeV," *Phys. Rev. C* **84** (2011) 024906, arXiv:1102.1957 [nucl-ex]. 22

[76] U. W. Heinz and M. Jacob, "Evidence for a new state of matter: An Assessment of the results from the CERN lead beam program," arXiv:nucl-th/0002042. 23

[77] **PHENIX** Collaboration, K. Adcox *et al.*, "Formation of dense partonic matter in relativistic nucleus-nucleus collisions at RHIC: Experimental evaluation by the PHENIX collaboration," *Nucl. Phys. A* **757** (2005) 184–283, arXiv:nucl-ex/0410003. 23

[78] **STAR** Collaboration, J. Adams *et al.*, "Experimental and theoretical challenges in the search for the quark gluon plasma: The STAR Collaboration's critical assessment of the evidence from RHIC collisions," *Nucl. Phys. A* **757** (2005) 102–183, `arXiv:nucl-ex/0501009`. 23

[79] M. Gyulassy and L. McLerran, "New forms of QCD matter discovered at RHIC," *Nucl. Phys. A* **750** (2005) 30–63, `arXiv:nucl-th/0405013`. 23

[80] E. Shuryak, "Physics of Strongly coupled Quark-Gluon Plasma," *Prog. Part. Nucl. Phys.* **62** (2009) 48–101, `arXiv:0807.3033 [hep-ph]`. 23

[81] S. Giorgini, L. P. Pitaevskii, and S. Stringari, "Theory of ultracold atomic Fermi gases," *Rev. Mod. Phys.* **80** (2008) 1215–1274, `arXiv:0706.3360 [cond-mat.other]`. 23

[82] **Fermi-LAT** Collaboration, R. P. Johnson, "Recent results from the Fermi gamma-ray space telescope," *PoS* **ICHEP2010** (2010) 434. 23

[83] C. Cao, E. Elliott, J. Joseph, H. Wu, J. Petricka, T. Schäfer, and J. E. Thomas, "Universal Quantum Viscosity in a Unitary Fermi Gas," *Science* **331** (2011) 58, `arXiv:1007.2625 [cond-mat.quant-gas]`. 23

[84] G. Policastro, D. T. Son, and A. O. Starinets, "The Shear viscosity of strongly coupled N=4 supersymmetric Yang-Mills plasma," *Phys. Rev. Lett.* **87** (2001) 081601, `arXiv:hep-th/0104066`. 23

[85] P. Kovtun, D. T. Son, and A. O. Starinets, "Holography and hydrodynamics: Diffusion on stretched horizons," *JHEP* **10** (2003) 064, `arXiv:hep-th/0309213`. 23

[86] J. M. Maldacena, "The Large N limit of superconformal field theories and supergravity," *Adv.Theor.Math.Phys.* **2** (1998) 231–252, `arXiv:hep-th/9711200 [hep-th]`. 23

[87] A. Vilenkin, "EQUILIBRIUM PARITY VIOLATING CURRENT IN A MAGNETIC FIELD," *Phys. Rev. D* **22** (1980) 3080–3084. 23, 25

[88] K. Fukushima, D. E. Kharzeev, and H. J. Warringa, "The Chiral Magnetic Effect," *Phys. Rev.* **D78** (2008) 074033, `arXiv:0808.3382 [hep-ph]`. 23, 25

[89] F. Becattini, F. Piccinini, and J. Rizzo, "Angular momentum conservation in heavy ion collisions at very high energy," *Phys. Rev. C* **77** (2008) 024906, `arXiv:0711.1253 [nucl-th]`. 23, 24

[90] **STAR** Collaboration, L. Adamczyk *et al.*, "Global Λ hyperon polarization in nuclear collisions: evidence for the most vortical fluid," *Nature* **548** (2017) 62–65, `arXiv:1701.06657 [nucl-ex]`. 23, 24, 25, 35, 43, 44, 92, 100

[91] W. Florkowski, R. Ryblewski, and A. Kumar, "Relativistic hydrodynamics for spin-polarized fluids," *Prog. Part. Nucl. Phys.* **108** (2019) 103709, `arXiv:1811.04409 [nucl-th]`. 23, 25, 33, 34, 35, 37, 45, 52, 53, 55, 60, 61, 63, 64, 70, 80, 110

[92] Z.-T. Liang and X.-N. Wang, "Globally polarized quark-gluon plasma in non-central A+A collisions," *Phys. Rev. Lett.* **94** (2005) 102301, `arXiv:nucl-th/0410079 [nucl-th]`. [Erratum: Phys. Rev. Lett.96,039901(2006)]. 23

[93] A. Einstein and W. de Haas, "Experimenteller Nachweis der Ampereschen Molekularstroeme," *Deutsche Physikalische Gesellschaft, Verhandlungen* **17** (1915) 152. 24

[94] S. J. Barnett, "Gyromagnetic and electron-inertia effects," *Rev. Mod. Phys.* **7** (Apr, 1935) 129–166. 24

[95] **STAR** Collaboration, J. Adam *et al.*, "Global Polarization of Ξ and Ω Hyperons in Au+Au Collisions at $\sqrt{s_{NN}}$ = 200 GeV," *Phys. Rev. Lett.* **126** no. 16, (2021) 162301, `arXiv:2012.13601 [nucl-ex]`. 24

[96] **STAR** Collaboration, J. Adam *et al.*, "Global polarization of Λ hyperons in Au+Au collisions at $\sqrt{s_{NN}}$ = 200 GeV," *Phys. Rev. C* **98** (2018) 014910, `arXiv:1805.04400 [nucl-ex]`. 24, 35, 103

[97] F. Becattini, I. Karpenko, M. Lisa, I. Upsal, and S. Voloshin, "Global hyperon polarization at local thermodynamic equilibrium with vorticity, magnetic field and feed-down," *Phys. Rev.* **C95** no. 5, (2017) 054902, `arXiv:1610.02506 [nucl-th]`. 24, 31, 34

[98] J.-H. Gao, Z.-T. Liang, Q. Wang, and X.-N. Wang, "Global polarization effect and spin-orbit coupling in strong interaction," *Lect. Notes Phys.* **987** (2021) 195–246, `arXiv:2009.04803 [nucl-th]`. 25

[99] F. Becattini and M. A. Lisa, "Polarization and Vorticity in the Quark–Gluon Plasma," *Ann. Rev. Nucl. Part. Sci.* **70** (2020) 395–423, `arXiv:2003.03640 [nucl-ex]`. 25

[100] E. Speranza and N. Weickgenannt, "Spin tensor and pseudo-gauges: from nuclear collisions to gravitational physics," *Eur. Phys. J. A* **57** no. 5, (2021) 155, `arXiv:2007.00138 [nucl-th]`. 25, 32, 33, 34, 53

[101] A. Jaiswal *et al.*, "Dynamics of QCD matter — current status," *Int. J. Mod. Phys. E* **30** no. 02, (2021) 2130001, `arXiv:2007.14959 [hep-ph]`. 25

[102] F. Becattini, J. Liao, and M. Lisa, "Strongly Interacting Matter Under Rotation: An Introduction," *Lect. Notes Phys.* **987** (2021) 1–14, `arXiv:2102.00933 [nucl-th]`. 25

[103] J. L. Francesco Becattini and M. Lisa, eds., *Strongly Interacting Matter under Rotation*. Lecture Notes in Physics. Springer, 2021. 25

[104] S. Bhadury, J. Bhatt, A. Jaiswal, and A. Kumar, "New developments in relativistic fluid dynamics with spin," *Eur. Phys. J. ST* **230** no. 3, (2021) 655–672, `arXiv:2101.11964 [hep-ph]`. 25

[105] F. Becattini, "Spin and polarization: a new direction in relativistic heavy ion physics," `arXiv:2204.01144 [nucl-th]`. 25

[106] J.-H. Gao, S.-W. Chen, W.-T. Deng, Z.-T. Liang, Q. Wang, and X.-N. Wang, "Global quark polarization in non-central A+A collisions," *Phys. Rev.* **C77** (2008) 044902, `arXiv:0710.2943 [nucl-th]`. 25

[107] Q. Wang, "Global and local spin polarization in heavy ion collisions: a brief overview," *Nucl. Phys.* **A967** (2017) 225–232, `arXiv:1704.04022 [nucl-th]`. 25

[108] D. E. Kharzeev and D. T. Son, "Testing the chiral magnetic and chiral vortical effects in heavy ion collisions," *Phys. Rev. Lett.* **106** (2011) 062301, `arXiv:1010.0038 [hep-ph]`. 25, 35

[109] D. E. Kharzeev, J. Liao, S. A. Voloshin, and G. Wang, "Chiral magnetic and vortical effects in high-energy nuclear collisions – status report," *Prog. Part. Nucl. Phys.* **88** (2016) 1–28, `arXiv:1511.04050 [hep-ph]`. 25

[110] W.-T. Deng and X.-G. Huang, "Vorticity in Heavy-Ion Collisions," *Phys. Rev. C* **93** no. 6, (2016) 064907, `arXiv:1603.06117 [nucl-th]`. 25

[111] Y. Hidaka, S. Pu, and D.-L. Yang, "Relativistic Chiral Kinetic Theory from Quantum Field Theories," *Phys. Rev. D* **95** no. 9, (2017) 091901, `arXiv:1612.04630 [hep-th]`. 25, 44

[112] **CMS** Collaboration, V. Khachatryan *et al.*, "Observation of charge-dependent azimuthal correlations in p-Pb collisions and its implication for the search for the chiral magnetic effect," *Phys. Rev. Lett.* **118** no. 12, (2017) 122301, `arXiv:1610.00263 [nucl-ex]`. 25

[113] **CMS** Collaboration, A. M. Sirunyan *et al.*, "Constraints on the chiral magnetic effect using charge-dependent azimuthal correlations in pPb and PbPb collisions at the CERN Large Hadron Collider," *Phys. Rev. C* **97** no. 4, (2018) 044912, `arXiv:1708.01602 [nucl-ex]`. 25

[114] Y.-C. Liu, L.-L. Gao, K. Mameda, and X.-G. Huang, "Chiral kinetic theory in curved spacetime," *Phys. Rev. D* **99** no. 8, (2019) 085014, `arXiv:1812.10127 [hep-th]`. 25

[115] J. Zhao and F. Wang, "Experimental searches for the chiral magnetic effect in heavy-ion collisions," *Prog. Part. Nucl. Phys.* **107** (2019) 200–236, `arXiv:1906.11413 [nucl-ex]`. 25

[116] **STAR** Collaboration, J. Adam *et al.*, "Charge separation measurements in $p(d)$+Au and Au+Au collisions; implications for the chiral magnetic effect," `arXiv:2006.04251 [nucl-ex]`. 25

[117] **STAR** Collaboration, M. Abdallah *et al.*, "Search for the chiral magnetic effect with isobar collisions at $\sqrt{s_{NN}}$=200 GeV by the STAR Collaboration at the BNL Relativistic Heavy Ion Collider," *Phys. Rev. C* **105** no. 1, (2022) 014901, `arXiv:2109.00131 [nucl-ex]`. 25

[118] M. Buzzegoli, "Thermodynamic equilibrium of massless fermions with vorticity, chirality and electromagnetic field," `arXiv:2011.09974 [hep-th]`. 25

[119] D. E. Kharzeev, L. D. McLerran, and H. J. Warringa, "The Effects of topological charge change in heavy ion collisions: 'Event by event P and CP violation'," *Nucl. Phys.* **A803** (2008) 227–253, `arXiv:0711.0950 [hep-ph]`. 25, 107

[120] **STAR** Collaboration, B. I. Abelev *et al.*, "Azimuthal Charged-Particle Correlations and Possible Local Strong Parity Violation," *Phys. Rev. Lett.* **103** (2009) 251601, arXiv:0909.1739 [nucl-ex]. 25

[121] D. E. Kharzeev and H.-U. Yee, "Chiral Magnetic Wave," *Phys. Rev. D* **83** (2011) 085007, arXiv:1012.6026 [hep-th]. 25

[122] D. E. Kharzeev, "The Chiral Magnetic Effect and Anomaly-Induced Transport," *Prog. Part. Nucl. Phys.* **75** (2014) 133–151, arXiv:1312.3348 [hep-ph]. 25

[123] P. Bozek, "Azimuthal angle dependence of the charge imbalance from charge conservation effects," *Phys. Rev. C* **97** no. 3, (2018) 034907, arXiv:1711.02563 [nucl-th]. 25

[124] X. An *et al.*, "The BEST framework for the search for the QCD critical point and the chiral magnetic effect," *Nucl. Phys. A* **1017** (2022) 122343, arXiv:2108.13867 [nucl-th]. 25

[125] **STAR** Collaboration, M. Abdallah *et al.*, "Search for the Chiral Magnetic Effect via Charge-Dependent Azimuthal Correlations Relative to Spectator and Participant Planes in Au+Au Collisions at $\sqrt{s_{NN}} = 200\,\text{GeV}$," *Phys. Rev. Lett.* **128** no. 9, (2022) 092301, arXiv:2106.09243 [nucl-ex]. 25

[126] L. Yin, D. Hou, and H.-c. Ren, "Chiral magnetic effect and three-point function from AdS/CFT correspondence," *JHEP* **09** (2021) 117, arXiv:2102.04851 [hep-th]. 25

[127] D. E. Kharzeev, "Chiral magnetic effect in heavy ion collisions and beyond," 4, 2022. arXiv:2204.10903 [hep-ph]. 25

[128] F. Becattini and I. Karpenko, "Collective Longitudinal Polarization in Relativistic Heavy-Ion Collisions at Very High Energy," *Phys. Rev. Lett.* **120** no. 1, (2018) 012302, arXiv:1707.07984 [nucl-th]. 26, 27, 31

[129] S. A. Voloshin, "Vorticity and particle polarization in heavy ion collisions (experimental perspective)," arXiv:1710.08934 [nucl-ex]. [EPJ Web Conf.17,10700(2018)]. 26, 94

[130] **STAR** Collaboration, J. Adam *et al.*, "Polarization of Λ ($\bar{\Lambda}$) hyperons along the beam direction in Au+Au collisions at $\sqrt{s_{NN}} = 200$ GeV," *Phys. Rev. Lett.* **123** no. 13, (2019) 132301, arXiv:1905.11917 [nucl-ex]. 25, 26, 92, 94, 100

[131] X.-L. Xia, H. Li, Z.-B. Tang, and Q. Wang, "Probing vorticity structure in heavy-ion collisions by local Λ polarization," *Phys. Rev. C* **98** (2018) 024905, arXiv:1803.00867 [nucl-th]. 27, 31

[132] I. Karpenko and F. Becattini, "Study of Λ polarization in relativistic nuclear collisions at $\sqrt{s_{NN}} = 7.7$ –200 GeV," *Eur. Phys. J.* **C77** no. 4, (2017) 213, arXiv:1610.04717 [nucl-th]. 27, 31, 94

[133] Y. Sun and C. M. Ko, "Azimuthal angle dependence of the longitudinal spin polarization in relativistic heavy ion collisions," *Phys. Rev.* **C99** no. 1, (2019) 011903, arXiv:1810.10359 [nucl-th]. 27, 31

[134] S. Bader and S. Parkin, "Spintronics," *Annual Review of Condensed Matter Physics* **1** no. 1, (2010) 71–88. 27

[135] R. Takahashi, M. Matsuo, M. Ono, K. Harii, H. Chudo, S. Okayasu, J. Ieda, S. Takahashi, S. Maekawa, and E. Saitoh, "Spin hydrodynamic generation," *Nature Physics* **12** no. 1, (Jan., 2016) 52–56. 27, 44

[136] A. Hirohata, K. Yamada, Y. Nakatani, I.-L. Prejbeanu, B. Diény, P. Pirro, and B. Hillebrands, "Review on spintronics: Principles and device applications," *Journal of Magnetism and Magnetic Materials* **509** (Sept., 2020) 166711. https://hal.archives-ouvertes.fr/hal-03192774. 27

[137] **STAR** Collaboration, M. S. Abdallah *et al.*, "Global Λ-hyperon polarization in Au+Au collisions at $\sqrt{s_{NN}}$=3 GeV," *Phys. Rev. C* **104** no. 6, (2021) L061901, arXiv:2108.00044 [nucl-ex]. 27, 100

[138] **ALICE** Collaboration, S. Acharya *et al.*, "Global polarization of $\Lambda\bar{\Lambda}$ hyperons in Pb-Pb collisions at $\sqrt{s_{NN}} = 2.76$ and 5.02 TeV," *Phys. Rev. C* **101** no. 4, (2020) 044611, arXiv:1909.01281 [nucl-ex]. 27

[139] **ALICE** Collaboration, S. Acharya *et al.*, "Polarization of Λ and $\overline{\Lambda}$ hyperons along the beam direction in Pb-Pb collisions at $\sqrt{s_{NN}} = 5.02$ TeV," arXiv:2107.11183 [nucl-ex]. 27, 100

[140] Y. B. Ivanov, V. Toneev, and A. Soldatov, "Estimates of hyperon polarization in heavy-ion collisions at collision energies $\sqrt{s_{NN}} = 4$–40 GeV," *Phys. Rev. C* **100** no. 1, (2019) 014908, arXiv:1903.05455 [nucl-th]. 27

[141] X.-G. Deng, X.-G. Huang, Y.-G. Ma, and S. Zhang, "Vorticity in low-energy heavy-ion collisions," *Phys. Rev. C* **101** no. 6, (2020) 064908, arXiv:2001.01371 [nucl-th]. 27

[142] Y. Guo, J. Liao, E. Wang, H. Xing, and H. Zhang, "Hyperon polarization from the vortical fluid in low-energy nuclear collisions," *Phys. Rev. C* **104** no. 4, (2021) L041902, arXiv:2105.13481 [nucl-th]. 27

[143] A. Ayala, I. Domínguez, I. Maldonado, and M. E. Tejeda-Yeomans, "Rise and fall of Λ and Λ^- global polarization in semi-central heavy-ion collisions at HADES, NICA and RHIC energies from the core-corona model," *Phys. Rev. C* **105** no. 3, (2022) 034907, arXiv:2106.14379 [hep-ph]. 27

[144] X.-G. Deng, X.-G. Huang, and Y.-G. Ma, "Lambda polarization in ^{108}Ag $+^{108}$Ag and ^{197}Au $+^{197}$Au collisions around a few GeV," arXiv:2109.09956 [nucl-th]. 27

[145] D. Teaney, J. Lauret, and E. V. Shuryak, "A Hydrodynamic description of heavy ion collisions at the SPS and RHIC," arXiv:nucl-th/0110037 [nucl-th]. 27

[146] P. Bozek and I. Wyskiel, "Rapid hydrodynamic expansion in relativistic heavy-ion collisions," *Phys. Rev. C* **79** (2009) 044916, arXiv:0902.4121 [nucl-th]. 27

[147] P. Romatschke, "New Developments in Relativistic Viscous Hydrodynamics," *Int. J. Mod. Phys. E* **19** (2010) 1–53, arXiv:0902.3663 [hep-ph]. 27, 30, 83

[148] C. Gale, S. Jeon, and B. Schenke, "Hydrodynamic Modeling of Heavy-Ion Collisions," *Int. J. Mod. Phys. A* **28** (2013) 1340011, arXiv:1301.5893 [nucl-th]. 27

[149] A. Jaiswal and V. Roy, "Relativistic hydrodynamics in heavy-ion collisions: general aspects and recent developments," *Adv. High Energy Phys.* **2016** (2016) 9623034, arXiv:1605.08694 [nucl-th]. 27

[150] P. Romatschke and U. Romatschke, *Relativistic Fluid Dynamics In and Out of Equilibrium*. Cambridge Monographs on Mathematical Physics. Cambridge University Press, 5, 2019. arXiv:1712.05815 [nucl-th]. 27, 28

[151] W. Florkowski, M. P. Heller, and M. Spalinski, "New theories of relativistic hydrodynamics in the LHC era," *Rept. Prog. Phys.* **81** no. 4, (2018) 046001, arXiv:1707.02282 [hep-ph]. 27

[152] S. Schlichting and D. Teaney, "The First fm/c of Heavy-Ion Collisions," *Ann. Rev. Nucl. Part. Sci.* **69** (2019) 447–476, arXiv:1908.02113 [nucl-th]. 27

[153] B. Schenke, "The smallest fluid on Earth," *Rept. Prog. Phys.* **84** no. 8, (2021) 082301, arXiv:2102.11189 [nucl-th]. 27

[154] L. Rezzolla and O. Zanotti, *Relativistic Hydrodynamics*. OUP Oxford, 2013. 27, 70

[155] C. Eckart, "The thermodynamics of irreversible processes. i. the simple fluid," *Phys. Rev.* **58** (Aug, 1940) 267–269. 27

[156] L. Landau and E. Lifshitz, *Fluid Mechanics: Volume 6*. No. v. 6 in Course of Theoretical Physics. Elsevier Science, 2013. 27

[157] W. Hiscock and L. Lindblom, "Stability and causality in dissipative relativistic fluids," *Annals Phys.* **151** (1983) 466–496. 28

[158] W. A. Hiscock and L. Lindblom, "Generic instabilities in first-order dissipative relativistic fluid theories," *Phys. Rev. D* **31** (1985) 725–733. 28

[159] D. A. Teaney, R. C. Hwa, and X.-N. Wang, *Viscous Hydrodynamics and the Quark Gluon Plasma*, pp. 207–266. World Scientific, 2010. arXiv:0905.2433 [nucl-th]. 28

[160] G. S. Denicol, H. Niemi, E. Molnar, and D. H. Rischke, "Derivation of transient relativistic fluid dynamics from the Boltzmann equation," *Phys. Rev.* **D85** (2012) 114047, arXiv:1202.4551 [nucl-th]. [Erratum: Phys. Rev.D91,no.3,039902(2015)]. 28

[161] S. De Groot, W. Van Leeuwen, and C. Van Weert, *Relativistic Kinetic Theory. Principles and Applications*. North Holland, 1, 1980. 28, 29, 32, 33, 34, 35, 43, 44, 45, 53, 56, 60, 61, 62, 108, 110

[162] C. Cercignani and G. M. Kremer, *The Relativistic Boltzmann Equation: Theory and Applications*. Springer, 2002. 28, 70

[163] A. Jaiswal, "Formulation of relativistic dissipative fluid dynamics and its applications in heavy-ion collisions," other thesis, 8, 2014. 30

[164] F. Becattini, V. Chandra, L. Del Zanna, and E. Grossi, "Relativistic distribution function for particles with spin at local thermodynamical equilibrium," *Annals Phys.* **338** (2013) 32–49, `arXiv:1303.3431 [nucl-th]`. 31, 56, 57, 78

[165] F. Becattini, L. Csernai, and D. J. Wang, "Λ polarization in peripheral heavy ion collisions," *Phys. Rev.* **C88** no. 3, (2013) 034905, `arXiv:1304.4427 [nucl-th]`. [Erratum: Phys. Rev.C93,no.6,069901(2016)]. 31

[166] L.-G. Pang, H. Petersen, Q. Wang, and X.-N. Wang, "Vortical Fluid and Λ Spin Correlations in High-Energy Heavy-Ion Collisions," *Phys. Rev. Lett.* **117** no. 19, (2016) 192301, `arXiv:1605.04024 [hep-ph]`. 31

[167] Y. Xie, D. Wang, and L. P. Csernai, "Global Λ polarization in high energy collisions," *Phys. Rev. C* **95** no. 3, (2017) 031901, `arXiv:1703.03770 [nucl-th]`. 31

[168] Y. Sun and C. M. Ko, "Λ hyperon polarization in relativistic heavy ion collisions from a chiral kinetic approach," *Phys. Rev. C* **96** no. 2, (2017) 024906, `arXiv:1706.09467 [nucl-th]`. 31

[169] H. Li, L.-G. Pang, Q. Wang, and X.-L. Xia, "Global Λ polarization in heavy-ion collisions from a transport model," *Phys. Rev. C* **96** no. 5, (2017) 054908, `arXiv:1704.01507 [nucl-th]`. 31

[170] D.-X. Wei, W.-T. Deng, and X.-G. Huang, "Thermal vorticity and spin polarization in heavy-ion collisions," *Phys. Rev. C* **99** no. 1, (2019) 014905, `arXiv:1810.00151 [nucl-th]`. 31, 100, 103

[171] J.-H. Gao and Z.-T. Liang, "Relativistic Quantum Kinetic Theory for Massive Fermions and Spin Effects," *Phys. Rev. D* **100** no. 5, (2019) 056021, `arXiv:1902.06510 [hep-ph]`. 31

[172] Y. B. Ivanov, V. Toneev, and A. Soldatov, "Vorticity and Particle Polarization in Relativistic Heavy-Ion Collisions," *Phys. Atom. Nucl.* **83** no. 2, (2020) 179–187, `arXiv:1910.01332 [nucl-th]`. 31

[173] J. I. Kapusta, E. Rrapaj, and S. Rudaz, "Hyperon polarization in relativistic heavy ion collisions and axial U(1) symmetry breaking at high temperature," *Phys. Rev. C* **101** no. 3, (2020) 031901, `arXiv:1910.12759 [nucl-th]`. 31

[174] C. Yi, S. Pu, and D.-L. Yang, "Reexamination of local spin polarization beyond global equilibrium in relativistic heavy ion collisions," *Phys. Rev. C* **104** no. 6, (2021) 064901, `arXiv:2106.00238 [hep-ph]`. 31

[175] S. Ryu, V. Jupic, and C. Shen, "Probing early-time longitudinal dynamics with the Λ hyperon's spin polarization in relativistic heavy-ion collisions," *Phys. Rev. C* **104** no. 5, (2021) 054908, `arXiv:2106.08125 [nucl-th]`. 31

[176] X.-Y. Wu, C. Yi, G.-Y. Qin, and S. Pu, "Local and global polarization of Λ hyperons across RHIC-BES energies: the roles of spin hall effect, initial condition and baryon diffusion," *Phys. Rev. C* **105** (2022) 064909, `arXiv:2204.02218 [hep-ph]`. 31

[177] W. Florkowski, A. Kumar, R. Ryblewski, and A. Mazeliauskas, "Longitudinal spin polarization in a thermal model," *Phys. Rev. C* **100** no. 5, (2019) 054907, `arXiv:1904.00002 [nucl-th]`. 31

[178] F. Becattini, M. Buzzegoli, and A. Palermo, "Spin-thermal shear coupling in a relativistic fluid," *Phys. Lett. B* **820** (2021) 136519, `arXiv:2103.10917 [nucl-th]`. 32

[179] F. Becattini, M. Buzzegoli, G. Inghirami, I. Karpenko, and A. Palermo, "Local Polarization and Isothermal Local Equilibrium in Relativistic Heavy Ion Collisions," *Phys. Rev. Lett.* **127** no. 27, (2021) 272302, `arXiv:2103.14621 [nucl-th]`. 32, 34

[180] B. Fu, S. Y. F. Liu, L. Pang, H. Song, and Y. Yin, "Shear-Induced Spin Polarization in Heavy-Ion Collisions," *Phys. Rev. Lett.* **127** no. 14, (2021) 142301, `arXiv:2103.10403 [hep-ph]`. 32

[181] W. Florkowski, A. Kumar, A. Mazeliauskas, and R. Ryblewski, "Effect of thermal shear on longitudinal spin polarization in a thermal model," `arXiv:2112.02799 [hep-ph]`. 32, 102

[182] X.-L. Sheng, Q. Wang, and D. H. Rischke, "Lorentz-covariant kinetic theory for massive spin-1/2 particles," `arXiv:2202.10160 [nucl-th]`. 32

[183] S. Lin and Z. Wang, "Shear induced polarization: Collisional contributions," `arXiv:2206.12573 [hep-ph]`. 32

[184] C. Itzykson and J. B. Zuber, *Quantum Field Theory*. International Series In Pure and Applied Physics. McGraw-Hill, New York, 1980. `http://dx.doi.org/10.1063/1.2916419`. 32, 45, 63

[185] S. Weinberg, *The Quantum theory of fields. Vol. 1: Foundations*. Cambridge University Press, 6, 2005. 32, 62

[186] F. J. Belinfante, "On the current and the density of the electric charge, the energy, the linear momentum and the angular momentum of arbitrary fields," *Physica* **7** (1940) 449–474. 32

[187] F. W. Hehl, "On the Energy Tensor of Spinning Massive Matter in Classical Field Theory and General Relativity," *Rept. Math. Phys.* **9** (1976) 55–82. 32, 33, 34

[188] L. Tinti and W. Florkowski, "Particle polarization, spin tensor and the Wigner distribution in relativistic systems," `arXiv:2007.04029 [nucl-th]`. 32, 33

[189] F. Belinfante, "On the spin angular momentum of mesons," *Physica* **6** no. 7, (1939) 887–898. 33

[190] F. Belinfante, "On the current and the density of the electric charge, the energy, the linear momentum and the angular momentum of arbitrary fields," *Physica* **7** no. 5, (1940) 449–474. 33

[191] L. Rosenfeld *Mem. Acad. Roy. Bel.* **18** no. 1, (1940) . 33

[192] J. Hilgevoord and S. Wouthuysen, "On the spin angular momentum of the dirac particle," *Nuclear Physics* **40** (1963) 1–12. 34

[193] J. Hilgevoord and E. De Kerf, "The covariant definition of spin in relativistic quantum field theory," *Physica* **31** no. 7, (1965) 1002–1016. 34

[194] M. Buzzegoli, "Pseudo-gauge dependence of the spin polarization and of the axial vortical effect," `arXiv:2109.12084 [nucl-th]`. 34

[195] N. Weickgenannt, D. Wagner, and E. Speranza, "Pseudogauges and relativistic spin hydrodynamics for interacting Dirac and Proca fields," *Phys. Rev. D* **105** no. 11, (2022) 116026, `arXiv:2204.01797 [nucl-th]`. 34

[196] E. Leader and C. Lorcé, "The angular momentum controversy: What's it all about and does it matter?," *Phys. Rept.* **541** no. 3, (2014) 163–248, `arXiv:1309.4235 [hep-ph]`. 34

[197] A. D. Gallegos, U. Gürsoy, and A. Yarom, "Hydrodynamics of spin currents," *SciPost Phys.* **11** (2021) 041, `arXiv:2101.04759 [hep-th]`. 34, 35

[198] N. Weickgenannt, E. Speranza, X.-l. Sheng, Q. Wang, and D. H. Rischke, "Generating Spin Polarization from Vorticity through Nonlocal Collisions," *Phys. Rev. Lett.* **127** no. 5, (2021) 052301, `arXiv:2005.01506 [hep-ph]`. 35, 37, 44, 45, 49, 51, 52, 53, 59

[199] N. Weickgenannt, E. Speranza, X.-l. Sheng, Q. Wang, and D. H. Rischke, "Derivation of the nonlocal collision term in the relativistic Boltzmann equation for massive spin-1/2 particles from quantum field theory," *Phys. Rev. D* **104** no. 1, (2021) 016022, `arXiv:2103.04896 [nucl-th]`. 35, 37, 44, 45, 49, 51, 52, 53, 59

[200] D. Montenegro and G. Torrieri, "Causality and dissipation in relativistic polarizable fluids," *Phys. Rev. D* **100** no. 5, (2019) 056011, `arXiv:1807.02796 [hep-th]`. 35

[201] D. Montenegro and G. Torrieri, "Linear response theory and effective action of relativistic hydrodynamics with spin," *Phys. Rev. D* **102** no. 3, (2020) 036007, `arXiv:2004.10195 [hep-th]`. 35

[202] W. M. Serenone, J. a. G. P. Barbon, D. D. Chinellato, M. A. Lisa, C. Shen, J. Takahashi, and G. Torrieri, "Λ polarization from thermalized jet energy," *Phys. Lett. B* **820** (2021) 136500, `arXiv:2102.11919 [hep-ph]`. 35

[203] G. Torrieri and D. Montenegro, "Linear response hydrodynamics of a relativistic dissipative fluid with spin," `arXiv:2207.00537 [hep-th]`. 35

[204] K. Hattori, M. Hongo, X.-G. Huang, M. Matsuo, and H. Taya, "Fate of spin polarization in a relativistic fluid: An entropy-current analysis," *Phys. Lett. B* **795** (2019) 100–106, `arXiv:1901.06615 [hep-th]`. 35, 44

[205] K. Fukushima and S. Pu, "Spin hydrodynamics and symmetric energy-momentum tensors – A current induced by the spin vorticity –," *Phys. Lett. B* **817** (2021) 136346, `arXiv:2010.01608 [hep-th]`. 35

[206] S. Li, M. A. Stephanov, and H.-U. Yee, "Nondissipative Second-Order Transport, Spin, and Pseudogauge Transformations in Hydrodynamics," *Phys. Rev. Lett.* **127** no. 8, (2021) 082302, `arXiv:2011.12318 [hep-th]`. 35

[207] D. She, A. Huang, D. Hou, and J. Liao, "Relativistic Viscous Hydrodynamics with Angular Momentum," `arXiv:2105.04060 [nucl-th]`. 35

[208] A. Daher, A. Das, W. Florkowski, and R. Ryblewski, "Equivalence of canonical and phenomenological formulations of spin hydrodynamics," `arXiv:2202.12609 [nucl-th]`. 35

[209] Z. Cao, K. Hattori, M. Hongo, X.-G. Huang, and H. Taya, "Gyrohydrodynamics: Relativistic spinful fluid with strong vorticity," `arXiv:2205.08051 [hep-th]`. 35

[210] J. Hu, "Kubo formulae for first-order spin hydrodynamics," *Phys. Rev. D* **103** no. 11, (2021) 116015, `arXiv:2101.08440 [hep-ph]`. 35

[211] Y. Hidaka and D.-L. Yang, "Nonequilibrium chiral magnetic/vortical effects in viscous fluids," *Phys. Rev. D* **98** no. 1, (2018) 016012, `arXiv:1801.08253 [hep-th]`. 35, 44

[212] D.-L. Yang, K. Hattori, and Y. Hidaka, "Effective quantum kinetic theory for spin transport of fermions with collsional effects," *JHEP* **20** (2020) 070, `arXiv:2002.02612 [hep-ph]`. 35, 44

[213] Z. Wang, X. Guo, and P. Zhuang, "Equilibrium Spin Distribution From Detailed Balance," *Eur. Phys. J. C* **81** no. 9, (2021) 799, `arXiv:2009.10930 [hep-th]`. 35, 44

[214] X.-L. Sheng, N. Weickgenannt, E. Speranza, D. H. Rischke, and Q. Wang, "From Kadanoff-Baym to Boltzmann equations for massive spin-1/2 fermions," *Phys. Rev. D* **104** no. 1, (2021) 016029, `arXiv:2103.10636 [nucl-th]`. 35, 44

[215] N. Weickgenannt, D. Wagner, E. Speranza, and D. Rischke, "Relativistic second-order dissipative spin hydrodynamics from the method of moments," `arXiv:2203.04766 [nucl-th]`. 35

[216] J. Hu, "Relativistic first-order spin hydrodynamics via the Chapman-Enskog expansion," *Phys. Rev. D* **105** no. 7, (2022) 076009, `arXiv:2111.03571 [hep-ph]`. 35

[217] M. A. Stephanov and Y. Yin, "Chiral Kinetic Theory," *Phys. Rev. Lett.* **109** (2012) 162001, `arXiv:1207.0747 [hep-th]`. 35

[218] J.-Y. Chen, D. T. Son, M. A. Stephanov, H.-U. Yee, and Y. Yin, "Lorentz Invariance in Chiral Kinetic Theory," *Phys. Rev. Lett.* **113** no. 18, (2014) 182302, `arXiv:1404.5963 [hep-th]`. 35

[219] E. V. Gorbar, D. O. Rybalka, and I. A. Shovkovy, "Second-order dissipative hydrodynamics for plasma with chiral asymmetry and vorticity," *Phys. Rev.* **D95** no. 9, (2017) 096010, `arXiv:1702.07791 [hep-th]`. 35

[220] S. Shi, C. Gale, and S. Jeon, "From chiral kinetic theory to relativistic viscous spin hydrodynamics," *Phys. Rev. C* **103** no. 4, (2021) 044906, `arXiv:2008.08618 [nucl-th]`. 35, 44, 47

[221] M. P. Heller, A. Serantes, M. Spaliński, V. Svensson, and B. Withers, "Convergence of hydrodynamic modes: insights from kinetic theory and holography," *SciPost Phys.* **10** no. 6, (2021) 123, `arXiv:2012.15393 [hep-th]`. 35

[222] A. D. Gallegos and U. Gürsoy, "Holographic spin liquids and Lovelock Chern-Simons gravity," *JHEP* **11** (2020) 151, `arXiv:2004.05148 [hep-th]`. 35

[223] M. Garbiso and M. Kaminski, "Hydrodynamics of simply spinning black holes & hydrodynamics for spinning quantum fluids," *JHEP* **12** (2020) 112, `arXiv:2007.04345 [hep-th]`. 35

[224] M. Hongo, X.-G. Huang, M. Kaminski, M. Stephanov, and H.-U. Yee, "Relativistic spin hydrodynamics with torsion and linear response theory for spin relaxation," *JHEP* **11** (2021) 150, `arXiv:2107.14231 [hep-th]`. 35

[225] A. D. Gallegos, U. Gursoy, and A. Yarom, "Hydrodynamics, spin currents and torsion," `arXiv:2203.05044 [hep-th]`. 35

[226] D. T. Son and P. Surowka, "Hydrodynamics with Triangle Anomalies," *Phys. Rev. Lett.* **103** (2009) 191601, `arXiv:0906.5044 [hep-th]`. 35

[227] D. Montenegro, L. Tinti, and G. Torrieri, "The ideal relativistic fluid limit for a medium with polarization," *Phys. Rev.* **D96** no. 5, (2017) 056012, `arXiv:1701.08263 [hep-th]`. 35

[228] D. Montenegro, L. Tinti, and G. Torrieri, "Sound waves and vortices in a polarized relativistic fluid," *Phys. Rev.* **D96** no. 7, (2017) 076016, `arXiv:1703.03079 [hep-th]`. 35

[229] X.-G. Huang, P. Huovinen, and X.-N. Wang, "Quark Polarization in a Viscous Quark-Gluon Plasma," *Phys. Rev. C* **84** (2011) 054910, `arXiv:1108.5649 [nucl-th]`. 35

[230] X. Li, Z.-F. Jiang, S. Cao, and J. Deng, "Evolution of global polarization in relativistic heavy-ion collisions within a perturbative approach," `arXiv:2205.02409 [nucl-th]`. 35

[231] W. Florkowski, B. Friman, A. Jaiswal, and E. Speranza, "Relativistic fluid dynamics with spin," *Phys. Rev.* **C97** no. 4, (2018) 041901, `arXiv:1705.00587 [nucl-th]`. 35, 57, 60, 61, 62, 67

[232] W. Florkowski, B. Friman, A. Jaiswal, R. Ryblewski, and E. Speranza, "Spin-dependent distribution functions for relativistic hydrodynamics of spin-1/2 particles," *Phys. Rev.* **D97** no. 11, (2018) 116017, `arXiv:1712.07676 [nucl-th]`. 35, 57, 65, 68, 78, 79, 99

[233] W. Florkowski, B. Friman, A. Jaiswal, and E. Speranza, "Relativistic hydrodynamics of particles with spin 1/2," *Acta Phys. Polon. Supp.* **10** (2017) 1139, `arXiv:1708.04035 [hep-ph]`. 35

[234] W. Florkowski, B. Friman, A. Jaiswal, R. Ryblewski, and E. Speranza, "Fluid dynamics for relativistic spin-polarized media," *Acta Phys. Polon. Supp.* **11** (2018) 507, `arXiv:1810.01709 [nucl-th]`. 35

[235] W. Florkowski, A. Kumar, and R. Ryblewski, "Thermodynamic versus kinetic approach to polarization-vorticity coupling," *Phys. Rev.* **C98** no. 4, (2018) 044906, `arXiv:1806.02616 [hep-ph]`. 35, 37, 43, 44, 45, 47, 49, 50, 55, 58, 59, 60, 61, 62, 64, 70, 78, 80

[236] W. Florkowski, A. Kumar, and R. Ryblewski, "Spin Potential for Relativistic Particles with Spin 1/2," *Acta Phys. Polon. B* **51** (2020) 945–959, `arXiv:1907.09835 [nucl-th]`. 35

[237] R. Hakim, *Introduction to relativistic statistical mechanics: classical and quantum.* World scientific, Singapore, 2011. `https:cds.cern.ch/record/1379544`. 35, 44, 45

[238] H.-H. Peng, J.-J. Zhang, X.-L. Sheng, and Q. Wang, "Ideal Spin Hydrodynamics from the Wigner Function Approach," *Chin. Phys. Lett.* **38** no. 11, (2021) 116701, `arXiv:2107.00448 [hep-th]`. 35

[239] H. T. Elze, M. Gyulassy, and D. Vasak, "Transport Equations for the QCD Quark Wigner Operator," *Nucl. Phys.* **B276** (1986) 706–728. 35, 45

[240] D. Vasak, M. Gyulassy, and H. T. Elze, "Quantum Transport Theory for Abelian Plasmas," *Annals Phys.* **173** (1987) 462–492. 35, 43, 44, 45, 46, 47, 49, 50

[241] H.-T. Elze and U. W. Heinz, "Quark - Gluon Transport Theory," *Phys. Rept.* **183** (1989) 81–135. [,117(1989)]. 35

[242] P. Zhuang and U. W. Heinz, "Relativistic quantum transport theory for electrodynamics," *Annals Phys.* **245** (1996) 311–338, `arXiv:nucl-th/9502034 [nucl-th]`. 35, 45

[243] W. Florkowski, J. Hufner, S. P. Klevansky, and L. Neise, "Chirally invariant transport equations for quark matter," *Annals Phys.* **245** (1996) 445–463, `arXiv:hep-ph/9505407 [hep-ph]`. 35, 45

[244] W. Florkowski, A. Kumar, R. Ryblewski, and R. Singh, "Spin polarization evolution in a boost invariant hydrodynamical background," *Phys. Rev. C* **99** no. 4, (2019) 044910, `arXiv:1901.09655 [hep-ph]`. 35, 40

[245] R. Singh, G. Sophys, and R. Ryblewski, "Spin polarization dynamics in the Gubser-expanding background," *Phys. Rev. D* **103** no. 7, (2021) 074024, `arXiv:2011.14907 [hep-ph]`. 35, 40

[246] R. Singh, M. Shokri, and R. Ryblewski, "Spin polarization dynamics in the Bjorken-expanding resistive MHD background," *Phys. Rev. D* **103** no. 9, (2021) 094034, `arXiv:2103.02592 [hep-ph]`. 35, 40

[247] W. Florkowski, R. Ryblewski, R. Singh, and G. Sophys, "Spin polarization dynamics in the non-boost-invariant background," *Phys. Rev. D* **105** no. 5, (2022) 054007, `arXiv:2112.01856 [hep-ph]`. 35, 40

[248] R. Singh, M. Shokri, and S. M. A. T. Mehr, "Relativistic magnetohydrodynamics with spin," `arXiv:2202.11504 [hep-ph]`. 35, 41

[249] S. Bhadury, W. Florkowski, A. Jaiswal, and R. Ryblewski, "Relaxation time approximation with pair production and annihilation processes," *Phys. Rev. C* **102** no. 6, (2020) 064910, `arXiv:2006.14252 [hep-ph]`. 35

[250] S. Bhadury, W. Florkowski, A. Jaiswal, A. Kumar, and R. Ryblewski, "Relativistic dissipative spin dynamics in the relaxation time approximation," *Phys. Lett. B* **814** (2021) 136096, `arXiv:2002.03937 [hep-ph]`. 35

[251] S. Bhadury, W. Florkowski, A. Jaiswal, A. Kumar, and R. Ryblewski, "Dissipative Spin Dynamics in Relativistic Matter," *Phys. Rev. D* **103** no. 1, (2021) 014030, `arXiv:2008.10976 [nucl-th]`. 35

[252] S. Bhadury, W. Florkowski, A. Jaiswal, A. Kumar, and R. Ryblewski, "Relativistic spin-magnetohydrodynamics," `arXiv:2204.01357 [nucl-th]`. 35

[253] V. E. Ambrus, R. Ryblewski, and R. Singh, "Spin waves in spin hydrodynamics," `arXiv:2202.03952 [hep-ph]`. 35, 40, 70

[254] A. Monnai, *Relativistic Dissipative Hydrodynamic Description of the Quark-Gluon Plasma Relativistic Dissipative Hydrodynamic Description of the Quark-Gluon Plasma*. PhD thesis, Tokyo U., New-York, 2014. 35, 70

[255] V. E. Ambrus, "Transport coefficients in ultrarelativistic kinetic theory," *Phys. Rev. C* **97** no. 2, (2018) 024914, `arXiv:1706.05310 [physics.flu-dyn]`. 35, 70

[256] J. Hu, "Linear mode analysis and spin relaxation," *Phys. Rev. D* **105** no. 9, (2022) 096021, `arXiv:2204.12946 [hep-ph]`. 35

[257] J. Hu, "The linear mode analysis from spin transport equation," `arXiv:2202.07373 [hep-ph]`. 35

[258] J. Hu and Z. Xu, "Propagation of spin waves," `arXiv:2205.15755 [hep-ph]`. 35

[259] A. Das, W. Florkowski, A. Kumar, R. Ryblewski, and R. Singh, "Semi-classical kinetic theory for massive spin-half fermions with leading-order spin effects," `arXiv:2203.15562 [hep-th]`. 40

[260] R. Singh, "Conformal transformations of conservation equations in spin hydrodynamics," *Acta Phys. Polon. B* **52** (2021) 1081, `arXiv:2104.01009 [hep-ph]`. 40

[261] R. Singh, "Hydrodynamics formalism with Spin dynamics," *Acta Phys. Polon. Supp.* **14** (2021) 461, `arXiv:2009.07067 [nucl-th]`. 40

[262] R. Singh, "Formalism of hydrodynamics with spin degrees of freedom," *PoS* **LHCP2020** (2021) 236, `arXiv:2009.05130 [nucl-th]`. 40

[263] R. Ryblewski and R. Singh, "Relativistic hydrodynamics for spin-polarized media," *Acta Phys. Polon. B* **51** (2020) 1537, `arXiv:2004.02544 [nucl-th]`. 40

[264] R. Singh, "Boost-invariant description of polarization within hydrodynamics with spin," *Acta Phys. Polon. Supp.* **13** (2020) 931, `arXiv:2001.05592 [hep-ph]`. 40

[265] A. Das, W. Florkowski, R. Ryblewski, and R. Singh, "Quantum baryon number fluctuations in subsystems of a hot and dense relativistic gas of fermions," `arXiv:2105.02125 [nucl-th]`. 41

[266] A. Das, W. Florkowski, R. Ryblewski, and R. Singh, "Pseudogauge dependence of quantum fluctuations of the energy in a hot relativistic gas of fermions," *Phys. Rev. D* **103** no. 9, (2021) L091502, `arXiv:2103.01013 [nucl-th]`. 41

[267] A. Das, W. Florkowski, R. Ryblewski, and R. Singh, "Quantum Fluctuations of Energy in Subsystems of a Hot Relativistic Gas," *Acta Phys. Polon. B* **52** no. 12, (2021) 1395, `arXiv:2012.05662 [hep-ph]`. 41

[268] R. Singh, "A compact formula for the quantum fluctuations of energy," *Rev. Mex. Fis. Suppl.* **3** no. 3, (2022) 0308115, `arXiv:2110.02727 [nucl-th]`. 41

[269] R. Singh, "Quantum fluctuations of baryon number density," *J. Phys. Conf. Ser.* **2105** no. 15, (2021) 012006, `arXiv:2109.08201 [nucl-th]`. 41

[270] R. Singh, "Mathematical expressions for quantum fluctuations of energy for different energy-momentum tensors," *PoS* **LHCP2021** (2021) 161, `arXiv:2109.11068 [quant-ph]`. 41

[271] C. Cercignani, "Theory and application of the boltzmann equation. elsevier, 1975." *Journal of Fluid Mechanics* **81** no. 4, (1977) 793–794. 43

[272] G. S. Denicol and D. H. Rischke, *Microscopic Foundations of Relativistic Fluid Dynamics*. Springer Cham, 1, 2021. 43, 59

[273] E. Wigner, "On the quantum correction for thermodynamic equilibrium," *Phys. Rev.* **40** (Jun, 1932) 749–759. 43, 46

[274] X.-l. Sheng, D. H. Rischke, D. Vasak, and Q. Wang, "Wigner functions for fermions in strong magnetic fields," *Eur. Phys. J. A* **54** no. 2, (2018) 21, `arXiv:1707.01388 [hep-ph]`. 43

[275] **STAR** Collaboration, J. Adam *et al.*, "Global polarization of Λ hyperons in Au+Au collisions at $\sqrt{s_{NN}}$ = 200 GeV," *Phys. Rev. C* **98** (2018) 014910, `arXiv:1805.04400 [nucl-ex]`. 43, 44, 92

[276] D. Kobayashi, T. Yoshikawa, M. Matsuo, R. Iguchi, S. Maekawa, E. Saitoh, and Y. Nozaki, "Spin current generation using a surface acoustic wave generated via spin-rotation coupling," *Phys. Rev. Lett.* **119** (Aug, 2017) 077202. 44

[277] M. Matsuo, Y. Ohnuma, and S. Maekawa, "Theory of spin hydrodynamic generation," *Phys. Rev. B* **96** (Jul, 2017) 020401. 44

[278] J.-h. Gao, S. Pu, and Q. Wang, "Covariant chiral kinetic equation in the Wigner function approach," *Phys. Rev. D* **96** no. 1, (2017) 016002, `arXiv:1704.00244 [nucl-th]`. 44

[279] D.-L. Yang, "Side-Jump Induced Spin-Orbit Interaction of Chiral Fluids from Kinetic Theory," *Phys. Rev. D* **98** no. 7, (2018) 076019, `arXiv:1807.02395 [nucl-th]`. 44

[280] J.-h. Gao, J.-Y. Pang, and Q. Wang, "Chiral vortical effect in Wigner function approach," *Phys. Rev. D* **100** no. 1, (2019) 016008, `arXiv:1810.02028 [nucl-th]`. 44

[281] A. Huang, S. Shi, Y. Jiang, J. Liao, and P. Zhuang, "Complete and Consistent Chiral Transport from Wigner Function Formalism," *Phys. Rev. D* **98** no. 3, (2018) 036010, `arXiv:1801.03640 [hep-th]`. 44, 45, 47

[282] H. T. Elze, M. Gyulassy, and D. Vasak, "Transport Equations for the QCD Gluon Wigner Operator," *Phys. Lett. B* **177** (1986) 402–408. 45

[283] J.-H. Gao, Z.-T. Liang, S. Pu, Q. Wang, and X.-N. Wang, "Chiral Anomaly and Local Polarization Effect from Quantum Kinetic Approach," *Phys. Rev. Lett.* **109** (2012) 232301, `arXiv:1203.0725 [hep-ph]`. 45

[284] R.-H. Fang, L.-G. Pang, Q. Wang, and X.-N. Wang, "Polarization of massive fermions in a vortical fluid," *Phys. Rev.* **C94** no. 2, (2016) 024904, `arXiv:1604.04036 [nucl-th]`. 45

[285] R.-H. Fang, J.-Y. Pang, Q. Wang, and X.-N. Wang, "Pseudoscalar condensation induced by chiral anomaly and vorticity for massive fermions," *Phys. Rev.* **D95** no. 1, (2017) 014032, `arXiv:1611.04670 [nucl-th]`. 45

[286] N. Weickgenannt, X.-L. Sheng, E. Speranza, Q. Wang, and D. H. Rischke, "Kinetic theory for massive spin-1/2 particles from the Wigner-function formalism," *Phys. Rev. D* **100** no. 5, (2019) 056018, `arXiv:1902.06513 [hep-ph]`. 45, 49, 107

[287] X.-G. Huang, P. Mitkin, A. V. Sadofyev, and E. Speranza, "Zilch Vortical Effect, Berry Phase, and Kinetic Theory," *JHEP* **10** (2020) 117, `arXiv:2006.03591 [hep-th]`. 45

[288] J.-H. Gao, Z.-T. Liang, and Q. Wang, "Quantum kinetic theory for spin-1/2 fermions in Wigner function formalism," *Int. J. Mod. Phys. A* **36** no. 01, (2021) 2130001, `arXiv:2011.02629 [hep-ph]`. 47, 49, 50

[289] Y. Hidaka, S. Pu, Q. Wang, and D.-L. Yang, "Foundations and Applications of Quantum Kinetic Theory," `arXiv:2201.07644 [hep-ph]`. 49

[290] J. Zamanian, M. Marklund, and G. Brodin, "Scalar quantum kinetic theory for spin-1/2 particles: Mean field theory," *New J. Phys.* **12** (2010) 043019, `arXiv:0910.5165 [cond-mat.quant-gas]`. 52

[291] R. Ekman, F. A. Asenjo, and J. Zamanian, "Fully relativistic kinetic equation for spin-1/2 particles in the long scale-length approximation," *Phys. Rev. E* **96** no. 2, (2017) 023207, `arXiv:1702.00722 [physics.plasm-ph]`. 52

[292] R. Ekman, H. Al-Naseri, J. Zamanian, and G. Brodin, "Relativistic kinetic theory for spin-1/2 particles: Conservation laws, thermodynamics, and linear waves," *Phys. Rev. E* **100** no. 2, (2019) 023201, `arXiv:1904.08727 [physics.plasm-ph]`. 52

[293] F. Jüttner, "Das Maxwellsche Gesetz der Geschwindigkeitsverteilung in der Relativtheorie," Jan., 1911. 57

[294] C. Cercignani and G. M. Kremer, *The relativistic Boltzmann equation: theory and applications.* 2002. 59

[295] F. W. Olver, D. W. Lozier, R. F. Boisvert, and C. W. Clark, *NIST handbook of mathematical functions hardback and CD-ROM.* Cambridge university press, 2010. 60, 72

[296] M. Mathisson, "Neue mechanik materieller systemes," *Acta Phys. Polon.* **6** (1937) 163–2900. 63

[297] J. D. Jackson, "Classical Electrodynamics," *John Wiley & Sons Inc.* (1998) 808. 67, 68, 70, 76

[298] W. Florkowski and R. Ryblewski, "Projection method for boost-invariant and cylindrically symmetric dissipative hydrodynamics," *Phys. Rev.* **C85** (2012) 044902, arXiv:1111.5997 [nucl-th]. 68, 81

[299] M. Martinez, R. Ryblewski, and M. Strickland, "Boost-Invariant (2+1)-dimensional Anisotropic Hydrodynamics," *Phys. Rev.* **C85** (2012) 064913, arXiv:1204.1473 [nucl-th]. 68, 81

[300] M. Alqahtani, M. Nopoush, and M. Strickland, "Quasiparticle equation of state for anisotropic hydrodynamics," *Phys. Rev. C* **92** no. 5, (2015) 054910, arXiv:1509.02913 [hep-ph]. 68, 81

[301] P. A. M. Dirac, "On the theory of quantum mechanics," 1926. 73

[302] A. Zannoni, "On the quantization of the monoatomic ideal gas," 1999. 73

[303] S. Floerchinger and M. Martinez, "Fluid dynamic propagation of initial baryon number perturbations on a Bjorken flow background," *Phys. Rev.* **C92** no. 6, (2015) 064906, arXiv:1507.05569 [nucl-th]. 73

[304] J. K. Lubański, "Sur la theorie des particules élémentaires de spin quelconque. I," *Physica* **9** (1942) 310–324. 77

[305] L. H. Ryder, *QUANTUM FIELD THEORY.* Cambridge University Press, 6, 1996. 77

[306] F. Cooper and G. Frye, "Comment on the Single Particle Distribution in the Hydrodynamic and Statistical Thermodynamic Models of Multiparticle Production," *Phys. Rev. D* **10** (1974) 186. 78

[307] R. Ryblewski, "Monte-Carlo statistical hadronization in relativistic heavy-ion collisions," in *53rd Winter School of Theoretical Physics: Understanding the Origin of Matter from QCD.* 12, 2017. arXiv:1712.05213 [nucl-th]. 78, 83

[308] E. Leader, "Spin in Particle Physics," *Cambridge University Press* (2001) . 79

[309] **BRAHMS** Collaboration, I. G. Bearden *et al.*, "Charged meson rapidity distributions in central Au+Au collisions at s(NN)**(1/2) = 200-GeV," *Phys. Rev. Lett.* **94** (2005) 162301, arXiv:nucl-ex/0403050. 82, 86

[310] R. P. Feynman, "Very high-energy collisions of hadrons," *Phys. Rev. Lett.* **23** (1969) 1415–1417. 86

[311] J. Bjorken, "Highly Relativistic Nucleus-Nucleus Collisions: The Central Rapidity Region," *Phys. Rev. D* **27** (1983) 140–151. 86

[312] **Particle Data Group** Collaboration, P. A. Zyla *et al.*, "Review of Particle Physics," *PTEP* **2020** no. 8, (2020) 083C01. 87

[313] **ALICE** Collaboration, S. Acharya *et al.*, "Global polarization of $\Lambda\bar{\Lambda}$ hyperons in Pb-Pb collisions at $\sqrt{s_{NN}}$ = 2.76 and 5.02 TeV," *Phys. Rev. C* **101** no. 4, (2020) 044611, arXiv:1909.01281 [nucl-ex]. 92

[314] S. A. Voloshin, "Polarized secondary particles in unpolarized high energy hadron-hadron collisions?," arXiv:nucl-th/0410089 [nucl-th]. 92

[315] W. Florkowski and R. Ryblewski, "On the interpretation of Λ spin polarization measurements," arXiv:2102.02890 [hep-ph]. 92

[316] M. Abramowitz and I. A. Stegun, eds., *Handbook of Mathematical Functions with Formulas, Graphs and Mathematical Tables.* Dover Publications, Inc., New York, 1965. 96

[317] **STAR** Collaboration, Z. Xu, "STAR Highlights," *Nucl. Phys. A* **1005** (2021) 121894. 100

[318] X.-G. Huang, "Electromagnetic fields and anomalous transports in heavy-ion collisions — A pedagogical review," *Rept. Prog. Phys.* **79** no. 7, (2016) 076302, arXiv:1509.04073 [nucl-th]. 107, 109

[319] L. Oliva, P. Moreau, V. Voronyuk, and E. Bratkovskaya, "Influence of electromagnetic fields in proton-nucleus collisions at relativistic energy," *Phys. Rev. C* **101** no. 1, (2020) 014917, arXiv:1909.06770 [nucl-th]. 107

[320] V. Roy, S. Pu, L. Rezzolla, and D. Rischke, "Analytic Bjorken flow in one-dimensional relativistic magnetohydrodynamics," *Phys. Lett.* **B750** (2015) 45–52, arXiv:1506.06620 [nucl-th]. 107

[321] S. Pu, V. Roy, L. Rezzolla, and D. H. Rischke, "Bjorken flow in one-dimensional relativistic magnetohydrodynamics with magnetization," *Phys. Rev.* **D93** no. 7, (2016) 074022, arXiv:1602.04953 [nucl-th]. 107

[322] G. Inghirami, L. Del Zanna, A. Beraudo, M. H. Moghaddam, F. Becattini, and M. Bleicher, "Numerical magneto-hydrodynamics for relativistic nuclear collisions," *Eur. Phys. J.* **C76** no. 12, (2016) 659, arXiv:1609.03042 [hep-ph]. 107

[323] A. Dash, V. Roy, and B. Mohanty, "Magneto-Vortical evolution of QGP in heavy ion collisions," *J. Phys. G* **46** no. 1, (2019) 015103, arXiv:1705.05657 [nucl-th]. 107

[324] M. Shokri and N. Sadooghi, "Novel self-similar rotating solutions of nonideal transverse magnetohydrodynamics," *Phys. Rev. D* **96** no. 11, (2017) 116008, arXiv:1705.00536 [nucl-th]. 107, 110, 111, 113

[325] W. Florkowski, A. Kumar, and R. Ryblewski, "Vortex-like solutions and internal structures of covariant ideal magnetohydrodynamics," *Eur. Phys. J. A* **54** no. 10, (2018) 184, arXiv:1803.06695 [nucl-th]. 107

[326] M. Shokri and N. Sadooghi, "Evolution of magnetic fields from the $3 + 1$ dimensional self-similar and Gubser flows in ideal relativistic magnetohydrodynamics," *JHEP* **11** (2018) 181, arXiv:1807.09487 [nucl-th]. 107, 111

[327] M. Shokri, "Generalization of Bantilan-Ishi-Romatschke flow to Magnetohydrodynamics," *JHEP* **01** (2020) 011, `arXiv:1911.06196 [hep-th]`. 107

[328] G. Inghirami, M. Mace, Y. Hirono, L. Del Zanna, D. E. Kharzeev, and M. Bleicher, "Magnetic fields in heavy ion collisions: flow and charge transport," *Eur. Phys. J. C* **80** no. 3, (2020) 293, `arXiv:1908.07605 [hep-ph]`. 107

[329] U. Gangopadhyaya and V. Roy, "Order-by-order Anisotropic Transport Coefficients of a Magnetised Fluid: a Chapman-Enskog Approach," `arXiv:2206.12197 [nucl-th]`. 107

[330] J. Hernandez and P. Kovtun, "Relativistic magnetohydrodynamics," *JHEP* **05** (2017) 001, `arXiv:1703.08757 [hep-th]`. 107, 108

[331] J. D. Bekenstein and E. Oron, "New conservation laws in general-relativistic magnetohydrodynamics," *Phys. Rev. D* **18** (Sep, 1978) 1809–1819. `https://link.aps.org/doi/10.1103/PhysRevD.18.1809`. 108

[332] L. Parker and D. Toms, *Quantum Field Theory in Curved Spacetime: Quantized Fields and Gravity*. Cambridge Monographs on Mathematical Physics. Cambridge University Press, 2009. 108

[333] P. Kovtun, "Thermodynamics of polarized relativistic matter," *JHEP* **07** (2016) 028, `arXiv:1606.01226 [hep-th]`. 109

[334] I. A. Karpenko, P. Huovinen, H. Petersen, and M. Bleicher, "Estimation of the shear viscosity at finite net-baryon density from $A + A$ collision data at $\sqrt{s_{\mathrm{NN}}} = 7.7 - 200$ GeV," *Phys. Rev. C* **91** no. 6, (2015) 064901, `arXiv:1502.01978 [nucl-th]`. 112

[335] V. Borka Jovanovic, S. R. Ignjatovic, D. Borka, and P. Jovanovic, "Constituent quark masses obtained from hadron masses with contributions of Fermi-Breit and Glozman-Riska hyperfine interactions," *Phys. Rev. D* **82** (2010) 117501, `arXiv:1011.1749 [hep-ph]`. 112

[336] S. S. Gubser, S. S. Pufu, and A. Yarom, "Entropy production in collisions of gravitational shock waves and of heavy ions," *Phys. Rev. D* **78** (2008) 066014, `arXiv:0805.1551 [hep-th]`. 112

[337] G. Aarts and A. Nikolaev, "Electrical conductivity of the quark-gluon plasma: perspective from lattice QCD," *Eur. Phys. J. A* **57** no. 4, (2021) 118, `arXiv:2008.12326 [hep-lat]`. 112

[338] S. S. Gubser, "Symmetry constraints on generalizations of Bjorken flow," *Phys. Rev. D* **82** (2010) 085027, `arXiv:1006.0006 [hep-th]`. 115, 117, 121

[339] S. S. Gubser and A. Yarom, "Conformal hydrodynamics in Minkowski and de Sitter spacetimes," *Nucl. Phys. B* **846** (2011) 469–511, `arXiv:1012.1314 [hep-th]`. 115, 117, 121

[340] S. S. Gubser, S. S. Pufu, and A. Yarom, "Off-center collisions in AdS(5) with applications to multiplicity estimates in heavy-ion collisions," *JHEP* **11** (2009) 050, `arXiv:0902.4062 [hep-th]`. 115

[341] M. Csanád, M. I. Nagy, and S. Lökös, "Exact solutions of relativistic perfect fluid hydrodynamics for a QCD equation of state," *Eur. Phys. J. A* **48** (2012) 173, `arXiv:1205.5965 [nucl-th]`. 115

[342] H. Marrochio, J. Noronha, G. S. Denicol, M. Luzum, S. Jeon, and C. Gale, "Solutions of Conformal Israel-Stewart Relativistic Viscous Fluid Dynamics," *Phys. Rev. C* **91** no. 1, (2015) 014903, `arXiv:1307.6130 [nucl-th]`. 115, 121

[343] S. S. Gubser and W. van der Schee, "Complexified boost invariance and holographic heavy ion collisions," *JHEP* **01** (2015) 028, `arXiv:1410.7408 [hep-th]`. 115

[344] G. S. Denicol, U. W. Heinz, M. Martinez, J. Noronha, and M. Strickland, "New Exact Solution of the Relativistic Boltzmann Equation and its Hydrodynamic Limit," *Phys. Rev. Lett.* **113** no. 20, (2014) 202301, `arXiv:1408.5646 [hep-ph]`. 115

[345] M. Nopoush, R. Ryblewski, and M. Strickland, "Anisotropic hydrodynamics for conformal Gubser flow," *Phys. Rev. D* **91** no. 4, (2015) 045007, `arXiv:1410.6790 [nucl-th]`. 115

[346] M. Strickland, M. Nopoush, and R. Ryblewski, "Anisotropic hydrodynamics for conformal Gubser flow," *Nucl. Phys. A* **956** (2016) 268–271, `arXiv:1512.07334 [nucl-th]`. 115

[347] A. Dash and V. Roy, "Hydrodynamic attractors for Gubser flow," *Phys. Lett. B* **806** (2020) 135481, `arXiv:2001.10756 [nucl-th]`. 115

[348] D.-L. Wang, X.-Q. Xie, S. Fang, and S. Pu, "Analytic solutions of relativistic dissipative spin hydrodynamics with radial expansion in Gubser flow," *Phys. Rev. D* **105** no. 11, (2022) 114050, `arXiv:2112.15535 [hep-ph]`. 115

[349] R. Baier, P. Romatschke, D. T. Son, A. O. Starinets, and M. A. Stephanov, "Relativistic viscous hydrodynamics, conformal invariance, and holography," *JHEP* **04** (2008) 100, `arXiv:0712.2451 [hep-th]`. 117, 120

[350] S. Bhattacharyya, S. Lahiri, R. Loganayagam, and S. Minwalla, "Large rotating AdS black holes from fluid mechanics," *JHEP* **09** (2008) 054, `arXiv:0708.1770 [hep-th]`. 117, 120

[351] R. Loganayagam, "Entropy Current in Conformal Hydrodynamics," *JHEP* **05** (2008) 087, `arXiv:0801.3701 [hep-th]`. 117, 119, 120

[352] H. Kastrup, "On the Advancements of Conformal Transformations and their Associated Symmetries in Geometry and Theoretical Physics," *Annalen Phys.* **17** (2008) 631–690, `arXiv:0808.2730 [physics.hist-ph]`. 118

[353] L. Fabbri, "Conformal Gravity with Dirac Matter," *Annales Fond. Broglie* **38** (2013) 155–165, `arXiv:1101.2334 [gr-qc]`. 118

[354] "Journal für die reine und angewandte mathematik,". `http://gdz.sub.uni-goettingen.de/dms/load/img/?PPN=GDZPPN002153882&IDDOC=266356`. 119

[355] M. M. G. Ricci and T. Levi-Civita, "Méthodes de calcul différentiel absolu et leurs applications," *Mathematische Annalen* **54** (1901) 125–201. `https://link.springer.com/article/10.1007/BF01454201`. 119

[356] S. Carroll, *Spacetime and Geometry: An Introduction to General Relativity.* Benjamin Cummings, 2003. 119

[357] R. M. Wald, *General relativity.* Chicago Univ. Press, Chicago, IL, 1984. https://cds.cern.ch/record/106274. 119, 120

[358] V. Faraoni, E. Gunzig, and P. Nardone, "Conformal transformations in classical gravitational theories and in cosmology," *Fund. Cosmic Phys.* **20** (1999) 121, arXiv:gr-qc/9811047. 119

[359] J. Callan, Curtis G., S. R. Coleman, and R. Jackiw, "A New improved energy - momentum tensor," *Annals Phys.* **59** (1970) 42–73. 120

[360] J. Wess, "Conformal invariance and the energy-momentum tensor," *Springer Tracts Mod. Phys.* **60** (1971) 1–17. 120

[361] P. Di Francesco, P. Mathieu, and D. Senechal, *Conformal Field Theory.* Graduate Texts in Contemporary Physics. Springer-Verlag, New York, 1997. 120

[362] M. Forger and H. Romer, "Currents and the energy momentum tensor in classical field theory: A Fresh look at an old problem," *Annals Phys.* **309** (2004) 306–389, arXiv:hep-th/0307199. 120